

# NW European Gas Atlas

British Geological Survey (BGS), Bundesanstalt für Geowissenschaften und Rohstoffe (BGR), Danmarks og Grønlands Geologiske Undersøgelse (GEUS), Panstwowy Instytut Geologiczny (PGI), Nederlands Instituut voor Toegepaste Geowetenschappen TNO (NITG-TNO),

The European Union

**Editor: Lokhorst, A. (NITG-TNO)**

## ***Section A (Geology)***

Compilers:

Denmark: Laier, T.

Germany: Kockel, F.

The Netherlands: Geluk, M.C.

Poland: Pokorsky, J. & Milaczewski, L.

United Kingdom: Lott, G.K.

## ***Section B (Geochemistry)***

Compilers:

Denmark: Laier, T.

Germany: Gerling, P.

The Netherlands: Fermont, W.J.J., David, P. & Geluk, M.C.

Poland: Kotarba, M.

United Kingdom: Nicholson, R.A.

## ***GIS Development***

Denmark: Platen, F., von

Germany: Heckers, J.

The Netherlands: Brugge, J.V.M. & Diapari, L.

Poland: Milaczewski, L. & Milaczewska, E..

United Kingdom: Adlam, K.

## **Table of contents**

### **1. INTRODUCTION**

### **2. TECHNICAL ASPECTS**

#### 2.1. Data sources

Note 1. Surface sampling procedure for natural gases

Note 2. Analytical Procedures

#### 2.2 Classification of gases

#### 2.3 Condensate analysis

### **3. GEOLOGY**

#### 3.1 Dinantian (Tournaisian and Viséan), distribution and facies

#### 3.2 Namurian (A-B), distribution and facies

#### 3.3 Westphalian, distribution and facies

#### 3.4 Pre-Permian surface, structural contours

#### 3.5 Pre-Permian subcrop

#### 3.6 Top pre-Permian, maturity

#### 3.7 Rotliegend volcanics, distribution and thickness

#### 3.8 Rotliegend sediments, distribution and thickness

#### 3.9 Rotliegend sediments: facies

#### 3.10 Zechstein 2 (Staßfurt Carbonate), distribution and facies

#### 3.11 Middle Buntsandstein, distribution and facies

#### 3.12 Lower Toarcian (Posidonia shales), distribution and facies

#### 3.13 "Upper Jurassic" (Oxfordian to Berriasian), distribution and facies

#### 3.14 Salt structures (Rotliegend and Zechstein salt)

#### 3.15 Intrusives (Palaeozoic and Mesozoic)

### **4. DISTRIBUTION OF SELECTED GAS COMPONENTS AND PARAMETER**

#### 4.1 Methane

#### 4.2 Stable Carbon Isotope Ratios of Methane

#### 4.3 The Molecular Composition of Gaseous Hydrocarbons $C_1/(C_2+C_3)$

#### 4.4 Nitrogen

#### 4.5 Carbon Dioxide

#### 4.6 Calorific Value

#### 4.7 Density

#### 4.8 Miscellaneous

##### 4.8.1 Hydrogen Sulphide

##### 4.8.2 Mercury

##### 4.8.3 Helium

## **5. THE GENETIC CHARACTERISATION OF GASEOUS HYDROCARBONS AND NITROGEN**

### **5.1 Carboniferous Reservoirs**

5.1.1 Production province C1: Upper Carboniferous Reservoirs in the UK and Dutch North Sea Sectors

5.1.2 Production province C2: Upper Carboniferous Reservoirs in the eastern part of the Netherlands and in NW Germany

5.1.3 Production province C3: Carboniferous Reservoirs in northern Poland

### **5.2 Rotliegend Reservoirs**

5.2.1 Production province R1: Rotliegend Reservoirs in the UK and Dutch North Sea (west of the island of Ameland)

5.2.2 Production province R2: Rotliegend Reservoirs on the Friesland platform, the Groningen High and the Ems Estuary

5.2.3 Production province R3: Rotliegend Reservoirs between Bremen and the Altmark area (northern Germany)

5.2.4 Production province R4: Rotliegend Reservoirs in Poland northeast of the Wolsztyn High

5.2.5 Production province R5: Rotliegend Reservoirs in Poland southwest of the Wolsztyn High

### **5.3 Zechstein Reservoirs**

5.3.1 Production province Z1: Zechstein Reservoirs in the eastern part of the Netherlands and in NW Germany

5.3.2 Production province Z2: Zechstein Reservoirs in Poland

### **5.4 Post-Zechstein Reservoirs**

5.4.1 Production province M1: Post-Zechstein Reservoirs in the Danish North Sea Sector

5.4.2 Production province M2: Post-Zechstein Reservoirs in the Central Graben of the Dutch North Sea

5.4.3 Production province M3: Post-Zechstein Reservoirs in the SW Netherlands

5.4.4 Production province M4: Post-Zechstein Reservoirs in the eastern part of the Netherlands and in NW Germany

## **6. REFERENCES**

## **APPENDIX: PUBLIC DOMAIN GAS FIELD COMPOSITION DATA**

## 1. INTRODUCTION

Oil and gas has been produced from the Northwest European onshore and offshore areas for several decades, but little has been done on an international basis so far to compare gas composition from different gas fields, or to correlate gas composition with provenance. Natural gas consisting predominantly of methane with varying amounts of the higher homologues ethane, propane, butane, etc., is sometimes also combined with undesirable non-combustibles and contaminants such as nitrogen, carbon dioxide and hydrogen sulphide.

Substantial amounts of data on gas composition exist, for a small part in the published literature and for the larger part in company records and archives of national geological surveys. There is a wide scatter in reliability and availability of these data. This was felt for long to be an undesirable situation.

Because traditionally the geological surveys of most European countries, on behalf of their governments, are the holders of most of the (both public and confidential) data concerning the geology and mineral resources of their countries, representatives of these surveys started a joint project to compile these gasdata. Comparable projects were initialised already in The Netherlands and in Germany.

The definitive project, partly financed by the European Union, (contract No JOU2-CT93-0295) started in January 1994. The participants were the British Geological Survey (BGS), the Bundesanstalt für Geowissenschaften und Rohstoffe (BGR), Danmarks Geologiske Undersøgelse, now Danmarks og Grønlands Geologiske Undersøgelse (GEUS) and the Rijks Geologische Dienst, now Netherlands Institute of Applied Geoscience TNO - *National Geological Survey* (NITG-TNO). From April 1995 on, the Panstwowy Instytut Geologiczny (PGI) of Poland also participated in the project, partly financed by the EU under the PECO programme (contract ERBCIPD-CT94-0502).

This report deals with the results of this inventory study whose main objectives were:

- to give a comprehensive overview of the composition and areal distribution of the natural gases in the Northwest European gasfields.
- to generate maps, displaying the calorific values of the hydrocarbon gases present;
- to give an overview of the amounts and areal distribution of the non-combustibles and contaminants (mainly CO<sub>2</sub>, and N<sub>2</sub>) in the natural gases.
- to characterise the origin of the gases by means of studying various isotope ratios

Initially the study area was situated between:

West:	4 degrees WL
East:	16 degrees EL
North:	57 degrees NL
South:	50 degrees NL

With the participation of the PGI the area was extended in the East to 22 degrees EL. The advantage of the participation of Poland made possible the complete coverage of the whole Southern Permian Basin, the main gasbearing basin of NW Europe.

These aforementioned objectives are achieved through the following work programme.

On the one hand, in addition to the compilation of existing data that are being collected, new information on gas composition including carbon and nitrogen isotopes are generated through the analytical programme of the project. The composition and isotopes were analysed from approximately 200 samples. Additionally several gas condensates were analysed as well. In order to obtain the necessary quality of the data, the analytical programme also included an inter-laboratory comparison and quality control with respect to the analysis of gases and isotopes. In order to facilitate the comparison between the common practice in the different countries, suggestions for uniform analytical procedures and definitions were made.

On the other hand, collection and compilation of additional geological data and information on reservoir rocks, possible source rocks, TOC and vitrinite reflectance was undertaken.



The two approaches are integrated to provide an atlas, with almost 50 maps, displaying the results of the study.

#### *About this report*

Chapter 2 of this report discusses mainly technical aspects related to the project. It discusses the datasources and their reliability, the technical aspects of the in-house analytical programme and quality control and various classification schemes of natural gases. Statistical analysis of the database containing the compositional data from more than 900 wells form a firm base. This chapter ends with the results of the analysis of condensates. Although condensates do not occur throughout the whole study area, they are important in some of the Danish, Dutch and German gas reservoirs and can give a lot of information concerning the provenance of the gases.

The following three chapter discuss in detail the results of the integrated studies. This part of the report is intended to be published as the accompanying text of the atlas on the CD ROM.

Chapter 3 discusses the geological background of the study as displayed on a series of maps. These maps contain the most up to date public information available on the area. The maps give insight into the distribution of the large scale petroleum-bearing geological units and their source rock characteristics.

Chapter 4 deals with the results of the distribution of the various components of the natural gases. The distribution of methane, nitrogen, carbon dioxide, calorific value and wetness (defined as  $C_1/(C_2+C_3)$ ), are displayed and discussed, differentiated into 4 reservoir horizons (Carboniferous, Rotliegend, Zechstein and Post-Zechstein (Mesozoic combined with a few Tertiary fields)).

Chapter 5 discusses the results of the isotope analyses of more than 500 wells. The results are plotted on a range of diagnostic diagrams. Separate plots for the main production areas are made, differentiated according to the age of the reservoirs. These isotope plots are the basis to characterise the genetic origin of most of the gases in the study area. This systematic determination of isotope ratios of C, H and N will improve the understanding of hydrocarbon gas provenance.

A major part of the work programme was the application of GIS techniques (in this case Arc\_Info) to compile the maps provided by the partners. Although GIS is a powerful tool to combine various maps and map elements, the time necessary to integrate maps from a variety of sources should not be overlooked. The Atlas will finally be published on CD ROM. The application of GIS techniques will enable the user of the atlas to combine the information for his own display and analysis

A final note on those who contributed to the results of the project and this report. A large group of participants (P. Gerling (BGR), M. Kotarba (AHG), R.A. Nicholson (BGS), F.B. Rispens (formerly RGD, now the Ministry of Economic Affairs, NL), W.J.J Fermont (NITG-TNO), P.David (NITG-TNO), T. Laier (GEUS) and H. Merta (GEONAFITA) was responsible for the geochemical part of the project, especially the collection and compilation of data and the in-house analytical programme. Technical aspects of the results of their work is reflected in chapter 2; W.J.J Fermont wrote the paragraph on the classification of gases, whereas R.A. Nicholson (BGS) was responsible for the text on datasources, assisted by P. Gerling (BGR), T. Laier (GEUS) and A. Lokhorst (NITG-TNO). W.J.J. Fermont (NITG-TNO) and T. Laier (GEUS) wrote the part on condensates.

F. Kockel (BGR) and M.C. Geluk (NITG-TNO) were responsible for the collection and compilation of most of the geological maps and also wrote the main part of the accompanying text of chapter 3. They were assisted by G.K. Lott (BGS), J. Pokorski (PGI) and L. Milaczewski (PGI).

The compilation of the geochemical maps, displaying the compositional data was done by M.C. Geluk (NITG-TNO), with the assistance of R.A. Nicholson (BGS), P. Gerling (BGR), L. Milaczewski (PGI) and T. Laier (GEUS), whereas P. Gerling (BGR) wrote the main part of the text, assisted by W.J.J. Fermont (NITG-TNO).

P. Gerling (BGR) made the diagnostic plots and wrote the text of chapter 5.

A tremendous effort has been made by those who were involved in the preparation of the maps. The integration and computerisation of geological and geochemical data on an international base was a challenging but time-consuming process carried out by J. Heckers (BGR), L. Diapari (NITG-TNO), L. Milaczewski (PGI), K. Adler (BGS) and F von Platen (GEUS). The results of this atlas will be

published on a CD ROM. The necessary software is developed by J.V.M. Brugge from Geodataware, who also advised on the application of the GIS techniques.

## 2. TECHNICAL ASPECTS

### Introduction.

This chapter deals with a variety of subjects related to the compilation of the data for the atlas. Because this compilation was an international effort, it was felt important that within the project group differences between the countries could at least be compared and if possible uniform or comparable approaches could be developed.

Two fields got special attention. The first concern was the reliability of the database, both of the collected existing data as well as the data obtained by the in-house analysis in the laboratories. Concerning the in-house analysis a special interlaboratory quality control programme was executed on a series of standard gassamples. A quality control on the existing data from various archives remained difficult, due to a lack of sufficient documentation of the recorded data. Paragraph 2.1 reports on these items.

Secondly the classification of natural gases got special attention. In day-to-day practice the terminology used, varies between the countries in Europe. Moreover different approaches are possible. More details are found in paragraph 2.2.

### 2.1. Data sources

#### Overview

Obtaining data from the project area has been the responsibility of the five different groups in the National Geological Surveys, each of which has adopted somewhat different approaches to data acquisition. Apart from the German sector, from where over 200 analyses have been published, there are only a very few published data in the scientific literature, those that are available are presented in Table 2.1. In the UK, where BGS has no formal role within the hydrocarbons industry, the majority of the data were received from individual oil companies following initial direct written requests to company exploration managers. This resulted in a set of data devoid of quality control information, and with some data more than thirty years old, obtained when analytical techniques were much less well developed. At the other extreme, for example in BGR, samples were collected and analysed in-house over a period of many years, leading to a comprehensive database comprising data of verified quality. Industry generally has been in favour of the project, although it is known that there has been disquiet in some areas concerning the confidentiality of data. Although data from the UK and Denmark is released into the public domain after five years, those from The Netherlands offshore must remain confidential for a period of ten years, whilst in Germany, no release of commercial data has yet been sanctioned. Many of the data gathered for the project are from recent discoveries, and as such are confidential for the period relevant to the country in which the data were produced.

#### The Netherlands

The RGD (now NITG-TNO) is mandated by the government of The Netherlands to provide advice on exploration and exploitation of its hydrocarbon resources, and in this role has been able to build up an extensive database to support the gas atlas project. A similar national project on the provenance and distribution of hydrocarbon gases has been running for a number of years. The NITG-TNO receives now on a routine base samples from the operating companies. Samples from all exploration and producing wells are collected by service companies, and returned to NITG-TNO for sub-sampling. Analyses of these sub-samples has been undertaken by a commercial laboratory, whose system of quality control has been ratified, and therefore ensures that there is confidence in all data produced. Although many of the data used for this project were obtained from this source, a significant amount of data were also supplied through service company laboratories and from petroleum company archives. As far as it concerns these older data, most of it comprises of compositional data, which are measured in laboratories all over the world. Condensate samples were analysed in-house by NITG-TNO

#### Germany

A substantial amount of data already existed in the public domain at the start of the project, and this was supplemented by additional data from a confidential database held in BGR. As the result of involvement in a national government/industry sponsored 'deep-gas' research project over a number of years, BGR has assumed responsibility for collecting its own gas samples, and undertaking all the necessary analyses in-house. For a community project such as the hydrocarbon gas atlas these are obviously ideal circumstances, as it is then possible to ensure good scientific control at all stages of

the sampling and analytical procedures, a situation which, unfortunately, was not possible for all of the partner organisations. BGR has therefore been able to build a comprehensive database of gas composition and isotopic measurements for gas samples obtained from virtually all hydrocarbon wells drilled throughout Germany, especially in the northern part. Some condensate samples have also been analysed.

### **United Kingdom**

As noted earlier, BGS does not now maintain a formal role within the hydrocarbons industry in respect of data holdings, but has in the past had a responsibility on behalf of the UK Government's Oil and Gas Division of the DTI, for the databasing of various borehole logs obtained during commercial exploration for oil and natural gas. Consequently no gas compositional or isotopic data were immediately available to BGS, other than the few found during literature searches. Letters were therefore written to oil companies operating in the UK, describing the aims of the project, with requests for release of the relevant data on a confidential basis. Responses received were variable, and it has taken more than two years to build a database that is tolerably representative of the UK sector; very few isotopic data were received. One or two companies have been particularly supportive of the project, and without their help and encouragement the task would have been doubly difficult; exceptionally a few recently-taken gas samples were offered to BGS for analysis. No data were received directly from service companies. One oil company, who has retained a significant archive of gas and condensate samples, made some of these available to BGS for analysis. Isotopic measurements on gases were made in a commercial laboratory and the condensates were sent to GEUS and NITG-TNO for evaluation. The UK database contains data from multiple wells for many fields, especially where fields are large, and hence one set of data would be unrepresentative. However, many data have been aggregated where multiple analyses have been obtained.

### **Denmark**

DGU (now GEUS) originally held few data, and had to negotiate with the oil companies operating in the Danish sector to obtain compositional data and new gas samples for isotopic analysis. Compositional data were determined in PVT laboratories, and isotopic data in GEUS. Not all exploration well analyses in the GEUS archive have been included in the project database, since similar gas compositions were often obtained for other wells in the same reservoir; however, chemical data from more than one well have been included in the database for reservoirs of large lateral extension. The Danish sector comprises a few offshore fields and only one onshore, and therefore provided a relatively small (although very important) contribution to the project. All Danish fields are condensate-rich, and GEUS therefore assumed responsibility for collecting and analysing condensates on behalf of the project in collaboration with NITG-TNO. NITG-TNO carried out analyses by high performance liquid chromatography (HPLC) and high resolution gas chromatography (HRGC), and GEUS by gas chromatography/mass spectrometry (GC/MS).

### **Poland**

Compositional and isotopic data held by the University of Mining and Metallurgy Krakow (AGH), and the Geological Bureau (GEONAFTA) of the Polish Oil and Gas Company were made available to the project through the Polish Geological Institute, Warsaw. All sampling in Poland was undertaken by GEONAFTA. The samples were analysed by the AGH laboratories, some samples were analysed in the BGR laboratories. Rock Eval measurements on source rocks were done by GEONAFTA.

### **In-house analytical programme**

Most data were collected from existing sources, and constituted mainly of compositional data. This implicated a severe lack of data on the isotopes. Therefore an in-house analytical programme with emphasis on the isotope data was set up. This in-house programme was done at the laboratories of the national geological surveys from Denmark, Germany and the United Kingdom. In Poland the University of Mining and Metallurgy carried out these analysis on behalf of the Polish Geological Survey, whereas ISOLAB a private company in the Netherlands participated in the Dutch programme.

One of the major problems for such an analytical programme is to acquire gassamples. The geological surveys depend on the operating oil companies, in most cases regulated by the laws in the various countries.

Again the situation varies per country. In Germany the Bundesanstalt für Geowissenschaften und Rohstoffe has direct access to the wells of the operators and has therefore the possibility to determine their own sampling device. See note 1 at the end of this chapter. In Denmark, The Netherlands and

Poland the geological surveys are entitled to get gas samples from the companies or have easy access, but are not at all involved in the sampling itself. In the United Kingdom the BGS is not entitled to obtain samples from industry and was fully dependant on the kindness of the operators.

Because of the high costs of storing, gas samples are generally not kept forever and therefore there is of course a limited possibility to obtain data from old wells. Because in the past isotope analysis were not done on a routine base, the final database of isotope data (516 data points) is much smaller than the database on compositional data (939 datapoints, from which 526 datapoints are presented in table 2.1. The remaining datapoints are confidential. Table 2.1 has been included in the appendix).

### **Inter-laboratory Quality Assurance**

To ensure comparability of gas analytical data from different laboratories, it is necessary to calibrate, or standardise, individual sample-handling procedures. First of all, the partners of participating laboratories compared extensively their routine practice on handling their analysis. An example of a protocol of the analytical procedures is given in note 2, at the end of this chapter.

However, the most effective means for ensuring compatibility of gas analysis, is for all partners to undertake the analysis of sub-sample of the same gases. To accomplish this, the project group decided that each laboratory should analyse aliquots of several different gas samples to be provided by the participants themselves.

The first of these inter-laboratory studies commenced in the spring of 1994, with gas standard EU3 being distributed to the other participants by RGD (now NITG-TNO) at the inaugural meeting of the project group in Haarlem. This sample was analysed in all of the laboratories with good reproducibility, see Table 2.2. EU3 was not (at this stage) distributed to Poland due to their late inclusion into the project under the PECO programme (January 1995).

The second of these exercises took place during the summer of 1994 with gas standard GB6, which derived from the natural gas field Thönse near Hannover/Germany. Several duplicate samples were taken from the well head by BGR staff in June 1994, and distributed amongst the partners during the second meeting in Hannover. Data shown in Table 2.2 display similar reproducibility to those obtained during the earlier exercise.

At the December meeting in Keyworth, a third gas sample was distributed by BGS, this sample was from a Jurassic reservoir sourced from Kimmeridge Clay. Data (Table 2.2) were more widely distributed compared to the previously measured gases EU3 and GB6, which may be due to the sub-sampling procedures employed (see comments relating to GB6 below). However, the data widen the range of carbon isotope ratios of methane, ethane and propane, and the  $\delta D$  of methane, to significantly more negative values. In contrast, the  $\delta^{13}C$  value of the carbon dioxide is about 5‰ heavier than those from the previously distributed gases. Due to lack of suitable laboratory facilities at the time BGS did not undertake the isotopic analysis of this particular sample.

To further widen the scope of the inter-laboratory study it was decided to purchase the international gas standards NGS-1 and NGS-2 distributed by the NIST (National Institute of Standards and Technology, US Department of Commerce), which has taken over custodial duties for these materials from the International Atomic Energy Authority (IAEA). The results of analyses undertaken as part of this current project agree very well with the data already published on these gases by JENDEN et al. 1988, DUMKE et al. 1989, SOHNS et al. 1994 (shown in Table 2.1). An additional sample EU2, from a Lower Cretaceous reservoir, was provided by Denmark, and distributed amongst four of the partners at the June 1995 meeting in Copenhagen. Data on this sample were also widely distributed compared to the previously measured gases, which may again be due to the sub-sampling procedures employed. Having still not identified a suitable laboratory to carry out the isotopic analyses, BGS did not receive sample EU2, however, the laboratory problem was partially resolved much later, and the NIST standards were subsequently analysed by an independent laboratory, on behalf of BGS, for isotopic composition only.

Table 2.2 is subdivided into separate data sheets for the single gases. Data from the individual laboratories are generally in acceptable agreement, mean values and standard deviations are calculated based on these results. Additionally, relative deviations are given for the molecular gas data. The data cover a broad range in both molecular and isotopic compositions (i.e. wet and rather dry HC gas compositions, variable nitrogen contents from 1 to 16%, variable CO<sub>2</sub> contents from 1 up

to 26%, carbon isotope ratios between -70 and -2‰, hydrogen isotope ratios between -200 and -130‰, and nitrogen isotope ratios ranging from -8 to +16‰). This broad range of compositional data is to be expected, bearing in mind the wide areal coverage represented by the project sampling programme.

The molecular and isotopic variations of the separate sub-samples 117369-117371 of GB6 (Table 2.2 - BGR data) show the range of data obtained related to both sampling procedures and analytical accuracy. Sample 117371 was re-analysed in September 1994 and again in June 1996. These latter data are in good agreement with those obtained in June 1994.

The large relative deviations for the molecular composition data of the higher molecular weight HC gases are most probably due to the very low absolute values, i.e. the close proximity of these values to the detection limits of the gas chromatography method employed for the determinations. However, relative deviations of more than 5% occur, sometimes even for the other higher concentration components. These deviations are often related to a single value from one specific laboratory.

All stable carbon isotope ratios for the HC gases are in acceptable agreement, and this is also true for the majority of the  $\delta^{13}\text{C}$  data on the carbon dioxide, however, the isotopic measurements on gas EU2 show quite a wide variation. The  $\delta\text{D}$  values on methane also agree for the gases NGS-1, NGS-2, EU3 and GB6, but the standard deviations of gases BGS and EU2 are again too large. The  $\delta\text{D}$  values from the Danish laboratory in particular seem to be isotopically too heavy. The database on nitrogen isotope ratios is small, and there are quite significant differences between the Netherlands and German data. The fact that other laboratories were not able to report reliable nitrogen isotope data for all of the samples, probably reflects the difficulties encountered when undertaking this particular analytical procedure. Analytical procedures for the analysis of methane and nitrogen in replicate gas samples from the Groningen field were reported by HUT et al. (1984).

## **Note 1. Surface sampling procedure for natural gases**

### 1. General remarks

Optimum recommendation: All gas samples within a project / sampling programme should be taken by the same person. The sampling procedures followed and the sampling devices should also be identical. Gas sampling should only be carried out during regular production, and as far as possible after the injection of inhibitors (especially in case of condensate sampling).

Unfortunately, in most cases these recommendations often cannot be followed due to established safety regulations, company interests etc.. However, the minimum requirement for surface sampling of natural gases is that gases should only be taken during production times.

### 2. Sampling devices

#### 2.1. Glass container

This type of gas-sample container can be routinely used for samples which are taken for conventional analysis of the molecular gas composition and stable isotopes (C, H, N, S) at normal atmospheric pressure. Beware of gas-sampling bulbs with valve stopcocks which are often not gas-tight. Instead, we highly recommended the use of gas-sampling tubes with one-way stopcocks and retaining devices. Stopcocks must be carefully greased to avoid any leakage. The type of grease used must be suitable for the ambient temperature encountered.

#### 2.2 Steel container

Steel containers are used for high-pressure gas samples. For noble gas analysis, especially in case of helium, He-tight welded materials, e.g. a WHITEY (trademark of the Swagelock Group of Companies) steel container with a WHITEY valve should be used. Care should be taken that the container is made from specific materials in case of sour-gas sampling.

### 3. Sampling procedure

Generally, four different 'types' of natural gas samples can be taken from producing wells:

- i) sample from the well head, atmospheric pressure,
- ii) sample from the well head, high pressure. Beware of the container specification!
- iii) atmospheric pressure sample from flow line after purification (moisture, liquid HC, H<sub>2</sub>S, Hg, etc.) and pressure adaptation to pipeline system,
- iv) high pressure sample from flow line, after purification and pressure adaptation to pipeline pressure.

Atmospheric pressure samples can be taken from both sampling points via a needle valve (for pressure adjustment) through a liquid separator into gas sampling bulbs. All devices can be connected with silicone or PVC tubings. At the end of this gas-sampling line, a bubble counter should be installed for visual control of the gas flow. The stopcocks of the gas container should be closed after allowing the gas to purge for 20 min.

In the case of lean and sour gases with H<sub>2</sub>S < 4 vol% a gas washing bottle filled with a zinc acetate solution should be installed at the end of the sampling line. H<sub>2</sub>S reacts with this alkaline solution and zinc sulphide precipitates. The precipitate can subsequently be analysed in the laboratory. In cases of higher H<sub>2</sub>S content, precipitation of zinc sulphide from the gas can be carried out in the laboratory.

High pressure gas samples should usually be taken from the flow line, to avoid moisture and liquid contamination in the steel container. In cases of low production pressure, gas samples have eventually to be taken at the well head, because gas-producing companies occasionally combine gas from a different well during gas purification in order to reach a certain pressure before the gas enters the pipeline system.

### 4. Data quality

BGR analysed atmospheric pressure gas samples from the well head and from the flow line of the same production well to detect possible molecular and/or isotopic differences occurring between these samples. The results are given in Table 1. In most cases both the molecular composition and the stable isotopes show significant differences between well-head gases and flow line gases. Because these differences cannot be clearly correlated with varying purification steps, and since sometimes a

different gas is added into producing plants before the gas enters the pipeline system, it is strongly recommended that atmospheric-pressure gas samples are taken only from the well-head.

#### 5. Actual standardisation in Germany

For safety reasons, German gas-producing companies have recently discussed the setting up of a new standard for surface sampling of natural gases. These regulations demand a heatable, pressure-reducing sampling unit which allows the taking of both high pressure (max. 1 MPa) and as low pressure (atmospheric) gas samples from the well head. The unit is furnished with pressure regulators (40 MPa to 1 Mpa and 1-0 MPa), spring safety valves and an explosion protected electrical heating plate (aluminium) to avoid freezing of the pressure regulators.

For sour gas sampling the use of a gas mask is essential, and a KOH-solution has to be used to precipitate the H<sub>2</sub>S passing the 'gas-sampling line' during the sampling of atmospheric pressure samples.



## Note 2. Analytical Procedures

The major constituents of natural gases (gaseous hydrocarbons, N<sub>2</sub>, CO<sub>2</sub>) were analysed in a gas chromatograph, running a temperature program and using thermal conductivity and flame ionisation detectors.

For isotope analysis, methane and ethane were isolated in a preparation line (e.g. in BGR's laboratory: gas chromatograph, packed column 1/4 inch OD stainless steel, 2.5 m length, Porapak Q). After subsequent oxidation in a CuO-oven (900°C) to water and carbon dioxide, the latter is used for stable carbon isotope analysis. The combustion water was reduced on zinc (450°C) to molecular hydrogen prior to isotope measurement. <sup>13</sup>C/<sup>12</sup>C and D/H were determined using Finnigan MAT type 251 and Finnigan MAT type DELTA D mass spectrometers. Isotope ratios are given as δ-values versus the standard materials PDB and SMOW for carbon and hydrogen, respectively. The analytical precision is ±0.2‰ for δ<sup>13</sup>C and ±3‰ for δD. Experimental details on the isotope technique are given by DUMKE et al. (1989).

In BGR, a GCIRMS system similar to that described by SOHNS et al. (1994). was set up to measure δ<sup>15</sup>N values on nitrogen gas. The gas chromatograph (packed column 1/8 inch OD stainless steel, 3 m length, 5Å molecular sieve, column temperature 75°C isothermal) is designed to isolate nitrogen before channelling into the MS (Finnigan MAT type 252) for isotope analysis. Isotope ratios are given as δ-values relative to the standard atmospheric nitrogen. The standard deviation of δ<sup>15</sup>N values is better than ±0.5‰.

A description of the analytical procedures concerning minor components in natural gases is given by the relevant authors, e.g. by OZIMA & PODOSEK (1983) for noble gases, by THODE et al. (1961) for H<sub>2</sub>S, and by MORRISON (1972) for mercury.

### *Analysis of Condensates*

Condensate Samples from natural gas fields in northern Germany were always taken on well-site at the liquid separator. The liquid was usually a mixture of condensate and formation water. The separation of these two substances was unproblematic due to their density differences.

No condensate preparation was performed prior to analysis.

The analytical procedure (whole-oil-chromatography) was done with the following set-up:

GC	: Packard 439, with deep-temperature equipment (LN <sub>2</sub> -cooling)
Injection	: one-column, injector 220°C
Carrier gas	: He
Flow	: 1 ml/min
Column	: 30 m, 0.25 mm id, 0.25 m DB5 coating
Temp. Program	: initial oven temp. -20°C, 1 min isotherm 10°C/min up to 0°C 4°C/min up to 295°C
Detector	: FID, 300°C

Detection: C<sub>6+</sub> hydrocarbons (alkanes + aromatics); isoprenoids (C<sub>14</sub>-C<sub>20</sub>) as far as occurring

Further analyses: δ<sup>13</sup>C on bulk condensates, with combustion at 850°C, isotope analysis with a Finnigan MAT 251 mass spectrometer.

## 2.2 Classification of gases

### Introduction

The classification of substances serves the objectives of those who ask for a classification. This implies that the classification of matter is basically subjective, because the user forms part of the classification system. Gaseous matters are no exception. There are many ways in which gases can be classified, based on the purpose of the user. For gases one can recognise for example:

- Compositional classifications
- Technical classifications
- Genetic classifications
- Economic classifications

Compositional classifications aim to describe the abundance, qualitatively and quantitatively, of single constituents of gases. Examples are for instance the amount of C<sub>2</sub>-C<sub>6</sub>, nitrogen, hydrogensulphide, or carbon dioxide. A problem in the classification of multi-component systems - as natural gases normally are - always arises when the classification aims to take into account more than one variable.

Whatever variable is applied for discrimination of different gases, the basis for a compositional classification is, that it describes the gases as they are, independent of circumstantial fact. As such, combined variables derived directly from the molecular gas composition, like density and calorific value, can be considered as compositional variables, too. By tradition, companies and countries have evolved relatively global classification systems for the description of natural gases. These classifications unfortunately lack basic assumptions and are interpreted in different ways in different countries. Examples are found in the Glossary of Natural Gas Reserves BGR/NLFB (1996). Here a summary is given of different interpretations used by different countries in Europe for example of wet gas, dry gas, sweet gas, and sour gas. From their summary it can be seen that agreement in Europe is not yet achieved with respect to the concept of classification, the definition of boundaries and the interpretation of terms. This atlas at least provides a numerical basis to substantiate a relevant classification of gases for NW-Europe.

Technical classifications are based on the fact that in certain applications gases behave in a specific manner. Such classifications describe physical/chemical properties of gases in order to estimate a certain behaviour within a certain technical environment. For example, the Wobbe Index *W*, the ratio of the gross calorific value to the square root of the relative density of a gas, is used as a measure for the energy input delivered to a burner via an injector. Gases of different compositions can yield the same Wobbe Index. Another example is the Reynolds number (*Re*), which is based on the kinematic viscosity of a gas, together with flow rate and pipe diameter dictates the flow type in a system. High *Re* numbers predict laminar flow, whereas high *Re* numbers predict turbulent flow in specified tubes. There are many of such technical classifications with the purpose of predicting the behaviour of gas under specific circumstances (for overview see GEERSSSEN, 1988). However, the aim of this study is to present, as precise as possible, an atlas of gas compositions. This atlas can be used for the consideration of technical applications in certain areas.

Genetic classifications aim to provide information upon the origin of the gases. It is assumed that chemical compounds present in the gases reflect in some way the geologic history of the gas, i.e., the depositional environment, the thermal maturity of the source or the post genetic history with respect to migration, oil maturation, or degradation. There are three major sources of information available, the molecular gross composition of gases, the isotopic composition of gases, and the presence or absence of biomarkers in the heavier fractions of the gases (For references see BORDENAVE (ed.), 1993; WHITICAR, 1993; PETERS & MOLDOWAN, 1993). In the case of the composition of gases the characteristic percentage range of gas constituents is from 100 to less than 1%. Concerning the absolute amount of stable isotopes and biomarkers the abundance is rather on ppm-scale or even less. Thus their presence does not influence the technical properties of the gases. The stable isotope composition and its use for classification is discussed elsewhere in this study. Biomarkers from the condensate fractions were not studied systematically and are left out of consideration.

The economical classification of gases, takes into account the quality of the gases, the volumes of the reserves, the presence of the infrastructure, transporting distance, the mondial price development, political stability and many other parameters. The Glossary of natural gas reserves (1996) describes combined compositional and economical classifications: "Wet (rich) gas is natural gas containing hydrocarbons heavier than methane in commercially extractable quantities". However commercially extractable quantities of condensates are time- and space dependent. It is related not only to gas composition, but also to the availability of infrastructure, distance to consumers, and market prices. As such, this definition of wet gas would be very volatile because unlike the geological data, many economical variables are relatively short-lived, making the definition confusing, multi-interpretable and therefore hardly useful.

### **The choice of a classification concept**

Having stated the differences between various classification concepts and purposes, it is worthwhile to ask which type of classification could be expected on the basis of the unique amount of data collected in this project. For petroleum geologists the best type of genetic classification should be based on representative reservoir samples, i.e. PVT samples, collected before the separator, including all types of heavier fractions, waxes, condensates, hydrargium. Such geological samples are necessary to understand the genetic history of petroleum systems were the hydrocarbons have been generated (MAGOON & DOW, 1994). Yet these samples are extremely expensive, and generally not available. At least the database used in this study is generally not derived from such samples.

For the gas market it is relevant to predict which type of hydrocarbon will enter the distribution system. This is the gas or nearly so, which downstream has passed the separator and eventually the clean-up plant, and from which sand, shale, water, heavy fractions, hydrargium and dissolved minerals have been removed. Fortunately for the geologist, the composition of these gases still contains valuable information, although they are not geological samples. Besides, there are additional sources of information available which help the geologists to interpret the gas occurrences. For instance, the Gas Oil Ratio, stable isotope compositions, as well as sub-ppm occurrences of biomarkers provide information upon the genetic history of the hydrocarbons present. Some of these subjects are presented elsewhere in this report.

From the other types of classifications it can be shortly stated that they are outside the scope of this project, for obvious reasons. There has not been made an inventory of the existing infrastructure, and no volumetric data are available on gas reserves. This leaves the conclusion that this atlas should provide a classification based on composition in a strict sense, without commercial, genetic interpretations (apart from the interpretations derived from the isotope studies).

Another relevant point in compositional classification is that they are based on the composition of the gases, theoretically ranging from 0-100 volume %, which are directly related to the chemical and physical properties and behaviour of these gases. This in contrast to the genetic classifications based on biomarkers and or isotope ratios, which are rather based on shifts in ratios at ppm-scale.

The ideal classification of gases, as far as possible, should:

- Match natural boundaries between types of gases,
- Provide relevant information about the composition of the gases,
- Provide relevant information of the spatial distribution of these gas types, and
- Meets customer requirements.

### **The classification of gases on the basis of gas composition**

For a compositional classification a number of techniques are available.

Classification can be based on single variables, or combined variables. In this chapter the available data are discussed in this order. In a similar way as has been described for the evaluation of the contour intervals, it has been attempted to choose as little categories as possible, but with maintenance of as much information as possible. In the table below some descriptive statistics of the parameters analysed are summarised. In the case of the calorific value and the density it was not always possible to calculate the compressibility factor because of the very high nitrogen content.

**Table 2.2.1 Statistical characteristics of all data**

total	C <sub>1</sub> vol.-%	C <sub>2</sub> vol.-%	C <sub>2</sub> - C <sub>6</sub> vol.-%	CO <sub>2</sub> vol.-%	N <sub>2</sub> vol.-%	H <sub>2</sub> S vol.-%	density (rel. dry air)	calorific value MJ/m <sup>3</sup>
n	939	939	939	935	939	939	908	908
minimum	0.01	0.00	0.00	0.00	0.00	0.00	0.51	1.28
maximum	99.62	11.53	28.72	78.75	97.60	38.00	1.32	66.04
mean	81.44	2.87	4.15	2.53	11.23	0.49	0.64	37.71
SD	11.24	1.43	2.10	0.32	13.81	0.00	0.08	6.91
SE	0.37	0.05	0.07	0.01	0.45	0.00	0.00	0.23
interval	3.32	0.38	0.96	2.63	3.25	1.27	0.03	2.16

In the following discussion relatively precise class intervals are presented. At the end of the chapter a generalised classification summary sheet, derived from the discussions is included.

### 1 Single variables

939 data points have been analysed. The following variables have been considered: methane, ethane, C<sub>2</sub>-C<sub>6</sub>, nitrogen, carbon dioxide, and hydrogensulphide. For the frequency analysis of each variable the number of classes was approximated as the square root of the number of observations, i.e. 30 classes. The class width W was approximated according to:

$$W = \frac{(MAX \text{ var}_i - MIN \text{ var}_i)}{\sqrt{n}}$$

where MAX en MIN are the maximum and minimum values of variable i and n is the number of observations.

#### *Methane*

The frequency distribution of methane is shown in figure 2.2.1. The class width of each interval is 3.32%. Methane shows a left skewed distribution pattern. Within this distribution there are three distinct minima. A subdivision in a minimum number of categories on the basis of methane, which best matches the observed data is given in table 2.2.2.

**Table 2.2.2 Classes of methane**

category	class range	methane content		observations	description
1	19 - 30	> 63%		91%	rich methane gas
2	12 - 18	> 40%	< 63%	5%	poor methane gas
3	6 - 11	> 20%	< 40%	4%	very poor methane gas
4	0 - 05	< 20%		1%	extremely poor methane gas

More than 90% of the 939 observations fall in the category of high methane gas.

#### *Ethane*

The frequency distribution of ethane is shown in figure 2.2.2. The class width of each interval is 0.38%. Ethane shows a right skewed frequency distribution in the range of 0-12%. One distinct minimum is present in class 6. A boundary is suggested between class 22 and 23. From this frequency distribution a classification on ethane is given in table 2.2.3.

**Table 2.2.3 Classes of ethane**

category	class range	ethane content		observations	description
1	1 - 6	< 2.3%	< 2.3%	40%	poor ethane gas
2	7 - 22	> 2.3%	< 8.4%	58%	medium rich ethane gas
3	23 - 30	> 8.4%	<12 %	2%	rich ethane gas

It might be necessary to subdivide further the low ethane gases into more categories, for instance for a proper recognition of gases with very low ethane contents, which are sometimes referred to as biogenic gases.

### *C<sub>2</sub>-C<sub>6</sub>*

It should be realised that the gases discussed here have already been processed. Most of them have been separated already in a low molecular and a high molecular fraction containing condensate and oil fractions from C<sub>6</sub>+ onward. Still, the downstream gases have significant differences with respect to the content of propane to hexane, although part of these gases are in fluid phase at room temperature. Due to equilibrium conditions the C<sub>2</sub>-C<sub>6</sub> content still mirrors the original composition of raw material after separation. As a consequence the gases delivered to the distribution system vary widely.

The frequency histogram is shown in figure 2.2.3. The class width of each interval for C<sub>2</sub>-C<sub>6</sub> is 0.96%. The C<sub>2</sub>-C<sub>6</sub> show a right skewed frequency distribution in the range of 0 to almost 30%. Significant minima in this frequency distribution are present in the classes 3 and 14. Above this interval the occurrences are scattered. From this frequency distribution a subdivision in C<sub>2</sub>-C<sub>6</sub> containing gases is given in table 2.2.4.

**Table 2.2.4 Classes of C<sub>2</sub>-C<sub>6</sub> content**

category	class range	C <sub>2</sub> -C <sub>6</sub> content		observations	description
1	1 - 3	< 3%	< 3%	43%	dry (lean) gas
2	4 - 14	> 3%	< 14%	54%	wet (rich) gas
3	15 - 30	> 14%		3%	associated gas

The terms proposed here, may give some (more) confusion, because they have been used frequently in different context en different meanings. There are some arguments to defend this classification. The current explanations of dry gas vary widely and are based on different properties and or classification concepts. In France and the Netherlands dry gas is defined as a gas which does not contain a heavy, easily condensable fraction under normal separation and transport conditions, leaving the question open what is easy and what is normal. In Germany the term dry gas is based on three variables, the dew point (< 0C at pipeline pressure), the percentage of H<sub>2</sub>S (< 1% ) and sales contract (?). In the UK dry gas is defined as non-associated gas containing less than 3 gallons of condensable hydrocarbons per 1000 cu.ft of gas.

For wet gas a comparable Babylonian captivity is noticed. In France and the Netherlands it is defined as a gas that remains in the gaseous phase in the reservoir rock, independent of the pressure, but from which a liquid phase condenses at standard conditions. In the UK it is opposite to the dry gas while it contains more than 3 gallons of condensable hydrocarbons per 1000 cu ft., and in Poland a gas is considered wet if it contains more then 12g C<sub>5</sub>+ hydrocarbons per m<sup>3</sup>.

### *Nitrogen*

The class width of each interval in the frequency histogram of nitrogen (figure 2.2.4) is 3.25%. Nitrogen shows an extremely right skewed frequency distribution in the range of 0 to almost 100%. It is difficult to extract significant minima from this frequency distribution. The first irregularity occurs between classes 5 and 6. One distinct minimum is present in class 13, another in class 18. From this frequency distribution a subdivision in nitrogen containing gases is presented in table 2.2.5.

**Table 2.2.5 Classes of nitrogen**

category	class range	nitrogen content	observations	description
1	1 - 5	< 16%	81%	poor nitrogen gas
2	6 - 13	> 16% < 42%	11%	medium rich nitrogen gas
3	14 - 18	> 43% < 60%	3%	rich nitrogen gas
4	19 - 30	> 60%	5%	very rich nitrogen gas

*Carbon dioxide*

The frequency distribution of carbon dioxide possesses a peculiar problem. In figure 2.2.5a the scores of all the data are shown in the histogram. The frequency distribution is extremely right skewed. The class interval is 2.63% . Almost 90% of the data fall within the first two classes. There are few data above 5%. A similar problem occurred when determining the contour intervals of the CO<sub>2</sub> map: at constant intervals no information was available from the maps because the majority of the data would have plotted within one contour interval. The histogram shows a distinct minimum at class 6.

Therefore the evaluation of CO<sub>2</sub> proceeded in two steps. First a class of CO<sub>2</sub> was separated at class 6. Then the class intervals and frequencies of the remaining data were recalculated. On the basis of the calculations of the 911 remaining data a new frequency distribution emerged with again 30 classes but now of 0.38% widthness of each class. This histogram is shown in figure 2.2.5b. The left skewed character of the frequency distribution is still present. A new minimum is observed at class 10. Distinct minima are not present in the skewed part of the histogram. However, the relatively large frequency jump between class 2 and 3 is used for the positioning of one more category boundary. From this frequency distribution analyses a subdivision on the basis of CO<sub>2</sub> is given in table 2.2.6.

**Table 2.2.6 Classes of CO<sub>2</sub>**

category	class range	CO <sub>2</sub> content	observations	description
1	b 1 - 2	< 0.8%	47%	sweet gas (1)
2	b 3 - 9	> 0.8% < 3.5%	36%	sour CO <sub>2</sub> gas
3	b 10 - 30	> 3.5% < 12%	14%	very sour CO <sub>2</sub> gas
4	a 6 - 30	> 12%	3%	extremely sour CO <sub>2</sub> gas

(1 ) note. Here we adopt the traditional term, which means that H<sub>2</sub>S should be absent as well.

The advantage of this classification schedule is that fits to a large amount of data, whereas major category intervals have economic relevance because of the corrosivity of sour gas.

*H<sub>2</sub>S*

The frequency distribution of all H<sub>2</sub>S data on the basis of 30 classes is shown in the histogram of figure 2.2.6a. The frequency distribution is extremely abnormal, with almost all data within class 1. The class interval is 1.27% and contains 94% of the data. The peak occurrence in class 1 is caused by 806 gases containing 0% of H<sub>2</sub>S.

Therefore only the 133 gases containing H<sub>2</sub>S were studied. From these gases 60 are above 1%. These are considered as extremely sour. and are further left out of the figure. Within the interval from >0 to <1% 73 gases are found. They are distributed over 8 classes of 0.13 vol% widthness. The histogram for the frequencies of H<sub>2</sub>S in this range is shown in the figure 2.2.6b. From this right skewed figure one distinct minimum is obtained at class 3. From this frequency distribution analyses and the above mentioned considerations a subdivision on the basis of H<sub>2</sub>S is given in table 2.2.7.

**Table 2.2.7 Classes of H<sub>2</sub>S**

category	class range	H <sub>2</sub> S content	observations	description
1	a 1	0.0 %	86%	sweet gas
2	b 1 - 2	> 0.0 % < 0.26%	6%	sour H <sub>2</sub> S gas
3	b 3 - 8	> 0.25% < 1.00 %	2%	very sour H <sub>2</sub> S gas
4	a > 8	> 1.0 %	6%	extremely sour H <sub>2</sub> S gas

The presence of H<sub>2</sub>S is of extreme importance, not only for environmental and safety regulations but also for the manufacturing of gas. Unfortunately, different countries have very different opinions concerning the classification of sweet gas on the basis of H<sub>2</sub>S. The classifications are summarised in table 2.2.8 (After BGR Glossary 1996).

Table 2.2.8 Summary of definitions for H<sub>2</sub>S used in several countries

country	boundary level sweet/sour gas	recalculated to vol%
FRG	5 mg/m <sup>3</sup>	0.033
UK and USA	1 vol%	1.000
CIS	0.013 vol% or 20 g/1000 m <sup>3</sup>	0.013 0.0013 (1)
PL	20 mg	0.0013

(1) presumably a typing error

As can be seen from the table there is a large discrepancy in the definitions of boundary conditions for sweet and sour gas. The advantage of the classification proposed here is that it relates the frequency of observed data with class intervals that make sense for the user.

#### Combined variables

Calorific value and density are physical/chemical properties of gases which are determined by the unique composition of gases. As such they mask the individual contribution of each single variable. In this chapter some discussion is presented upon the subdivision in various types of gases based on these characteristics. The calculations used for calorific values and densities, as well as the properties of individual gas compounds are discussed elsewhere in this report. In 27 cases the extremely high nitrogen content prevented exact calculations of the density, and calorific value, because the gas compositions were outside the confidence limits of the methods applied.

#### Calorific value

Calorific values used in this report are calculated on the basis of thermodynamic properties of the individual gas constituents of gas mixtures at standard P,T conditions (CRC 1984, GEERSSEN 1988). The range of calorific values is from almost zero to 64 MJ/m<sup>3</sup>. The class intervals used for the univariate analyses is 2.16 MJ/m<sup>3</sup>. In figure 2.2.7 the frequency distribution of calorific values is shown. The average calorific value of all samples amounts to 37.71 MJ/m<sup>3</sup>. For comparison the calorific value of the Groningen gasfield, which is used as a national standard, amounts 35.17 MJ/m<sup>3</sup>. On the basis of the mean 37.71 MJ/m<sup>3</sup> and the standard deviation of 6.09 MJ/m<sup>3</sup> four classes of calorific values were designed. The round off values are summarised below:

Table 2.2.8 Classes of calorific values

category	class range	range calorific value in MJ/m <sup>3</sup>	observations	description
1	0 - 13	< 30.80	12%	very low calorific gas
2	14 - 17	> 30.80 < 37.7	27%	low calorific gas
3	18 - 20	> 37.7 < 44.6	57%	high calorific gas
4	20 - 30	> 44.6	4%	very high calorific gas

The high values of the calorific values are invariably caused by admixtures of C<sub>2</sub>-C<sub>6</sub>, whereas low calorific values are caused either by the presence of nitrogen or carbon dioxide.

#### Density

The densities used in this report are calculated on the basis of the densities of single gas densities at standard P.T conditions, corrected with the compressibility factor z for gas mixtures (CRC 1984, GEERSSEN 1988). They are expressed relative to air density. The density range of the investigated samples varies from 0.5 to 1.4. The width of class intervals is 0.027. In figure 2.2.8 the frequency histogram of density is shown. The density shows a slightly right skewed unimodal distribution. Four classes are designed on the basis of the mean of 0.642 and a standard deviation of 0.078.

**Table 2.2.9 Classes of density values**

category	class range	range density rel. to air	observations	description
1	0 - 00	<0.56	00%	very light gas
2	00 - 0.64	>0.56 <0.64	00%	light gas
3	00 - 00	>0.64 <0.72	00%	heavy gas
4	00 - 00	> 0.72	0%	very heavy gas

Light gases are invariably rich in nitrogen, because it is the lightest constituent present in considerable amounts.. Heavy gases are either loaded by CO<sub>2</sub>, or by propane and higher hydrocarbons. Ethane does not influence the relative density significantly because its density is very close to that of air.

### Summary of classification

In the preceding text it was argued that a classification schedule should be based on numerical data. Although statistically more or less correct it leads to relatively unbalanced classification tables. Therefore, it is attempted in table 2.2.10 to present a smoothened general classification scheme, derived from the above mentioned data.

**Table 2.2.10 Summary sheet of classification**

variable	description	lower limit	upper limit
CH <sub>4</sub>	rich methane gas	> 65 %	100 %
	poor methane gas	> 40 %	< 65 %
	very poor methane gas	> 20 %	< 40 %
	extremely poor methane gas		< 20 %
C <sub>2</sub> H <sub>6</sub>	poor ethane gas		< 2 %
	medium rich ethane gas	> 2 %	< 8 %
	rich ethane gas	> 8 %	
C <sub>2</sub> -C <sub>6</sub>	dry (lean) gas		< 3 %
	wet (rich) gas	> 3 %	< 14 %
	associated gas	> 14 %	
N <sub>2</sub>	very poor nitrogen gas		< 15 %
	medium rich nitrogen gas	> 15 %	< 35 %
	rich nitrogen gas	> 35 %	< 55 %
	very rich nitrogen gas	> 55 %	
CO <sub>2</sub>	sweet gas		< 1 %
	sour CO <sub>2</sub> gas	> 1 %	< 4 %
	very sour CO <sub>2</sub> gas	> 4 %	< 12 %
	extremely sour CO <sub>2</sub> gas	> 12 %	
H <sub>2</sub> S	sweet gas	0.0 %	
	sour H <sub>2</sub> S gas	> 0.0 %	< 0.2%
	very sour H <sub>2</sub> S gas	> 0.2 %	< 1.0%
	extremely sour H <sub>2</sub> S gas	> 1.0 %	
Calorific value	very low calorific gas	< 30	
	low calorific gas	> 30	< 38
	high calorific gas	> 38	< 44
	very high calorific gas		> 44
Density	very light gas	< 0.55	
	light gas	> 0.55	< 0.65
	heavy gas	> 0.65	< 0.75
	very heavy gas		> 0.75

### Cluster analysis



A cluster analysis was carried out taking into account the molar percentages of the gas components using the statistical software package SPSS release 7.5 (NORUSIS 1997). The similarity measure for combining clusters used in this analysis is based on the squared Euclidean distances (D). The distance between two samples X and Y is the sum of the squared differences of each variable i, as expressed by:

$$D(X,Y) = \sum_i (X_i - Y_i)^2$$

In this investigation the Ward method for combining clusters has been applied (NORUSIS 1992). The results of the cluster analysis are shown in the summary dendrogram of figure 2.2.9. From the analysis it is evident that two main clusters are observed at a relative distance of 10. One cluster comprises the group of very high nitrogen gases, whereas all the other gases are collected in the second cluster. When considered at a relative distance of 3, 8 clusters emerge. From these clusters the statistical data are summarised in table 2.2.11.

**Table 2.2.11**

cluster 1	n=454	C <sub>1</sub>	C <sub>2</sub>	C <sub>3</sub>	C <sub>4</sub>	C <sub>5</sub>	C <sub>6</sub>	C <sub>2</sub> -C <sub>6</sub>	CO <sub>2</sub>	N <sub>2</sub>	H <sub>2</sub> S
min	.	83.43	0.00	0.00	0.00	0.00	0.00	0.00	0.00	0.00	0.00
max		99.62	11.53	3.36	2.40	4.00	4.60	13.60	7.81	10.40	2.90
mean		91.16	3.26	0.72	0.30	0.11	0.10	4.49	1.54	2.63	0.03
sd		2.94	1.71	0.57	0.28	0.23	0.34	2.59	1.70	1.78	0.19
cluster 2	n=6										
min		9.27	0.02	0.00	0.00	0.00	0.00	0.02	42.18	2.25	0.00
max		50.46	4.22	1.34	0.50	0.15	0.04	6.25	78.75	10.96	5.05
mean		31.27	0.89	0.27	0.11	0.04	0.02	1.33	61.85	4.17	1.32
sd		17.10	1.64	0.53	0.20	0.06	0.02	2.44	17.67	3.43	1.98
cluster 3	n=27										
min		61.92	0.24	0.00	0.00	0.00	0.00	0.26	0.03	18.84	0.00
max		71.69	9.08	4.34	1.91	0.83	0.35	15.52	3.22	33.58	2.80
mean		68.24	1.60	0.37	0.16	0.05	0.02	2.21	0.67	28.65	0.10
sd		2.63	1.97	0.99	0.48	0.17	0.07	3.60	1.00	3.33	0.54
cluster 4	n=90										
min		70.03	0.03	0.00	0.00	0.00	0.00	0.03	0.00	12.39	0.00
max		84.43	5.06	1.15	0.44	0.17	0.25	6.71	8.07	25.60	3.20
mean		79.34	1.39	0.18	0.06	0.02	0.02	1.66	1.04	17.80	0.09
sd		3.01	1.11	0.26	0.09	0.03	0.04	1.47	1.72	2.86	0.44
cluster 5	n=201										
min		67.91	0.14	0.00	0.00	0.00	0.00	0.15	0.00	0.00	0.00
max		90.91	11.45	7.95	5.90	1.90	10.45	28.72	5.25	13.45	0.60
mean		83.93	4.28	1.41	0.61	0.20	0.25	6.76	1.07	8.04	0.01
sd		3.74	2.45	1.54	0.86	0.30	0.99	5.07	0.96	3.23	0.05
cluster 6	n=72										
min		60.14	0.00	0.00	0.00	0.00	0.00	0.00	5.11	1.42	0.00
max		84.20	6.27	3.08	1.59	0.81	0.41	12.16	33.10	14.40	26.90
mean		76.98	1.03	0.22	0.12	0.04	0.03	1.44	11.94	4.44	5.20
sd		6.21	1.52	0.50	0.31	0.13	0.07	2.40	5.94	2.25	5.76

cluster 7	n=42										
min		23.10	0.00	0.00	0.00	0.00	0.00	0.00	6.43	0.00	
max		63.40	9.64	6.63	4.43	4.27	3.30	28.27	11.04	56.32	38.00
mean		50.70	1.43	0.37	0.21	0.13	0.09	2.22	1.23	43.90	1.13
sd		7.42	1.52	1.02	0.68	0.66	0.51	4.27	2.92	8.94	6.01
cluster 8	n=42										
min		0.01	0.00	0.00	0.00	0.00	0.00	0.00	59.73	0.00	
max		38.80	4.90	2.40	1.29	0.55	0.23	8.57	20.87	97.60	2.57
mean		25.90	0.84	0.23	0.12	0.04	0.02	1.25	1.36	71.33	0.10
sd		9.12	1.02	0.51	0.27	0.11	0.04	1.91	4.31	8.80	0.43

In addition, for these clusters the average calorific values and densities have been calculated. The results are summarised in table 2.2.12

**Table 2.2.12**

		density	calorific value
cluster 1 n=454	min	0.51	34.40
	max	0.75	51.18
	mean	0.61	41.03
	sd	0.03	2.27
cluster 2 n=6	min	0.92	3.89
	max	1.32	23.39
	mean	1.14	13.97
	sd	0.18	7.94
cluster 3 n=27	min	0.62	26.23
	max	0.80	38.46
	mean	0.68	29.49
	sd	0.04	2.74
cluster 4 n=90	min	0.57	29.14
	max	0.71	37.01
	mean	0.63	33.58
	sd	0.03	1.80
cluster 5 n=201	min	0.55	34.81
	max	0.96	63.75
	mean	0.64	40.49
	sd	0.07	4.14
cluster 6 n=72	min	0.62	25.21
	max	0.90	42.86
	mean	0.68	33.14
	sd	0.06	3.38
cluster 7 n=41	min	0.67	9.26
	max	1.00	26.41
	mean	0.75	22.06
	sd	0.05	3.04
cluster 8 n=16	min	0.75	1.28
	max	0.96	17.23
	mean	0.85	13.21
	sd	0.06	4.30

The clusters are all distinctly different. Each group will be shortly described hereafter.

**Cluster 1** Very rich methane gas

With 454 samples assigned to this cluster, cluster 1 comprises the most frequent type of gas. The gases of this cluster are characterised by a very high methane content, more than 90% on average, and ranging from 83 to 100%. The gases contain less C<sub>2+</sub> components as compared to cluster 5. The nitrogen content is low, 2.63% on average. The CO<sub>2</sub> content is 1.54% on average but H<sub>2</sub>S is virtually absent.

**Cluster 2** Extremely sour CO<sub>2</sub> gas

Cluster 2 is a extremely sour gas characterised by a dominance of more than 60% CO<sub>2</sub> and a high content of H<sub>2</sub>S of 1.32% at average. The nitrogen content is also very low. The average methane content is slightly more than 30%.

**Cluster 3** Medium rich nitrogen, rich methane, sweet gas

This cluster is a dry, sweet gas characterised by the concurrence of nitrogen with an average of 29% and methane with an average of 68%.

**Cluster 4** Medium rich nitrogen, rich methane, sour gas

This cluster is closely related to cluster 3. It shows at average a somewhat higher methane content, and a lower nitrogen content. The average abundance of CO<sub>2</sub> is above 1%.

**Cluster 5.** Rich methane, poor nitrogen, wet gas. This cluster is characterised by a high methane content, at average about 84% and a high C<sub>2</sub>-C<sub>6</sub> proportion, at average more than 6%.

**Cluster 6** Extremely sour H<sub>2</sub>S gas

This cluster is mainly characterised by the abundance of 5% of H<sub>2</sub>S and high percentages of CO<sub>2</sub>, up to 12% on average. Besides, the gas is rich in methane.

**Cluster 7** Extremely sour nitrogen rich gas

This cluster is characterised by more than 1% H<sub>2</sub>S on average, and high nitrogen contents, of more than 40% on average.

**Cluster 8** Very rich nitrogen gas

This cluster is mostly characterised by the dominance of nitrogen, at average more than 70%.

The clusters are also distinctly different with respect to density and calorific value in the table below the classification of gases, according to the previously mentioned classification schedules is shown in table 2.2.13

**Table 2.2.13**

			cluster							
			1	2	3	4	5	6	7	8
density	very low	< 55								
	low	> 55	x			x	x			
	high	> 65			x			x	x	
	very high	> 75		x						x
calorific value	very low	< 30		x	x				x	x
	low	> 30				x		x		
	high	> 38	x				x			
	very high	> 44								

As can be seen from this table there are several clusters with similar density and calorific value ranges, however, from the compositional data it can be seen that the compositions are entirely different. For example cluster 1 and 5 fall into the same categories of density and calorific value. However, from the compositions it can be seen that they are different with respect to nitrogen content, C<sub>2</sub>-C<sub>6</sub>, content en methane content. Similarly cluster 2 and 8 fall in the same density and calorific

value category. Cluster 2, however is dominated by carbon dioxide, and cluster 8 by nitrogen. And, finally, cluster 3 and cluster 7 fall in the same categories. Cluster 3 represents a sweet gas however, while cluster 7 is a sour gas.

The classification scheme for gases proposed here is straightforward, based on numerical data and it fits to boundaries within the European gas database. Furthermore, it is independent of market, infrastructure and economical considerations.

## 2.3 Condensate analysis

Condensates from over 100 wells were analysed by GC-MS to gain additional information about the origin of the hydrocarbons in various gas fields. The composition of the condensates varied from light hydrocarbons (C<sub>n</sub><20) to that of crude oils. Based on triterpane and sterane biomarkers which were present in about half the samples, interpretation could be made with respect to type and maturity of source rock for the condensates. A few gas fields in Mesozoic reservoirs have been sourced from moderately mature source rocks as indicated by the isotopes of gaseous hydrocarbons and the biomarker distribution of condensates. Thermal cracking cannot explain the occurrence of such gas accumulations, rather segregation of the gaseous hydrocarbons took place during secondary migration.

Hydrocarbon gases in gas fields may be either biogenic (bacterial) or thermogenic in origin. The two types of gases can easily be discriminated using stable isotopic analyses, biogenic gas being much more depleted in the heavy <sup>13</sup>C isotope, δ<sup>13</sup>C ranging from -60 to -100 ‰, compared to the thermogenic gases. All commercial gas fields described in this work contain thermogenic gases which in most cases were derived from highly mature source rocks, the gas being dry with a relatively heavy isotopic signature. The Gas Atlas Project also covers gas/condensate fields where different amounts of condensate are produced along with gas. Assuming that the formation of gas fields are due to thermal cracking of higher hydrocarbons either in the source rock or in the reservoir one may anticipate that condensates contain only lighter hydrocarbons, the C<sub>n</sub> range being dependent on the degree of thermal cracking. This is the case for many gas fields, although in some gas fields the chemical composition of the condensates is similar to that of a crude oil.

In some condensates, thermal cracking had clearly affected the biomarker distribution, but in most cases the biomarker distribution showed little or no effect of thermal cracking. The information gained from the biomarkers concerning type of source rock and thermal maturity was particularly useful for some gas reservoirs in Mesozoic rocks, which contain isotopically light gases. One example is the Tyra gas field in the Danish North Sea. The isotopic composition of the gases and the maturity indicators of the condensate both point to a moderately mature source rock for the gaseous and the liquid hydrocarbons.

Comparison of gas isotope data and C<sub>29</sub> sterane maturity indicators

Name	type	δ <sup>13</sup> C <sub>1</sub> (‰)	δ <sup>13</sup> C <sub>2</sub> (‰)	δ <sup>13</sup> C <sub>3</sub> (‰)	20S/(20S+20R) C <sub>29</sub>
Tyra	Gas/cond.	-46.6	-32.1	-28.6	0.29
Dan	Oil	-47.8	-31.0	-25.0	0.27

Furthermore, the hydrocarbons in the Dan oil field, 30 km south of Tyra field, are fairly similar to Tyra with respect to the isotopic composition of the gases and biomarker distribution in the liquid hydrocarbons. Thus, formation of a gas field like the Tyra field is most likely due to segregation of a gas phase during secondary migration, although the mechanism responsible for this is not fully understood. Only one out of seven Danish gas fields contains a light hydrocarbon condensate all; other fields have condensates which were generated from moderately mature to mature source rocks, the condensates showing no evidence of thermal cracking.

Comparison of biomarker distribution and gas composition including isotopic data in other areas is underway. The purpose of this study is to see if data indicate the same source for the gaseous and the liquid hydrocarbons in a given gas reservoir. Whether or not this is the case, information may be obtained which will allow interpretation of the migration route of the gas and thereby help to find the source of the gas. The biomarker data not only provide information on maturity of the source rock, but

can also provide information about the depositional environment for the source rock. Examples of the following types of source rocks were indicated by the biomarkers in the condensates: Carbonates; siliciclastics, evaporites and coals.

No attempt was made to map the condensate data which do not represent a systematic study as analyses were performed on the samples readily available, mostly Dutch and Danish condensates, in order to check the usefulness of condensate biomarker analyses. The results obtained during the Gas Atlas Project show that very useful information can be gained from the analyses of condensates. Thus, biomarker analyses are recommended for the condensates of gas/condensate fields.

### 3. GEOLOGY

Within NW Europe a substantial number of hydrocarbon plays have been discovered. As backdrop information to the geochemical maps, those plays have been selected which have controlled HC formation or entrapment over a substantial part of NW Europe. Distribution, facies and/or isopach maps have been constructed of most of the important source rocks (Dinantian, Namurian, Westphalian, Posidonia and Upper Jurassic) and reservoir rocks (Dinantian, Namurian, Westphalian, Rotliegend, Buntsandstein). Depth and sub-crop maps of the top of the Pre-Permian surface have been included as well as a maturity map of the top of the Pre-Permian. Additional maps displaying salt structures and igneous intrusives complete the atlas.

The maps have been constructed by the various geological surveys, and have been approved by them. Responsibility for national sectors of the maps therefore lies with the geological surveys.

Most of the Palaeozoic and Triassic reservoirs and source rocks are mapped. Only the pre-Devonian source rocks (Cambrian Alum Shale) and reservoir rocks (Pre-Cambrian to Silurian sandstones and carbonates), which sourced hydrocarbons in northern Poland and the adjacent Baltic area, have been excluded, since they are only significant to the north of the Caledonian Front. The major part of NW Europe lies within the Caledonian deformation area.

Mesozoic and Cainozoic reservoirs have only a basic coverage. These reservoirs display a great variability in time and space, and are often strongly controlled by processes like rifting. Furthermore, these reservoirs are only of importance in the western part of the study area, as there are no Mesozoic reservoirs in the eastern part of NW Europe. Mesozoic reservoirs not dealt with in the maps comprise the Keuper and Jurassic sandstones in NW Germany, the North Sea area, Lower Cretaceous sandstones, mainly in NW Germany and The Netherlands, Danian Chalk in the Danish Central North Sea and several Tertiary sandstones in The Netherlands.

#### 3.1 Dinantian (Tournaisian and Viséan), distribution and facies

##### Relevance to the European Gas Atlas

The mapped unit, includes in the Central European Basin, the oldest known gas generating source rocks of economic importance and shows their regional distribution. The unit includes minor reservoir horizons.

##### Data base

The map relies on subsurface well and mining data as well as surface outcrop studies. Seismic information on the extent of the platform carbonates are scarce. Most information is available from areas near the northern and southern margins of the basin (i.e. London-Brabant Massif, Mid North Sea High). In the area between (northwestern Germany, Southern North Sea), the top of the Dinantian is usually deeply buried and data are scarce or absent.

Modern key literature with additional references: (GB): CAMERON (1993), CAMERON et al. (1992), LEEDER (1992); (BE): PAPROTH et al. (1983a); (NL): ADRICHEM BOOGAERT, van & KOUWE (1993-1996); (DK): MICHELSEN (1971); (DE): DALLMEYER, FRANKE & WEBER (eds.) (1995), WALTER (1992), FRANKE, D. (1990); (PL): ZDANOWSKI & ZAKOWA (eds.) (1995).

##### Distribution

The distribution of Dinantian rocks in the Central European Basin is limited to the north by the Mid North Sea--Ringkøbing-Fyn High, and to the east by the western and southwestern margin of the East European Platform, in the territories of Lithuania, Poland and Ukraine. To the south, their extent is restricted by the Central European Suture, the southern margin of the Rhenohercynian ocean, which can be traced from the western boundary of the Moravian zone (main Moldanubian thrust zone) to the northern boundaries of the Fore-Sudetic Block (Odra Fault Zone), the Mid German Crystalline Zone (Northern Phyllite zone) and to the American Massif (Lizard Point thrust). The dominant feature within the depositional area is the London-Brabant- St. George's High, which was partly flooded and covered by platform limestones, which later were partly eroded and karstified.

##### Facies realms

Five main facies realms have been identified:

**1. The northern marginal facies** (Farne Gp., Elleboog Fm., Gozd Mb., Drzewiany Fm.) occurs along the southern fringe of the Devonian Old Red Continent (Mid North Sea-- Ringkøbing-Fyn High, East European Platform in Pomerania and the Lublin Basin). Littoral and terrestrial-fluviatile deposits of braided rivers and deltas prevail in the lower part, deltaic to shallow marine deposits in the upper part (Yoredale 'facies').

**2. The carbonate platform facies** (Carboniferous Limestone Gp, Zeeland Fm., Kohlenkalk, Kurowo Lmst. Fm.) extends north of the London-Brabant Massif in central GB, in Belgium (Campine) and the Netherlands, in the southern Anglo-Dutch Basin, in Schleswig-Holstein and northern Lower Saxony, southern Denmark (Falster), Rügen and NW-Pomerania as well as in Upper Silesia, the Holy Cross Mountains and the Malopolska Massif, Poland. South of the London-Brabant Massif it is known from south and southwest England, from Belgium (Namur and Dinant Basin) and from the Aachen region. It is represented by thick, often oolitic-oncolithic limestones with subordinate intercalations of claystones, silt- and sandstones, anhydrites and volcanics.

**3. Basinal facies within the carbonate platform.** Basins within the carbonate platform are known only from central England (Northumberland Basin, Stainmore Basin, Cleveland Basin, Widmerpool Basin and others). This facies may well exist in the central Anglo-Dutch Basin, the German part of the North Sea, northwestern Germany and in the Hiddensee Basin in the southern Baltic, but its existence has not been proved by drilling. Sediments are predominantly clastic delta-, pro-delta and basin deposits up to 6000 m thick.

**4. The facies of the "starved basin" and its flysch infill ("Culm"-Facies)** occurs in southwest England, in the eastern Rheinische Schiefergebirge, the Harz Mountains, in Wielkopolska, in the Holy Cross Mountains and west of the Upper Silesian Depression. It is represented by black shales, siliceous carbonates, siliceous shales and dark mudstones. The thickness can reach 600 m, but is generally much less. Gradually during Tournaisian and Viséan times, the starved basin was filled in from the SE and S in Germany, from the SW and W in Poland by flysch turbidity currents ("Culm"-greywackes), which reached a line from the East Sauerland anticline in the eastern Rheinische Schiefergebirge to the northwestern tip of the Harz Mountains and beyond to the Berlin area.

**5. The facies realm of olistostromes and gliding nappes** occurs in the eastern Rheinische Schiefergebirge (Giessen), in the Hessen depression (Werra-Grauwackengebirge) the southeastern Harz Mountains and the Fore-Sudetic Monocline (= Wielkopolska externides). In the SE and S, the distribution area is bounded by the Northern Phyllite Zone and its equivalents. The olistostromes consist of an argillaceous matrix with limestone and shale olistoliths (partly of Lower Palaeozoic age). The gliding nappes comprise Upper Devonian greywackes (Giessen, South Harz and Selke nappes).

#### **Reservoir rocks:**

Potentially productive reservoir rocks of Dinantian age been discovered only in Britain and Poland. Fluviatile and deltaic sandstones along the northern fringe of the basin (Fell Sandstone Fm., Scremerston Fm. and other deltaic deposits) may have potential productivity. In Poland the presence of reservoir rocks is proven by the occurrence of small oil/gas fields in Pomerania (Drzewiany Sandstone Fm. of Ivorian-Brigantian age and Kurowo Oolite Fm. of Ivorian age) as well as in the basement of the Carpathian foredeep (Lower Carboniferous Limestone). Such deeply buried sandstones are normally tight due to secondary cementation. However, secondary porosity and permeability has been observed in carbonates of Dinantian and Upper Devonian age, owing to pre-Namurian karstification in the Belgian Campine area, and to secondary dolomitization in the Rügen-Hiddensee realm of the southern Baltic Sea.

#### **Source rocks**

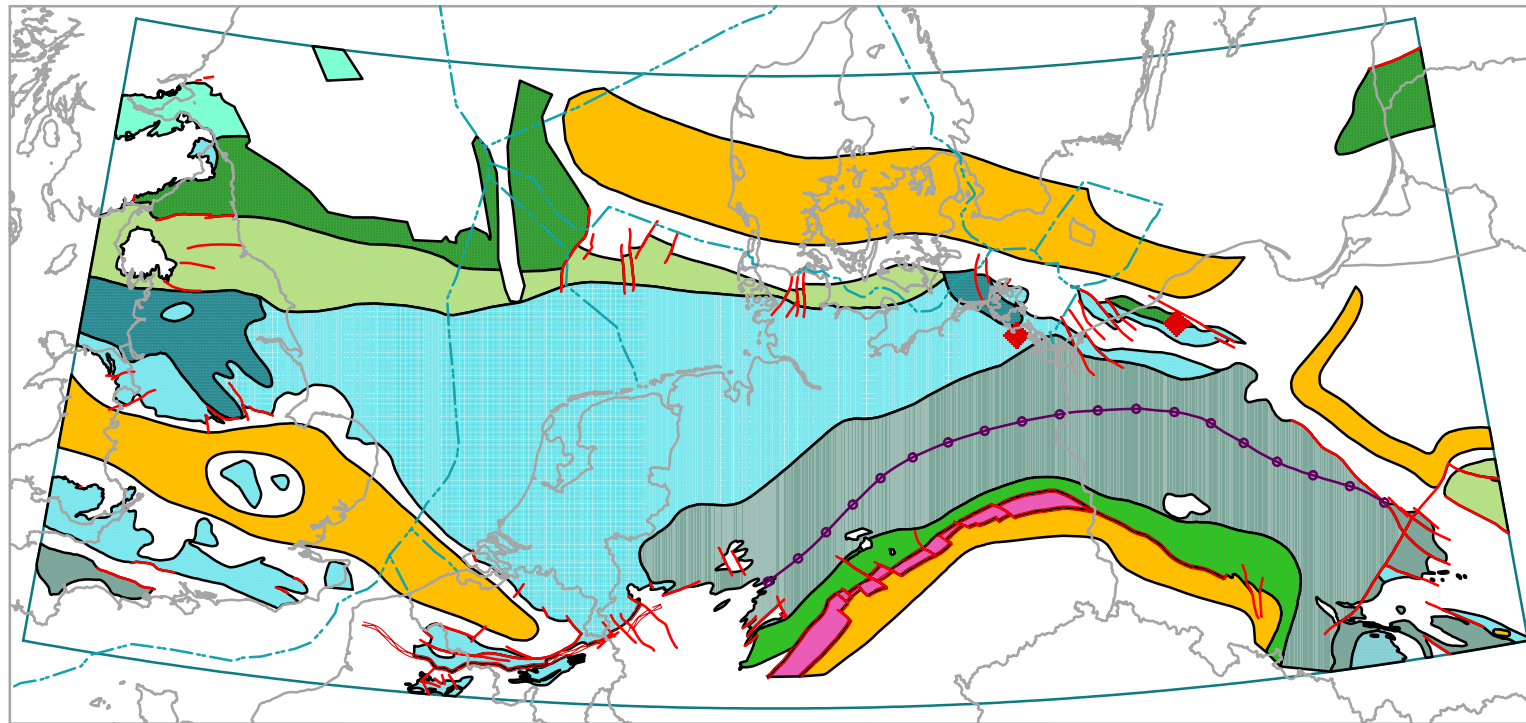
(see table 3.1)

Epoch	Stage	Southern North Sea, Central North Sea		Netherlands, southern offshore, onshore	Belgium Campine Basin	Germany, Rheinisch. Schiefergeb., Harz	Poland W Pomerania	Poland Holy Cross M.	Poland Malopolska SW of Krakow	Poland Wielkopolska	
Visean	Brigantian	Lower Bowland Shale (basinal facies) type I-II, ca. 7% TOC	Lower Yoredale facies (shallow marine/deltaic) type III, 0.89-1.87% TOC			distal flysch, dark shales and turbidites, dispersed organic matter type III, ca. <0.5- >2% TOC		Lechówek Fm. shales type I-II		distal flysch	
	Asbian	Oil Shale Group (lacustrine) type I, ca. 50% TOC	Scremerston Coal Group, (deltaic), type III, 1-3.8% TOC		Kulm-Tonschiefer type II, 0.5-5% TOC	Kieselige Übergangsschichten type I-II, <0.5->3% TOC					Zareby Fm. claystones, silicious shales alum shales type I-II
	Holkerian										
	Arundian				bituminous Carboniferous Limestone (Marbre noir etc.) (platform carbonates) type II, 6.2-10.7% TOC	Kulm-Kieselkalke type I-II, 0.5-12% TOC					
	Chadian					Kulm-Kieselschiefer type I-II, <0.5-12% TOC					
	Tournaisian	Ivorian					Untere Alaunschiefer type I, <0.5-12% TOC	Grzybowo Shale Mb., claystones type II 1.7% TOC			
Hastarian					Sch. Pont d'Arcole type I-II, 0.3-1.5% TOC		Trzebiechowo Mb., claystones type II, 1.2% TOC				

**Table 3.1: Dinantian source rocks in the Central European Basin** (light grey = marine, dark grey = non-marine, white = no known source rock)



# Dinantian -- Distribution and facies



- Offshore boundaries
- Topographic overview
- Volcanic centre
- Structural features
  - major fault
  - overthrust
  - N limit of Dinantian flysch
- Dinantian Facies
  - paleohigh
  - non-marine (lacustrine)
  - littoral / fluvial / deltaic
  - shallow marine / deltaic
  - carb.platform / sh. marine
  - carbonate platform / basin
  - intra-platform basin
  - starved basin, partly flysch
  - olisthostromes and nappes
  - Mid-European Suture
  - Study area outline

0 110 220 330 440 550 660 Kilometers



Projection : Lambert Conformal Conic  
 Spheroid : Bessel, 1841  
 Standard parallels : 51 N and 54 N  
 Central meridian : 9 E  
 Latitude of projection origin : 48 N  
 False easting : 7,500,000 m  
 False northing : 0 m

## 3.2 Namurian (A-B, Pendleian--Alportian/Marsdenian), distribution and facies

The Namurian can be broadly subdivided into a lower, predominantly marine part (displayed on the map) and an upper, predominantly paralic to deltaic part, not displayed. The boundary between the two units is diachronous and varies from basin to basin.

### Relevance to the European Gas Atlas

In the Central European Basin important marine and non-marine source rock horizons occur in the Namurian, which source both oil and gas fields in the region. Reservoir rocks have locally been encountered in the Southern North Sea area.

### Data base

The map relies on subsurface well data, mining information and surface outcrop studies. In the western part, most information is available from the northern and southern margins of the basin (i.e. Mid North Sea High, London-Brabant Massif). In the area in-between (northwest Germany, Southern North Sea), the Namurian is usually deeply buried and data are scarce or absent. Modern key literature with additional references: (GB): CAMERON (1993), CAMERON et al. (1992); (BE): PAPROTH et al. (1983a), LANGENAEKER & DUSAR (1992); (NL): ADRICHEM BOOGAERT, van & KOUWE (1993-1996); (DE): DALLMEYER, FRANKE & WEBER (eds.) (1995), WALTER (1992), FRANKE, D. (1990); (PL): ZDANOWSKI & ZAKOWA (eds.) (1995) and other published and unpublished reports.

### Distribution

The distribution of Namurian rocks in the Central European basin is limited in the north by the Mid North Sea--Ringkøbing-Fyn High and the southwestern margin of the East European Platform. In the south, the extent of Namurian rocks is limited by the Central European Suture (see text for Dinantian map). The present day distribution of the Namurian is more restricted than that of the Dinantian, due to pre-Westphalian and pre-Permian erosion. The dominant feature within the depositional area is the London-Brabant--St. George's High, which was successively flooded during Namurian A. Namurian sediments partly covered karstified Dinantian platform limestones.

### Facies domains in the Lower Namurian

#### 1. Deltaic and paralic facies

This facies is limited to Scotland and the Moray Firth area and in the intra-Sudetic Coal Basin in Poland.

#### 2. Shallow-marine/deltaic facies

The shallow marine-deltaic Yoredale facies (interbedded platform limestones and delta- to prodelta deposits) occupies a vast area south of the Mid North Sea High--Ringkøbing-Fyn High and to a lesser extent along the northeastern border of the London-Brabant--St. George's High and along the SW-border of the East European Platform (Lublin Trough, Terebin Fm.). The sequence is Pendleian to Arnsbergian in age.

In northern Schleswig-Holstein, southern Jutland, Rügen and western Pomerania the Namurian has been eroded prior to the Westphalian. In Vorpommern, the paralic Namurian began with the Alportian transgression.

#### 3. Bituminous shale facies (Pendleian to Alportian)

In central Britain, the Southern North Sea, the Campine area, and probably most of the Netherlands and in northwest Germany bituminous shales (Upper Bowland Shale Fm., Eden Shales and equivalents (GB), Geverik Mb. of the Epen Fm. (NL), Chokier Fm. (BE) cover the Dinantian carbonate platform as well as the intra-platform basins (see also 1. Dinantian). It is inferred, that this deep basin may have connections to the "starved basin" adjacent to the Northern Phyllite zone. Pro-delta and delta slope sedimentation of the Millstone Grit Fm. commenced at the northern rim of the Anglo-Dutch Basin and in Central England in the Pendleian (basal Namurian A), progressively filling the Bowland Shale Basin with pro-delta deposits, fan lobes, and lower and upper delta slope sediments of northern provenance. From the London-Brabant Massif in the south, delta and pro-delta sediments were deposited from the Kinderscoutian onwards in the Campine area and the southern Anglo-Dutch Basin. In Poland, mudstone deposits of this type occur in Pomerania and in Central Poland.

#### **4. "Starved basin"-facies with turbiditic infill**

In Germany, northwest of the Rheinische Schiefergebirge (Rhenish Massif) and the Harz Mountains, as well as in Wielkopolska and in the Upper Silesian depression, a starved basin existed, comparable with the Dinantian starved basin, containing black shales ("Hangende Alaunschiefer"), stretching up to Southern Mecklenburg and Szczecin in the North. Flysch turbidites infilled this starved basin progressively from the south and east. In the Upper Silesian Depression the marine environment with flysch sedimentation continued to the top of the basal Namurian A (Malinowice = Zalas Fm.)

#### **Facies domains in the paralic to deltaic Namurian (Namurian A to C; not displayed)**

In the Lublin Basin paralic sedimentation with intercalated coal seams commenced in the higher part of the Lower Namurian (Deblin Fm.).

Paralic sedimentation began in the Lower Namurian A with coal-bearing sediments (Petrkovice, Hrusov, Jaklovec and Poruba Beds), containing several marine incursions. Subsequently from the beginning of the Namurian B (Zarbrze and Ruda Beds) onwards, deltaic to fluvial molasse conditions prevailed.

In Wielkopolska and eastern Germany there is an hiatus between the marine Lower Namurian and the fluvial Westphalian D-Stephanian.

In Vorpommern deltaic and fluvial sedimentation started after a break in the Alportian. Coal seams occur in the Kinderscoutian and Yeadonian. The Namurian flysch fans did not prograde to the northern fringe of the basin.

In the Campine area, southern Netherlands and adjacent parts of West and East Germany, marine sedimentation lasted until the Late Kinderscoutian to higher Marsdenian (Early to Late Namurian B). Numerous marine incursions indicate an open marine environment towards the west.

In the Anglo-Dutch Basin, coal-bearing, paralic, delta plain deposits began with the higher Marsdenian (Namurian B) in the south, younging towards the north (Yeadonian; Namurian C) with braided river sediments and shallow lagoons and swamps (coal seams).

South and east of the London-Brabant-St. George High (Aachen, Namur Basin) no Namurian Flysch is developed. Already in the upper parts of the Namurian A fluvial/terrestrial deposits (Walhorn and Lower Stolberg beds of Chokerian and Alportian age) cover the thin marine claystones of the lowermost Namurian.

#### **Reservoir rocks**

Economically productive reservoir rocks of Namurian age occur in onshore GB and the Southern North Sea (Millstone Grit Fm.). Other fluvial and deltaic sandstones along the northern rim of the Anglo-Dutch Basin also have potential productivity. Deeply buried sandstones of pro-delta and flysch type are normally tight due to secondary cementation. This is also true for the fluvial deposits of meandering or braided rivers of Namurian age although fracture permeability may occur.

Coal seams of Late Namurian age may also be regarded as potential reservoir horizons for coal bed methane production.

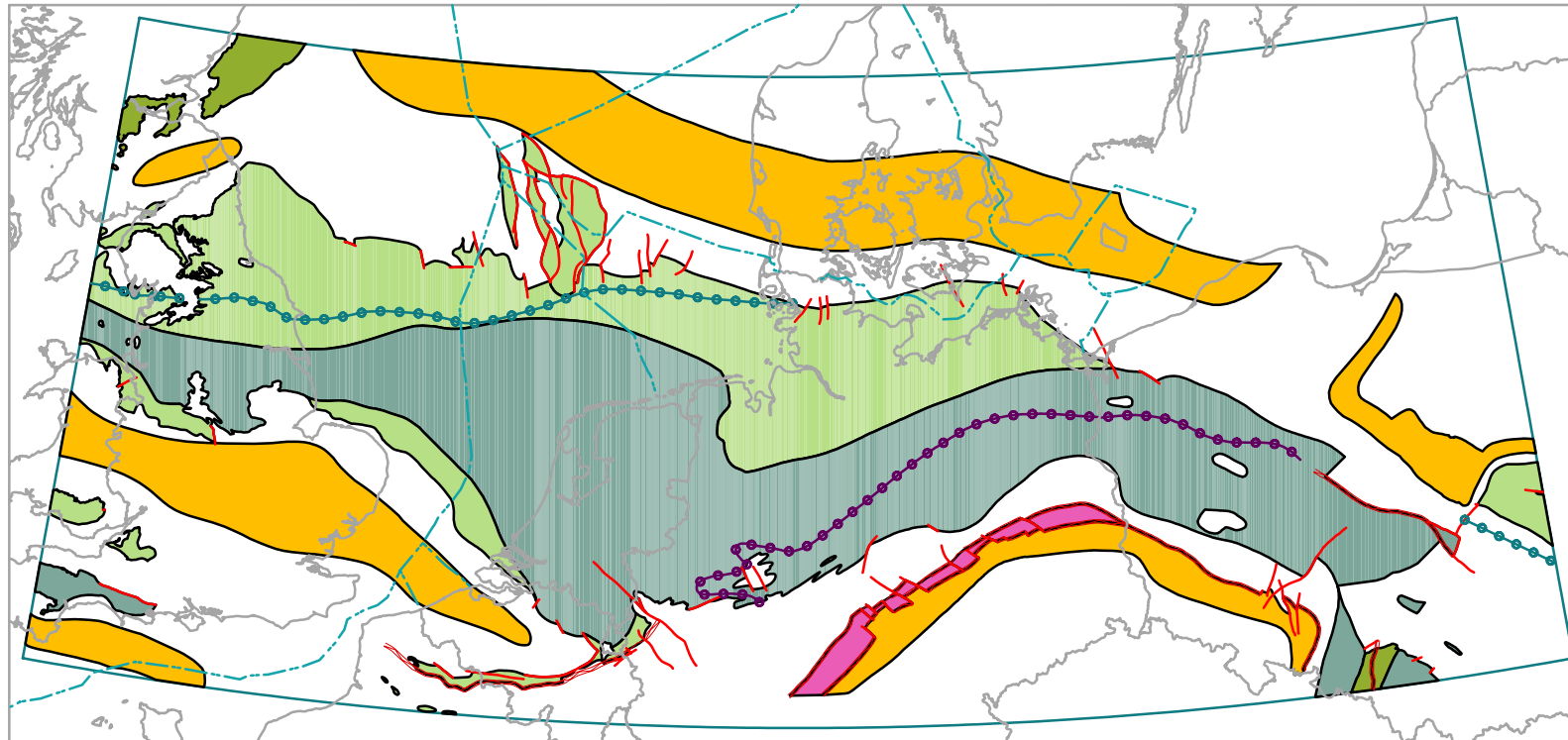
#### **Source rocks**

(see table 3.2)

Continental stages	Marine stages	GB onshore, Southern North Sea	GB/NL offshore, Central North Sea	Belgium, Campine Basin	Netherlands, onshore, southern offshore	Germany, Aachen district	Germany, Ruhr area	Germany, NW and NE,	Poland, Wielkopolska	Poland Upper Silesian depression	Poland, Lublin area
Namurian C	Yeadonian	Millstone Grit Fm (delta plain), type III,	Millstone Grit Fm (delta plain), type III,	Ransart Mb. type III (delta plain)	Baarlo Fm. (coastal plain) type III	Lower	Sprockhövel beds (delta plain) type III, 1.8-80% TOC	Namurian C (delta plain) type III		Ruda beds alluvial plain type III	Lower Korczmiska series (paralic) sandstone + mudstone type III 1.9-2.8% coal
	Namurian B	Marsdenian		0.5-5.4% TOC	Marsdenian-Kinderscoutian (delta plain), type III			Stolberg beds, (delta plain), type III		Namurian A-B, dispersed organic matter in distal Flysch <0.5->1% TOC type III	
Namurian A		Kinderscoutian		0.5-5.4% TOC							
	Alportian	Upper Bowland "hot shales", Edale shales and equivalents	Upper	Chokier "hot shales" type I and II, 0.3-1.2% TOC	Geverik Mb. (euxinic marine clays), type I + II				dispersed organic matter	Poruba beds (paralic) Jaklovec beds (paralic) Hrušov beds (paralic)	Bug Mbr. (paralic)
	Chokerian										Petrkovice beds (paralic)
	Arnsbergian	type I and II 2 - 60% TOC	Yoredale Fm. (shallow-marine/deltaic) type III				Hangende Alaunschiefer type I + II, 0.8-1.4% TOC	Hangende Alaunschiefer, type I + II, 0.8-1.4% TOC	in distal Flysch	type III 3.3% coal	Korczmin Mbr. (Yoredale facies, shallow marine/deltaic) type III
Pendleian								Namurian black shales type I + II	Zalas beds dispersed org. matter in Flysch		

**Table 3.2: Potential Namurian source rocks in the Central European Basin**  
(with type of kerogen, average TOC content and coal in % of total thickness)  
(light grey = marine, dark grey = non-marine depositional environment, white = no known source rock)

# Namurian A-B -- Distribution and facies



- Offshore boundaries
- Topographic overview
- Structural features
- major fault
- overthrust
- S limit Yoredale
- N limit Namurian A
- Namurian Facies
- paleohigh
- paralic
- shallow marine / deltaic
- starved basin, partly flysch
- phyllite zone
- Mid-European Suture
- Study area outline

0 110 220 330 440 550 660 Kilometers



Projection : Lambert Conformal Conic  
 Spheroid : Bessel, 1841  
 Standard parallels : 51 N and 54 N  
 Central meridian : 9 E  
 Latitude of projection origin : 48 N  
 False easting : 7,500,000 m  
 False northing : 0 m

### 3.3 Westphalian, distribution and facies

#### Relevance to the European Gas Atlas

The Westphalian coal seams are the most important source rocks for natural gas in Northern and Central Europe. More than 90% of the gas fields in GB, the Netherlands, and Germany found in the Carboniferous, Rotliegend, Zechstein and Buntsandstein reservoirs are sourced from Westphalian coal seams.

#### Data base

The map relies on seismic and well data, mining information as well as outcrop studies. Modern key literature with additional references: (GB): CAMERON (1993), CAMERON et al. (1992); (BE): PAPROTH et al. (1983b), LANGENAEKER & DUSAR (1992); (NL): ADRICHEM BOOGAERT, van & KOUWE (1993-1996), GELUK (1997); (DE): DALLMEYER, FRANKE & WEBER (eds.) (1995), DRODZDEWSKI et al. (1985), DRODZDEWSKI (1992), WALTER (1992), FRANKE, D. (1990), HOTH et al. (1990); (PL): ZDANOWSKI & ZAKOWA (eds.) (1995) and other published and unpublished reports.

#### Distribution

Westphalian beds occupy the inner part of the Central European depression from the Britain to Wielkopolska. The succession reaches a thickness of some 2000 m in the area between Northwest Germany and the British sector of the Southern North Sea. To the north, the basin was limited by the Mid North Sea--Ringkøbing-Fyn High. The southern margin was formed by the northward migrating Variscan Front. Outliers of the basin are known from Pomerania, Central Poland, the Fore-Sudetic Monocline, the Upper Silesian depression and the Lublin Basin. Another outlier is situated south of the London-Brabant--St. George High in the axis of the Namur Basin and below the Midi thrust. Locally also in the Paris Basin some Westphalian rocks occur beneath the Triassic. The southern and southeastern part of the Westphalian basin belongs to the folded Variscan molasse trough. The occurrences in northwestern and northern Germany, the Netherlands and British southern North Sea, Mecklenburg-Vorpommern and the occurrences in Pomerania, Central Poland, Lublin Basin and Upper Silesian Depression are only gently warped and form the Variscan Foreland. Locally in the foreland basin, e.g. in the southern North Sea wrench-tectonics strongly deformed the deposits. Intra-Variscan basins like the Saar-Nahe Basin or the intra-Sudetic basins have not been included in this study

#### Facies development

The lower part of the Westphalian, the Westphalian A and B (Langsetian and Duckmantian) were deposited on a low lying paralic plain, occupied by freshwater swamps and brackish lagoons. Meandering rivers brought channel sands onto the plain, crevasse channel and crevasse splay sands were shed into the interdistributary lagoons. Several marine incursions subdivide the succession into formations correlatable over the whole western part of the studied area. Locally, i. e. in the Ruhr area these marine horizons have reservoir potential. Cyclicity is common. Sand supply to the basin came both from southern and northern sources.

In the Pennine Basin 80 coal seams have been recorded, the amount of coal is estimated at 3-4% of the total thickness of the coal-bearing sequence in the Anglo-Dutch Basin. In the Ruhr Basin in Northwestern Germany > 98 seams are known. They amount to 0.8-1% of the total thickness in the Namurian C, to 2.5-2% in Westphalian A1, 5.5-6% in Westphalian A2, 4.5-5% in Westphalian B1 and 5-6% in Westphalian B2. These values have also been found valid for most of the Southern North Sea and on- and offshore areas of the Netherlands. Towards to the Mid North Sea High, the coal content decreases with the increase of the sand component in the succession.

In the Upper Silesian Depression the coal-bearing Zatlze and Orzesze beds of the Mudstone Series (Westphalian A and Early B) includes up to 5.6% coal and represents an alluvial plain environment in contrast to the Namurian paralic coal-bearing sequences. In the Lublin Basin the Kumów Mbr. (Namurian C to lower Westphalian A), containing 1.9-2.8% coal, still occurred in a paralic environment. The Lublin Fm. (Upper Westphalian A + B) contains up to 8.35% coal of limnic-fluviatile origin.

After the last marine basinwide incursion, the Aegirianum-horizon, (base of Westphalian C, Dorsten Beds, Bolsovian) the basin configuration, as well as the climate, in Western Europe were subject to change. Subsidence was concentrated more in fault-bounded depressions like the Ems Low, West

Netherlands Basin and parts of the Anglo-Dutch Basin. Uplift of the basin margins, in combination with some intra-basinal highs, resulted in a considerable increase in sand input to the basin (Ketch Mb., Dinkel Subgroup, Dorsten Beds, Cracow Sst.). In northwest Germany, the sand percentage increased from 12% in Westphalian B1 to 60% in Westphalian C. The climate, humid/tropical up to the middle part of the Westphalian C, gradually became dryer. Barren red sediments were deposited along the northern flank of the London-Brabant Massif (Brig Fm., Barren Red Group, Strijen Fm.). Reworked older Westphalian sporomorphs occur in the southern Netherlands and elsewhere. Coal seams are still frequent in the Lower Westphalian C (Upper Westoe Coal Fm., Dorsten Beds) but rapidly decrease in number and thickness subsequently. This trend continued into the Westphalian D; primary red beds are frequent, vertisol soils and finally even calcretes become typical features.

In NW-Germany the drainage system direction switched from west to north, the marine inlet to the west closed, the topography became more pronounced, braided rivers prevailed over meandering rivers and the ground water table lowered.

In the Upper Silesian depression the sand-rich Cracow Sandstone (Laziska and Libiaz beds, Westphalian B-D), with an average coal content of 3.3% and topped by the red Kwaczala arkoses of Stephanian age, obviously reflect this change in climate and relief. In the Lublin area only the lower parts of the Magnuszew Fm. (Westphalian C and ?D) contain a few thin coal seams, its upper part is barren. In the Polish gas provinces (Wielkopolska, western Pomerania) and in central Poland the Upper Westphalian to Stephanian rocks (Wolin Fm., Rega Fm.) do not contain coal seams.

In the entire sequence up to the higher parts of Westphalian C, in addition to the coal seams present, dispersed organic matter commonly occurs in the "barren", sandy and argillaceous intercalations and probably exceeds in volume the organic matter concentrated in the seams themselves.

#### **Reservoir rocks**

Potential reservoir rocks are formed by the fluvial sandstones, the percentage of which increases towards the top of the sequence from the Westphalian A (18-34%) and Westphalian B (12-47%) to a level of > 60% in the Westphalian C succession. Sedimentologically, they demonstrate a change from meandering to braided river and sheet flood deposits. Within the study area the sandstones, especially of the Westphalian C and D, have proven reservoir horizons. In the Southern North Sea, sandstones of the Westphalian A-Lower Westphalian B also form good reservoirs. Many such Westphalian gas accumulations produce from fracture permeability in the vicinity of major fault zones, in situations where leaching of cements has occurred below unconformities or early gas saturation subsequently prevented excessive cementation.

Coal seams of Westphalian age may also be regarded as reservoir horizons for coal bed methane.

#### **Source rocks**

(see table 3.3)

International stages	GB North Sea	Netherlands onshore	Belgium, Campine	Germany, Aachen district	Germany, Ruhr Area	Germany, Ibbenbüren	NW-German lowlands	Germany, Vorpommern	Poland, Upper Silesia	Poland, Lublin, Central Poland
Westphalian D						U. Ibbenbüren beds 0.9% coal	Westphalian D 0.2-0.8% coal		Libiaz beds, 3.3% coal	
Westphalian C Bolsovian	Schooner Fm 1-5% coal	Maurits Fm. 5-8% coal Type I + II	Maurage		Lembeck beds, 1-4% coal	L. Ibbenbüren beds 2.2% coal	Westphalian C (I-W) 1.2 - 3% coal	Jasmund beds 0.5-1% coal	Laziska beds, 3.3% coal	Magnuszew beds, very low
					Dorsten beds 2-4% coal		Westphalian C (A-H) 1-4% coal			
Westphalian B Duckmantian	Westoe Coal Fm. 5% coal		Eisden	Merkstein beds	Horst beds, 5-6% coal	U. Alstette beds		Lohme beds 2-5% coal		
Westphalian A Langsettian	Caister Coal Fm. 5% coal	<5% coal	Quaregnon	Alsdorf beds	Essen beds, 4.5-5% coal	L. Alstette beds	Westphalian B ca. 3% coal	Wiek beds 2-5% coal	Orzesze beds 5.6% coal	Lublin Fm. 8.2-8.3% coal
			Floriffoux	Kohlscheid beds	Bochum beds, 5.5-6% coal	Schafberg beds				Zaleze beds, 5.6% coal
Namurian C	Millstone Grit Fm < 1% coal	Baarlo Fm. 1% coal	Ransart	U. Stolberg beds	Witten beds, 2-2.5% coal		Westphalian A 2.8% coal	U. Barth beds 0.01% coal		
			Andenne	L. Stolberg beds	Sprockhövel beds, 0.8-1% coal		Namurian C 0.2-1% coal		Ruda beds, 8.4% coal	1.9-2.% coal

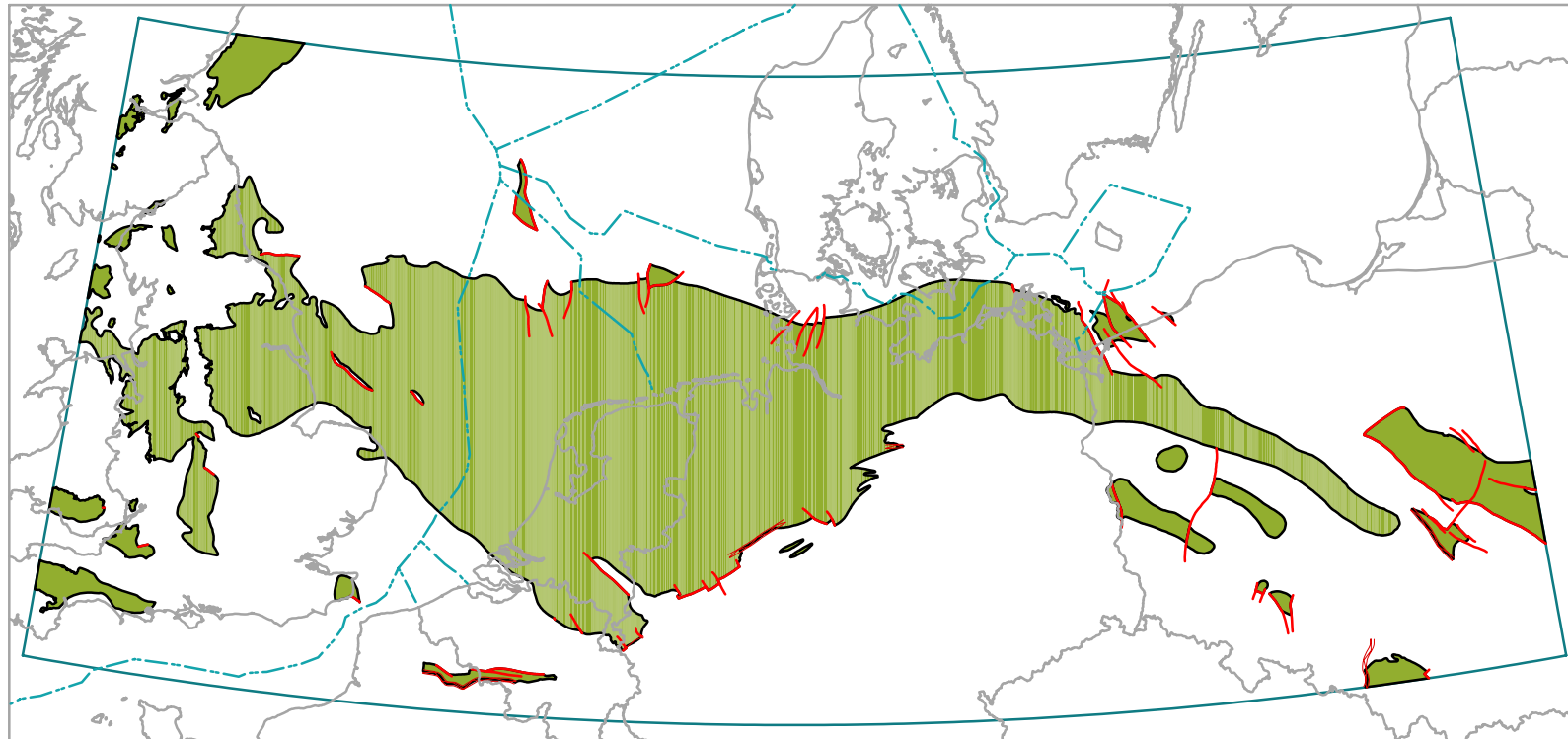
**Table 3.3: Westphalian source rock horizons in the Central European Basin**

(coal in % of total thickness)

(light grey = marine, dark grey = non-marine depositional environment, white = no known source rock)



# Westphalian -- Distribution and facies



- Offshore boundaries
- Topographic overview
- Structural features
- major fault
- overthrust
- Westphalian distribution
- Study area outline

0 110 220 330 440 550 660 Kilometers



Projection : Lambert Conformal Conic  
Spheroid : Bessel, 1841  
Standard parallels : 51 N and 54 N  
Central meridian : 9 E  
Latitude of projection origin : 48 N  
False easting : 7,500,000 m  
False northing : 0 m

### 3.4 Pre-Permian surface, structural contours

#### Relevance to the European Gas Atlas

The present-day depth of the pre-Permian surface represents the sum of all vertical tectonic movements (subsidence and uplift) since the beginning of the Permian (296 Ma Bp.) and have controlled the subsidence and maturation history of pre-Permian source rocks in the basin.

#### Data base

The map is constructed from the present day depth to the base Zechstein (Upper Permian), based mainly on seismics, by adding up the Upper (sedimentary) Rotliegend thickness and estimated total thickness of the Lower (volcanic) Rotliegend. Only major fault zones at the basal Zechstein level have been displayed, the isocontour intervals chosen indicate the degree of generalisation. Modern key literature with additional references: (GB): WHITTAKER (ed.) (1985); (NL): HEYBROEK (1974); (DK) (VEJBÆK & BRITZE (1994); (DE): HOFFMANN (1990), BALDSCHUHN, KOCKEL & FRISCH (ed.) (1996); (PL): POZARYSKI & KARNOWSKI. (1992) and unpublished reports.

#### Main structural features

Two Permian-Mesozoic basins, the Northern and Southern Permian Basins (Upper Permian) can be recognised, separated by the Mid North Sea High--Ringkøbing-Fyn High. In the southern basin the northwest--southeast trending Mid-Polish Trough has no direct prolongation into the North German Trough.

The North German Trough is differentiated into three subsidence centres: from east to west the Havel-Müritz Depression, the West Mecklenburg Depression and the Glückstadt Graben. Other important subsidence centres are the Horn Graben and the so far poorly known Central North Sea Graben.

The generally SW-NW and ESE-WNW trending Central European Basin is crosscut by structural elements trending NNE or NNW: the eastern margin of the Havel-Müritz Depression formed by the Rheinsberg lineament, the Eichsfeld-Altmark ridge, the fault systems bordering the Glückstadt Graben, the Horn Graben and the Central North Sea Graben.

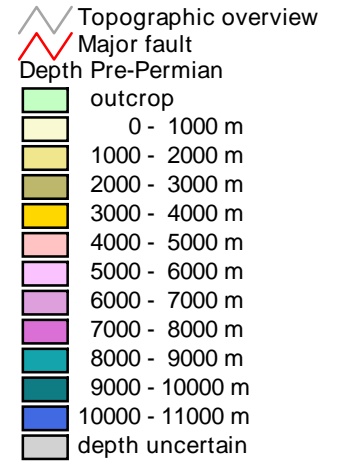
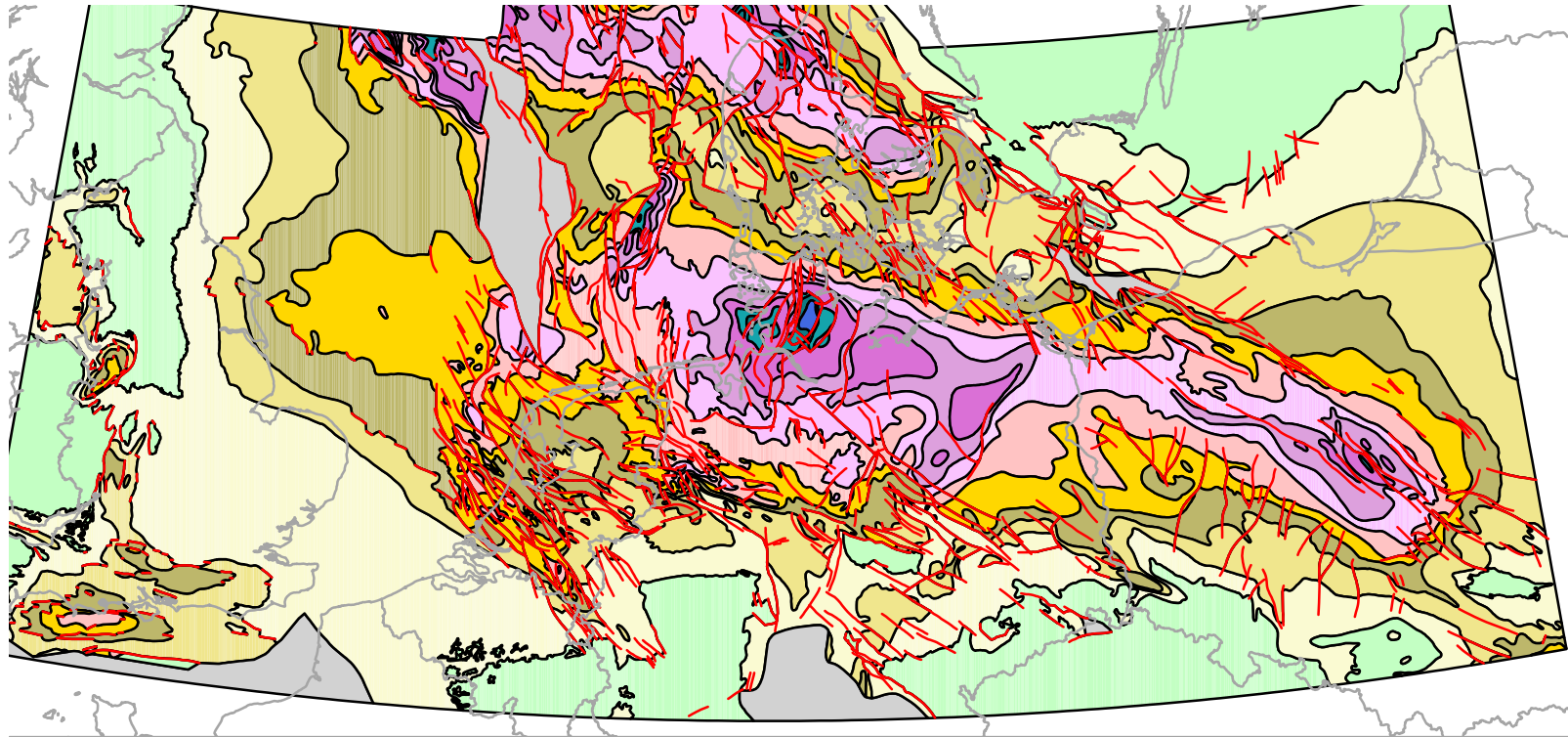
The greatest known present day depths are found in the Glückstadt Graben at > 10.000 m and in the Horn Graben at > 9.000 m. Depths in the Central North Sea Graben are expected to be of similar magnitude or even greater. Maximum depth in the Mid-Polish Trough is about 8.000 m (north of Lodz)

The parts of the basin, which became inverted during the Late Cretaceous do not always show up as present day ridges or horsts due to the differing intensity of the inversion process over the area. However, they are characterised by intense faulting and fragmentation into elongated narrow blocks (Mid-Polish Trough and its prolongation into the Baltic Sea, Glückstadt Graben, Lower Saxony Basin, Central and West Netherlands Basin, Broad Fourteens Basin and others). In some cases, the structural complexity of these basins had to be simplified in view of the scale of this map.

In the western part of the southern North Sea, the basin shallows and in Eastern England the base Zechstein surface crops out. The western part of the British Isles displays a different structural pattern. The picture is dominated here by isolated fault-bounded basins like the Irish Sea, Cheshire, Worcester and the Bristol Channel basins.

Separated from the southern North Sea area are the basins of southern England and the British Channel. The inverted Weald and Wessex Basin and the Eastern Bristol Channel Basin are still recognisable as lows. Tertiary inversion here has not compensated entirely for the previous Mesozoic subsidence pattern.

# Pre-Permian surface -- Structural contours



0 110 220 330 440 550 660 Kilometers



Projection : Lambert Conformal Conic  
 Spheroid : Bessel, 1841  
 Standard parallels : 51 N and 54 N  
 Central meridian : 9 E  
 Latitude of projection origin : 48 N  
 False easting : 7,500,000 m  
 False northing : 0 m

### 3.5 Pre-Permian subcrop

#### Relevance to the European Gas Atlas

The map has been compiled to show the present day distribution of all pre-Permian rock units in order to differentiate between areas with or without potential source rocks.

#### Data base

The map is compiled from well data and limited reflection seismic interpretation. This data base is patchy and in many regions, with limited exploration activities, insufficient. In some areas like Wielkopolska a differentiation between folded Dinantian and Namurian was not possible.

Modern key literature with additional references: (GB): CAMERON (1993), CAMERON et al. (1992); (NL): VAN WIJHE (1987), OUDMAYER & DE JAGER (1993), ADRICHEM BOOGAERT, van & KOUWE (1993-1996); (DK): VEJBÆK & BRITZE (1994); (DE): WALTER (1992), TEICHMÜLLER et al. (1984), FRANKE, D.(ed) (1990), FRANKE, D. et al. (1995, 1996); (PL): POZARYSKI & KARNOWSKI (1992) and unpublished reports.

#### Main features

Westphalian and Stephanian occur in the central parts of the Central European Basin and Namurian, Dinantian and older rocks subcrop in the marginal areas.

The boundaries of the basin are clearly discernible:

To the north the basin is bounded by the Baltic Shield-East European Platform with Precambrian basement and Early Palaeozoic sedimentary cover. This structural boundary does not coincide exactly with the margins of the Late Palaeozoic basin. The Caledonian outer front, separating deformed rocks of the Caledonian tectonic phase from those not affected by the Silurian-Early Devonian deformation, can be traced from Central Poland to Pomerania and into the Baltic, off Rügen island, through the western Baltic and southern Jutland into the North Sea, where it trends towards the northwest and north.

The southern margin of the Central European Late Palaeozoic basin coincides with the "Central European Suture", the subduction suture of the Devonian-Early Carboniferous Rhenohercynian ocean, which runs from the Lizard Point thrust in an eastern direction into the Saar-Nahe Basin, the Northern Phyllite Zone and the northern margin of the Mid German Crystalline Zone to the Odra fault, bounding the Sudetic Mountains to the northeast.

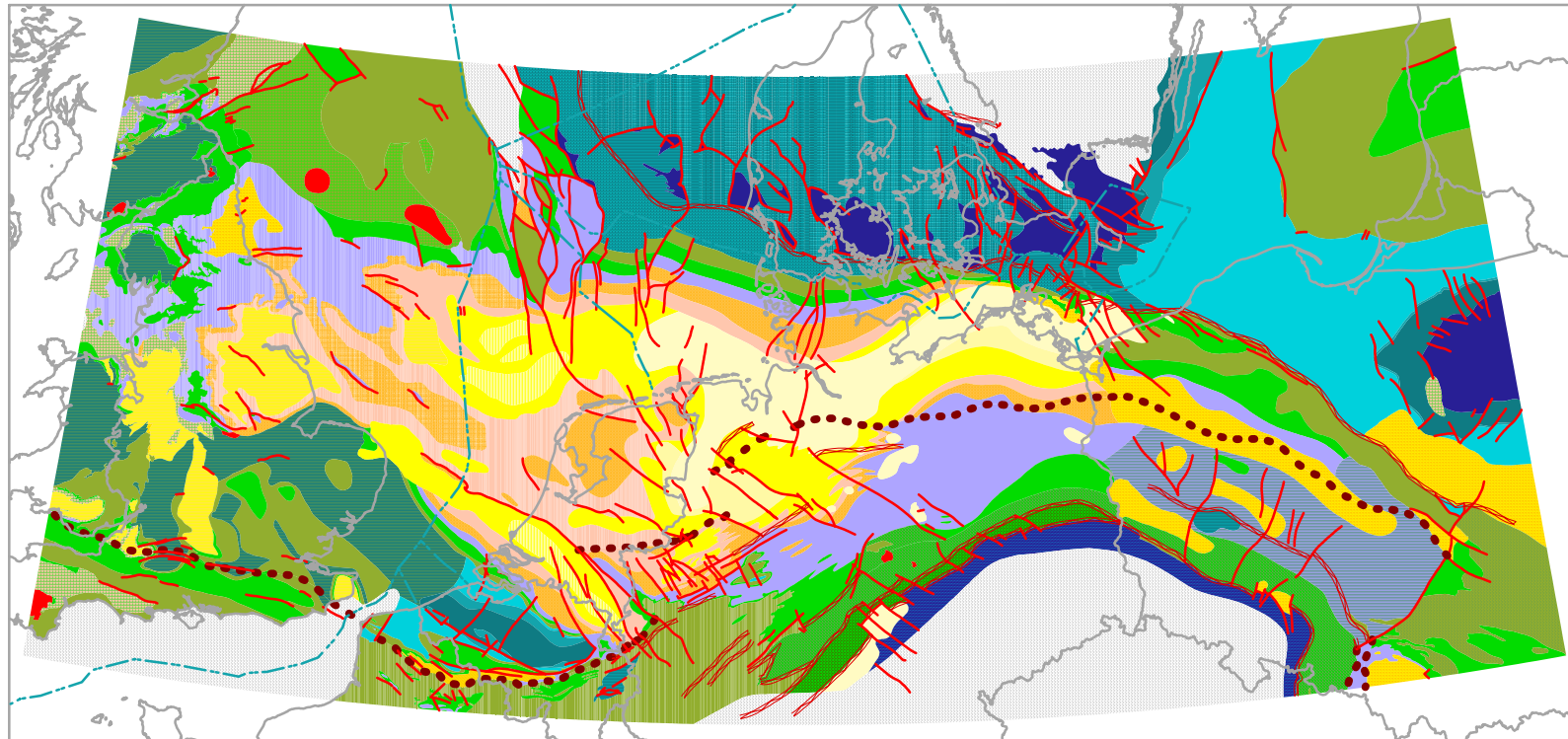
Within the Central European (Late Palaeozoic) Basin, the Variscan outer front separates areas strongly deformed in Late Westphalian to Stephanian times, from areas where the deformation has been less intense (block faulting, doming, reactivation of Caledonian structures). In the latter areas, however, locally strong, wrench-induced deformation may be observed.

The Variscan foreland shows broad warping or block faulting (Rügen), broad folding and thrusting along reactivated Caledonian thrust planes (Holy Cross Mountains) and updoming (Groningen High). In the Anglo-Dutch Basin the axes of these broad fold structures follow an southeast-northwest trend. Superimposed upon this broad folding is a pattern of complex wrench-deformation. A relationship between the Variscan folding and faulting and the underlying Caledonian structures is inferred.

The Variscan outer front, which is described as the pre-Permian subcrop of the northwestern to northernmost listric detachment plain, can be traced from Southern Ireland into South Wales, the Bristol district, Wessex and south Kent, into Northern France and the Faille du Midi-Aachen Thrust. East of the Rhine river it has been traced in northwestern Münsterland and into the Oldenburg-Bremen region. East of the river Weser it changes to a W-E direction, crossing the Lüneburg Heath, Southern Mecklenburg and reaching the Odra river south of Szczecin. It then trends southeast towards Lodz and is found, running roughly north-south again west of the Upper Silesian Depression. The obvious lateral displacements of the Variscan outer front are explained by the assumption of so called "tear faults", following the Peel Boundary Fault, the Osning Fault, the axial fault of the Lower Saxony Basin and the Pilica River Fault in Poland.

Most of the Polish and German gas fields lie within the folded Variscan molasse trough south and southwest of the Variscan outer front, whereas the Dutch and British gas fields occur in the Variscan foreland.

# Pre-Permian subcrop



- Offshore boundaries
- Topographic overview
- Structural features
  - major fault
  - overthrust
  - Variscan front
- Subcrop Pre-Permian
  - Stephanian
  - Westph. D + Stephanian
  - Westphalian D
  - Westphalian C + D
  - Westphalian C
  - Westphalian B
  - Westphalian A + B
  - Westphalian A
  - Westphalian, undiff.
  - Namurian
  - Dinantian + Namurian
  - Dinantian
  - Olisthostr. and nappes
  - Mid-European Suture
  - Carboniferous, undiff.
  - Variscite granitoids
  - Devon. and Carbonif.
  - Devonian
  - Devonian, locally older
  - Pre-Camb. to Devon.
  - Silurian
  - Ordovician
  - Cambro-Silurian
  - Cambro-Silurian, folded
  - Cambrian
  - Pre-Cambrian
  - M-German Crystal ridge
  - No data on the subject

0 110 220 330 440 550 660 Kilometers



Projection : Lambert Conformal Conic  
 Spheroid : Bessel, 1841  
 Standard parallels : 51 N and 54 N  
 Central meridian : 9 E  
 Latitude of projection origin : 48 N  
 False easting : 7,500,000 m  
 False northing : 0 m

### 3.6 Top pre-Permian, maturity

#### Relevance to the European Gas Atlas

This map presents the present-day maturity of potential pre-Permian source rocks.

#### Data base

The map relies on measurements of mean vitrinite reflection (Rr) of samples taken in wells and outcrops from the pre-Permian surface or slightly below (<300 m). No extrapolation of vitrinite reflection from coalification-depth trends in the overburden has been incorporated nor other methods employed. Isocontours have been interpolated between the data points, but in the case of buried magmatic bodies, adjusted to the trends of gravity and magnetic contouring.

Modern key literature with additional references: (GB): CORNFORD (1984), (NL): FERMONT et al. (1997); (DE): KOCH, KOCKEL & KRULL (1996), TEICHMÜLLER et al. (1984), BRAUN & WOLF (1994), EISERBECK et al. (1992), MÜLLER (1994); (PL): GROTEK (in press) and unpublished data and reports.

#### Causes of maturation

The maturity of pre-Westphalian source rocks in the Central European Basin is the combined effect of the following events:

- subsidence maturation in the Late Palaeozoic molasse trough;
- maturation caused by the Variscan folding (weak or no effect);
- maturation by the high heat flow during the Autunian;
- maturation by contact with Autunian lava flows and sills (weak or local);
- maturation by Late Variscan (Stephanian-Autunian) intrusive bodies;
- subsidence maturation during the Permian, Mesozoic and Cenozoic;
- maturation by Middle/Upper Jurassic and Early Cretaceous volcanic activity;
- maturation caused by high heat flow in the course of Late Cretaceous inversion;
- maturation by Late Cretaceous intrusive bodies;
- maturation by Early Tertiary volcanic activity;

#### Main features

In the **Polish** part of the basin maturity trends follow the NW-SE-configuration of the Permo-Mesozoic basin (see map No. 4). Values of < 3% Rr are reached in the axis of the trough. Towards the margins these values decrease towards <1% Rr. Positive anomalies (about 4% Rr) disturbing this regional trend are attributed to late Variscan (Stephanian to Autunian) magmatic intrusions, partly proven, partly inferred, and are located in some areas northeast of Wrocław and north of Częstochowa.

**North Germany** can be subdivided into two regions.

1. Münsterland, Ruhr area, Rheinische Schiefergebirge, Harz. Here the iso-reflectance contour lines again trace the Variscan fold pattern. Older (Devonian, Dinantian and Namurian) rocks are more mature (> 3% Rr) than Westphalian rocks (0.6-3% Rr). Present day maturity clearly results from subsidence prior to the Variscan folding. Exceptions are the contact haloes in the vicinity of Late Variscan intrusions like Erkelenz, Krefeld, Soest-Erwitte, Brocken and Ramberg (see map No. 15) and the increase of maturity within the Northern Phyllite zone south of Magdeburg due to stress metamorphism.

2. To the north the maturity differentiations inherited from the Palaeozoic have been homogenised by later maturation overprinting caused by Permo-Tertiary subsidence. The original maturity of 0.6-1% within the Westphalian increased to an average of 1.5 to 2.5% Rr. Intrusions of Late Variscan age (Velpke Asse-Roxförde NW of Magdeburg, Greifswald ["South Rügen pluton"]) and Late Cretaceous intrusions (Bramsche, Uchte, Vlotho, Solling, Neustadt-Heeßel) are marked by high maturity anomalies with values > 3% Rr. The large maturity anomaly in southern Mecklenburg and Northern Brandenburg is not well documented.

In most of the **Netherlands** part of the map, the isolines follow more closely the Mesozoic structural pattern. The Mesozoic highs (Friesland Platform, Groningen High, Texel-IJsselmeer High, Cleaverbank High) show values between 0.6-1.0% Rr. In the Mesozoic basins (Lower Saxony Basin, West and Central Netherlands Basin, Roer Valley Graben, Broad Fourteens Basin and Central North

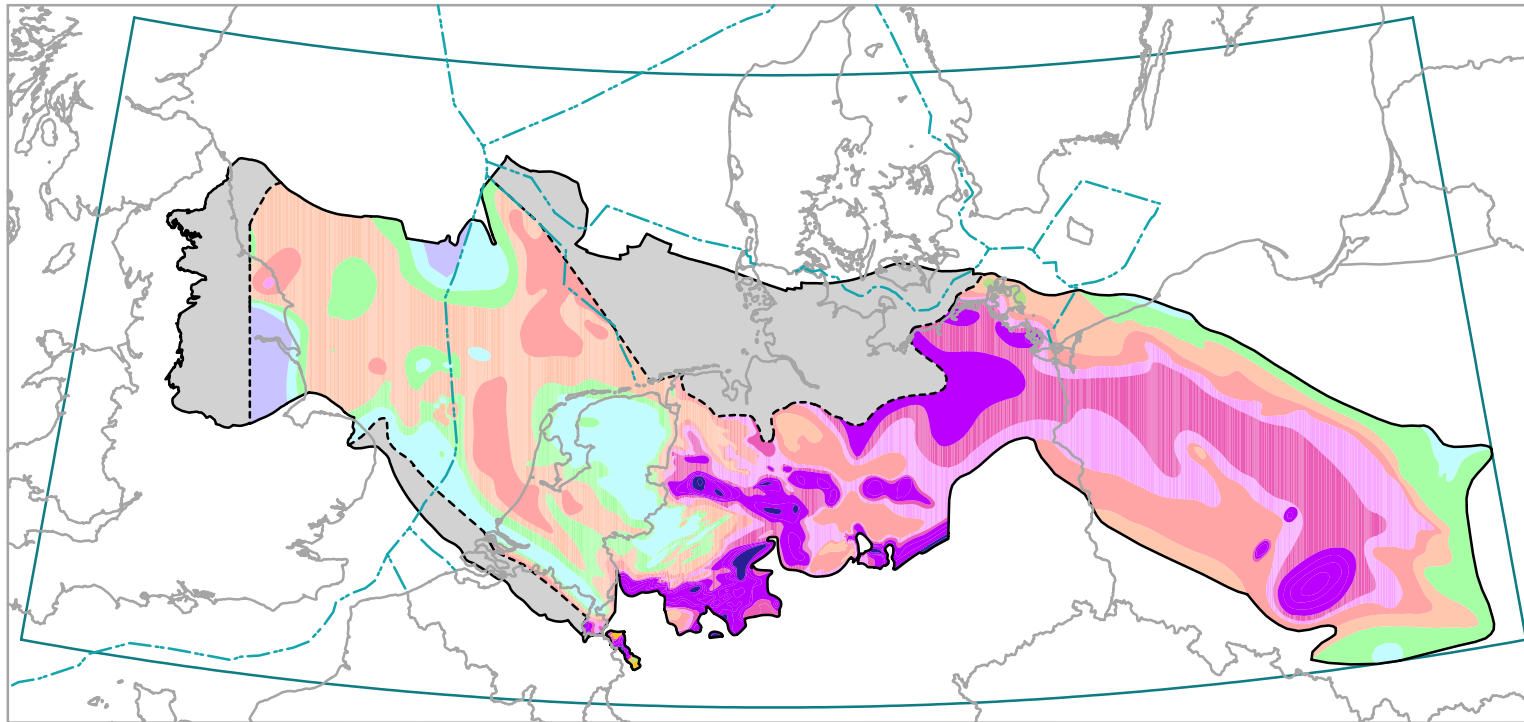
Sea Graben), values occur between 0.8 and 2.0% Rr. The increase in coalification towards the London-Brabant Massif (up to 4% Rr) can be attributed to pre-Permian subsidence.

In the **British** part of the map, only the Sole Pit Basin shows up as an area of higher maturation (up to 2% Rr).

In northern parts of Germany, the adjacent German North Sea and parts of the GB, information is too scattered to construct iso-reflection lines. Generally speaking, in areas with maturity values of >3.5% Rr at the Pre-Permian surface, gas deposits derived from Pre-Permian source rocks should not be expected.



# Top Pre-Permian -- Maturity



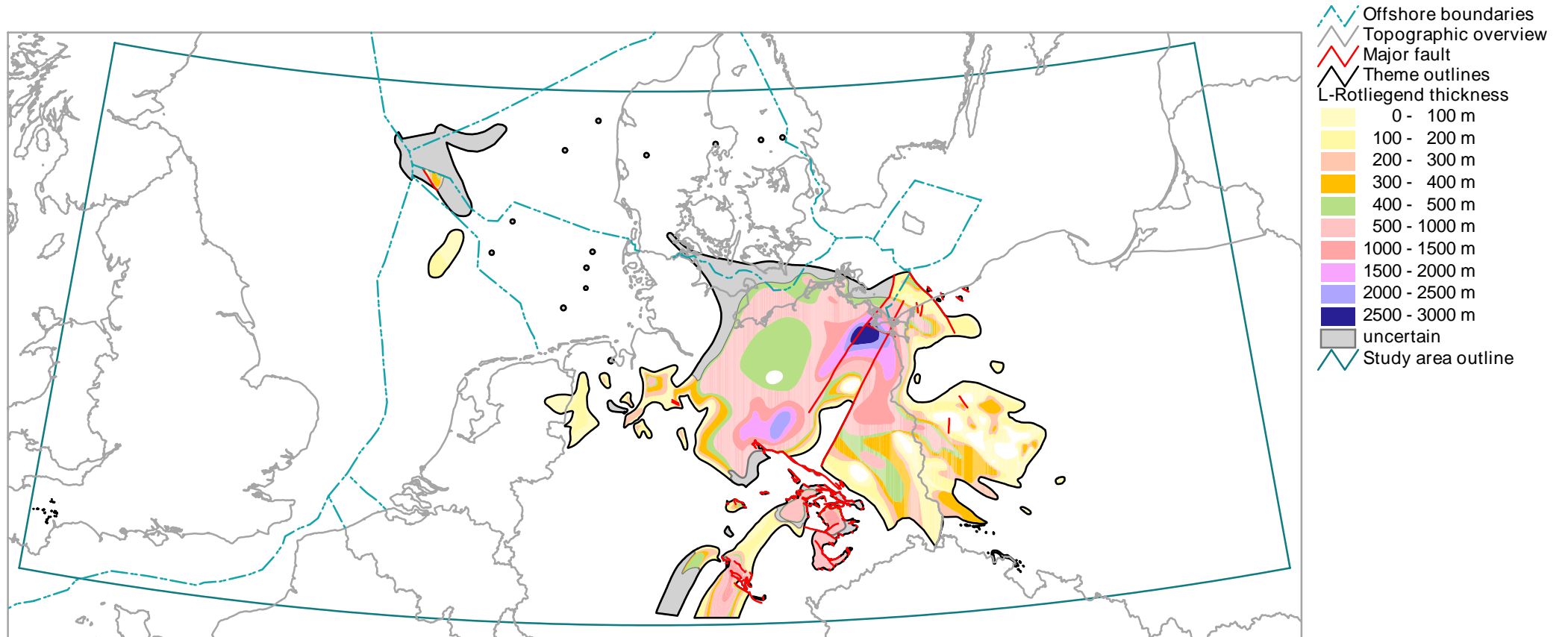
- Offshore boundaries
- Topographic overview
- Theme outlines
  - 160
  - 990
- Maturity Top Pre-Permian
  - 0.0 - 0.6 %
  - 0.6 - 0.8 %
  - 0.8 - 1.0 %
  - 1.0 - 1.5 %
  - 1.5 - 2.0 %
  - 2.0 - 2.5 %
  - 2.5 - 3.0 %
  - 3.0 - 5.0 %
  - 5.0 - 7.0 %
  - uncertain
- Study area outline

0 110 220 330 440 550 660 Kilometers



Projection : Lambert Conformal Conic  
 Spheroid : Bessel, 1841  
 Standard parallels : 51 N and 54 N  
 Central meridian : 9 E  
 Latitude of projection origin : 48 N  
 False easting : 7,500,000 m  
 False northing : 0 m

# Rotliegend volcanics -- Distribution and thickness



- Offshore boundaries
- Topographic overview
- Major fault
- Theme outlines
- L-Rotliegend thickness**
- 0 - 100 m
- 100 - 200 m
- 200 - 300 m
- 300 - 400 m
- 400 - 500 m
- 500 - 1000 m
- 1000 - 1500 m
- 1500 - 2000 m
- 2000 - 2500 m
- 2500 - 3000 m
- uncertain
- Study area outline

0 110 220 330 440 550 660 Kilometers



Projection : Lambert Conformal Conic  
 Spheroid : Bessel, 1841  
 Standard parallels : 51 N and 54 N  
 Central meridian : 9 E  
 Latitude of projection origin : 48 N  
 False easting : 7,500,000 m  
 False northing : 0 m

### 3.8 Rotliegend sediments, distribution and thickness

#### Relevance to the European Gas Atlas

The sedimentary Rotliegend comprises the economically most important gas reservoir horizons in the study area.

#### Data base

The construction of the map predominantly relies on well data and only locally on reflection seismic data. It shows the total residual thickness of the sedimentary Rotliegend. Its stratigraphical volume differs considerably in the different regions. Modern key literature with additional references: VERDIER (1996); (GB): CAMERON et al. (1992), GLENNIE (1990); (NL): WIJHE, van et al. (1980), GELUK et al. (1996); (DK): SØRENSEN & MARTINSEN (1987), (DE): PLEIN (ed.) (1995); (PL): HOFFMANN ET AL. (1997), POKORSKI (1989) and unpublished reports.

#### Distribution

The depositional area of the Rotliegend sediments can be subdivided into two regions, one to the north and one to the south of the Mid North Sea--Ringkøbing-Fyn High. North of these highs only isolated occurrences of Rotliegend sediments have been encountered, up to some 200 m in thickness. South of these highs the main sedimentation took place in the Southern Permian Basin. This basin did not yet form one entity, as it did later during the deposition of the Zechstein. During the deposition of the Rotliegend, a gradual expansion of the area of sedimentation occurred, beginning at fault-bounded depocenters in the eastern part of Germany.

The Central European Upper Rotliegend trough is limited in the north by the Mid North Sea--Ringkøbing-Fyn High, in the northeast more or less by the southwestern border of the East European Platform, although some isolated shallow basins occur on the platform itself. In the south the southern fringe of the basin is situated on the northern and northeastern part of the folded Variscan Rheno-Hercynian zone. In Poland, the Sudetes marks the southwestern present day boundary of the trough, in East Germany they mark the northeastern border of the Lausitz Block. West of the Elbe river the southern border is lobated. A large embayment existed in southern Lower Saxony and northern Hessen. A ridge west of this embayment, the Hunte Swell, extends north and nearly reaches Bremen. Another south-directed embayment, the Ems Low, follows the Ems River. In the Netherlands the basin extends southward and reaches the northeastern flank of the London-Brabant Massif, which also forms the basin limit in GB. The western boundary here is marked by the eastern flank of the Pennine High.

The most prominent outliers are in the north the fault-bounded Rønne Graben near Bornholm and in the south the NE-trending Saar-Saale Trough, extending from the Saarland to Leipzig.

#### Palaeogeography and facies development (see table 3.4 for nomenclature)

The oldest Rotliegend sediments of the Central European Permian basin - with the exception of the Saar-Saale Trough - are found in the fault-bounded Barnim (Brandenburg) Depression in East Germany (Grüneberg Fm.). They belong to the Lower Rotliegend. Slightly younger, but still within the Lower Rotliegend, are the Bebertal beds in the Beber-Graben (Flechtingen Block). Their equivalent in Poland is the locally occurring Obrzycko Member.

After the Saalian hiatus, sedimentation recommenced in the main trough in eastern Germany with the deposition of the Müritz Subgroup in the Mirow-, Parchim- and Schwaan-depocenters, in the Havel-Müritz and West-Mecklenburg depressions and in the Bebertal Graben (Föhrberg Mb.; fluvio-lacustrine fine-grained clastics with algal limestones). These sediments may have their equivalents in the Kornik Fm. in the Poznan Graben (PL).

After the Altmark I discordancy (base of Lower Havel Subgroup, Parchim Fm.) the local depocenters extended towards the west, occupying the Lower Elbe and German Bay depressions. In the centre of the depression clay deposition occurred in a playa lake setting, with separate depocenters in western Mecklenburg (Schwerin) and off the Elbe estuary, where sabkha sediments with evaporites are found. From the south in the Lüneburg Heath and the northern Hessen area (precursor of the Triassic Weser Trough) a system of structurally controlled wadi channels with fluvial sediments fed into the playa lake which was also being partly infilled by dune sands. Aeolian sediments also occur in the Havel-Müritz Depression. In Poland the lower part of the Drawa Subgroup (exclusively Pila Fm.) was

deposited in the rift basin as fluvial and aeolian sediments. At that time the Mid-Polish Trough also began to develop and later played a significant role in the Late Permian-Mesozoic structural history of the Polish Lowlands. The main sedimentary transport directions were steered by tectonically active fault zones. In the west and north only the Brande Trough and the Horn Graben were probably included in this area of sedimentation. The southern North Sea and the Netherlands were areas actively undergoing erosion.

After the Altmark II discordance (base of Mirow-Formation, Upper Havel Subgroup, base of Czaplonek Fm., Upper Drawa Subgroup) the playa lake in the centre of the basin widened and its southern margin overstepped the Elbe River to the south. Sabkha persisted to the west off the Elbe estuary. The wadis in the south were filled by aeolian sands. In Poland the sedimentary basin, infilled by the Czaplonek Fm predominantly developed within the Pomeranian unit of the rift basin. These fluvial and aeolian sediments were deposited along active fault scarps. The upper part of the sedimentary succession is dominated by claystones and siltstones of playa origin. The concentric lithofacies pattern that developed is typical of a stable sedimentary basin infill. In the west the Central North Sea Graben probably also lay within the sedimentation area.

After the Altmark III discordance and with the beginning of the Elbe Subgroup (base Dethlingen Fm. Lower Notec Subgroup, base of the Piaski Fm., Lower Silverpit Claystone Mb., Lower Slochteren Sst. Mb., Leman Sandstone Fm.) the depositional area gradually expanded, particularly towards the west into the southern North Sea area. The shoreline of the central sabkha lake in the Elbe estuary region moved some 10 km to the south. Sabkha conditions with evaporite sedimentation prevailed in the Lower Elbe region, the German and partly in the Netherlands and GB sectors of the North Sea. Fluvial deposits were shed northwards into the playa lake, and in the southern GB and NL-sector fluviually reworked sands and a vast area with dune sand deposits are found (Slochteren Fm., Leman Sandstone Fm.). In eastern Germany playa conditions with claystone and anhydrite deposition prevailed. The deposits of the Piaska Fm. in Poland significantly overstep the margins of the rift basin. A concentric pattern of facies distribution is again characteristic, with broad marginal areas dominated by coarse-grained sediments (fluvial sandstones initially and aeolian sands later). The depocenter at this time was located in the Mid-Polish Trough, where playa sedimentation prevailed.

In the Lower Hannover Fm. (Upper Notec Subgroup, Szubin Fm., Silverpit Fm., Upper Slochteren Fm.) beginning with the transgression of the Ameland Claystone the largest extent of the desert lake was reached, occupying the entire Lower Elbe region, parts of the Havel-Müritzer and Schwerin depression, nearly the entire German North Sea sector and extending almost to the GB coast. Deposition at the lake centre was dominated by evaporitic sediments while towards the margins claystones dominate. In the south, the wadis disappeared and were filled with playa sediments. In the Southern North Sea fluvial and aeolian deposits dominate (Upper Slochteren Sandstone, Leman Sandstone Fm.) In the upper part of the Hannover Fm. the largest extent of the depositional area of the Rotliegendes was reached, extending south to Rotterdam and into East Anglia and to the mouth of the Humber in the west. Playa deposits occupy the northern Netherlands (Ten Boer Mb.) and large parts of Lower Saxony, Mecklenburg-Vorpommern and Northern Brandenburg. Aeolian sedimentation persisted in most of the Netherlands onshore area, the GB Southern North Sea sector and is also found in Pomerania (Slupsk Depression) and along the southern fringe of the Mid-Polish Trough. In Szubin times, the palaeogeographical conditions in Poland remained similar to those during the sedimentation of the underlying Piaska Fm. In the marginal zones of the basin coarse clastic deposits (fluvial and aeolian) prevailed, whereas in the depocenter of the Mid-Polish Trough, in the Pomeranian and Kujawian areas, playa deposits predominated. Simultaneously conglomerates and sandstones of fluvial origin were deposited on the East European Platform (Warmia and Podlasie depressions) and aeolian sands in the Slupsk Depression.

## Main features

The map displays the following features:

In Poland three individual troughs generally trending NW-SE are developed. From NE to SW they are:

- the Mid-Polish Trough (> 1400 m), extending towards the SE, NE and SW of the Swietokrzyskie Uplift, bordering the East European Platform to the southwest
- the Silesian Trough (> 400 m) flanked to the northeast by the Wolsztyn High and to the southwest by the Luzyce (Lausitz) High
- the Luzyce (Lausitz) Trough (> 400 m) northeast of the Sudetic Uplift
- Isolated depressions of smaller dimension are the Poznan Graben (> 1.000) m, the East Fore-Sudetic Graben (> 400 m) and the Intra-Sudetic Trough.
- On the East European Platform several shallow depressions with a maximum thickness < 100 m are known: the Slupsk Depression in Eastern Pomerania, the Warmia Depression north of the Mazurian High and the Podlasie Depression in East Poland.

In Germany the main depocenters are:

- the Havel-Müritz Depression (> 1900 m)
- the Schwerin-Westmecklenburg Trough (> 2200 m) with extensions to the west into
- the Lower Elbe-German Bay Depression (1500 m). The original thicknesses from the central part of this large depocenter are not known, due to the later complications of mobilisation of the salt layers within the Elbe Subgroup (indicated in grey in the map).
- the Lausitz Depression (> 300 m) in southeastern Brandenburg extends into the Polish Luzyce Trough to the SE.

Other isolated depocentres are the synsedimentary rift system in northern Lower Saxony East of the Weser river, the Beber Graben (> 600 m) in the Altmark and the Barnim Depression (> 700 m) in Brandenburg north of Berlin. The latter containing Lower Rotliegend sediments at the base.

Further basins existed in Sachsen-Anhalt (Halle Basin), in Thuringia, Hessen, Rheinland-Pfalz (Saar-Nahe Basin, Trier) and Bavaria. Deposits in the Malmedy Graben (BE) and the Mechernich area (DE), previously considered to be Permian in age, are most likely to represent Lower Triassic deposition.

In the Netherlands the main area of sedimentation is situated in the northern offshore area (>700 m). Lying perpendicular to this depocenter is the north-south trending Off Holland Low in the southern North Sea (>300 m). In the onshore area are the contiguous Central Netherlands (>200 m) and West Netherlands basins (>100 m).

In the GB southern North Sea, up to 250 m of sediments were deposited in the western part of the Southern Permian Basin. Isolated from this basin, in the British onshore area, equivalent sediments occur in the fault-bounded Worcester, Celtic Sea, Bristol Channel and Irish Sea basins.

In the Danish onshore and North Sea areas, some isolated occurrences of Rotliegend sediments are found. In the western part of the Danish offshore up to 300 m of aeolian and fluvial sediments are occur north of the Ringkøbing-Fyn High. The Horn Graben appears to have been the most important area of sedimentation. Thick Rotliegend sediments occur in the synsedimentary Rønne Graben near Bornholm.

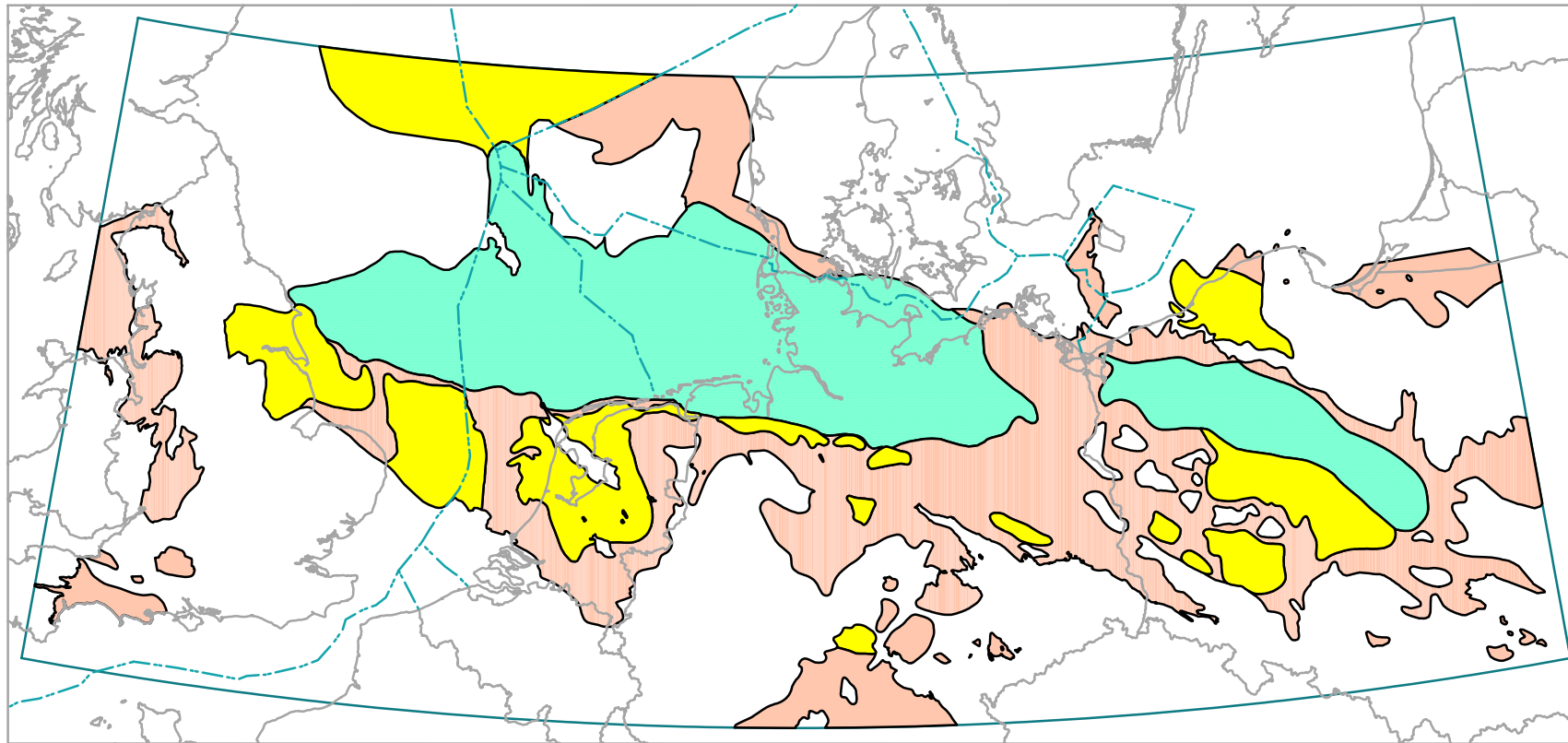
## Reservoir rocks

All sandstone deposits of the Rotliegend are potential reservoir rocks. Outstanding reservoir properties are shown by the aeolian sands of the Parchim Fm. (Schneverdingen and Büste Sandstone), the beach and reworked aeolian sands along the southern shore of the desert lake in Dethlingen and Hannover age in Germany and particularly the aeolian and reworked aeolian sands of this age in the Netherlands and GB (Slochteren Fm. and Leman Sandstone Fm). In Poland reservoir sandstones occur in the Drawa and Notec subgroups. Up to now, the known gas fields produce mainly from the Notec Subgroup, but within the Mid-Polish Trough reservoir sandstones are likely in the Notec as well as in the Drawa Subgroup. The reservoir properties of these sandstones, not only in Poland but also in the other regions depend, above all, on their early to meso-diagenetic history which has preserved their excellent poroperm characteristics.

GB		Netherlands			Germany			Poland		Tectonic pulses
Group	Formation	Group	Formation	Member	Group	Subgroup	Formation/Member	Sub-group	Formation/Member	
Rotliegend	Silverpit Fm. /	Upper Rotliegend Group	Silverpit Fm. /	U. Silverp. Clst./ Ten Boer Clst. Mb. U. Slochteren Sst. Mb. Silverpit Evaporite /Ameland Clst. Mb. L. Slochteren Sst. Mb.	Oberrotliegend II	Elbe	Hannover	Notec	Szubin	←Altmark IV
	Leman Sst. Fm.			L. Silverpit Clst. Mb. Hollum Clst. Mb.			Dethlingen		Piaski	
				Lower Slochteren Sst.		Havel	Mirow	Drawa	Czaplinek	←Altmark III
							Parchim		Pila	←Altmark II
					Oberrotliegend I	Müritz	Föhrberg	Müritz	Kornik	←Altmark I
							Unterrötliengend		Altmark	Uthmöden Bebertal Winkelstedt
		Grüneberg Roxförde Eiche		Wielkopolska						
Group	Inge Volcanics Formation	Lower Rotliegend Group	Emmen Volcanics Fm.				Flechting Bodendorf	-----		
		Limburg Gp.	De Lutte Fm.		Stefan		Mönchgut/ Süplingen		Swiniec	←Franconian

**Table 3.4: Correlation of the Rotliegend in Great Britain, the Netherlands, Germany and Poland. Hatching indicates a hiatus.**

# Rotliegend sediments -- Facies



- Offshore boundaries
- Topographic overview
- Upper Rotliegend Facies
  - aeolian
  - fluvial
  - lacustrine
- Study area outline

0 110 220 330 440 550 660 Kilometers



Projection : Lambert Conformal Conic  
Spheroid : Bessel, 1841  
Standard parallels : 51 N and 54 N  
Central meridian : 9 E  
Latitude of projection origin : 48 N  
False easting : 7,500,000 m  
False northing : 0 m

### 3.9 Rotliegend sediments: facies

#### Relevance to the European Gas Atlas

The sedimentary Rotliegend forms the economically most important gas reservoir horizons in the study area.

#### Data base

The construction of the map predominantly relies on published data, supported by released well-data. It shows the distribution of facies in the upper part of the sedimentary Rotliegend, approximating to the middle part of the Hannover Formation. Modern key literature with additional references: (GB): CAMERON et al. (1992), GLENNIE (1990); (NL): GEORGE & BERRY (1994), VERDIER (1996), WIJHE, van et al. (1980), (DK): SØRENSEN & MARTINSEN (1987), (DE): GAST (1988, 1991), LINDERT et al. (1990), PLEIN (ed.) (1995); (PL): HOFFMANN ET AL. (1997), POKORSKI (1989) and unpublished reports.

#### Facies development

Three facies realms have been identified for the Rotliegend sediments:

- 1. Aeolian sediments** cover large areas south of the playa lake in the southern North Sea area, in Pomerania (Slupsk Depression) and south of the Mid-Polish Trough. In northern Germany, they cover smaller areas and occur close to the margin of the playa lake. These sediments were deposited in the areas lying between the main fluvial systems.
- 2. Fluvial and sabkha sediments** were deposited in the lows along which the main fluvial systems were situated (Off Holland Low, Ems Low, Weser Trough), and in the Thuringian Basin, the Rønne Graben, Horn Graben and Northern Permian Basin. At the margins of the playa lake sabkha and beach sands were deposited. The latter forming good reservoirs in northwest Germany. Fluvial deposits occur on the East European Platform in the Warmia and Podlasie depressions.
- 3. The distribution of playa lake sediments** pinpoint the depocenters of the basin. They comprise clay- and siltstone successions which in the Southern North Sea and northern Germany also include halite intercalations. These evaporites attain a great thickness in northern Germany, the Netherlands and the British offshore sectors and they have been extensively mobilised during the Mesozoic to form a number of salt structures. In the Mid-Polish Trough on the other hand, only fine-grained clastic sediments are present. Near the margins of the basin, e.g. the Mid North Sea High, intercalations of sandstones occur.



### 3.7 Rotliegend volcanics, distribution and thickness

#### Relevance to the European Gas Atlas

This map has been compiled in order to estimate depths of the pre-Permian surface by adding Rotliegend residual thickness to the seismically mapped depths of the base Zechstein. In some cases gas bearing sandstones occur in association with these volcanic rocks (German North Sea).

#### Data base

The map is compiled from well data. Modern key literature with additional references: (GB): CAMERON et al. (1993), EDMONDS et al. (1975), (NL): GELUK (1997); (DK): AGHABAWA (1993), (DE): BENEK (1995), HOTH et al. (1993a), PLEIN (ed.) 1995; (PL): HOFFMANN ET AL. (1997), POKORSKI (1989) and unpublished reports.

#### Main features

The greatest accumulation of Rotliegend volcanics is confined to the Polish Lowlands and Northern Germany. Important outliers are recorded from Saxony (Leipzig), Sachsen-Anhalt (Halle) and Thuringia (Thuringian forest etc.), from the Danish onshore area, the Horn and Central North Sea.

The maximum thickness of volcanics is reached in Poland in the Szczecin area (> 500 m and south of the Warta river east of Frankfurt/Oder (> 1500 m).

In Germany maximum thicknesses are reached in a NE-SW-trending depocenter between Usedom and Neuruppin (> 2500 m), in the Altmark depocenter, which extends to the Flechtingen and Velpke-Asse area (> 2000 m), in the Berlin area (> 1000 m), in the Halle (> 500 m) and Leipzig (> 100 m) depocenters, in the Eisenach-Hessian depocenter (> 1400 m), in a depocenter NE of Bremen (> 500 m), in the Ems Depression (> 100 m) and in several smaller outliers. The volcanics of the Saar-Nahe Depression have not been included in the map.

In the southwestern England, Denmark and the North Sea area, data are scarce and contouring of the thickness nearly impossible based on data currently available. The maximum thickness is found in the Central North Sea Graben at the 5 country junction (>150 m).

#### Petrological succession

The volcanics in Germany can be subdivided into several different eruption phases:

- an Upper Rotliegend basaltic phase within the Havel Group.
- a rhyolite phase (Uthmöden + Föhrberg Fm)
- a post-ignimbritic phase with andesitoids at the base and rhyolitic lavas (Winkelstedt Fm.),
- an explosive eruption phase with compositionally different rhyolitic ignimbrites (Roxförde Fm.),
- a basal, probably Stephanian andesite phase (Flechtingen Fm.) with basalts and andesitoides,

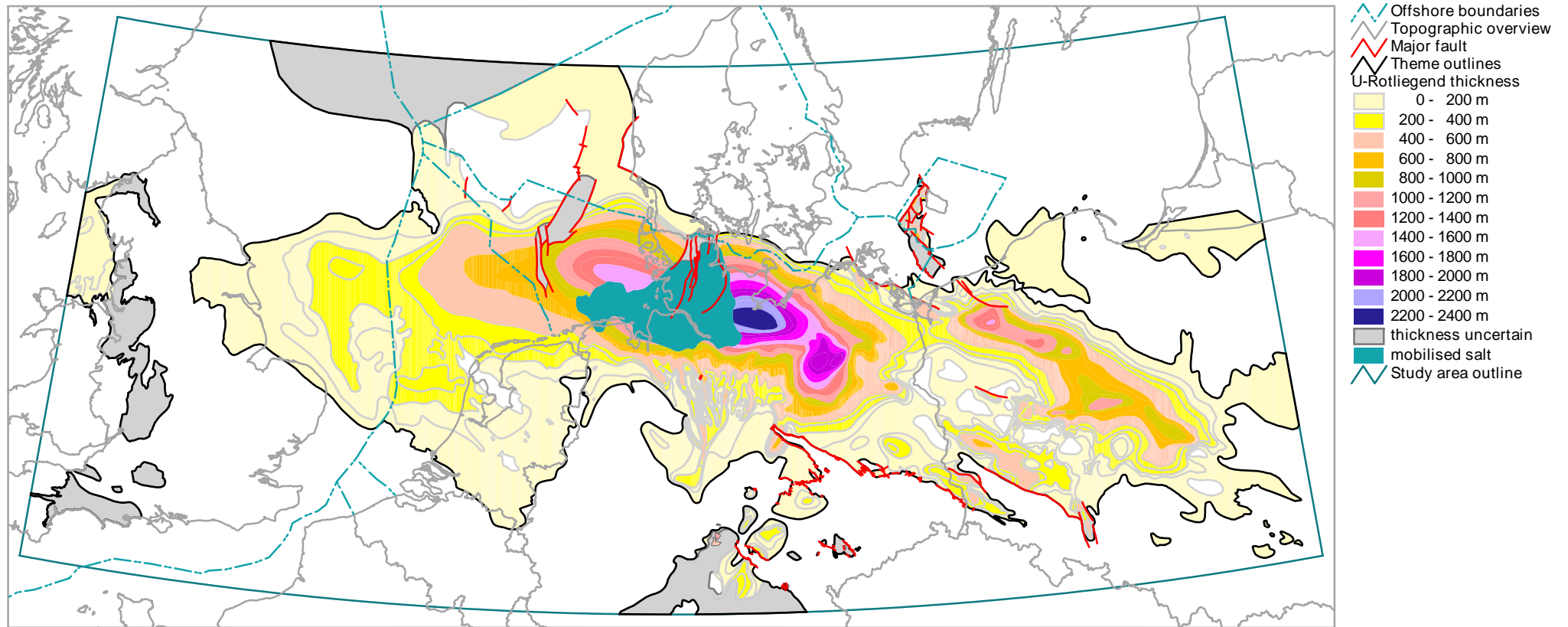
Rhyolite and basaltic phases are missing in Rügen and Vorpommern, as well as in NW-Germany, where only the andesitic and to a certain extent the ignimbritic phases are preserved. In other areas the volcanic sequence has not been studied in detail.

The depocenters of the ignimbrites have been ascribed to Early Permian calderas and volcano-tectonic depressions like the Friedland-Mirow, the Flechtingen and Altmark the NW-Saxony (Leipzig)- and the Rochlitz caldera/depression.

Increased coalification of the pre-Permian rocks in the vicinity of the volcanic depocenters has not been observed but it is assumed, that a generally increased heat flow in the Central European Early Permian basin existed.

The age of the volcanics is well constrained by geophysical and stratigraphical data. The oldest basalts and andesites are Stephanian (Ghzelian) in age, the bulk is Asselian and Sakmarian in age, the younger basalts occur in the Havel Subgroup (Tartarian). The eruption phase lasted ca. 32 Ma (ca. 297- ca. 265 Ma Bp.)

# Rotliegend sediments -- Distribution and thickness



0 110 220 330 440 550 660 Kilometers



Projection : Lambert Conformal Conic  
 Spheroid : Bessel, 1841  
 Standard parallels : 51 N and 54 N  
 Central meridian : 9 E  
 Latitude of projection origin : 48 N  
 False easting : 7,500,000 m  
 False northing : 0 m

### 3.10 Zechstein 2 (Staßfurt Carbonate), distribution and facies

#### Relevance to the European Gas Atlas

Economically important reservoir horizons occur within the Zechstein throughout the study area. The most productive reservoir is the Zechstein 2 (Staßfurt) Carbonate; other reservoirs are formed by the Zechsteinkalk, the Platy Dolomite and the Hewett or Zechstein 4 Sandstone. The Zechstein also contains organic-rich source rocks (Kupferschiefer, Stinkschiefer) which source some minor gas-fields. The Zechstein halites represent the primary reservoir seal for the Palaeozoic gas plays in the Central European Basin.

#### Data base

The map relies on well data and outcrop investigations, facies analyses and partly on 3D-reflection seismic. Modern key literature with additional references: (GB): CAMERON et al. (1992), TAYLOR & COLTER (1975), TAYLOR (1986), HARWOOD & SMITH (1986), (DK): CLARK & TALLBACKA (1980), VEJBÆK (1990); (NL): SANDE, van de. et al. (1996), BAAN, van der (1990), GELUK et al. (in press); (DE): STROHMENGER et al. (1996), SANNEMANN et al. (1978), PIESKE & SCHRETZENMAYR (1984), GÖRING & ZAGORA (1993), RASCH & ZAGORA (1993); (PL): WAGNER (1994), PERYT (1992)

#### Facies development

The deposits of the Zechstein 2 (Staßfurt) Carbonate can be subdivided into three main facies realms: the **platform, slope and basinal facies**. The platform developed upon the thick anhydrite deposits of the Zechstein 1 (Werra) cycle along the margins of the Southern Permian Basin. The slope accreted laterally upon the slope of the Zechstein 1 Anhydrite accumulation and the basinal facies occupies the floor of the deep basin. These differences in facies are due to a submarine relief of >200 m between platform and basin floor during early Staßfurt times. The basin itself was subsequently quite rapidly filled by the Staßfurt halite. In this way most of the relief of the basin floor, which formed in Zechstein 1-times, was smoothed out. .

1. The **platform facies** comprises several subfacies types, which all represent shallow supratidal to subtidal environments. The thickness of the carbonate on this platform may range up to 50 m. The platform is also characterised by a wide variety of sub-environments, which sometimes display rapid variations in facies over small distances. Isolated occurrences of platform carbonates along the southern margin of the basin in Germany, Poland and the Netherlands correspond mainly to small carbonate built-ups.
2. The **slope facies** ranges from subtidal (between fair- and storm-weather wave base) to a deep marine facies at the toe of the slope. The thickest occurrences of the Staßfurt Carbonate are developed in this facies (30-200 m). The unit is mostly composed of fine-grained, dolomitised carbonates. Sea-level lowering during deposition of this unit led to leaching, erosion and redeposition of these slope sediments.
3. The **basinal facies** comprises thin deposits (5-20 m), with a very uniform thickness and facies and distribution. Near the lower slope bituminous carbonates ("Stinkkalke") occur and in the basin centre the carbonate content diminishes and only bituminous shales ("Stinkschiefer") remain.

#### Main features

Extended platform areas, sometimes with broad slope realms are found along the northeastern, eastern and southern fringe of the basin, whereas along the northern margin, coinciding with the southern slope of the Ringkøbing-Fyn High the platform and slope are rather narrow. The widest platform/slope rim is situated in southern Oldenburg (Germany) and in the German-Netherlands border region, where the bulk of the most productive Zechstein gas fields has been found.

In addition to the Staßfurt Carbonate, the distribution of the Hewett Sandstone is shown on the map. The Hewett Sandstone forms an important reservoir unit in the British sector of the southern North Sea. From a consideration of the regional development of the Zechstein cycles the Hewett Sandstone is now considered to form part of the Zechstein 4-5 cycle.

#### Reservoir rocks

Zechstein 1 Carbonate (Zechsteinkalk) reservoirs occur in Wissey and the Southern North Sea Basin (GB/NL). In some Polish gasfields, the Zechsteinkalk forms a single reservoir together with the Rotliegend deposits.

The Zechstein 2 (Staßfurt) Carbonate forms a good reservoir rock in the platform and upper slope facies in Southern Oldenburg, Emsland and the Eastern Netherlands, Eastern Brandenburg, Vorpommern, Thuringia and Poland. In Poland important oil deposits are found in this carbonates. Reservoir properties are highly dependent on early (eogenetic) diagenetic controls. On the platform meteoric leaching or contemporaneous dolomitization in the sabkha setting of the shallow subtidal to supratidal carbonates created vuggy, moldic and intracrystalline porosity. In the turbiditic slope carbonates dolomitization caused by percolation of aragonite undersaturated and dolomite-oversaturated water from the deeper marine environment lead to fabric-selective, intraparticle and moldic porosity development. Later dedolomitization (calcitization) may often totally destroyed this porosity. Sediments of the middle and lower slope and the basinal facies normally have little or no porosity.

The Plattendolomite (Zechstein 3 Carbonate) is a reservoir rock in the Emsland, Süoldenburg, eastern and western Netherlands, the GB southern North Sea and in Poland.

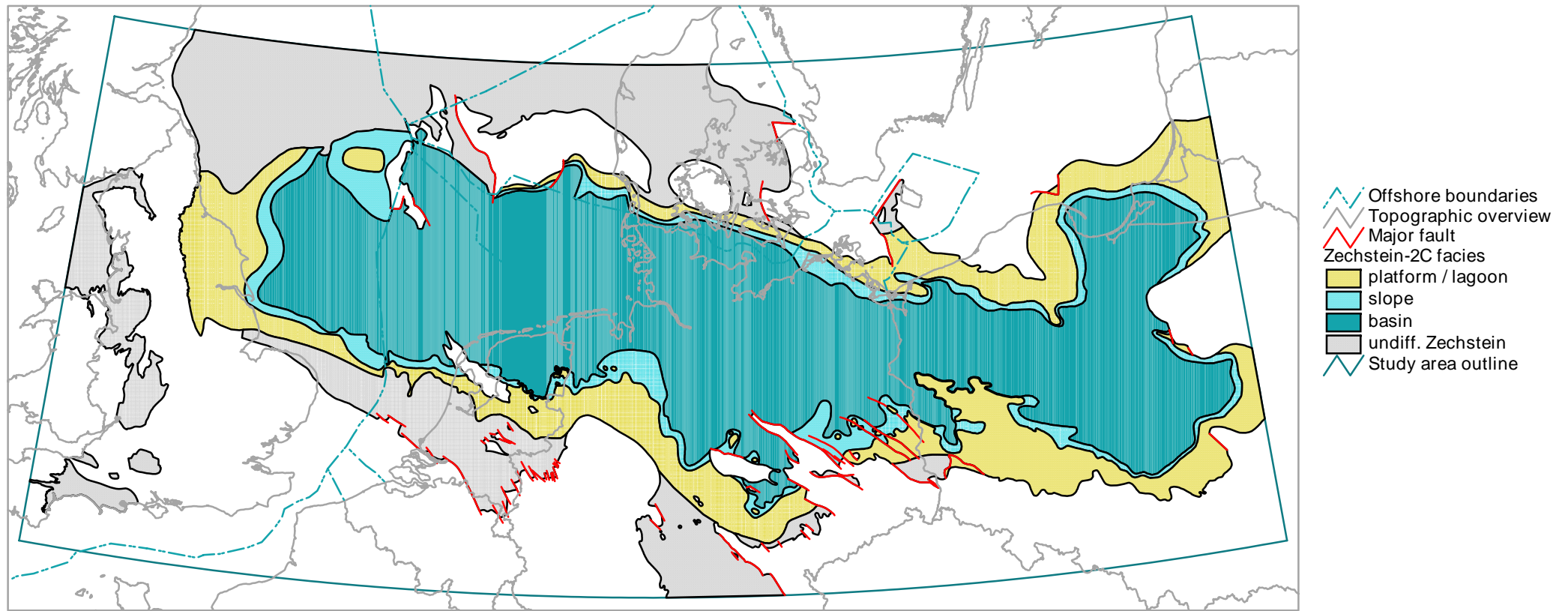
The Hewett Sandstone (NL: Z4 Sandstone Mb.) forms an important reservoir rock in the British southern North Sea. In the British sector, this unit was long considered to belong to the Triassic (JOHNSON et al., 1994); regional considerations of the Polish, German and Netherlands stratigraphic sequences now suggest it should be included in the Zechstein.

#### **Source rocks**

Kupferschiefer (base of Werra = Zechstein 1 cycle) (productivity uncertain)

Stinkkalk-Stinkschiefer = basinal equivalents to the Staßfurt Carbonate (Zechstein 2). Both layers source smaller hydrocarbon-deposits (natural gas, condensates and oil) in the southern North Sea, Thuringia, Vorpommern, East Brandenburg, the Southern Baltic and Poland.

# Zechstein 2 (Stassfurt Carbonate) -- Distribution and facies



0 110 220 330 440 550 660 Kilometers



Projection : Lambert Conformal Conic  
Spheroid : Bessel, 1841  
Standard parallels : 51 N and 54 N  
Central meridian : 9 E  
Latitude of projection origin : 48 N  
False easting : 7,500,000 m  
False northing : 0 m

### 3.11 Middle Buntsandstein, distribution and facies

#### Relevance to the European Gas Atlas

The map has been chosen for display, because economically important hydrocarbon-reservoir horizons occur within the Buntsandstein succession in Britain, the Netherlands and Germany. The most productive reservoirs occur in the Middle or Main Buntsandstein, which consists of a series of sheet sands with an almost basin-wide distribution.

#### Data-base

The map relies on seismic and well data, and to a lesser degree on outcrop mapping. Modern key literature used for the compilation are: (GB): CAMERON et al. (1993), CAMERON et al. (1992), JOHNSON, WARRINGTON & STOKER (1994); (DK): BERTELSEN (1980), VEJBÆK & BRITZE (1994), VEJBÆK (1990); (NL): GELUK & RÖHLING (1997), Van ADRICHEM BOOGAERT & KOUWE (1993-1996); GELUK et al. (1996); (DE): RÖHLING (1991a, b), HOTH et al. (1993b); (PL): SZYPERKO-TELLER (1997).

#### Distribution

The original extent of the Buntsandstein basin covers the major part of the study area. The depositional area was delineated by the Fennoscandian High in the north, the London-Brabant and Bohemian massifs to the south, the Mazurian-Byelorussian High to the east and the Irish Massif, Welsh and Grampian highs to the west. After deposition of the Middle Buntsandstein, rifting movements during the so-called Hardegsen Phase caused uplift and erosion of the Mid North Sea--Ringkøbing-Fyn High and a number of northeast trending swells in GB, NL and Germany. The absence of the Buntsandstein in the northern Netherlands onshore area and on the Cleaverbank High, however, can be attributed mainly to the Kimmerian (Middle Jurassic--Early Cretaceous) tectonic phases.

#### Facies development

The map shows the outline of the deposits of the Middle Buntsandstein. The deposits of the Buntsandstein can be subdivided into three depositional realms. The major part of the basin is occupied by lacustrine sediments, whereas in the vicinity of the basin margins braidplain and fluvial facies were developed. In the northern part of the Central North Sea Graben the Middle Buntsandstein has only been locally preserved (GOLDSMITH et al., 1995).

1. The **lacustrine facies** occupies the greatest part of the Triassic basin. The sediments are represented by the classical Germanic Triassic, in which sheet sandstones (Volpriehausen, Detfurth, Hardegsen and Solling). alternate with clay- and siltstones. These sandstones can be traced, from Poland into the southern North Sea. They were deposited in both fluvial and aeolian environments. The fluvial deposits were laid down near the margins of the lake; aeolian deposits prevail in the Central North Sea Graben. The lacustrine facies typically shows great thicknesses in northwestern Germany (>3.500 m in the Glückstadt Graben, 3.400 m in the Horn Graben) and central Poland (>1.500 m in the Mid-Polish Trough). In Poland, some marine oolitic deposits occur which are considered to point to a connection with the Tethys.

2. The **fluvial facies** displays massive sandstones in the Middle Buntsandstein intercalated between the fine-grained sediments of the Lower and Upper Buntsandstein. These are represented by the widespread Bunter Sandstone Fm GB, DK), but equivalent sandstone developments are present the southern Netherlands, Germany and Poland. The deposits in this facies range up to 350 m in thickness.

3. The **braidplain facies** contains sandy developments throughout the Buntsandstein. The facies is generally present at the margins of the Triassic basin. It is represented by the Skagerak Fm. (DK), Sherwood Sandstone Gp. (GB) and the Nederweert Mb., Main Buntsandstein Subgroup and Röt Fringe Sandstone Mb. (NL). Occasionally aeolian or alluvial fan deposits have been recorded. The deposits in this facies can reach up to 1000 m in thickness in the Norwegian-Danish Basin, 700 m in the southern Netherlands and 500-600 m in the British onshore areas. Isolated occurrences are found in the Malmedy Graben (BE) and the Mechernich and Trier areas (DE).

#### Reservoir rocks

The fluvial to aeolian sandstones of the Buntsandstein form reservoir rocks in both the British onshore and offshore areas, the Irish Sea, the southern North Sea, the southern Netherlands, the

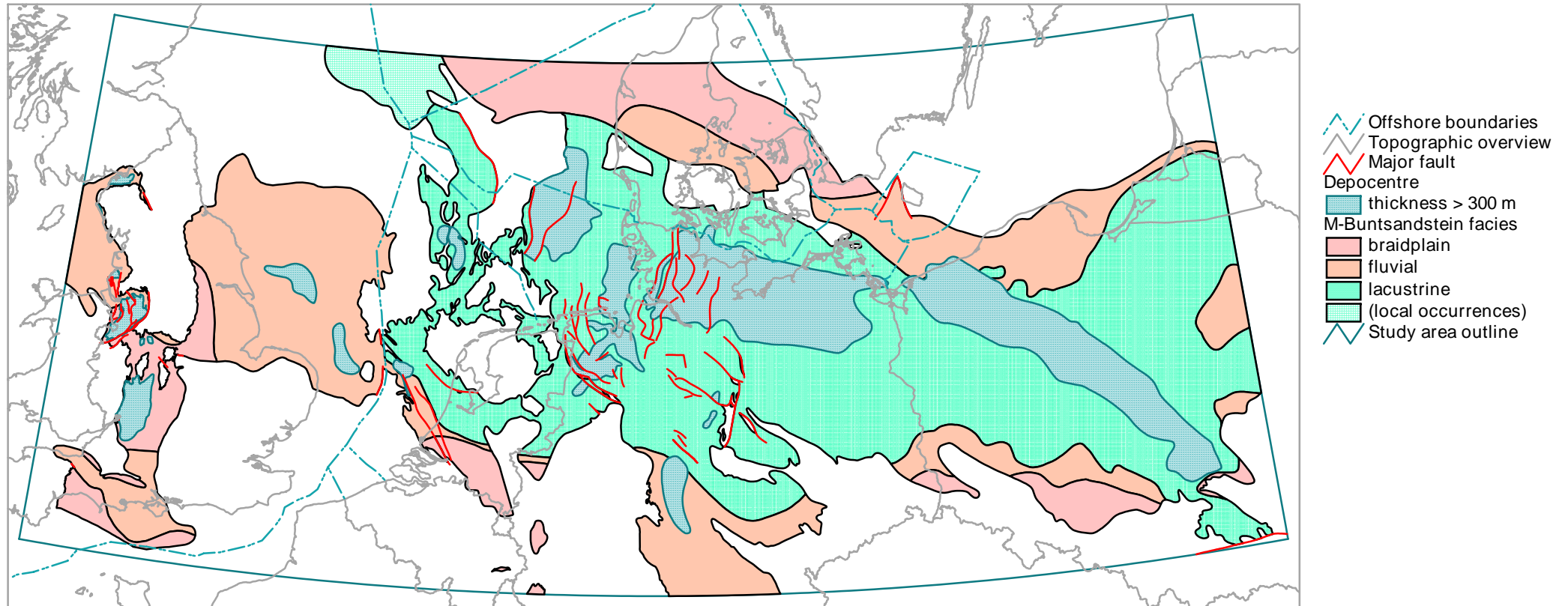
eastern Netherlands, northwestern Germany and Southern Denmark (Tønder). Salt plugging of the reservoir is known to be a problem near Zechstein salt domes (DRONKERT & REMMELTS, 1993).

Apart from the major reservoirs of the Middle Buntsandstein, local reservoirs are formed by the Amethyst Member of the Lower Buntsandstein (GB), the Josephine and Judy Sandstones in the central North Sea (GB), leached oolite beds in the Lower Buntsandstein in the eastern Netherlands (Rogenstein Mb.) and Rhaetic Sandstone in northwest Germany.

**Source rocks**

The Buntsandstein succession is composed predominantly of red-beds and is devoid of source-rocks. Only the Keuper succession contains some coaly beds or coal seams.

# Buntsandstein (Middle) -- Distribution and facies



0 110 220 330 440 550 660 Kilometers



Projection : Lambert Conformal Conic  
 Spheroid : Bessel, 1841  
 Standard parallels : 51 N and 54 N  
 Central meridian : 9 E  
 Latitude of projection origin : 48 N  
 False easting : 7,500,000 m  
 False northing : 0 m



## 3.12 Lower Toarcian (Posidonia shales), distribution and facies

### Relevance to the European Gas Atlas

The Posidonia Shale forms an important oil source rock in the western part of the study area (Northwest Germany, southern North Sea). Its suitability for gas generation has been demonstrated in northwest Germany and the Netherlands.

### Data base

Since Lower Toarcian shales form a very good seismic reflector in the western part of the study area, the compilation of this map predominantly relies mainly on seismic data, with additional well data. Modern key literature with additional references: (GB): LOTT & KNOX (1995), CAMERON et al. (1992), HAMBLIN et al. (1992); (DK): DAMTOFT et al. (1992), MICHELSEN (1989a, b), (NL): ADRICHEM BOOGAERT, van & KOUWE (1993-1996); (DE): BINOT et al. (1993); (PL): FELDMAN-OLSZEWSKA (1988).

### Distribution

The present-day distribution of the Lower Toarcian shales is limited to sites of the main Mesozoic basins: the Sole Pit, Cleveland, Wessex and Weald basins (GB); the Paris Basin (FR); the Roer Valley Graben, West Netherlands Basin, Central Netherlands Basin, (NL); Central North Sea Graben, the Lower Saxony Basin, the Prignitz Basin and some smaller basins in Schleswig-Holstein, (DE); and the Mid-Polish Trough (PL). Important palaeogeographic highs in the study area were the Welsh High, the Grampian High, the London-Brabant Massif, the Rhenish Massif, the Bohemian Massif and the Fenno-Scandian High.

### Facies development

Three facies domains have been discerned:

#### 1. Source rock facies (carbonaceous mudstones)

In the central part of the studied area, the Lower Toarcian shales form a source rock facies. Typically, the unit is developed as a black, partly limy shale, with a thickness of several tens of meters (20-50 m) in the Lower Saxony Basin, Central Netherlands Basin, West Netherlands Basin, Broad Fourteens Basin and the Central North Sea Graben. The shales have been preserved only in the central parts of these basins. In the Paris Basin in France the source rock facies ("schiste carton") reaches thicknesses between 10 and >50 m. In the Sole Pit Basin and the Cleveland Basin, just a thin organic-rich spike occurs (Jet Rock Member of the Whitby Mudstone Formation); towards the west, the unit passes into a non-source rock facies.

#### 2. Mixed facies (carbonaceous/non carbonaceous mudstones and sandstones)

In the eastern part of Germany, a gradual eastward decrease of the source-rock potential of the Lower Toarcian (Posidonia Shales) occurs. North of the Elbe river and in the Altmark a facies change occurs over a 50-70 km wide zone into the "green series", a greenish grey silty, chlorite-bearing brackish-water mudstone succession, which still has some source rock potential. The "green series" itself is as whole barren. This facies also occurs in the Danish part of the Central North Sea Graben and the Danish-Norwegian Basin.

#### 3. Non-source rock facies (non-carbonaceous mudstones and sandstones)

In the eastern part of Eastern North Germany ("the green series") and in Poland, Toarcian deposits form a sandy succession. In the Mid-Polish Trough the thickness is <300 m, in the Kalisz-Kamiensk Graben <100 m and in the Koszalin-Chojnice Graben <200 m. In the Wessex -Weald Basins in Britain, the Toarcian comprises poorly carbonaceous sandstones and claystones of varying thickness.

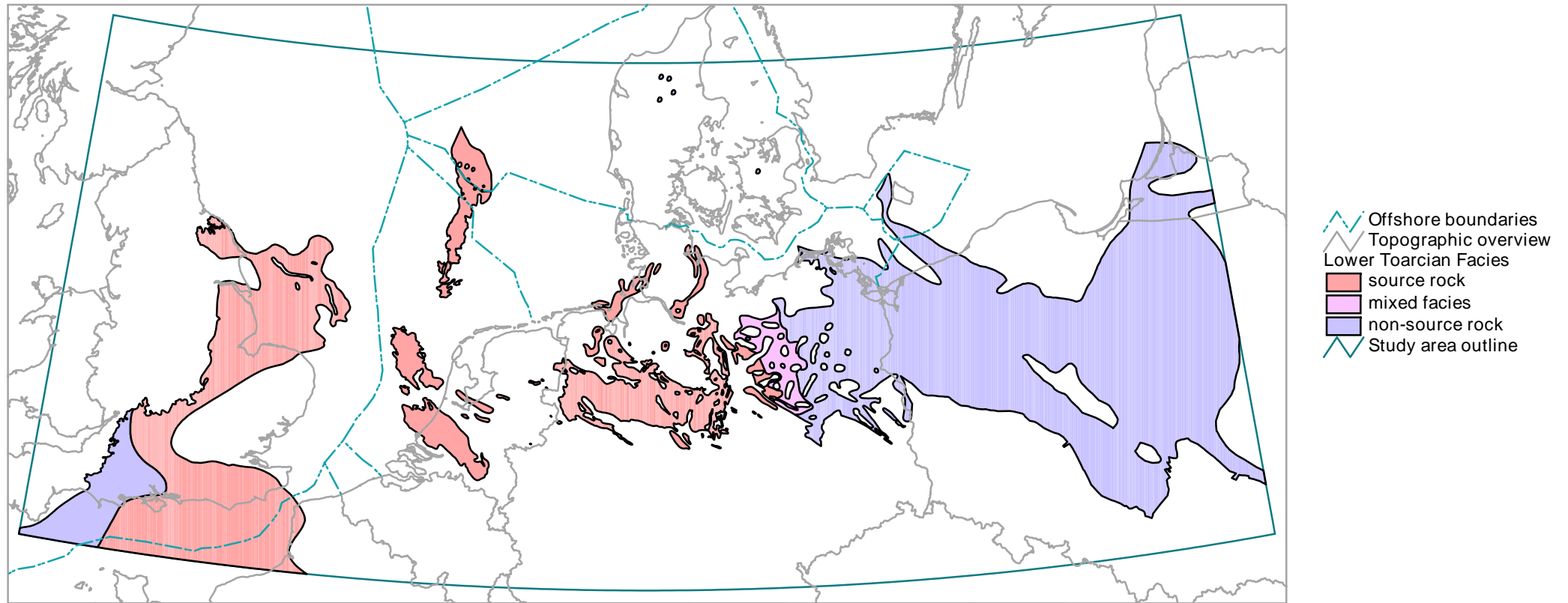
### Source-rocks

Source-rocks of the Lower Toarcian are predominantly type I (+ II), within the Broad Fourteens Basin TOC contents of up to 5% occur. In some parts of Northwest Germany according to the maturity values, TOC contents of > 12% occur. The Lower Toarcian shale sources nearly all the oil fields in the eastern and central Lower Saxony Basin, in Schleswig Holstein and in the Paris Basin as well as wet gas and condensate deposits in areas of high maturity in Northwest Germany (Thönse, Löhningen). Apart from the Lower Toarcian, thin organic-rich claystones locally occur in the Hettangian to Pliensbachian claystones (Central Netherlands Basin, West Netherlands Basin, Broad Fourteens Basin).

**Reservoir rocks**

Within the Lower Jurassic succession, Hettangian and Aalenian sandstones locally form reservoir rocks in Germany. Several Middle Jurassic sandstone units are important hydrocarbon bearing strata in the Danish-Norwegian Basin, in the Lower Saxony Basin, the Schleswig Holstein troughs and the Central North Sea Graben; the same applies to time-equivalent limestones in the Paris Basin. In the Wessex Basin (GB) the Late Toarcian Bridgeport Sandstone Formation and Middle Jurassic oolitic limestones are an important reservoir horizons.

# Lower Toarcian (Posidonia shales) -- Distribution and facies



0 110 220 330 440 550 660 Kilometers



Projection : Lambert Conformal Conic  
Spheroid : Bessel, 1841  
Standard parallels : 51 N and 54 N  
Central meridian : 9 E  
Latitude of projection origin : 48 N  
False easting : 7,500,000 m  
False northing : 0 m

### 3.13 “Upper Jurassic” (Oxfordian to Berriasian), distribution and facies

#### Relevance to the European Gas Atlas

The “Upper Jurassic” (Oxfordian to Berriasian) comprise both source rock for oil and gas and reservoir rocks in the North Sea area (Central North Sea Graben, Danish-Norwegian Basin, Sole Pit Trough).

#### Data base

The compilation of this map relies on seismic and well data. Modern key literature with additional references: (GB): LOTT & KNOX (1995), CAMERON et al (1992). WHITTAKER et al. (1985); (DK): DAMTOFT et al. (1992), VEJBÆK (1992); (NL): ADRICHEM BOOGAERT, van & KOUWE (1993-1996), WONG et al. (1989); (DE): DULCE et al. (1993), BALDSCHUHN, KOCKEL & FRISCH (ed.) (1996); (PL): NIEMCZYCKA (1997).

#### Distribution

The occurrence of “Upper Jurassic” rocks is limited mainly to the Late Jurassic rift basins. These are the Sole Pit Trough, Cleveland Basin, Wessex-Weald Basin, Portland Wight Basin (GB), Central North Sea Graben, Danish-Norwegian Basin, Vlieland Basin, Broad Fourteens Basin, West Netherlands Basin, Central Netherlands Basin, Roer Valley Graben (NL), Lower Saxony Basin, Prignitz Basin (NL, DE) and the Mid-Polish Trough (PL). The broad similarity of the marine deposits in the western part of the study area suggest, that between several of these basins during deposition a connection existed. An exception is the Lower Saxony Basin (DE), which stood out as an isolated basin with evaporitic to lacustrine deposition. Highs bordering the basins were the Grampian High, Welsh High, London-Brabant Massif, Cleaver Bank High, Mid North Sea High, Ringkøbing-Fyn High, North Netherlands High, Pompeckj Block, Rhenish Massif, Bohemian Massif. In part these highs formed only low-lying barriers between the different basins, and may as such have been covered with sediments. Many of the highs were accentuated and their cover was eroded during the Early Cretaceous.

#### Facies development

Four different facies domains have been identified:

##### 1. Berriasian source-rock facies (organic-rich limnic shales)

The occurrence of this facies is limited to the Lower Saxony Basin (Bückeberg Fm., Coevorden Fm.). Parts of the so-called “Germanic Wealden” are developed as an organic-rich paper shale (Wealden-3, -4 and -6) in the western part of the basin. These source-rocks generated the major part of the oil in the German Emsland area, and minor quantities of gas. They are of limnic origin and belong to source-rock type I. Towards the west, the deposits grade into paralic sediments in the Central Netherlands Basin, towards the east into fluvio-deltaic sandy deposits with intercalated coal seams..

##### 2. Ryazanian source rock facies (bituminous marine mudstones)

These deposits comprise the source-rocks in the central and northern North Sea areas. The most important of these are known as the Clay Deep Fm. (NL) and the Hot Unit of the Farsund Fm. (DK). They attain a thickness of up to 60 m. Towards the south, these source-rocks grade into paralic sediments.

##### 3. Kimmeridgian source rock facies (bituminous marine mudstones)

The Kimmeridge Clay is a mudstone succession showing complex cyclic variations in its organic matter and carbonate content. In its type area the middle part of the unit, contains numerous bituminous mudstone beds. Similar coeval developments occur in the Paris and Weald basins and in the Sole Pit Trough.

##### 4. Non-source rock facies

In other areas, the “Upper Jurassic” is developed in a non-source rock facies. This facies includes a fluvial to paralic development in the Vlieland Basin, Broad Fourteens Basin, West Netherlands Basin, Central Netherlands Basin and the Roer Valley Graben (NL) and isolated occurrences of sandy, fluvial to paralic deposits in secondary rim synclines of salt structures on the Pompeckj Swell (DE) and the North Netherlands High. In the Mid-Polish Trough, the “Upper Jurassic” is represented by a calcareous facies.

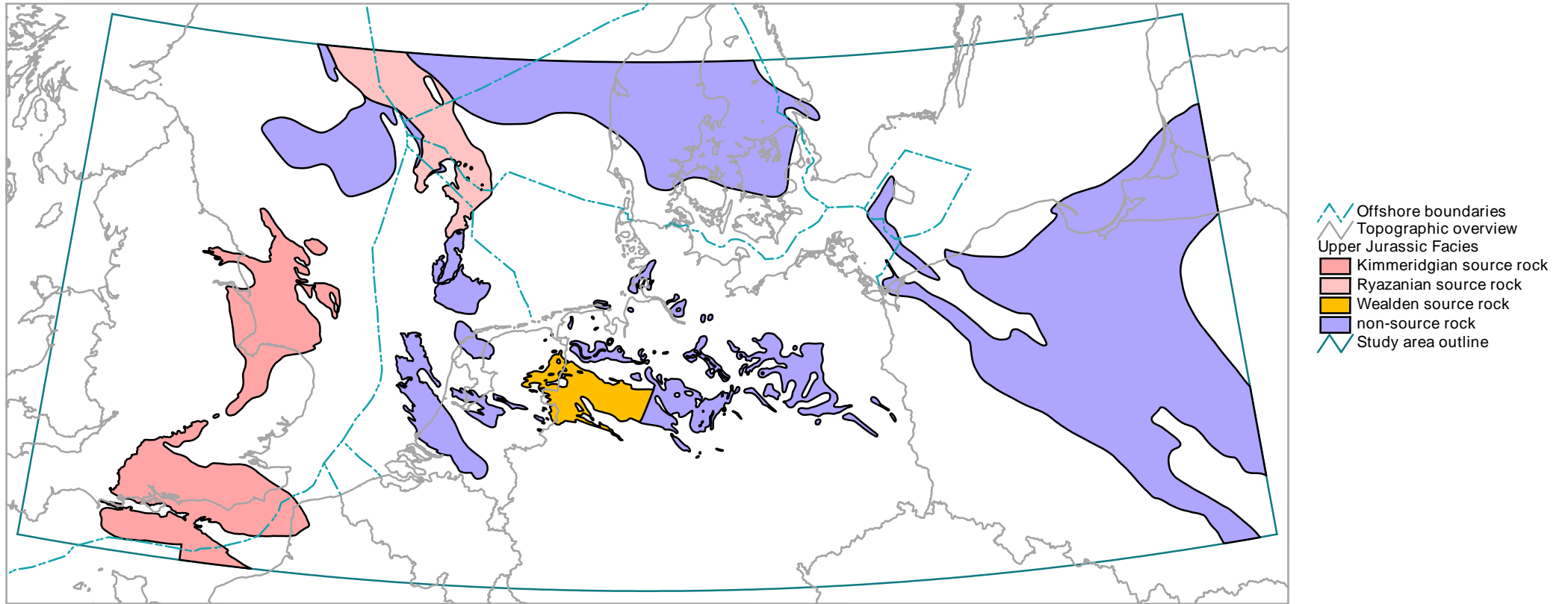
#### Source rocks

Limnic source rocks of the Berriasian in the Lower Saxony Basin comprise Type I + II source rocks; their TOC varies from 1.2 up to 5.1%. Source rocks occurring in the western part of the study area (Kimmeridgian-Ryazanian) comprise Type I + II kerogen. The TOC content of the Kimmeridgian varies between 5-10%. Furthermore, paralic deposits occurring in many basins in the Netherlands contain abundant coal layers in places; these form potential Type III source rocks. They are, however, generally of low maturity.

### **Reservoir rocks**

The "Upper Jurassic" contains a great number of reservoir horizons in the area. Upper Jurassic sandstones form important reservoirs in the Norwegian-Danish Basin and the Central North Sea Graben (Oxfordian - Ryazanian). In the Lower Saxony Basin (DE) "Upper Jurassic" sandstones (Oxfordian, Early Kimmeridgian, Ryazanian (Bückeberg sandstone) and carbonates (Kimmeridgian, Portlandian) form reservoirs in places. In the West Netherlands Basin there are Portlandian-Ryazanian sandstone reservoirs. In both these basins, however, the main reservoirs occur in Lower Cretaceous sandstones

# "Upper Jurassic" (Oxfordian to Berriasian) -- Distribution and facies



0 110 220 330 440 550 660 Kilometers



Projection : Lambert Conformal Conic  
Spheroid : Bessel, 1841  
Standard parallels : 51 N and 54 N  
Central meridian : 9 E  
Latitude of projection origin : 48 N  
False easting : 7,500,000 m  
False northing : 0 m

### 3.14 Salt structures (Rotliegend and Zechstein salt)

#### Relevance to the European Gas Atlas

The extensive development of salt structures within the Central European Basin, often with a subsurface relief of several kilometres, has produced a significant structural grain to the study area.

#### Data base

Modern key literature with additional references includes: (GB): JENYON (1985, 1986,), JACKSON ET AL (1995); (DK): VEJBÆK & BRITZE (1994); (NL): GELUK (1995), REMMELTS (1995, 1996); (DE): KOCKEL (ed. (1995), BALDSCHUHN, KOCKEL & FRISCH (ed.) (1996), ZGI (1990), (PL): DADLEZ (1977, 1980).

#### Salt structures

Only the salt pillows and salt diapirs consisting of Rotliegend and Zechstein 2-7 salts are considered in the map. Other salt structures (salt intrusions, salt-lubricated thrusts, stratiform layers) and salt pillows formed by the Werra Salt (Z1), Upper Buntsandstein, Middle Muschelkalk, Middle Keuper or Upper Jurassic salts have been omitted. Salt structures containing Rotliegend salt are limited to the central parts of the Upper Rotliegend desert lake in the Elbe Estuary, in Schleswig-Holstein and the German Bight. All the other salt structures displayed consist only of Zechstein salts.

By definition salt pillows (domes) are salt with intact or nearly intact sedimentary cover. Salt plugs (diapirs) are structures, which pierce this cover and are capped by sediments much younger than the Upper Permian. Pillows are structures of relatively low amplitude in comparison with salt diapirs. They are normally accompanied by other halokinetic features which affect neighbouring sediments such as primary or secondary rim synclines. Their outline (round, oval or elongated = salt wall) merely expresses irregularities in the underlying basement and is not a criteria for classification.

#### Salt pillows

Salt pillows contain, at their core, a considerably greater vertical thickness of salt than was originally deposited, because of salt migration.. The tectonically mobilised salt migrated more or less horizontally into the structure causing upwarping of the post-Permian sedimentary cover. Tensional stresses in this sedimentary cover formed crest grabens and faults. Salt pillows are most typical of regions without intense faulting of the underlying pre-Permian basement. Salt diapirs do not inevitably form from all salt pillows, but most diapirs are normally generated from earlier salt pillows.

Salt pillows developed only in structurally quiet areas like the Friesland Platform, Groningen Block, West Schleswig Block, East Holstein-Mecklenburg Block, Northern and Eastern Brandenburg. They are also very common in the area of the Pomeranian-Kujavian Swell and the inverted Mid-Polish Trough where Zechstein salt deposits reached their greatest thickness. Areas with limited primary salt thickness like the Hunte Swell in Southern Oldenburg or in the Subhercynian realm, north of the Harz Mountain, are also devoid of salt diapirs. In Poland salt pillows do not occur in those parts of the Zechstein basin, situated to the northeast of the Teisseyre-Tornquist zone or on the East European Platform, which is less tectonically deformed. Small pillows consisting of Werra Salt in the German-Netherlands border region have not been shown in the map. Areas in which the Zechstein is partly or completely eroded as locally on the Cleaver Bank High or the Schillgrund High also show no evidence of halokinetic structures.

#### Salt diapirs

Salt diapirs as a rule straddle major basement faults or fault zones. Often several diapirs may be connected by salt pillow bridges, straddling the same basement fracture zone. The position shape and orientation of their long axis usually reflect the fault pattern and block limits in the underlying pre-Permian basement. Structures which have all exerted considerable influence on the trend of the salt structures in the basin include: the NW-SE trending in the Pomeranian-Kujavian inversion structure, the NW-SE trending Central German Fault Zone (= Mitteldeutsche Abbrüche) - Uelzen Lineament (= Elbe Lineament), the Aller Lineament, the NNE-direction of the Reinsberg lineament, the Braunschweig-Gifhorn fracture zone and the internal and border faults of the Glückstadt Graben, the Horn Graben and the Central North Sea Graben, the Terschelling Basin, the western margin of the Lower Saxony Basin as well as the strongly fractured Ems Estuary region. In Poland the occurrence of salt diapirs is concentrated in the Pomeranian-Kujavian swell. They are less numerous than the salt pillows and are often surrounded by residual pillows.

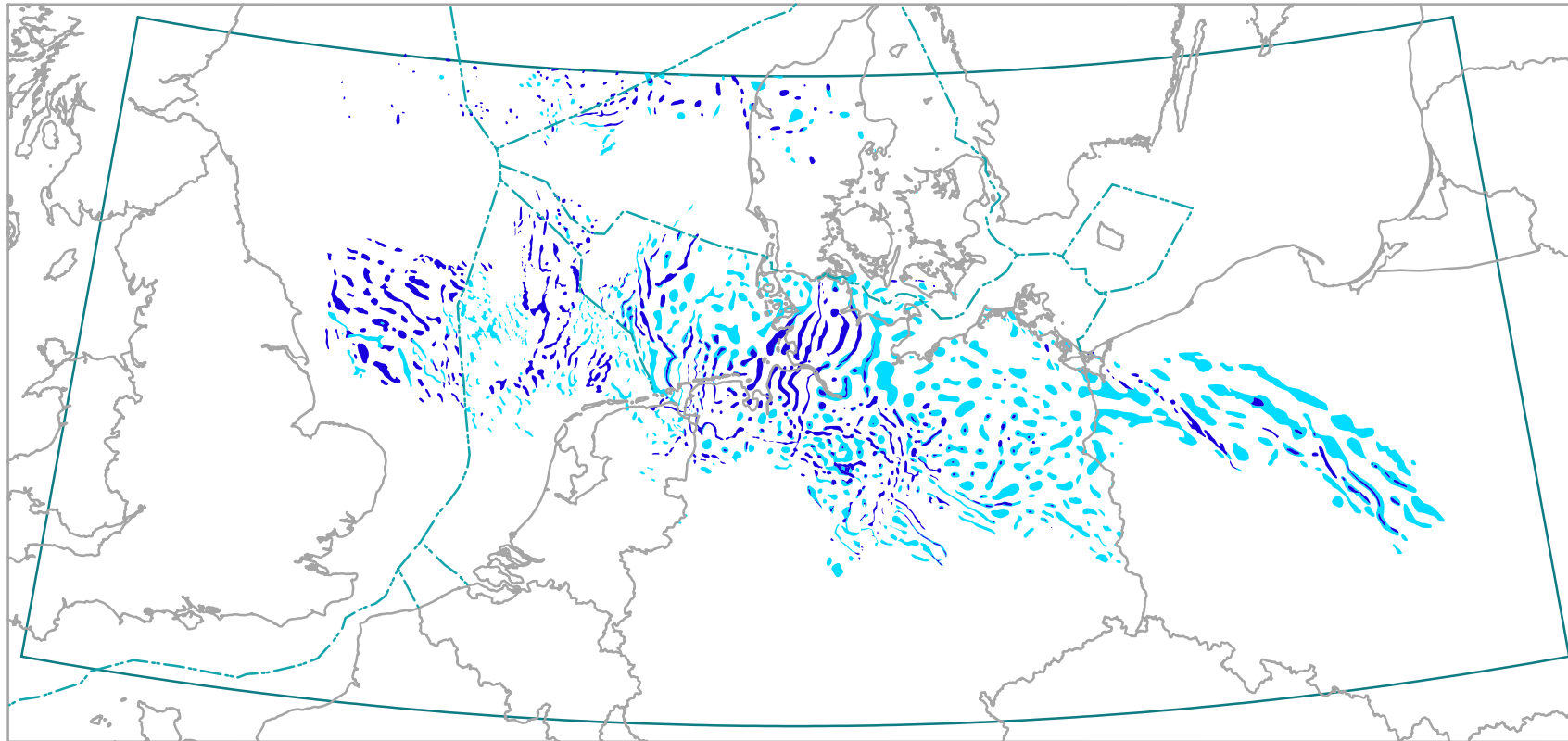
The age of the diapiric piercement of the salt diapirs coincides with extensional tectonic pulses primarily in the Scythian, Middle Keuper, Middle Jurassic to Early Cretaceous and Palaeogene. Diapiric piercement can be dated by the first filling of the secondary rim sinks. In compressional regimes, such as that which occurred during Late Cretaceous inversion, salt diapirs may be overprinted and reshaped, squeezed and compressed and in some cases may even detach from the host Permian salt layer and form salt balls freely floating in the Mesozoic sediments.

The culminations of salt pillows and the deformed sedimentary flanks of diapirs in some areas form hydrocarbon-traps within Mesozoic reservoirs (e.g. in the Central North Sea Graben and in the Lower Saxony Basin). In offshore Denmark and in Northwest Germany hydrocarbon traps have formed in Upper Triassic, Jurassic, Maastrichtian and Danian reservoirs on the tops of salt diapirs. Nevertheless salt plugging of the reservoirs in the vicinity of salt diapirs may reduce the reservoir properties considerably (DRONKERT & REMMELTS, 1993).

Several authors have suggested that the higher heat conductivity of the salt may generate a potential chimney effect and thus diminished maturity below the salt structures. In areas of high maturity of source rocks this would have a positive effect on gas productivity.



# Salt structures -- (Rotliegend and Zechstein salt)



- Offshore boundaries
- Topographic overview
- Salt structures
  - dome
  - pillow
- Study area outline

0 110 220 330 440 550 660 Kilometers



Projection : Lambert Conformal Conic  
Spheroid : Bessel, 1841  
Standard parallels : 51 N and 54 N  
Central meridian : 9 E  
Latitude of projection origin : 48 N  
False easting : 7,500,000 m  
False northing : 0 m

### 3.15 Intrusives (Palaeozoic and Mesozoic)

#### Relevance to the European Gas Atlas

Igneous intrusives are of relevance to the study as an aid to understanding the complex organic maturation patterns present in the source rocks.

#### Data base

This map is based on maturity data, with supporting gravity and magnetic anomaly data and some well and seismic data. Modern key literature with additional references includes: (GB): DONATO ET AL (1983); PHAROAH ET AL (1996); (DE): TEICHMÜLLER & TEICHMÜLLER (1950, 1982), TEICHMÜLLER et al. (1984), KOCH, KOCKEL & KRULL (1997); (PL): JACKOWICZ (1994), GROCHOLSKI & RYKA (1995).

#### Distribution

Intrusives have been identified throughout the entire study area. The age of some these intrusions have been dated either by direct sampling and radiometric age determination or by dating the roof sediments affected by the coalification halo

#### Palaeozoic intrusives

In Poland three marked coalification anomalies within the Carboniferous rocks have been observed in the Variscan Externides E and NE of Wrocław. Rr-values in the vicinity rise to 4 and 4.5% respectively. These coalification anomalies coincide with gravity and magnetic anomalies. An intrusive body of acid composition has been drilled northwest of Poznań in the Chrzypsko well.

In Germany several late Variscan intrusive bodies have been either proved or inferred.

Their influence (> 3.3% Rr at the top Pre-Permian) has been observed in central and southern Rügen island and on the adjacent main land, coinciding with a strong magnetic anomaly. Basic and acid dikes (probably apophyses) have been drilled.

The magnetic, gravity and magnetotelluric anomaly of Pritzwalk (East Elbian Massif) is interpreted by some authors to be caused by a Late Variscan basic or ultrabasic intrusion (mantle diapir) with its top at 18 km depth.

High coalification (> 4% Rr in the Namurian) in the Magdeburg-Roxförde-Velpke Asse area, partly coinciding with the gravity anomaly of Magdeburg, is very likely to have been caused by an acid intrusion and its apophyses, drilled in Flechtingen and Velpke Asse and radiometrically (Rb/Sr) dated  $264 \pm 9$  Ma.

Well known, and radiometrically (Rb/Sr) dated (292 Ma and 296 Ma Bp.), are the granitic intrusions of Brocken, Oker and Ramberg in the Harz Mountains with their contact metamorphic haloes.

In the Lippstadt Dome and the Warstein region a magnetic anomaly coincides with a strong coalification anomaly in the Devonian (>4.6% Rr). It is inferred to be caused by a granitic intrusion at ca. 3000 m depth.

At Krefeld a weak magnetic and coalification anomaly (> 2.8% Rr) is possibly caused by a pre-Upper Permian gabbroic intrusion at 3000 m depth.

Near the German-Dutch border at Erkelenz a strong magnetic (but no gravity) anomaly coincides with a strong coalification anomaly in the Westphalian A (3.2-3.6% Rr). A similar anomaly has also been observed in the southeastern Netherlands. Hydrothermal influences point to a Late Variscan basic to ultrabasic intrusion at 3-4 km depth.

Near Monschau in the High Venn a Late Variscan tonalitic intrusion (Lammersdorf) has caused a strong magnetic and coalification anomaly (> 6% Rr).

On the Cleaverbank High and in other areas of the southern North Sea, small Variscan intrusives have locally been encountered.

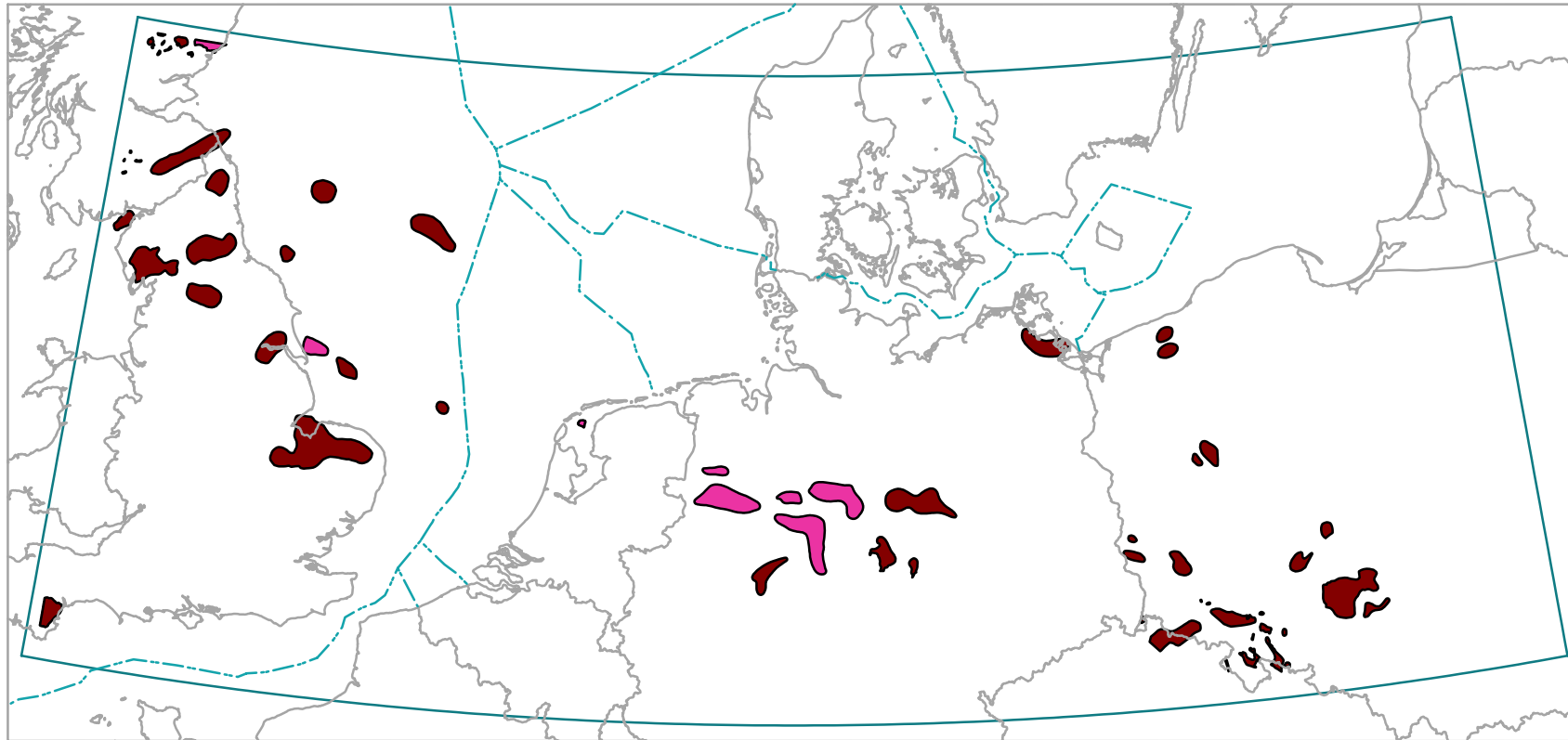
#### Mesozoic intrusives

Mesozoic intrusions thermally affect not only the pre-Permian basement but also the Mesozoic cover. In the Central North Sea Graben area Middle Jurassic intrusions are of widespread occurrence. They also occur locally in other areas. A Late Jurassic intrusion, with associated volcanoclastics, has been encountered in the Vlieland Basin in the Netherlands (Zuidwal).

Coalification anomalies in combination with magnetic and gravity anomalies and partly associated with hydrothermal indications are well known from the central part of the Lower Saxony Basin (DE): Bramsche Massif, Uchte Massif and Vlotho Massif, with a prolongation to the southeast into the Solling, and with the recently discovered Neustadt-Heessel anomaly. Intrusions or apophyses are inferred from the coalification and gravity anomalies of Nordhorn and Apeldorn. The age of these intrusions is not precisely known. Geological data point to an age between Valanginian and Campanian or Aptian to Campanian, apatite fission track data to a thermal event at 100 to 70 Ma Bp.

The thermal impact of both these Late Variscan and the Mesozoic intrusive bodies on the Palaeozoic and Mesozoic source rocks in their vicinity should not be underestimated. They are surrounded by large haloes in which all potential source rocks, even the Liassic and Early Cretaceous ones, are completely overcooked and do not have any remaining hydrocarbon-potential. Additionally in the vicinity of the Mesozoic intrusive bodies high CO<sub>2</sub>-contamination of the natural gases occur and a higher percentage of mantle originated helium has been measured.

# Intrusives -- (Palaeozoic and Mesozoic)



- Offshore boundaries
- Topographic overview
- Intrusive body
  - Mesozoic age
  - Palaeozoic age
- Study area outline

0 110 220 330 440 550 660 Kilometers



Projection : Lambert Conformal Conic  
Spheroid : Bessel, 1841  
Standard parallels : 51 N and 54 N  
Central meridian : 9 E  
Latitude of projection origin : 48 N  
False easting : 7,500,000 m  
False northing : 0 m

## 4. DISTRIBUTION OF SELECTED GAS COMPONENTS AND PARAMETER

### Introduction

The geochemical signatures of natural gases can provide information about its source, e.g. whether it is of bacterial origin or thermally generated at a variety of stages and/or kerogen types. Additionally, gas mixtures from different sources or altered gases can often be identified (e.g. SCHOELL 1983, WHITICAR 1990). Inter- or intra-reservoir correlation, determination of hydrocarbon source potential and migration pathways, and input into basin analysis models are among the immediate applications of geochemical information obtained from subsurface natural gases. All these applications are based on the fact that there are significant and predictable compositional variations between the various gas types.

Beside this local (genetic) information the distribution of gas constituents or physical gas parameter on a regional scale can provide valuable information about the natural gas quality either for exploration purposes or for gas trading companies. For this gas atlas, we have decided to map methane ( $\text{CH}_4$ ), nitrogen ( $\text{N}_2$ ), carbon dioxide ( $\text{CO}_2$ ), the gas composition methane/(ethane+propane) [ $\text{C}_1/(\text{C}_2+\text{C}_3)$ ], the stable carbon isotope ratios of methane ( $\delta^{13}\text{CH}_4$ ), calorific values, and gas densities. These parameter are chosen since they are most important ones to describe the natural gas quality. Most data already existed, some had to be measured (e.g. carbon and nitrogen isotopes) or even calculated (e.g. physical gas parameter).

Our strategy was to map the above mentioned parameter separately for four reservoir horizons identified in the study area: Carboniferous, Rotliegend, Zechstein, and post-Zechstein. Carboniferous reservoirs comprise mainly Upper Carboniferous (Namurian, Westphalian) in the western part of the study area, and both Lower and Lower Carboniferous (Dinantian) in Poland. Post-Zechstein reservoirs occur mainly in the Buntsandstein, but sometimes in Jurassic, Cretaceous and Cenozoic strata. There are no post-Zechstein reservoirs in Poland and eastern Germany.

Contouring intervals were determined using a statistical approach. It appeared that the application of a straightforward linear contour interval for most of the parameters would have obscured valuable information. For example, the  $\text{CO}_2$  percentage of gases is a very important parameter, and provides information concerning the corrosivity of the natural gas in pipelines. The application of a linear contour interval covering the range of 0 to 45%  $\text{CO}_2$  in Rotliegend gases would have placed 96% of the data within the 0-4.5% interval of  $\text{CO}_2$ . For commercial reasons related to the choice of resistant transporting and clean-up materials and economic strategies companies are much more interested in information pertaining to the interval between 0 and 2%  $\text{CO}_2$ . Maps based on the linear contour intervals would not provide such information.

Another example is the spatial distribution of nitrogen. In the case of a linear contour interval covering the range of  $\text{N}_2$  percentages in the Rotliegend gases would place 86% of the observations in 2 intervals between 0 and 17%. In this case a reasonable map would have been obtained for the eastern part of the study area. However, subtle differences in the percentages of  $\text{N}_2$  in the natural gases produced in the centre of the study area - the area where a large amount of gas is produced - would have been obscured.

The same conclusion can be made for the distribution of methane. 84% of the datapoints lie within the in the two intervals of 80-90, and 90-100% of  $\text{CH}_4$ . Subtle differences in the western part of the study area would be obscured.

Similar conclusions can be made for all the other gas components as well as for the physical parameters of gas density and calorific value.

Therefore it was attempted to choose contour intervals for each parameter in such a way that each interval contains more or less the same amount of data. This results in maps with a reasonable spread in information density. The procedure is briefly described here. Using the contour intervals calculated in this way, each map will show a balanced amount of information per contour interval. In practice, however, the contours intervals were approximated to enlarge the readability of the maps.

The following paragraphs will start each with a general introduction about the mapped parameter followed by a description of the relevant four maps.

## 4.1 Methane

Methane is produced in nature through two dominant processes, methanogenesis and thermogenesis. During methanogenesis the two dominant metabolic processes forming microbial methane are reduction of CO<sub>2</sub> and fermentation of acetate (e.g. WHITICAR et al., 1986). These two processes are each dominant in a different depositional environment: reduction of CO<sub>2</sub> in marine settings and fermentation of acetate in freshwater settings. Methanogens, the micro-organisms which perform methanogenesis, are achaeobacteria which live only in anaerobic, reducing environments.

Thermal methane is formed as organic matter in buried sediments is subjected to elevated temperatures (ca. 60°C) and undergoes decomposition. In case of sapropelic organic matter, this process typically involves generation of oil and gaseous products like methane and higher weight hydrocarbons (e.g. HUNT, 1989). Although methane dominated in such gases heavier gaseous hydrocarbons (i.e. higher alkanes) are present in considerably amounts. Such gases have a 'wet' gas signature. In case of thermal alteration of humic organic matter, however, the heavier hydrocarbon gases are only found in low concentrations. The prevailing methane usually makes up more than 90% of the gaseous hydrocarbons ('dry' gas signature).

In the late stages of thermogenesis, as temperatures increase above 120-150°C, higher hydrocarbon gases occur only in traces. Methane becomes the predominant product, generated by thermal cracking of kerogen, bitumen, and oil. This is valid for any type of organic matter.

According to RICE & CLAYPOOL (1981), 20 percent of all known commercial gas accumulations are composed of microbial gas, whereas 80 percent are of thermogenic origin. Actually this estimate is under debate as the classification of NW Siberian gases is insecure.

The following explanations briefly describe the four maps which display the methane contouring within the four reservoir horizons Carboniferous, Rotliegend, Zechstein, and post-Zechstein.

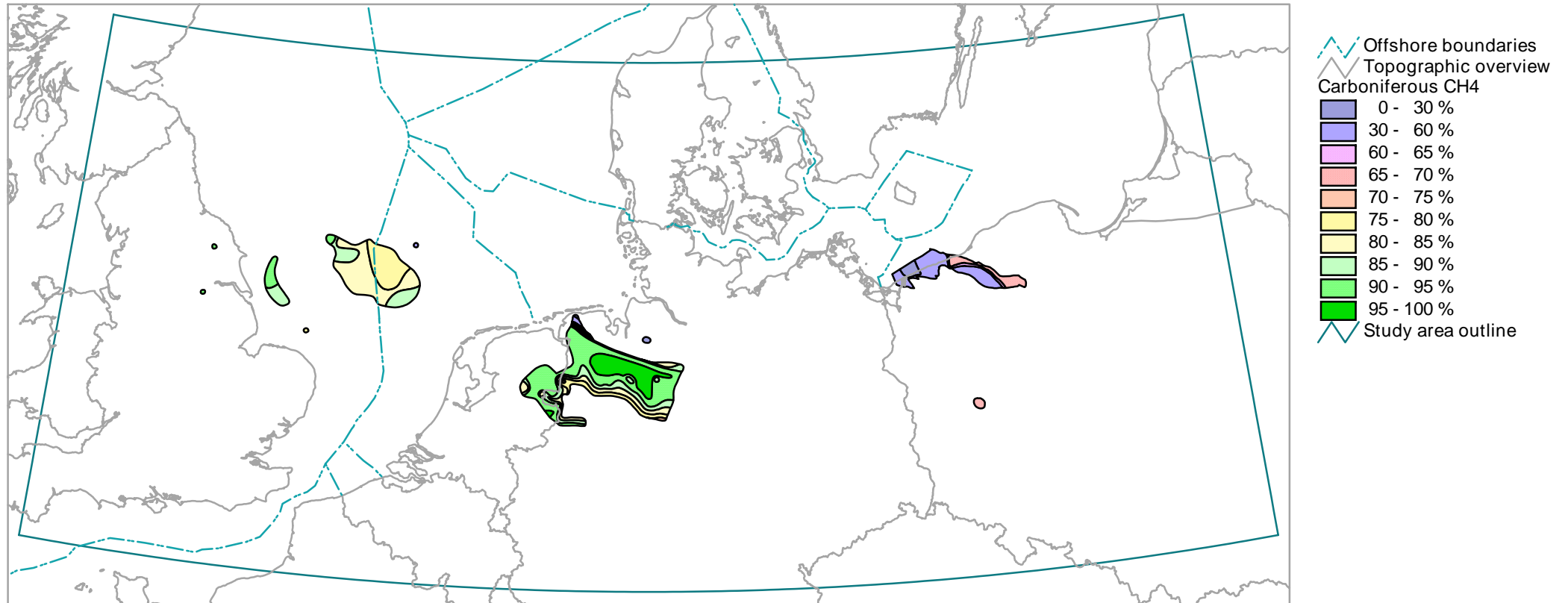
The methane content in **Carboniferous** gases is based on reservoir data and DSTs. In the North Sea and onshore UK, CH<sub>4</sub>-contents usually exceed 75%. The same is valid for NW Germany and the eastern part of the Netherlands. In this area, methane contents rapidly decrease at the southern as well as at the northeastern rim. In Poland, CH<sub>4</sub>-contents are generally below 75%.

The methane content in **Rotliegend** strata is based on reservoir data and DSTs. Almost in the entire area from the UK until middle Germany, CH<sub>4</sub>-contents exceed 80%. Interestingly, the methane contents decrease towards NE in a short distance along the northeastern rim of the Rotliegend-fairway in NW Germany. From the large reservoir Altmark onwards to the east, methane contents decrease below 30%, but increase again in Poland up to more than 80% in the Fore-Sudetic Monocline.

The CH<sub>4</sub>-contents in **Zechstein** strata is based on reservoir data and DSTs. In the North Sea, in the Netherlands as well as in NW Germany, methane contents are regularly above 70%. Small areas with lower CH<sub>4</sub>-concentrations are often due to TSR (Thermochemical Sulphate Reduction, see 4.8.1) or intrusives. In Poland, methane contents are rather low, they rarely exceed 65%.

The CH<sub>4</sub>-content in **post-Zechstein** gases is based on reservoir data and DST's. The methane content is usually higher than 70%. Only a few areas contain natural gas with lower methane concentrations.

# CH4 contour map - Carboniferous reservoir gas

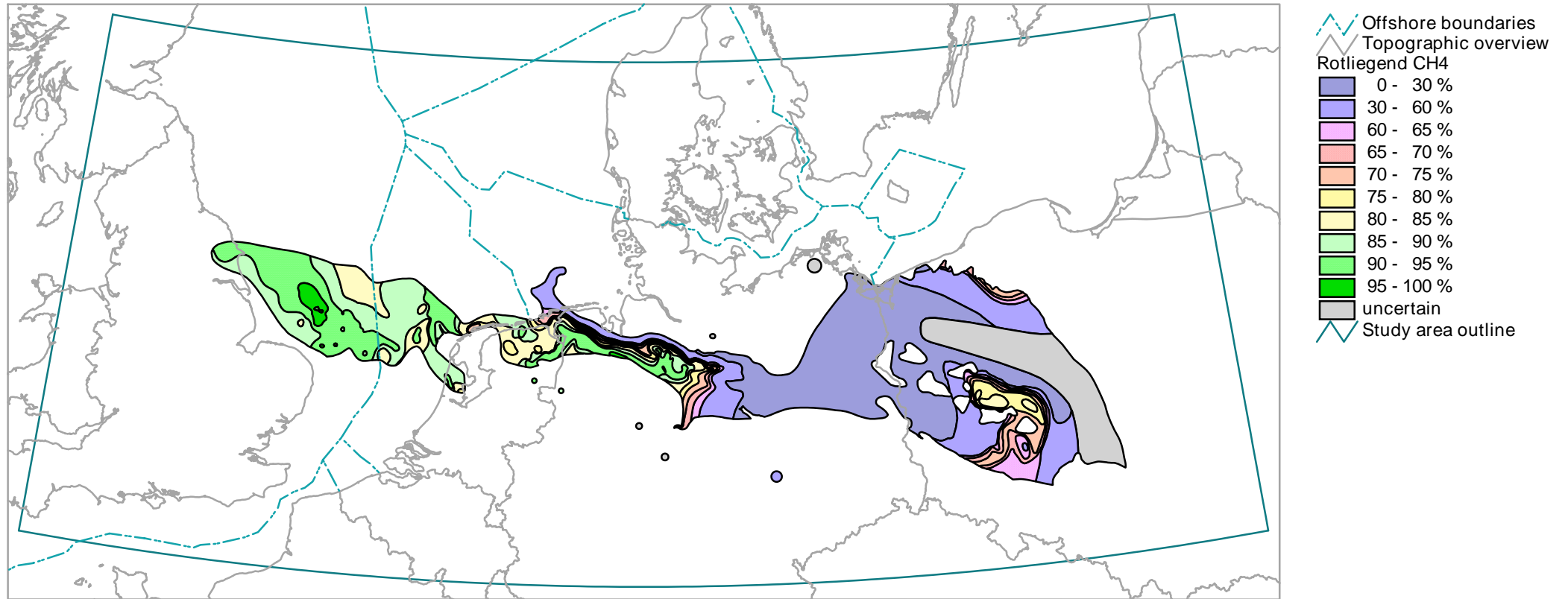


0 110 220 330 440 550 660 Kilometers



Projection : Lambert Conformal Conic  
Spheroid : Bessel, 1841  
Standard parallels : 51 N and 54 N  
Central meridian : 9 E  
Latitude of projection origin : 48 N  
False easting : 7,500,000 m  
False northing : 0 m

# CH4 contour map - Upper Rotliegend reservoir gas



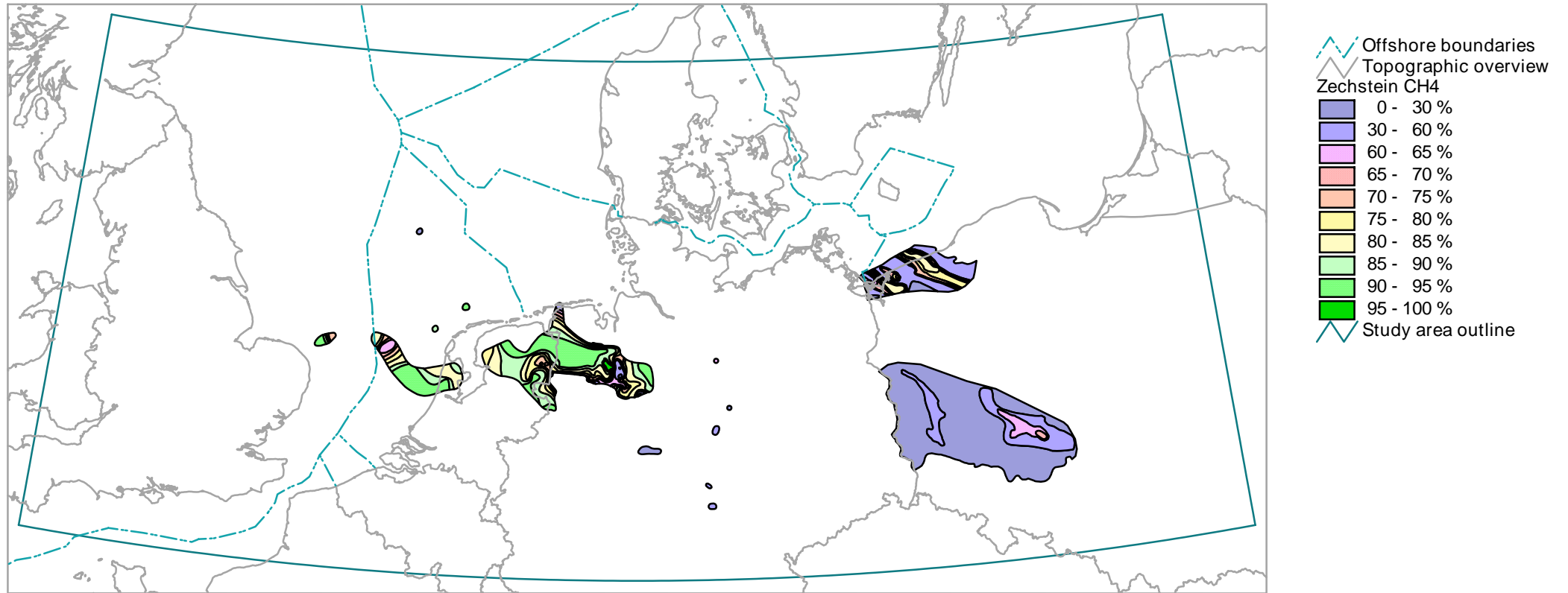
0 110 220 330 440 550 660 Kilometers



Projection : Lambert Conformal Conic  
Spheroid : Bessel, 1841  
Standard parallels : 51 N and 54 N  
Central meridian : 9 E  
Latitude of projection origin : 48 N  
False easting : 7,500,000 m  
False northing : 0 m



# CH4 contour map - Zechstein reservoir gas

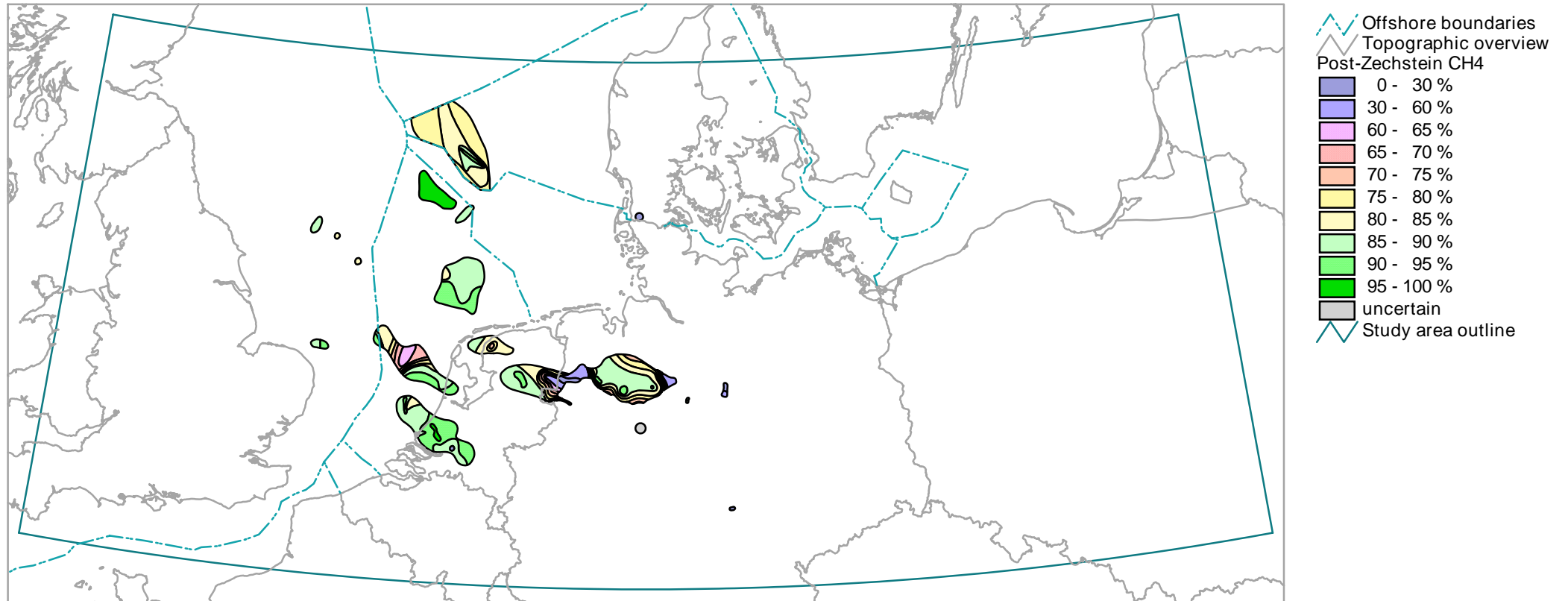


0 110 220 330 440 550 660 Kilometers



Projection : Lambert Conformal Conic  
Spheroid : Bessel, 1841  
Standard parallels : 51 N and 54 N  
Central meridian : 9 E  
Latitude of projection origin : 48 N  
False easting : 7,500,000 m  
False northing : 0 m

# CH4 contour map - Post-Zechstein reservoir gas



0 110 220 330 440 550 660 Kilometers



Projection : Lambert Conformal Conic  
Spheroid : Bessel, 1841  
Standard parallels : 51 N and 54 N  
Central meridian : 9 E  
Latitude of projection origin : 48 N  
False easting : 7,500,000 m  
False northing : 0 m

## 4.2 Stable Carbon Isotope Ratios of Methane

The origin of methane is closely related to the diagenetic and thermal alteration of organic matter (see 4.1). Stable carbon isotopes give important information on their genetic history.

Methanogens cause enrichment of lighter isotope during methanogenesis, producing values of  $\delta^{13}\text{C} < -60\text{‰}$  whereas thermogenic values are typically  $> -50\text{‰}$ . Values between  $-60$  and  $-50\text{‰}$  are often attributed to mixing of thermal and microbial gases. Oil-associated gases have  $\delta^{13}\text{CH}_4$  values between  $-50$  and about  $-35\text{‰}$ . Late-stage thermal gases (formed during metagenesis) have higher isotopic signatures because the available organic matter is enriched in  $^{13}\text{C}$  due to earlier fractionation which preferentially removed  $^{12}\text{C}$ .

Generally, carbon isotope ratios of thermal gases are thought to increase with increasing maturity of their precursors. This is explained through a kinetic isotope effect by which  $^{12}\text{C}$ - $^{12}\text{C}$  bonds of the kerogen are preferentially cracked leading to an enrichment of  $^{13}\text{C}$  in the precursor sites, whereas light hydrocarbons are depleted in  $^{13}\text{C}$  compared to the kerogen.

Carbon isotopes have been used for a long time to characterise the generation of natural gases. In an empirical approach STAHL (1968) and STAHL & CAREY (1975) were the first to use qualitatively the stable carbon isotope composition of methane to characterise type and maturity of the source rock, as well as its post-genetic history. Later on numerous other researchers came up with further suggestions how to use stable carbon isotopes of gases in hydrocarbon exploration (see Chapter 5).

SCHOELL (1980) introduced a combination of stable carbon and hydrogen isotopes of methane to determine its origin. He was able to differentiate using D/H ratios between bacterial and thermogenic methane of various origins. Similar to  $^{13}\text{C}/^{12}\text{C}$  ratios, D/H ratios increase with increasing rank of the source materials. Fig. 4.1 shows a diagnostic plot in which carbon and hydrogen isotope ratios of methane are plotted against each other. This 'CD-diagram', developed by SCHOELL (1980, 1984) and WHITICAR et al. (1986) contains certain fields for common bacterial and thermogenic methane gases. The field of thermal methane is further subdivided in areas for non-associated gases from marine and terrestrial precursor materials (after SCHOELL, 1984).

However, it came out that the C/D diagram is of greater importance when determining methane from the various methanogenic pathways than for a characterisation of thermal methane gases. In order to describe the genesis of natural gases from the deep subsurface, carbon isotopes are more relevant. Consequently, we decided to map  $\delta^{13}\text{C}$ -values of methane.

The following explanations briefly describe the four maps which display the contouring of methane stable carbon isotope ratios ( $\delta^{13}\text{CH}_4$ ) within the Carboniferous, Rotliegend, Zechstein, and post-Zechstein.

The distribution of  $\delta^{13}\text{CH}_4$ -values in **Carboniferous** strata based on reservoir data. In the North Sea, carbon isotope ratios are between  $-33$  and  $-36\text{‰}$ . Data are rather light ( $^{12}\text{C}$ -enriched) compared to those from NW Germany and the eastern part of the Netherlands (mostly  $-27$  till  $-21\text{‰}$ ). In Poland,  $\delta^{13}\text{CH}_4$ -values vary between  $-33$  and  $-27\text{‰}$ .

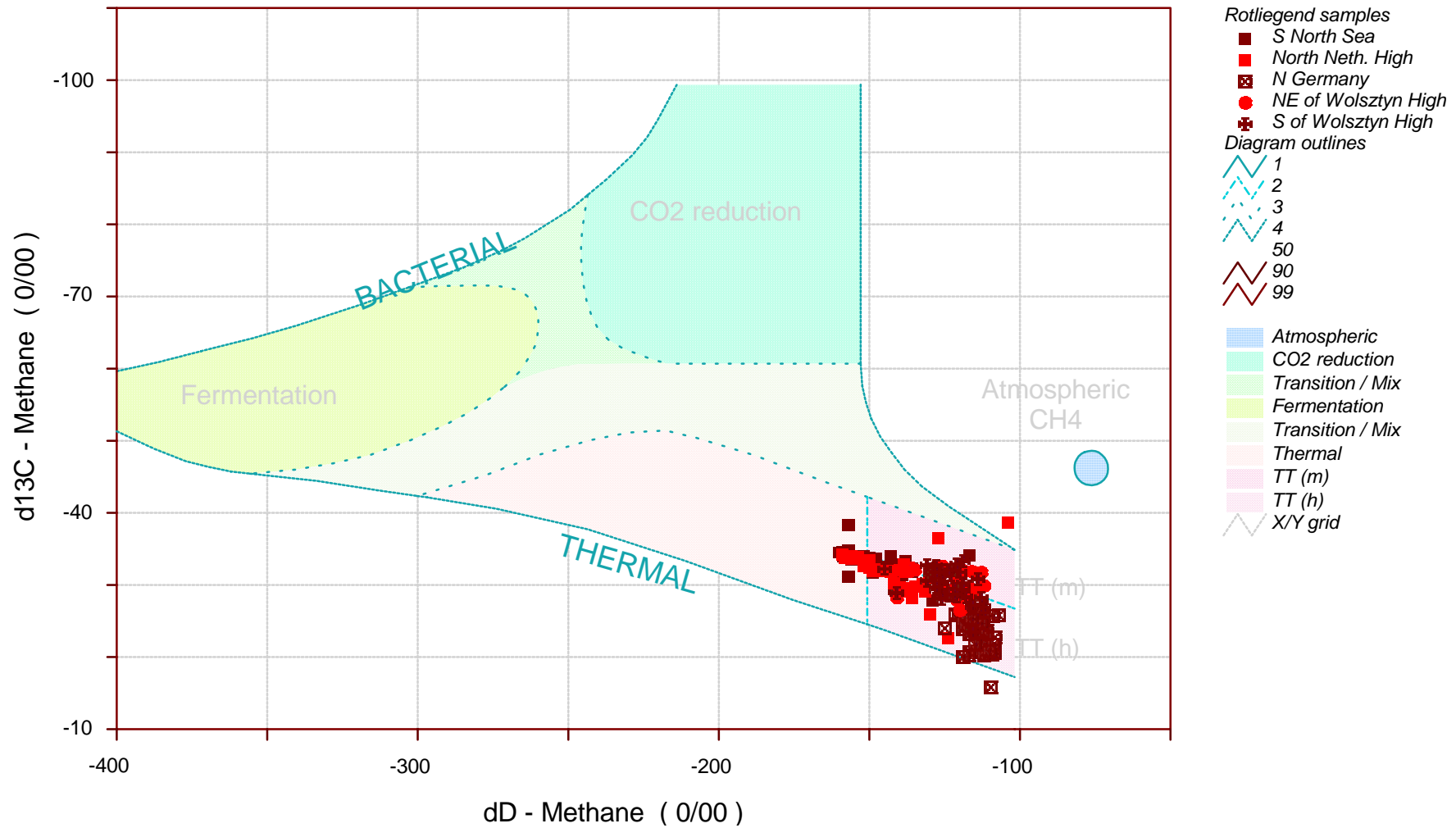
The distribution of  $\delta^{13}\text{CH}_4$ -values in **Rotliegend** strata is based on reservoir data. Data show a kind of undulation. They start with rather heavy or  $^{13}\text{C}$ -enriched  $\delta^{13}\text{CH}_4$ -values in the Southern North Sea (mostly  $-30$  till  $-24\text{‰}$ ), proceed eastward with more negative values in the Netherlands (mostly  $-36$  till  $-27\text{‰}$ ), have again rather heavy values in Germany with most  $\delta^{13}\text{CH}_4$ -values  $> -27\text{‰}$ , and end in Poland with comparatively  $^{13}\text{C}$ -depleted values (most  $\delta^{13}\text{CH}_4$ -values  $< -27\text{‰}$ ).

The distribution of  $\delta^{13}\text{CH}_4$ -values in **Zechstein** gases is based on reservoir data. In the North Sea, in the Netherlands as well as in NW Germany,  $\delta^{13}\text{CH}_4$ -values are in most cases between  $-30$  and  $-21\text{‰}$ , sometimes even more  $^{13}\text{C}$ -enriched (TSR!). In contrast, Polish data are comparable  $^{12}\text{C}$ -enriched ( $\delta^{13}\text{CH}_4$ -values  $< -42\text{‰}$ ).

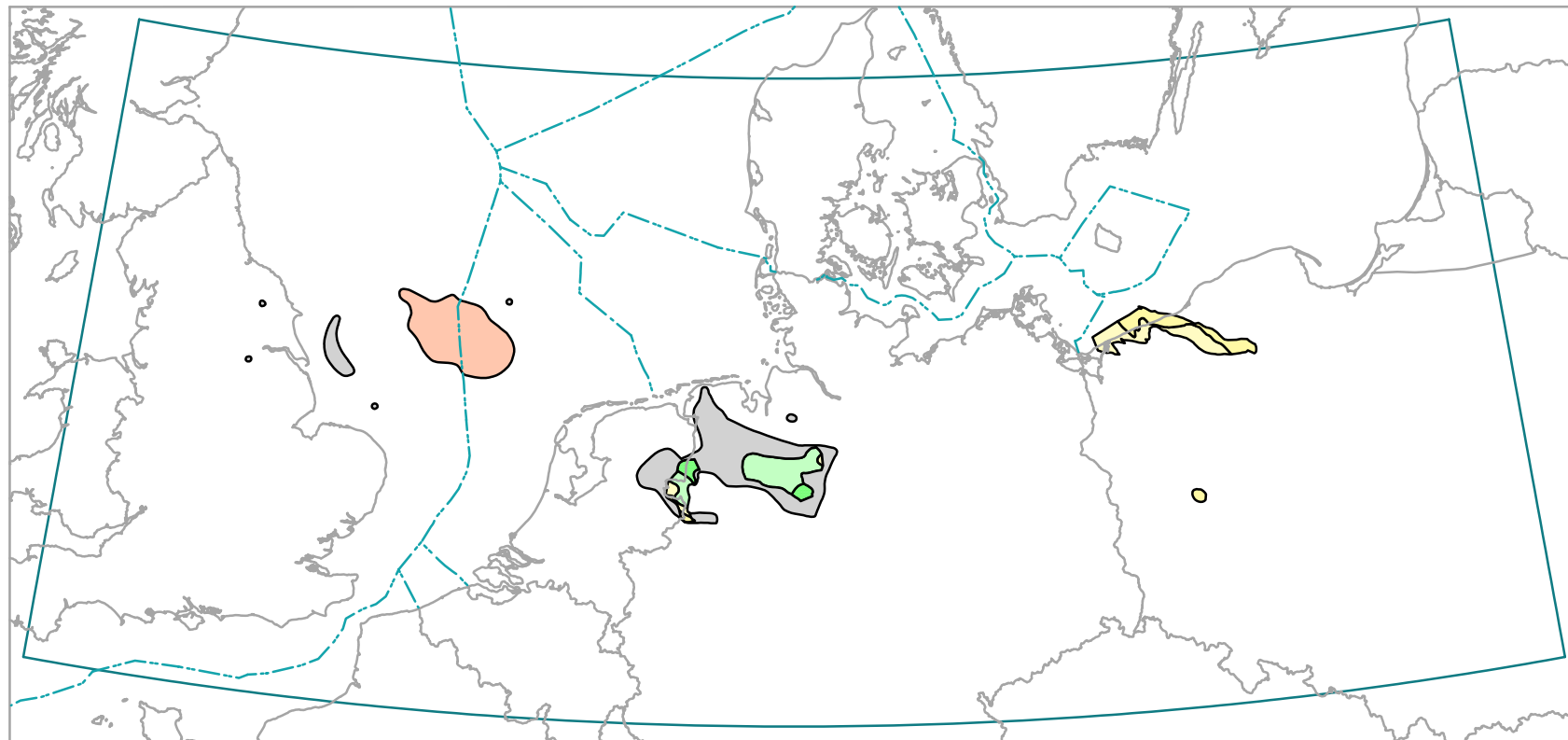
The distribution of  $\delta^{13}\text{CH}_4$ -values in **post-Zechstein** gases is based on reservoir data. There is a clear E-W trend with rather heavy carbon isotope ratios in Germany and the border area with the

Netherlands (most  $\delta^{13}\text{CH}_4 > -27\text{‰}$ ) and less  $^{13}\text{C}$ -enriched methane gases in the SW Netherlands (most  $\delta^{13}\text{CH}_4$ -values between  $-30$  and  $-39\text{‰}$ ) and offshore Denmark ( $\delta^{13}\text{CH}_4$ -values  $< -45\text{‰}$ ).

**Fig. 4.1 Diagnostic plot  
dD-CH<sub>4</sub> vs. d<sup>13</sup>C-CH<sub>4</sub>**



# d13C-CH4 contour map - Carboniferous reservoir gas



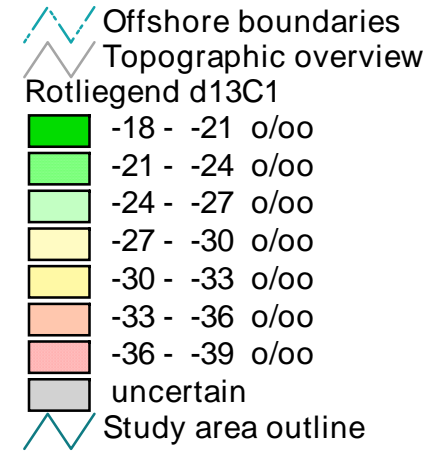
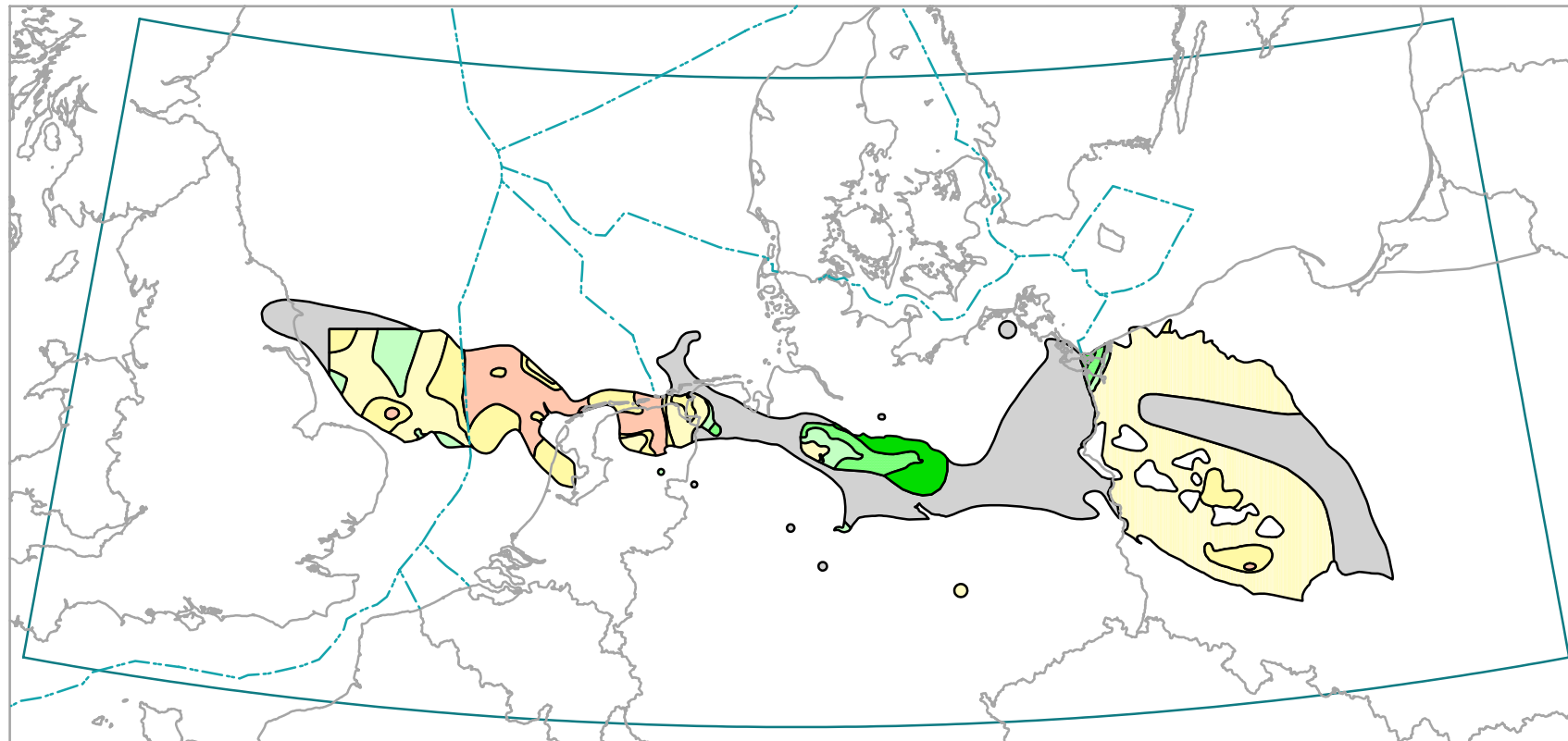
- Offshore boundaries
- Topographic overview
- Carboniferous d13C1
  - 21 - -24 ‰
  - 24 - -27 ‰
  - 27 - -30 ‰
  - 30 - -33 ‰
  - 33 - -36 ‰
  - uncertain
- Study area outline

0 110 220 330 440 550 660 Kilometers



Projection : Lambert Conformal Conic  
Spheroid : Bessel, 1841  
Standard parallels : 51 N and 54 N  
Central meridian : 9 E  
Latitude of projection origin : 48 N  
False easting : 7,500,000 m  
False northing : 0 m

# d13C-CH4 contour map - Upper Rotliegend reservoir gas

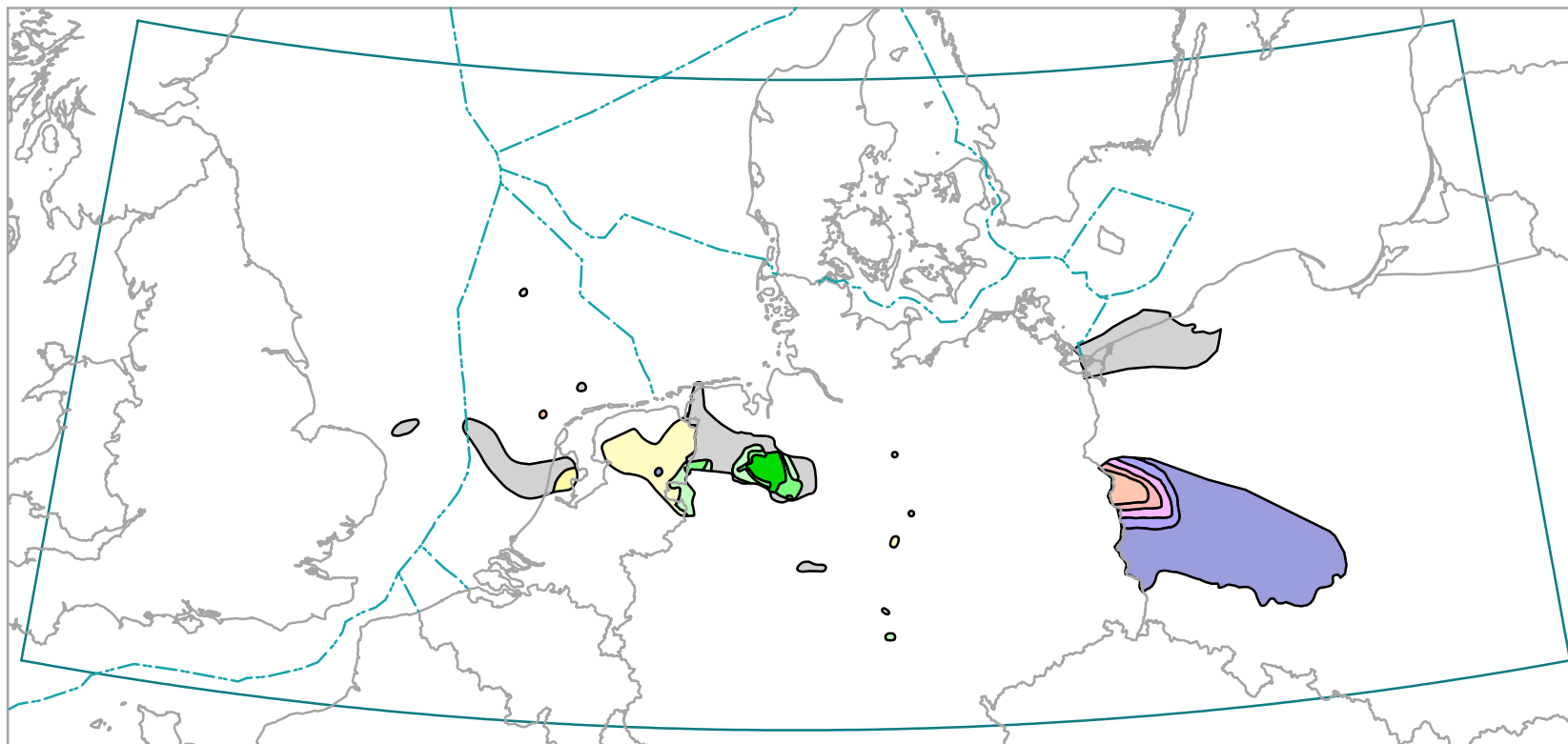


0 110 220 330 440 550 660 Kilometers



Projection : Lambert Conformal Conic  
 Spheroid : Bessel, 1841  
 Standard parallels : 51 N and 54 N  
 Central meridian : 9 E  
 Latitude of projection origin : 48 N  
 False easting : 7,500,000 m  
 False northing : 0 m

# d13C-CH4 contour map - Zechstein reservoir gas



- Offshore boundaries
- Topographic overview
- Zechstein d13C1
- 18 - -21 o/oo
- 21 - -24 o/oo
- 24 - -27 o/oo
- 27 - -30 o/oo
- 30 - -33 o/oo
- 33 - -36 o/oo
- 36 - -39 o/oo
- 39 - -42 o/oo
- 42 - -45 o/oo
- 45 - -48 o/oo
- uncertain
- Study area outline

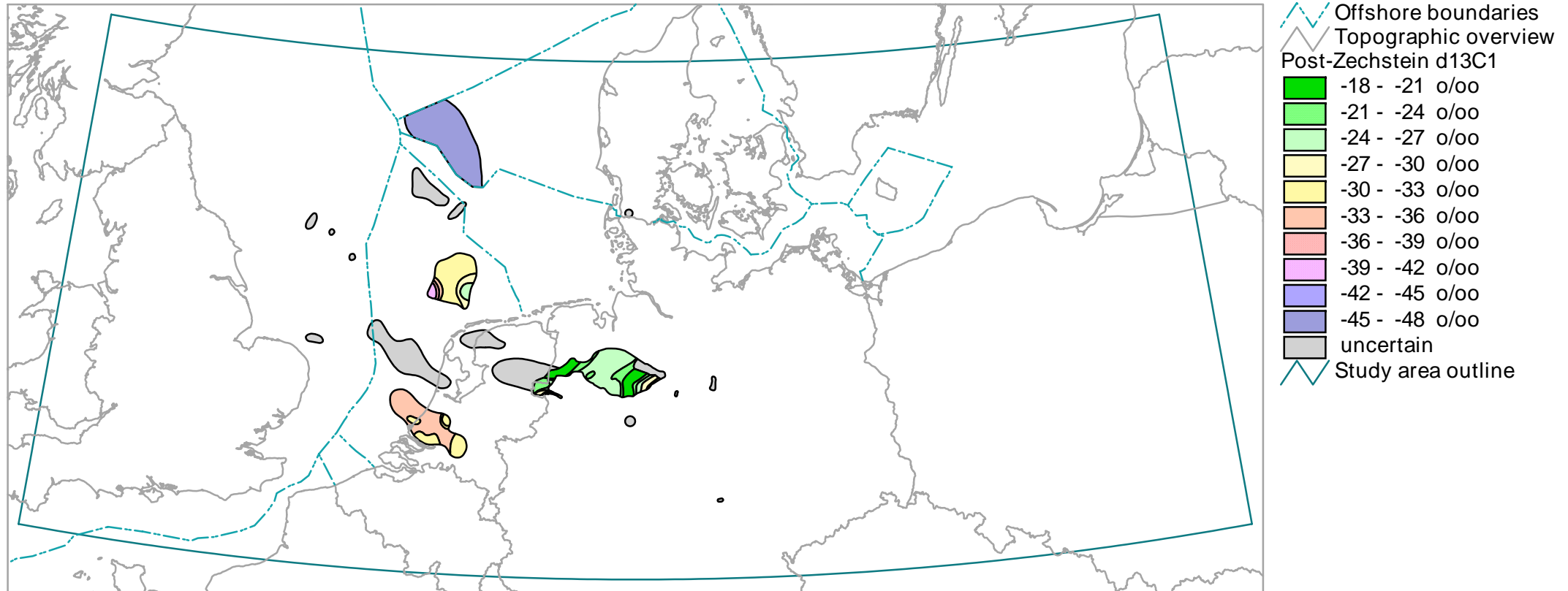
0 110 220 330 440 550 660 Kilometers



Projection : Lambert Conformal Conic  
 Spheroid : Bessel, 1841  
 Standard parallels : 51 N and 54 N  
 Central meridian : 9 E  
 Latitude of projection origin : 48 N  
 False easting : 7,500,000 m  
 False northing : 0 m



# d13C-CH4 contour map - Post-Zechstein reservoir gas



0 110 220 330 440 550 660 Kilometers



Projection : Lambert Conformal Conic  
 Spheroid : Bessel, 1841  
 Standard parallels : 51 N and 54 N  
 Central meridian : 9 E  
 Latitude of projection origin : 48 N  
 False easting : 7,500,000 m  
 False northing : 0 m

### 4.3 The Molecular Composition of Gaseous Hydrocarbons $C_1/(C_2+C_3)$

Thermogenically produced gas can be distinguished from microbially generated gas by use of methane stable isotope and methane/(ethane + propane) [ $C_1/(C_2+C_3)$ ] ratios (BERNARD et al., 1976; FABER & STAHL, 1984). Microbial methane is enriched in  $^{12}C$  ( $\delta^{13}CH_4 < -50\text{‰}$ ) and contains only trace amounts of higher alkanes:  $C_1/(C_2+C_3)$  ratios are typically  $\gg 100$ . Thermogenic methane, formed during catagenesis, is depleted in  $^{12}C$  ( $\delta^{13}CH_4 > -50\text{‰}$ ) and has an abundance of higher alkanes, usually with values of  $C_1/(C_2+C_3) < 100$ . Gaseous hydrocarbons generated during metagenesis, however, are again dominated by methane in their molecular composition ( $C_1/(C_2+C_3)$  can reach values above 200) and enriched in  $^{13}C$  ( $\delta^{13}CH_4 > -35\text{‰}$ ).

This combination of  $\delta^{13}CH_4$  values and  $C_1/(C_2+C_3)$  ratios can be used to characterise gaseous hydrocarbons (Fig. 4.2). The diagram permits bacterially generated methane to be distinguished from thermogenic hydrocarbon gases, with a further distinction between thermogenic gases from marine and terrestrial source rocks.

The following explanations briefly describe the four maps which display the contouring of the gas ratios  $C_1/(C_2+C_3)$  within the reservoir horizons Carboniferous, Rotliegend, Zechstein, and post-Zechstein.

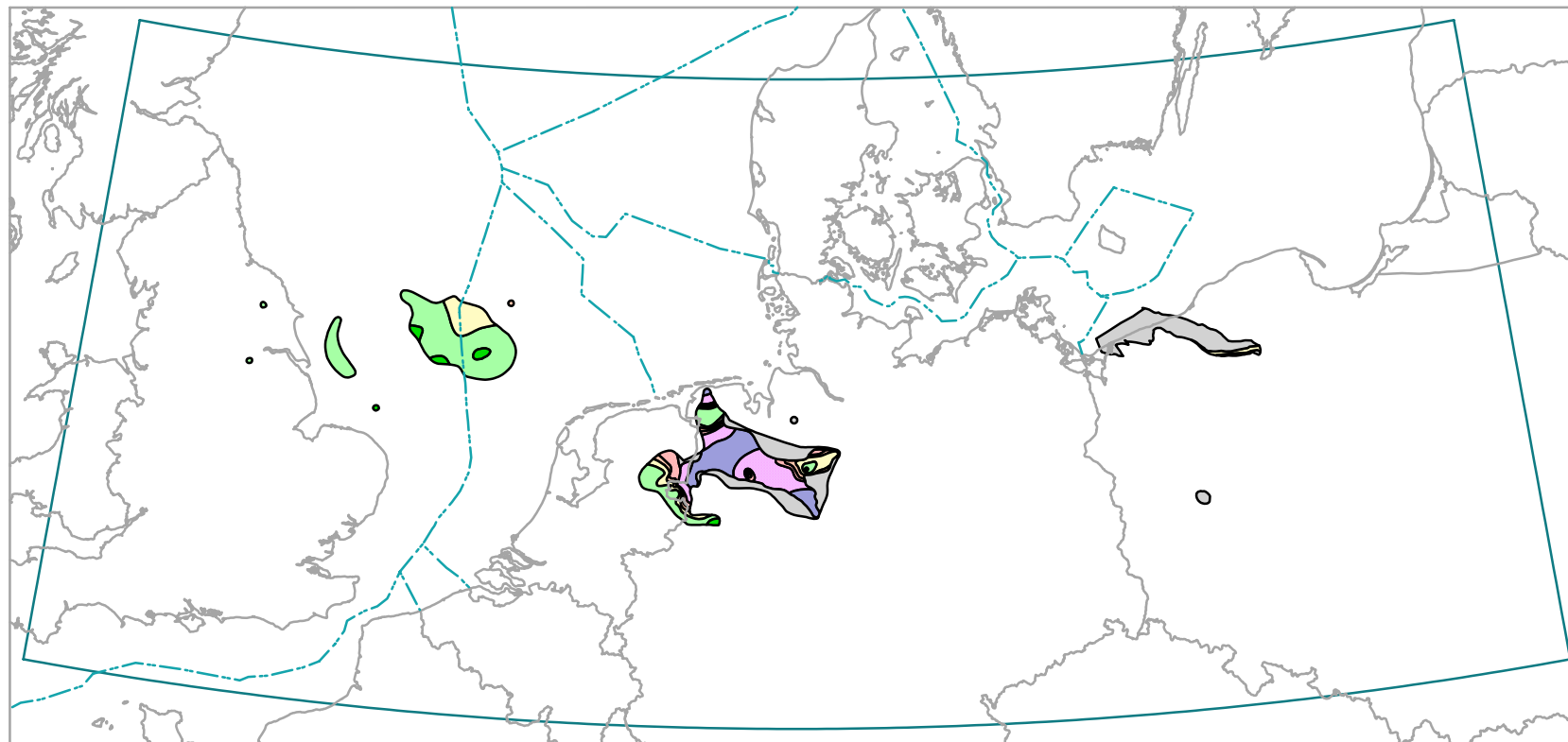
The  $C_1/(C_2+C_3)$  ratios in **Carboniferous** gases are based on reservoir data and DSTs.  $C_1/(C_2+C_3)$  ratios are high ( $>100$  to  $>200$ ) in the Netherlands-German border area. In the southern North Sea,  $C_1/(C_2+C_3)$  ratios indicate that the rather wet gases (ratios from  $<10$  to  $50$ ). Gases become dryer in a northward direction. In N Poland, spotwise information indicate relative wet gases ( $C_1/(C_2+C_3) = 25 - 50$ ).

The  $C_1/(C_2+C_3)$  ratios in **Rotliegend** strata based on reservoir data and DSTs. There is a clear division in rather wet gases in the British and the Dutch area (ratios  $C_1/(C_2+C_3)$  usually  $<50$ ) and more dry gases in Germany and Poland (most  $C_1/(C_2+C_3) > 50$ ).

The  $C_1/(C_2+C_3)$  ratios in **Zechstein** strata based on reservoir data and DSTs. Gas ratios are quite high in NW Germany and in the NE Netherlands, often exceeding 200. Towards central Netherlands,  $C_1/(C_2+C_3)$  ratios decrease down to  $< 50$ . Such wet gas compositions occur as well in the North Sea and in Poland.

The  $C_1/(C_2+C_3)$  ratios in **post-Zechstein** strata based on reservoir data and DSTs. Dry gases occur in NW Germany ( $C_1/(C_2+C_3) >100$ ) and some parts of the North Sea. In contrast, gas ratios offshore Denmark ( $C_1/(C_2+C_3) <25$ ) as well as in on- and offshore areas in the SW Netherlands (mostly  $C_1/(C_2+C_3) < 25$ ) are comparably wet. In the Dutch Central North Sea area,  $C_1/(C_2+C_3)$  ratios vary strongly between  $<10$  and  $>200$

# Wetness contour map - Carboniferous reservoir gas



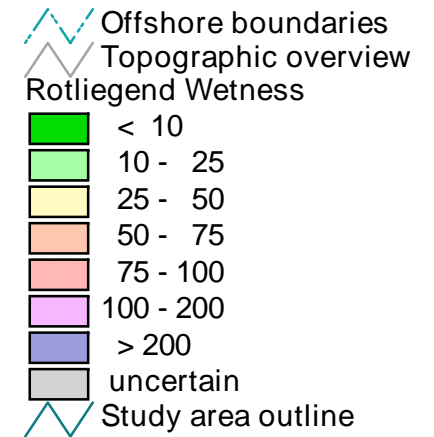
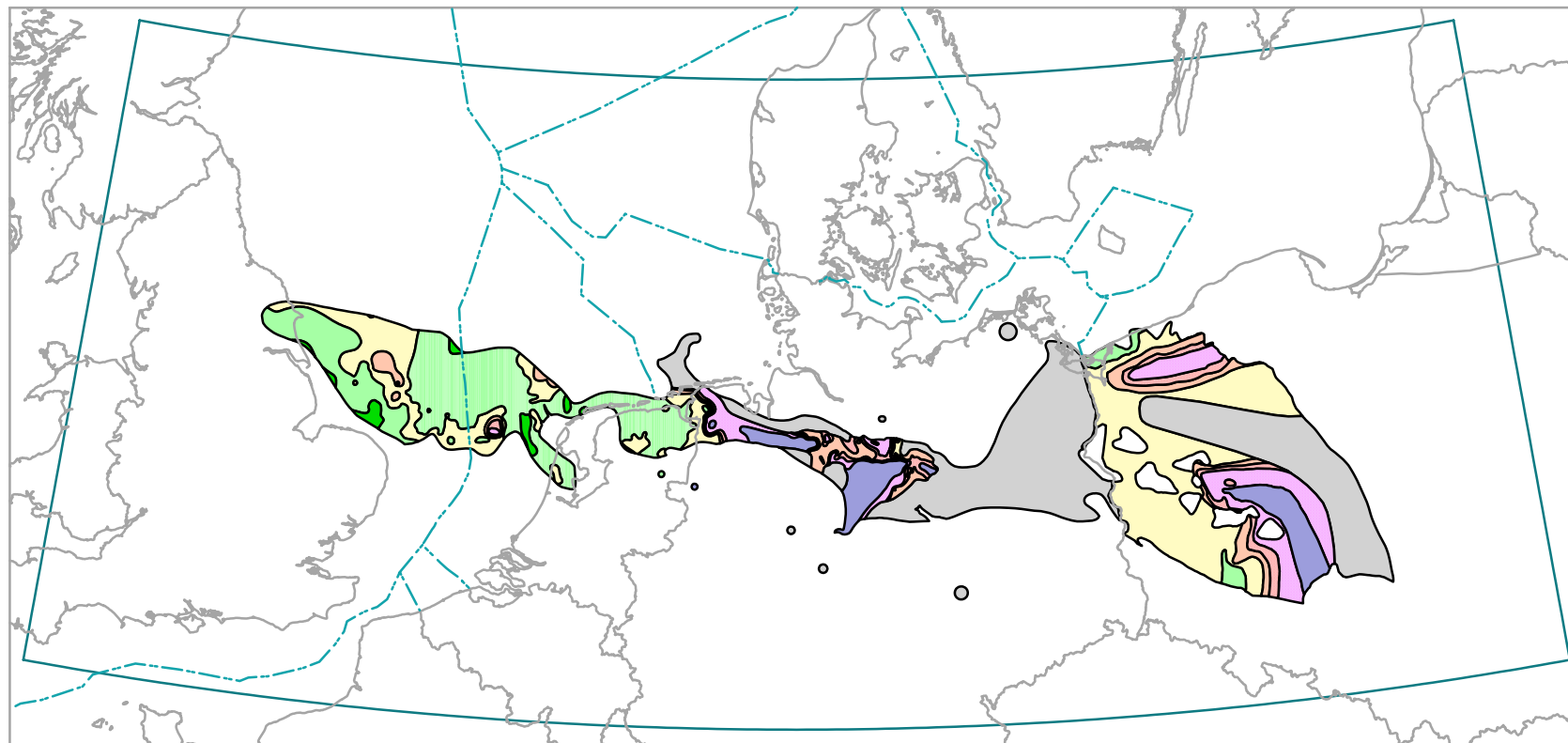
- Offshore boundaries
- Topographic overview
- Carboniferous Wetness**
- < 10
- 10 - 25
- 25 - 50
- 50 - 75
- 75 - 100
- 100 - 200
- > 200
- uncertain
- Study area outline

0 110 220 330 440 550 660 Kilometers



Projection : Lambert Conformal Conic  
 Spheroid : Bessel, 1841  
 Standard parallels : 51 N and 54 N  
 Central meridian : 9 E  
 Latitude of projection origin : 48 N  
 False easting : 7,500,000 m  
 False northing : 0 m

# Wetness contour map - Upper Rotliegend reservoir gas

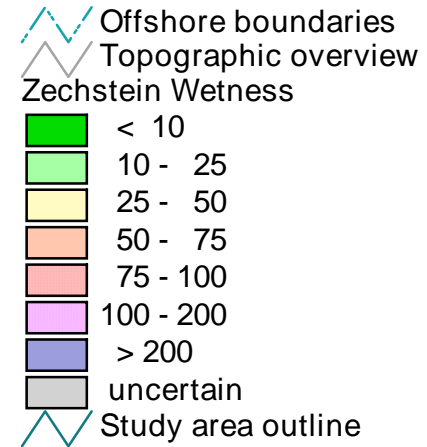
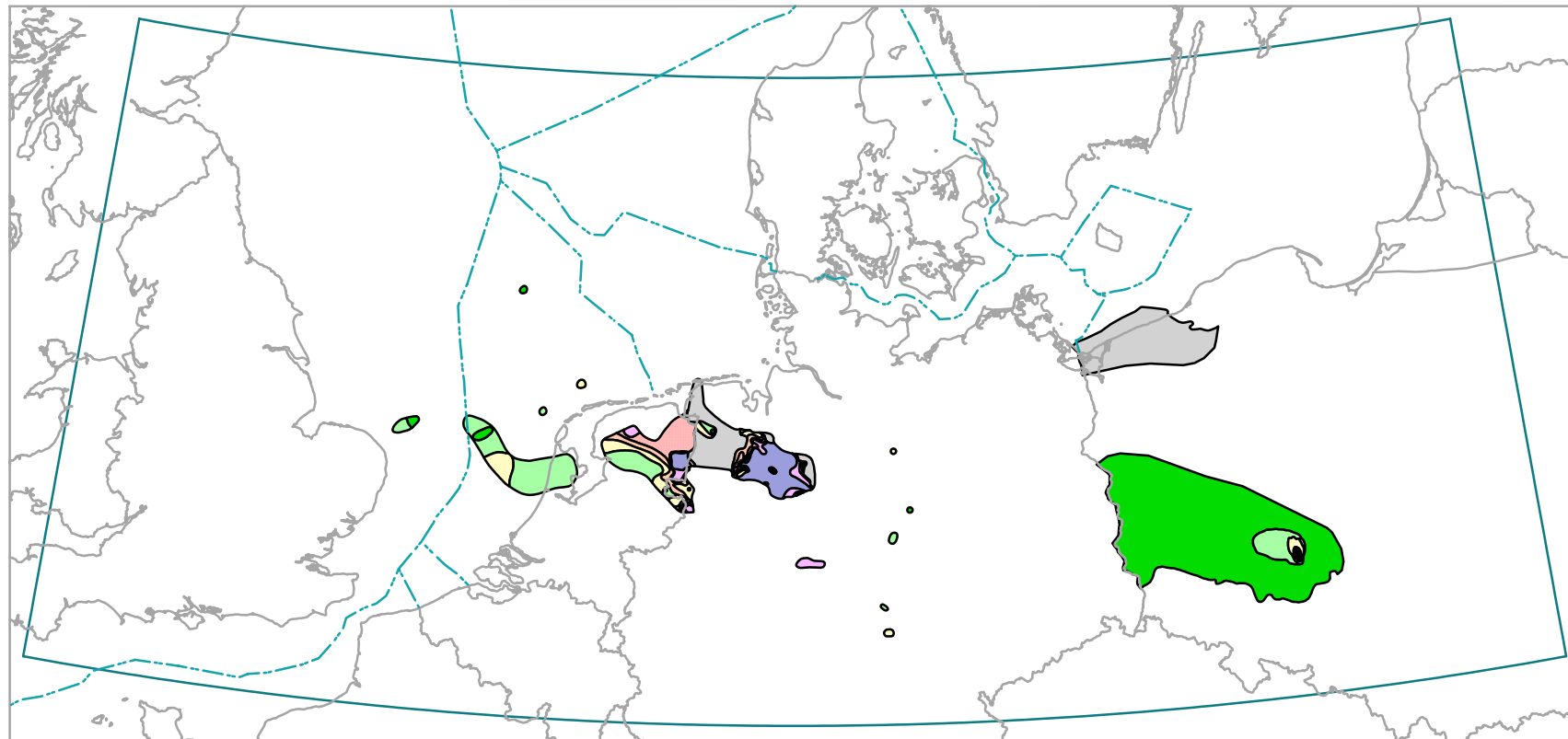


0 110 220 330 440 550 660 Kilometers



Projection : Lambert Conformal Conic  
 Spheroid : Bessel, 1841  
 Standard parallels : 51 N and 54 N  
 Central meridian : 9 E  
 Latitude of projection origin : 48 N  
 False easting : 7,500,000 m  
 False northing : 0 m

# Wetness contour map - Zechstein reservoir gas

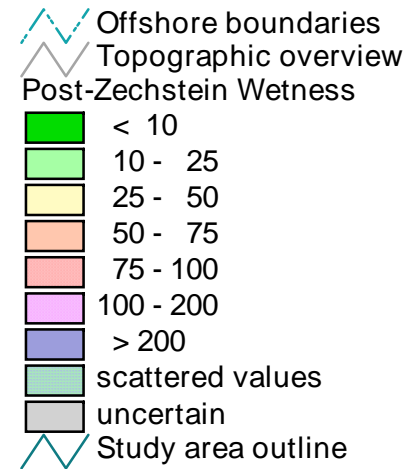
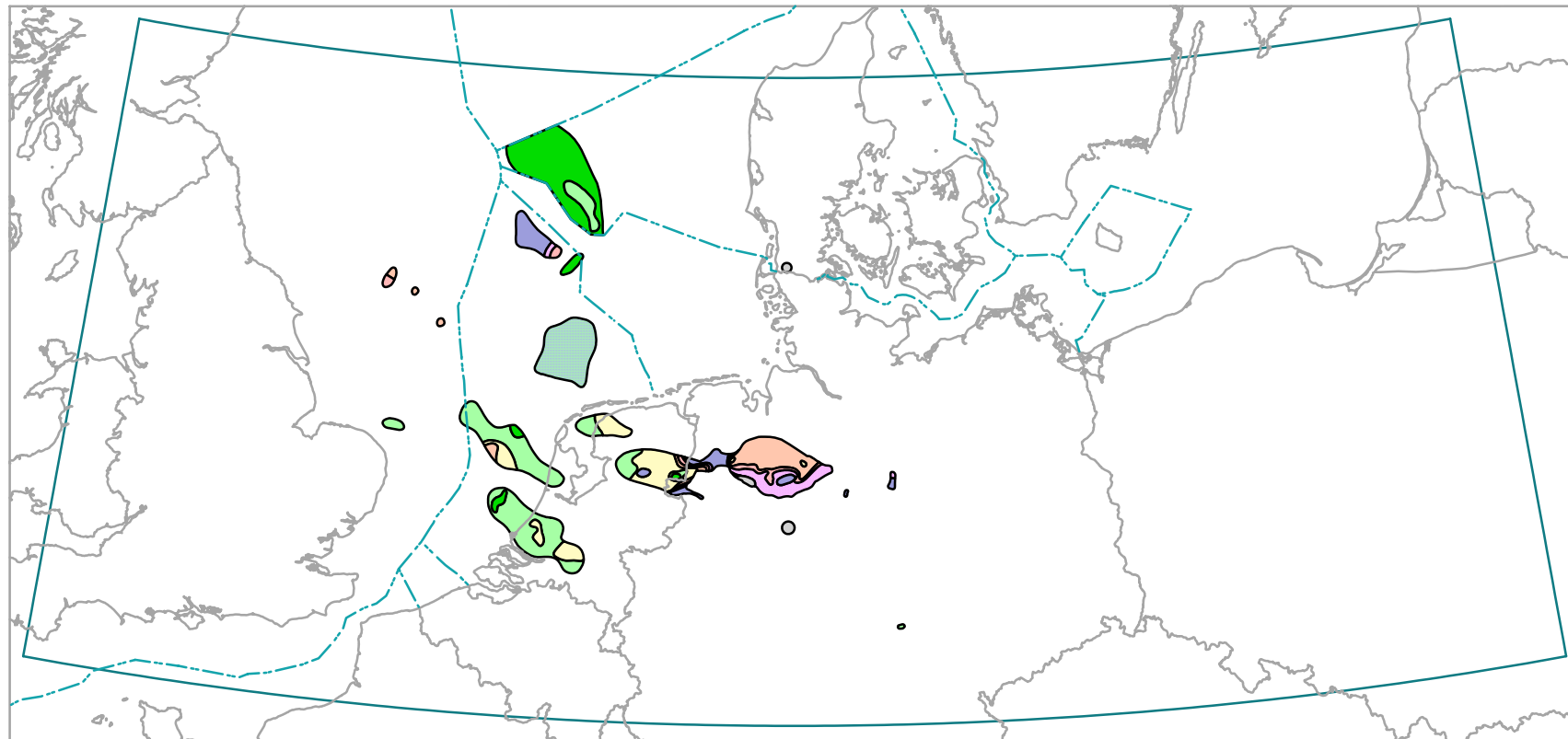


0 110 220 330 440 550 660 Kilometers



Projection : Lambert Conformal Conic  
 Spheroid : Bessel, 1841  
 Standard parallels : 51 N and 54 N  
 Central meridian : 9 E  
 Latitude of projection origin : 48 N  
 False easting : 7,500,000 m  
 False northing : 0 m

# Wetness contour map - Post-Zechstein reservoir gas



0 110 220 330 440 550 660 Kilometers



Projection : Lambert Conformal Conic  
Spheroid : Bessel, 1841  
Standard parallels : 51 N and 54 N  
Central meridian : 9 E  
Latitude of projection origin : 48 N  
False easting : 7,500,000 m  
False northing : 0 m

## 4.4 Nitrogen

In most natural gases nitrogen is a minor component, and together with hydrocarbons gases, probably released from organic matter. However, in certain areas of the world the nitrogen content in dry natural gases can make up to more than 80%, e.g. up to 87% in the California Great Valley (JENDEN et al., 1988) or up to 88% in northern Germany (GERLING et al., 1997). In those cases nitrogen seems to have diverse origins.

Many authors have discussed the origin of nitrogen-rich natural gases based on molecular and isotopic gas compositions as well as on pyrolysis experiments. In general, three different generation processes have been proposed for the generation of nitrogen:

- The release of nitrogen from sedimentary organic matter controlled by maturity and type of kerogen (e.g. KLEIN & JÜNTGEN, 1972, BOIGK et al., 1976, SWEENEY et al., 1978, STIEHL & LEHMANN, 1980, KETTEL, 1982, ROHRBACK et al., 1983, KROOSS et al., 1993),
- the derivation from aquifers charged with meteoric waters (e.g. GOEBEL et al., 1984),
- 'Tiefenstickstoff' (deep nitrogen) which is supposed to originate from igneous or metamorphic basement rocks (e.g. MÜLLER et al., 1976, HAENDEL et al., 1986, JENDEN et al., 1988, EVERLIEN & HOFFMANN, 1991).

Under the framework of BGR's research project titled 'Deep Gas', GERLING et al. (1997) developed a diagnostic plot which allows to differentiate between nitrogen generated through thermal alteration from terrestrial organic matter and from sapropelic organic matter (Fig. 4.3). Data from pyrolysis experiments and from autochthonous Zechstein gases is the basis of this diagnostic plot.

GERLING et al. (1996) investigated several oil-associated gases trapped in the Stassfurt carbonates (Zechstein 2). The gases contain between 20 and 70% nitrogen with  $\delta^{15}\text{N}$  values between +15 and +28‰. Gases encountered in Stassfurt halites (Na2) and Leine halites (Na3) within the Zechstein series had nitrogen contents of 70% and 15% and isotopic values +32‰ and +15‰ respectively. Since the Zechstein reservoir interval is often a closed system, enveloped by the Werra Anhydrites (A1) below and Anhydrites and Halites of the Zechstein 2 cycle (A2 and Na2) above, conditions in the past may have been conducive for trapping of early diagenetically released nitrogen. Although these findings do not include nitrogen characteristics from highly mature sapropelic organic matter we assume to have a first benchmark to identify nitrogen from marine precursor materials.

In order to correlate nitrogen evolving from Upper Carboniferous coals with those gases occurring in natural gas deposits, hydrous pyrolysis experiments were performed on a series of different mature coal samples from northern Germany.  $\delta^{15}\text{N}$  values of nitrogen gas released from coals start with -7.7‰ at the lowest rank and increase with coalification up to values around +4‰. Nitrogen contents in those gases vary from below 1% up to 37%. Similar experiments were carried out on a series of Upper Namurian shales with TOC contents ranging between 5-10%. These contained predominantly vitrinite-dominated organic matter and had original maturities between 3-6% vitrinite reflectance (Rr). The results from these experiments show a systematic shift of about 3‰ in nitrogen isotopes towards lighter values compared to Westphalian coals (see Fig. 4.3). The nitrogen contents in those gases vary between 23 and 76%.

The following explanations briefly describe the four maps which display the nitrogen contouring within the reservoir horizons Carboniferous, Rotliegend, Zechstein, and post-Zechstein.

The nitrogen content in **Carboniferous** strata based on reservoir data and DSTs. In the North Sea and onshore UK,  $\text{N}_2$ -contents usually are below 10%. The same is valid for NW Germany and the eastern part of the Netherlands. In this area, nitrogen contents rapidly increase towards the intrusives of Bramsche-Vlotho-Uchte and Apeldorn, as well as at the northeastern rim. In Poland,  $\text{N}_2$ -contents are generally above 20%, sometimes even above 60%.

The nitrogen content in **Rotliegend** gases is based on reservoir data and DSTs. In the entire area from the UK up to the coast of the Netherlands, nitrogen contents do not exceed 10%. Until middle Germany,  $\text{N}_2$ -contents are still below 20% except along the northeastern rim of the Rotliegend-fairway where the  $\text{N}_2$ -contents increase towards NE in a short distance. From the large reservoir Altmark

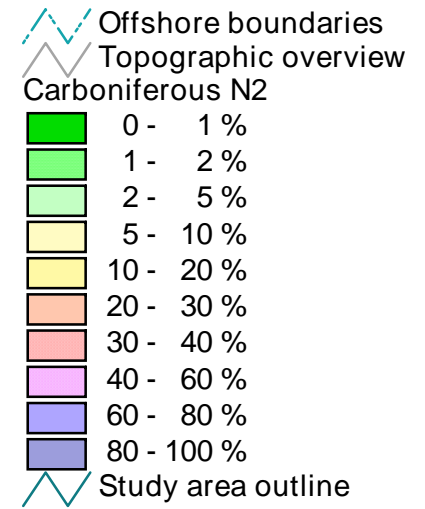
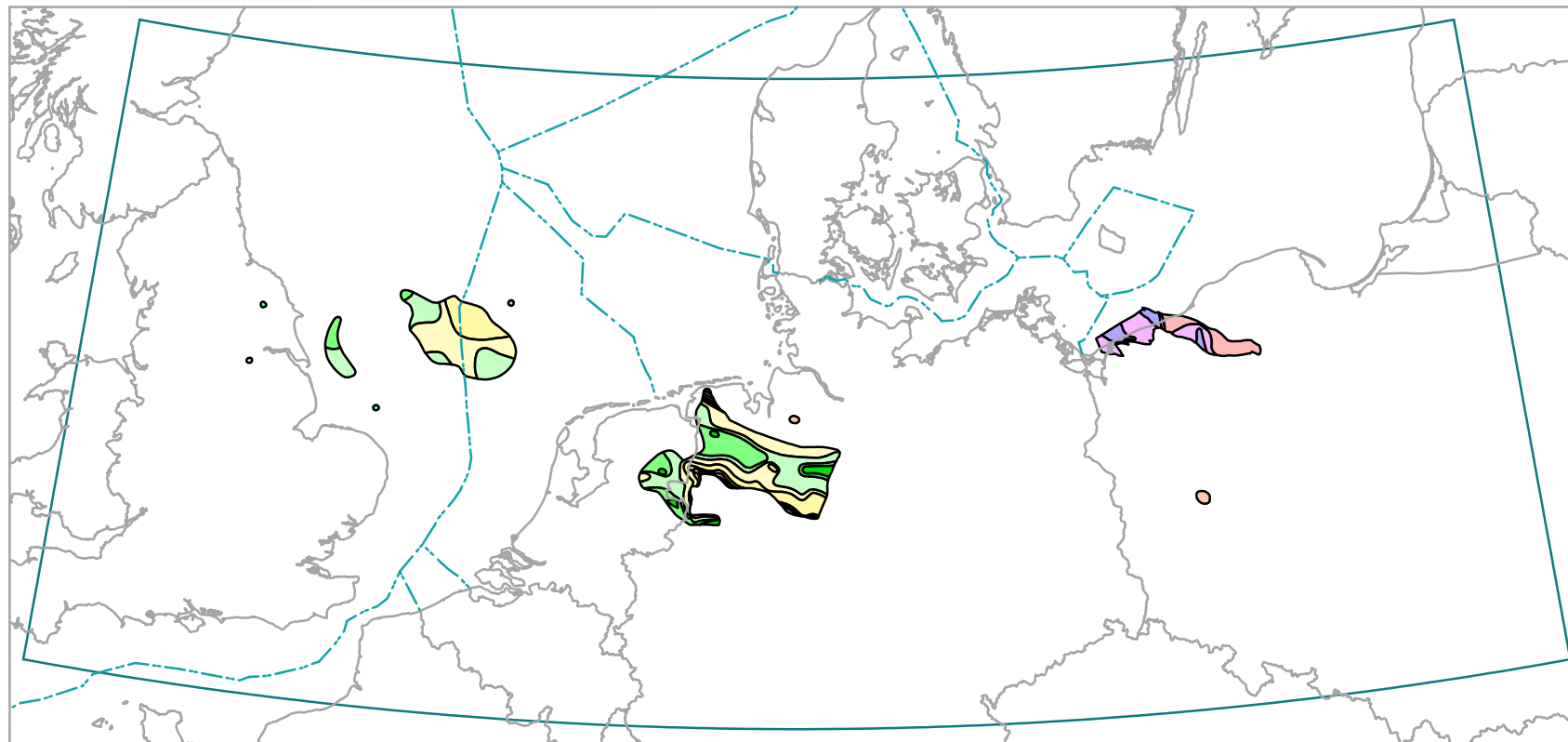
onwards to the east, nitrogen contents increase to more than 80% but decrease in Poland, however, below 20% in the Fore-Sudetic Monocline.

The N<sub>2</sub>-contents in **Zechstein** gases is based on reservoir data and DSTs. In the North Sea, in the Netherlands as well as in NW Germany, nitrogen contents are regularly below 10%. Increasing N<sub>2</sub>-concentrations occur especially around the intrusives of Bramsche-Vlotho-Uchte and Apeldorn. In Poland, nitrogen contents are always above 10%, often even higher.

The N<sub>2</sub>-content in **post-Zechstein** gases based on reservoir data and DSTs. The nitrogen content is rather high (N<sub>2</sub>-content >10%) in NW Germany and the E Netherlands. In the SW Netherlands and the North Sea this gas usually does not exceed 10%, except in the Broad Fourteens Basin, where the nitrogen content increases up to 30%.



# N2 contour map - Carboniferous reservoir gas

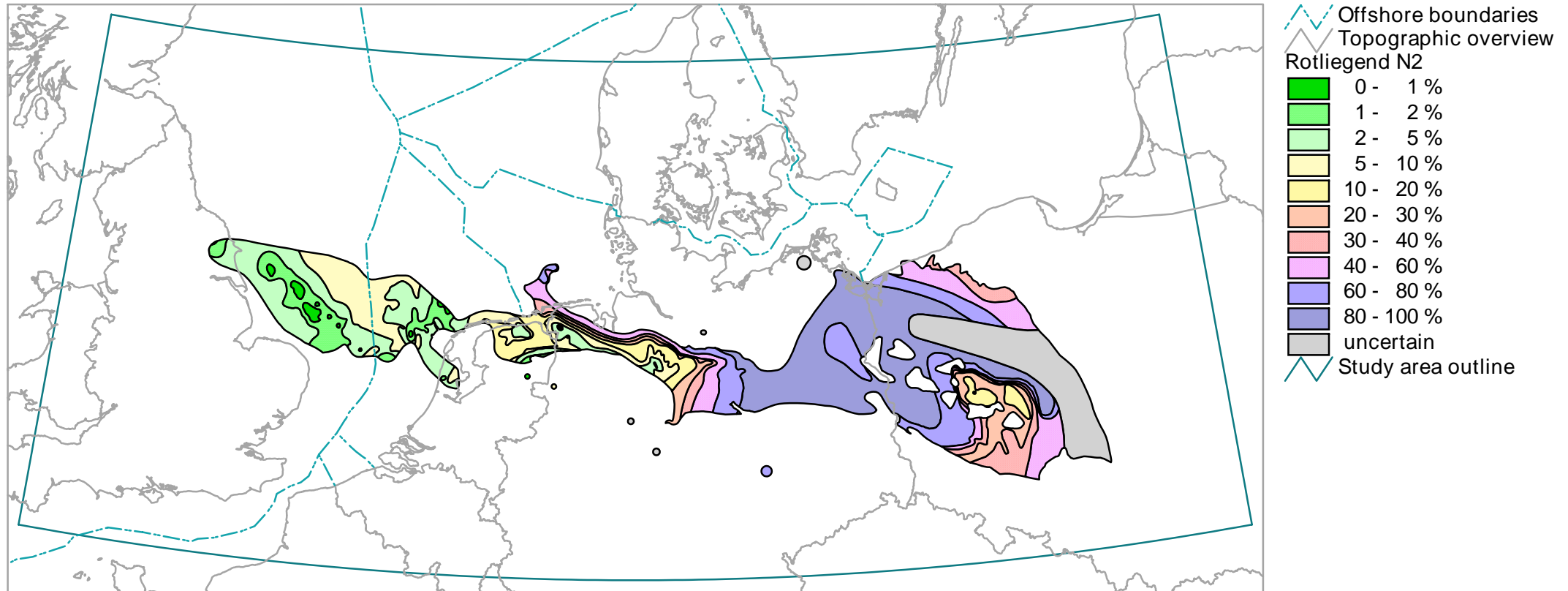


0 110 220 330 440 550 660 Kilometers



Projection : Lambert Conformal Conic  
 Spheroid : Bessel, 1841  
 Standard parallels : 51 N and 54 N  
 Central meridian : 9 E  
 Latitude of projection origin : 48 N  
 False easting : 7,500,000 m  
 False northing : 0 m

# N2 contour map - Upper Rotliegend reservoir gas

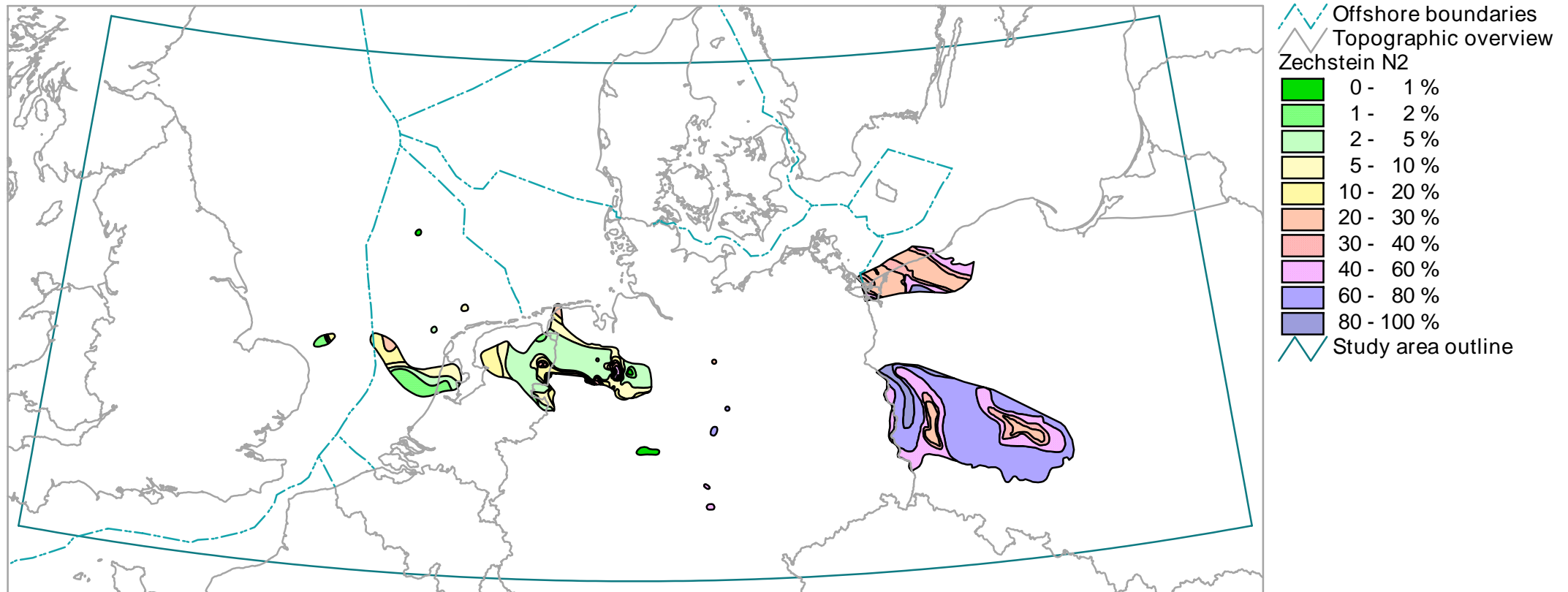


0 110 220 330 440 550 660 Kilometers



Projection : Lambert Conformal Conic  
Spheroid : Bessel, 1841  
Standard parallels : 51 N and 54 N  
Central meridian : 9 E  
Latitude of projection origin : 48 N  
False easting : 7,500,000 m  
False northing : 0 m

# N2 contour map - Zechstein reservoir gas

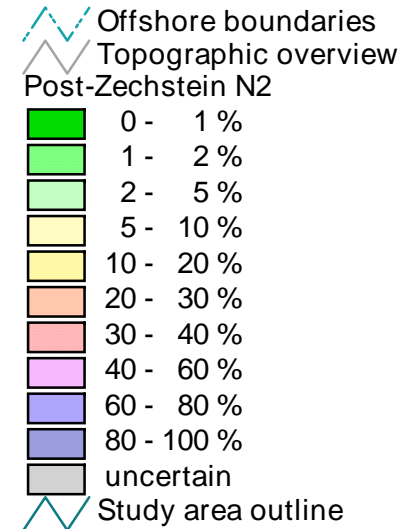
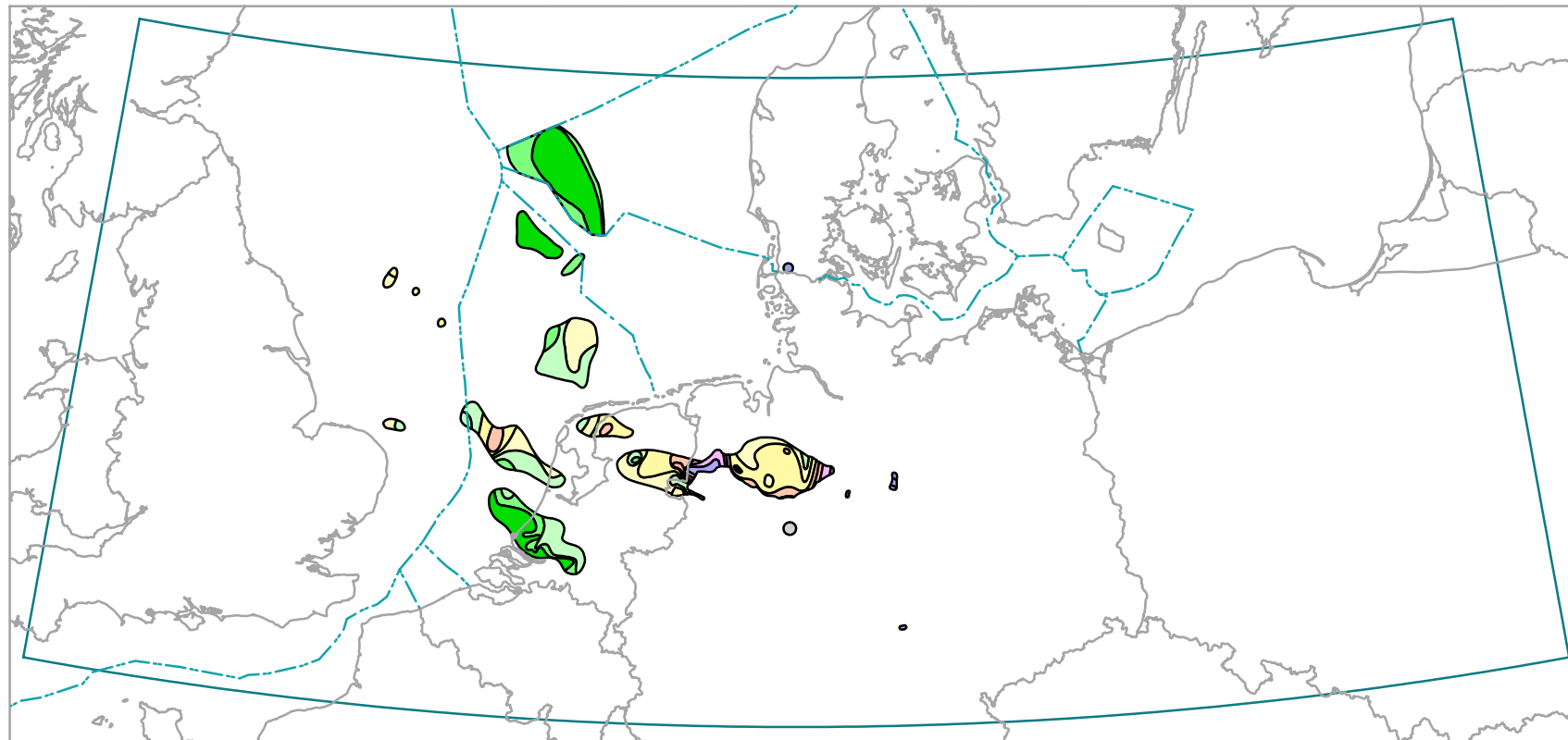


0 110 220 330 440 550 660 Kilometers



Projection : Lambert Conformal Conic  
Spheroid : Bessel, 1841  
Standard parallels : 51 N and 54 N  
Central meridian : 9 E  
Latitude of projection origin : 48 N  
False easting : 7,500,000 m  
False northing : 0 m

# N2 contour map - Post-Zechstein reservoir gas



0 110 220 330 440 550 660 Kilometers



Projection : Lambert Conformal Conic  
 Spheroid : Bessel, 1841  
 Standard parallels : 51 N and 54 N  
 Central meridian : 9 E  
 Latitude of projection origin : 48 N  
 False easting : 7,500,000 m  
 False northing : 0 m

## 4.5 Carbon Dioxide

Carbon dioxide is a common non-hydrocarbon gas in petroleum reservoirs. In some cases it is even the dominant component. The CO<sub>2</sub> levels in the investigated natural gas fields vary between < 1% up to >50%. Carbon isotope ratios are frequently used to characterise the source of carbon in the CO<sub>2</sub>.

Four processes can basically be distinguished in the origin of carbon dioxide:

- The decomposition of the organic substance (decarboxylation) takes place in particular during the early deposition and generates a CO<sub>2</sub>, ending with the same  $\delta^{13}\text{C}$  ratios as that of the precursor materials:  $\delta^{13}\text{C}$  ratios are usually < -20 ‰.
- The dissociation of carbonates is caused either by thermal influence or by contact with acidic waters. The CO<sub>2</sub> emitted during this process is usually isotopically similar to the destroyed carbonate, i.e. the  $\delta^{13}\text{C}$  ratios vary around zero.
- The thermo-chemical sulphate reduction (TSR), only occurring in Zechstein reservoirs, is connected with an oxidation of hydrocarbons. The generated CO<sub>2</sub> is isotopically similar to the decomposed hydrocarbons:  $\delta^{13}\text{C}$  ratios < -20 ‰.
- Deep sourced carbon dioxide like juvenile exhalations, metamorphic fluids or even from the mantle have CO<sub>2</sub> with  $\delta^{13}\text{C}$  ratios of between approx. -7 and -2‰.

This isotopic spectrum has clear intrinsic contradictions which make a genetic characterisation difficult. This problem is exacerbated in natural conditions because overlaps occur in the above mentioned processes, which have either taken place chronologically or as a result of synchronicity. Hence we decided to present only the carbon dioxide contents of natural gases.

The following explanations briefly describe the four maps which display the carbon dioxide contouring within the reservoir horizons Carboniferous, Rotliegend, Zechstein and post-Zechstein.

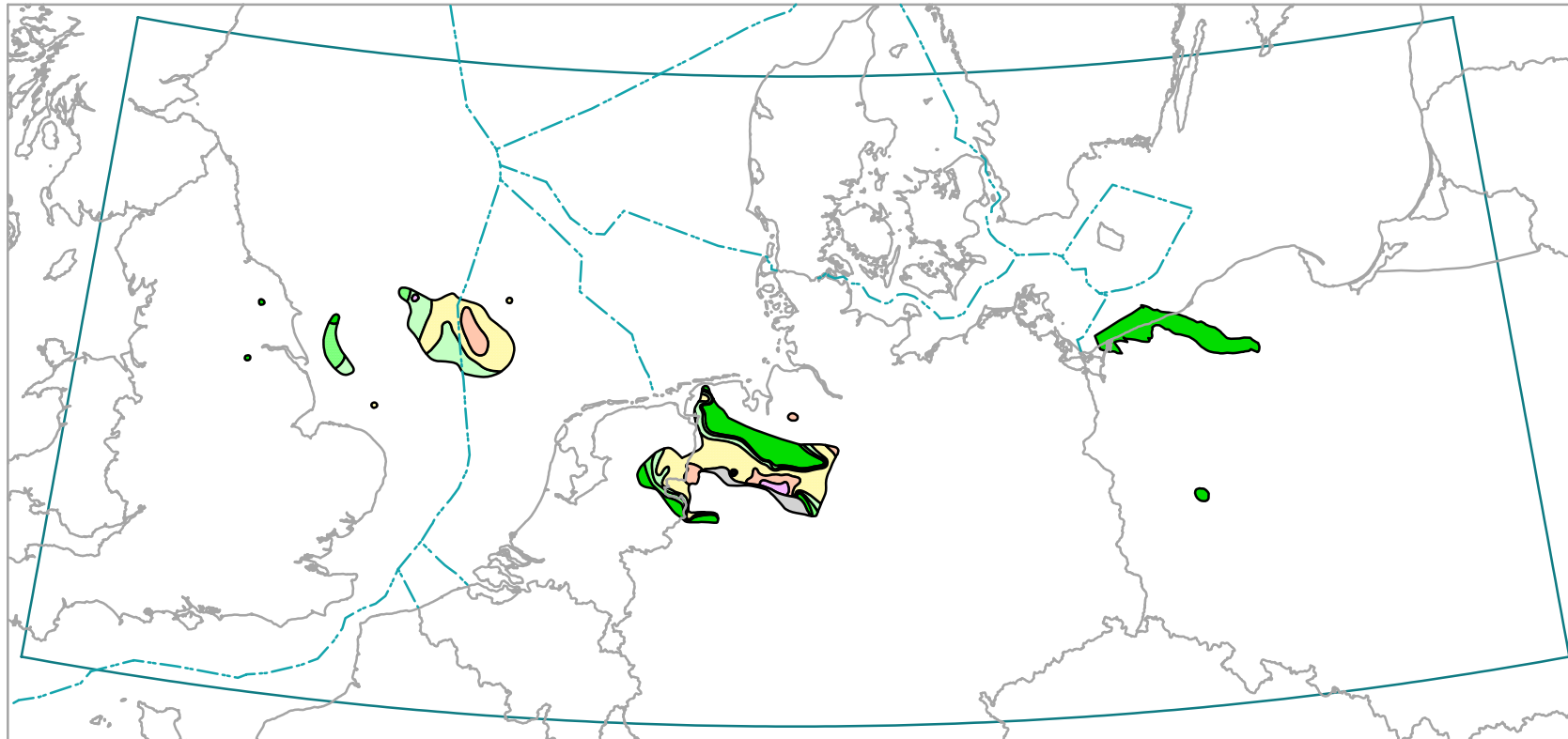
The carbon dioxide content in **Carboniferous** gases is based on reservoir data and DSTs. In the North Sea and onshore UK, CO<sub>2</sub>-contents are below 5%, towards the coast of UK even decreasing below 1%. In NW Germany and the eastern part of the Netherlands CO<sub>2</sub>-contents are between <0.5% and - locally - more than 5%. Elevated concentration occur around the intrusives of Bramsche-Vlotho-Uchte and Apeldorn. In Poland, CO<sub>2</sub>-contents are generally below 1%.

The carbon dioxide content in **Rotliegend** gases is based on reservoir data and DSTs. In the entire area, CO<sub>2</sub>-contents rarely exceed 2%. Spots with more than 50% occur in relation with intrusives in NW Germany. Slightly elevated contents (up to 5%) are observed in the Southern North Sea area.

The CO<sub>2</sub>-contents in **Zechstein** gases is based on reservoir data and DSTs. In NW Germany and the border area to the Netherlands carbon dioxide contents are often above 5% or even higher. Those elevated CO<sub>2</sub>-contents surround the intrusives of Bramsche-Vlotho-Uchte and Apeldorn. Moreover, TSR occurs in this area which generates as well CO<sub>2</sub> (cf. paragraph 4.8.1) In the remainder part of the Netherlands and in the North Sea CO<sub>2</sub>-contents usually are below 5%. In Poland, carbon dioxide contents rarely exceed 2%.

The CO<sub>2</sub>-content in **post-Zechstein** gases is based on reservoir data and DSTs. The carbon dioxide content in the entire area is usually below 2%. Only a few areas contain natural gas with higher CO<sub>2</sub> concentrations, such as the SW Netherlands, locally in the Broad Fourteens Basin and in the Danish Central North Sea Graben.

# CO2 contour map - Carboniferous reservoir gas



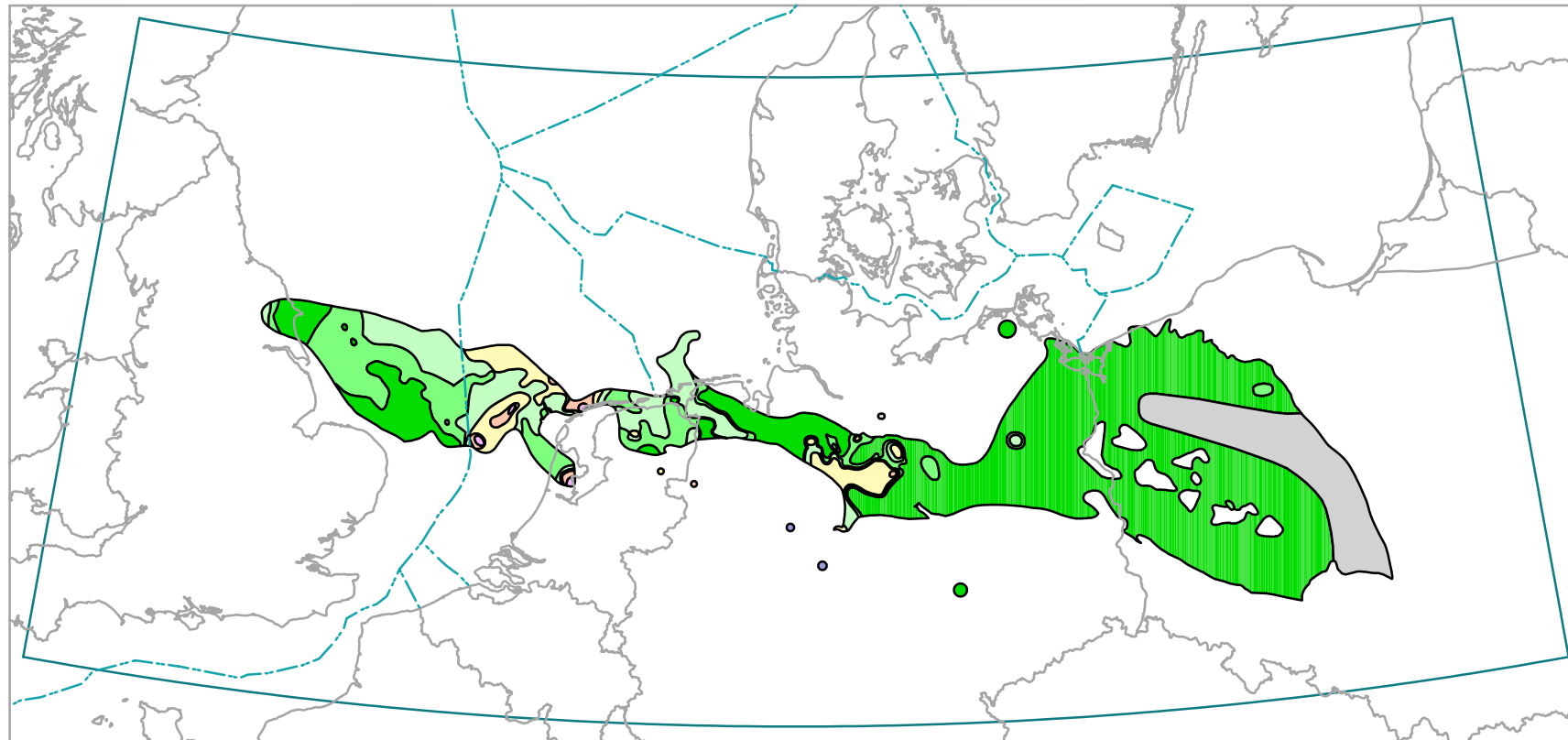
- Offshore boundaries
- Topographic overview
- Carboniferous CO2
  - 0.0 - 0.5 %
  - 0.5 - 1.0 %
  - 1.0 - 2.0 %
  - 2.0 - 5.0 %
  - 5.0 - 10.0 %
  - 10.0 - 20.0 %
  - uncertain
- Study area outline

0 110 220 330 440 550 660 Kilometers



Projection : Lambert Conformal Conic  
Spheroid : Bessel, 1841  
Standard parallels : 51 N and 54 N  
Central meridian : 9 E  
Latitude of projection origin : 48 N  
False easting : 7,500,000 m  
False northing : 0 m

# CO2 contour map - Upper Rotliegend reservoir gas



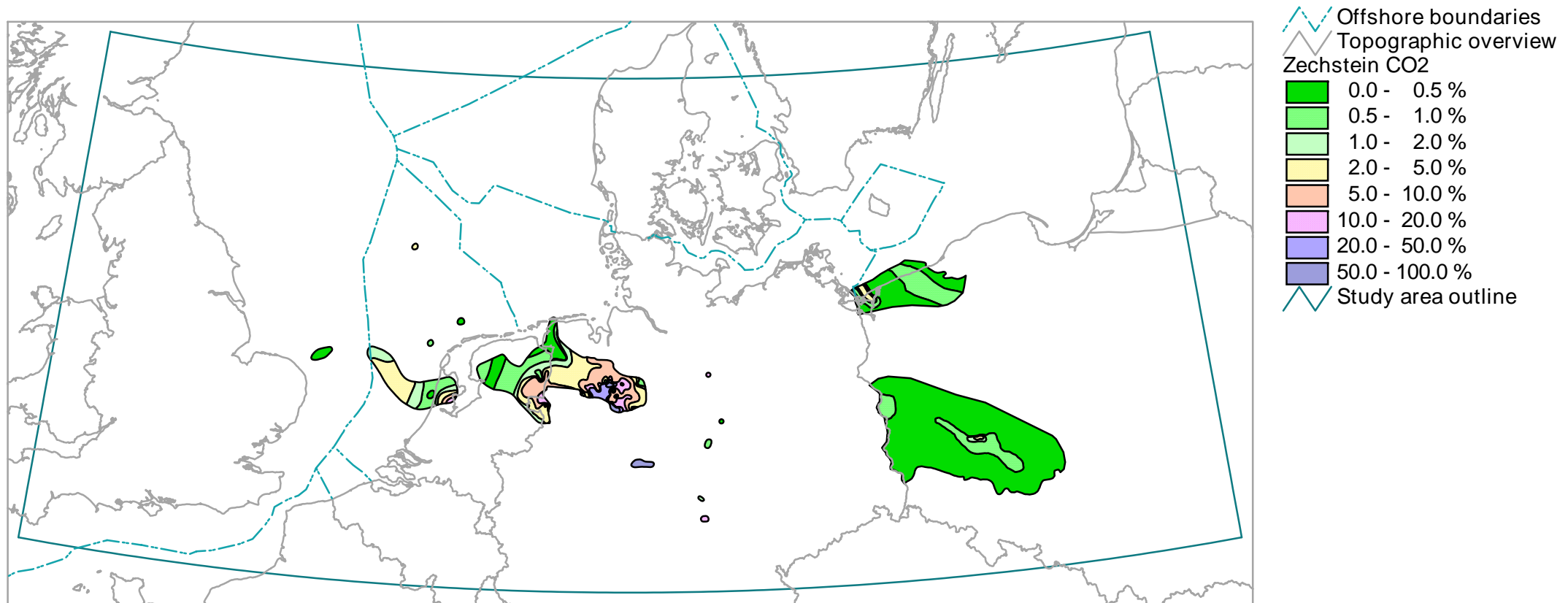
- Offshore boundaries
- Topographic overview
- Rotliegend CO2
  - 0.0 - 0.5 %
  - 0.5 - 1.0 %
  - 1.0 - 2.0 %
  - 2.0 - 5.0 %
  - 5.0 - 10.0 %
  - 10.0 - 20.0 %
  - 50.0 - 100.0 %
  - uncertain
- Study area outline

0 110 220 330 440 550 660 Kilometers



Projection : Lambert Conformal Conic  
Spheroid : Bessel, 1841  
Standard parallels : 51 N and 54 N  
Central meridian : 9 E  
Latitude of projection origin : 48 N  
False easting : 7,500,000 m  
False northing : 0 m

# CO2 contour map - Zechstein reservoir gas



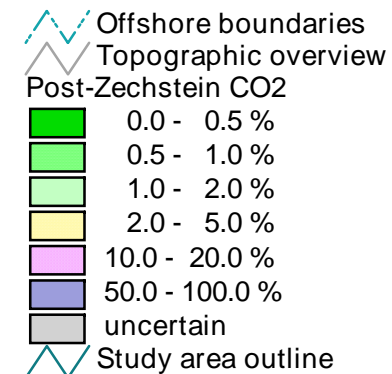
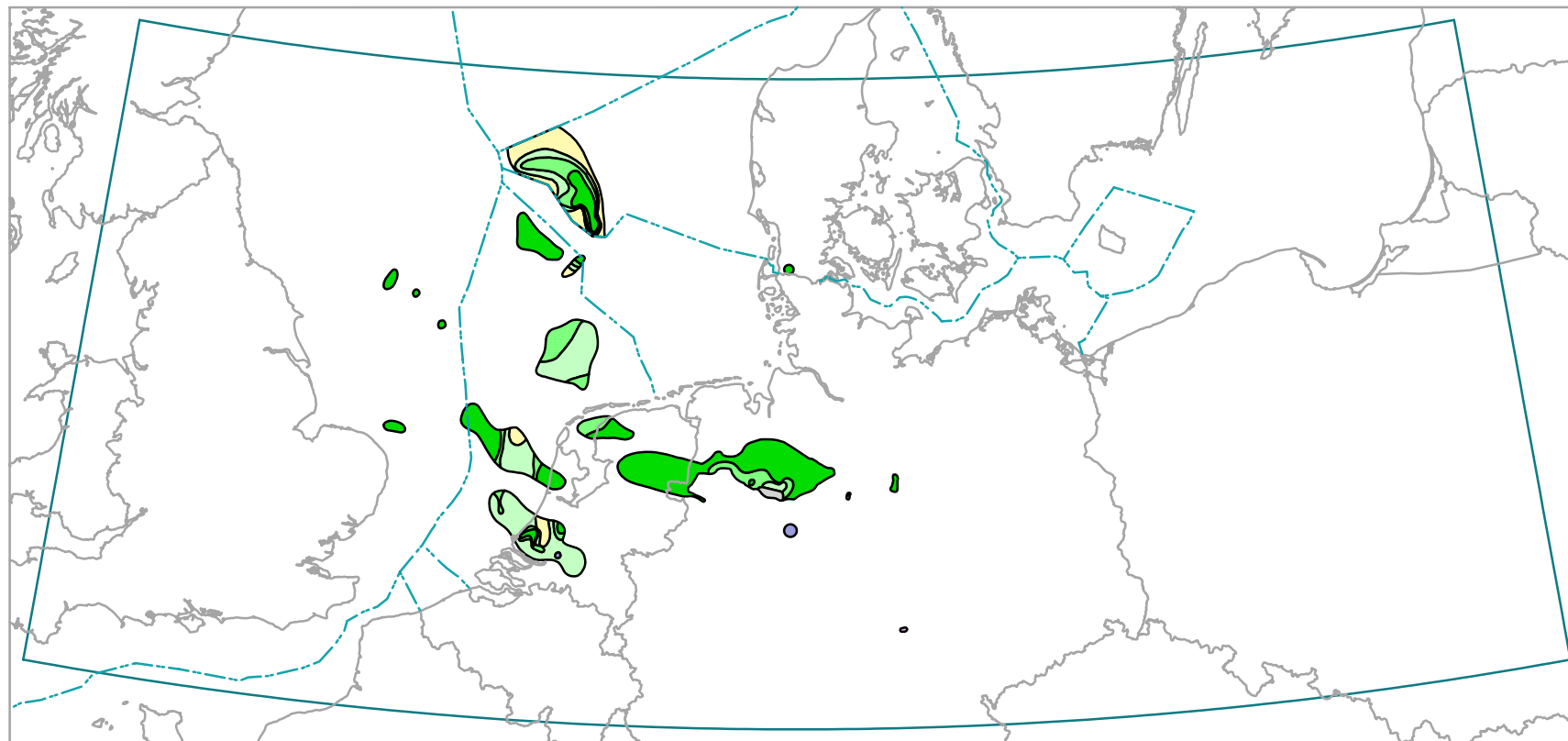
0 110 220 330 440 550 660 Kilometers



Projection : Lambert Conformal Conic  
 Spheroid : Bessel, 1841  
 Standard parallels : 51 N and 54 N  
 Central meridian : 9 E  
 Latitude of projection origin : 48 N  
 False easting : 7,500,000 m  
 False northing : 0 m



# CO2 contour map - Post-Zechstein reservoir gas



0 110 220 330 440 550 660 Kilometers



Projection : Lambert Conformal Conic  
Spheroid : Bessel, 1841  
Standard parallels : 51 N and 54 N  
Central meridian : 9 E  
Latitude of projection origin : 48 N  
False easting : 7,500,000 m  
False northing : 0 m

## 4.6 Calorific Value

The available database was far from complete. From many wells used for this study only GC data on gas compositions were available. Therefore it was necessary to calculate the calorific value on the basis of thermodynamic properties. The calorific value has been calculated according to:

$$H_i = \sum n_i \cdot Q_i$$

where

$H_i$  = heat of combustion  
 $n_i$  = the volume fraction of component  $i$   
 $Q_i$  = the calorific value of component  $i$

The calculated calorific values are expressed in MJ/m<sup>3</sup>, at standard conditions e.g. 15° C and 101325 kPa. The calculated combustion enthalpies (kJ/mol) of individual gas components have been derived from CODATA list of standard formation enthalpies (COX et al. 1989, LIDE [ed] 1992).

Most frequently the available data provide no information upon the presence of alkane isomers. The isomers of butane and pentane show differences in standard enthalpies of less than 0.5%. Therefore the calculations for the higher alkanes were based on the data for n-alkanes.

In those cases where measured and calculated calorific data were available, we were able to compare the results and perform a quality screening procedure. In cases of discrepancy the data were removed from the database.

The contour values of the calorific value maps are calculated according to the principle of equal amounts of data within the contour intervals. For the four reservoir intervals maps are presented of the calorific value distribution. The calorific value maps are not easy to interpret. The relative contribution of mineral gases N<sub>2</sub>, CO<sub>2</sub>, but not H<sub>2</sub>S to the calorific value is negative, whereas the presence of the higher alkanes causes an increase of the calorific value. For reference the calorific values of pure gases are given in the table below :

<u>component</u>	<u>calorific value (MJ/kg)</u>
CH <sub>4</sub>	32,81
C <sub>2</sub> H <sub>6</sub>	58,40
C <sub>3</sub> H <sub>8</sub>	83,51
n-C <sub>4</sub> H <sub>10</sub>	108,62
n-C <sub>5</sub> H <sub>12</sub>	133,76
n-C <sub>6</sub> H <sub>14</sub>	158,87
H <sub>2</sub> S	21,17
O <sub>2</sub>	0
N <sub>2</sub>	0
CO <sub>2</sub>	0
He	0

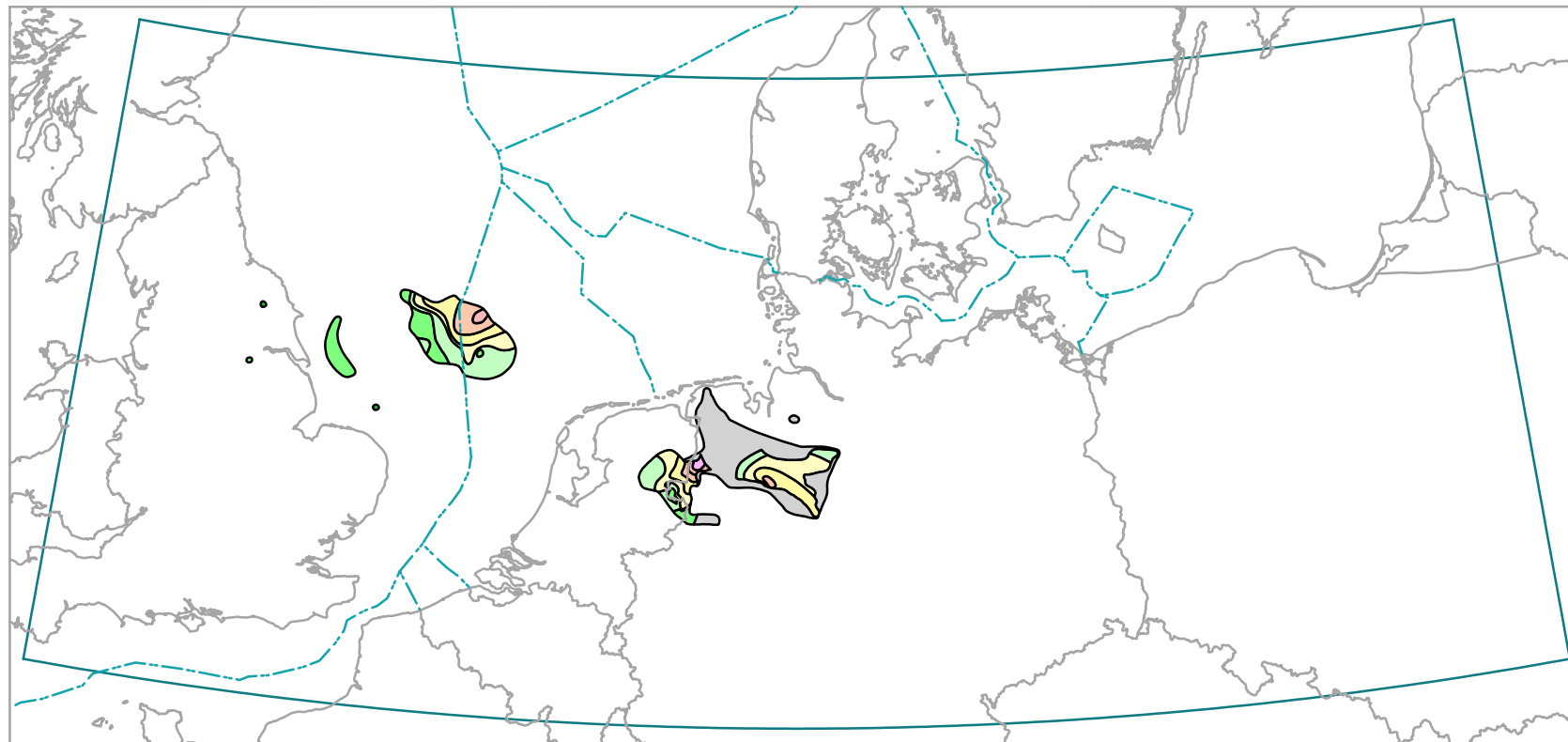
Calorific values from **Carboniferous** gases show low values in the eastern part of the study area (15 to 30 MJ/kg), due to high percentages of nitrogen. Around the German/Dutch boundary and in the Southern North Sea, calorific values are much higher, ranging over short distances from 32 to 43 MJ/kg. A southward increase is observed in this area. Obviously, higher calorific values in these areas are caused by relative contributions of the higher alkanes.

In the calorific values of **Rotliegend** gases distinct a distinct E-W trend. Highest calorific values are observed in the UK offshore and onshore areas, up to 45 MJ/kg. To the east there is an irregular decrease, first due to the decrease of C<sub>2+</sub> and subsequently followed by the increase of nitrogen content. Irregularities superimposed on this trend can be attributed to minor fluctuations in the relative proportions of C<sub>2+</sub> versus mineral gases. As compared with the Carboniferous data the Rotliegend gas occurrences in the whole area have relatively higher calorific values.

The **Zechstein** gases however, in those areas where they do occur, have lower calorific values again, as can be seen from the contourmap. This is partly caused, at least in Germany by relatively high abundance of CO<sub>2</sub>, which reduce the calorific value.

The calorific values in the **post-Zechstein** show a different pattern. In large parts of the Southern and Central North Sea calorific values range from 42 to 46 MJ/kg. These gas occurrences are rich in C<sub>2+</sub>, which can be linked to the contributions of Jurassic source rocks. i.e. Posidonia and/or Kimmeridge shales. These have high potentials for oil, relative to the Westphalian source rocks. They generally did not contribute to hydrocarbon accumulations in older strata.

# Calorific Value contour map - Carboniferous reservoir gas



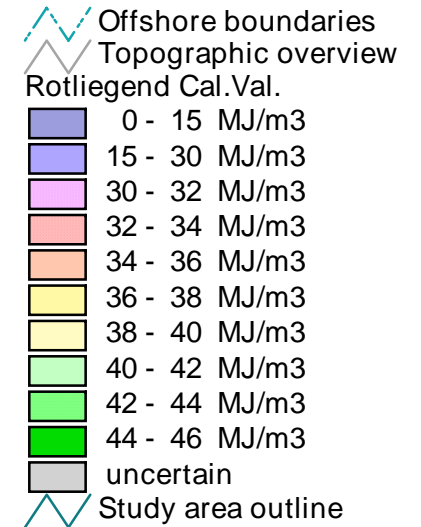
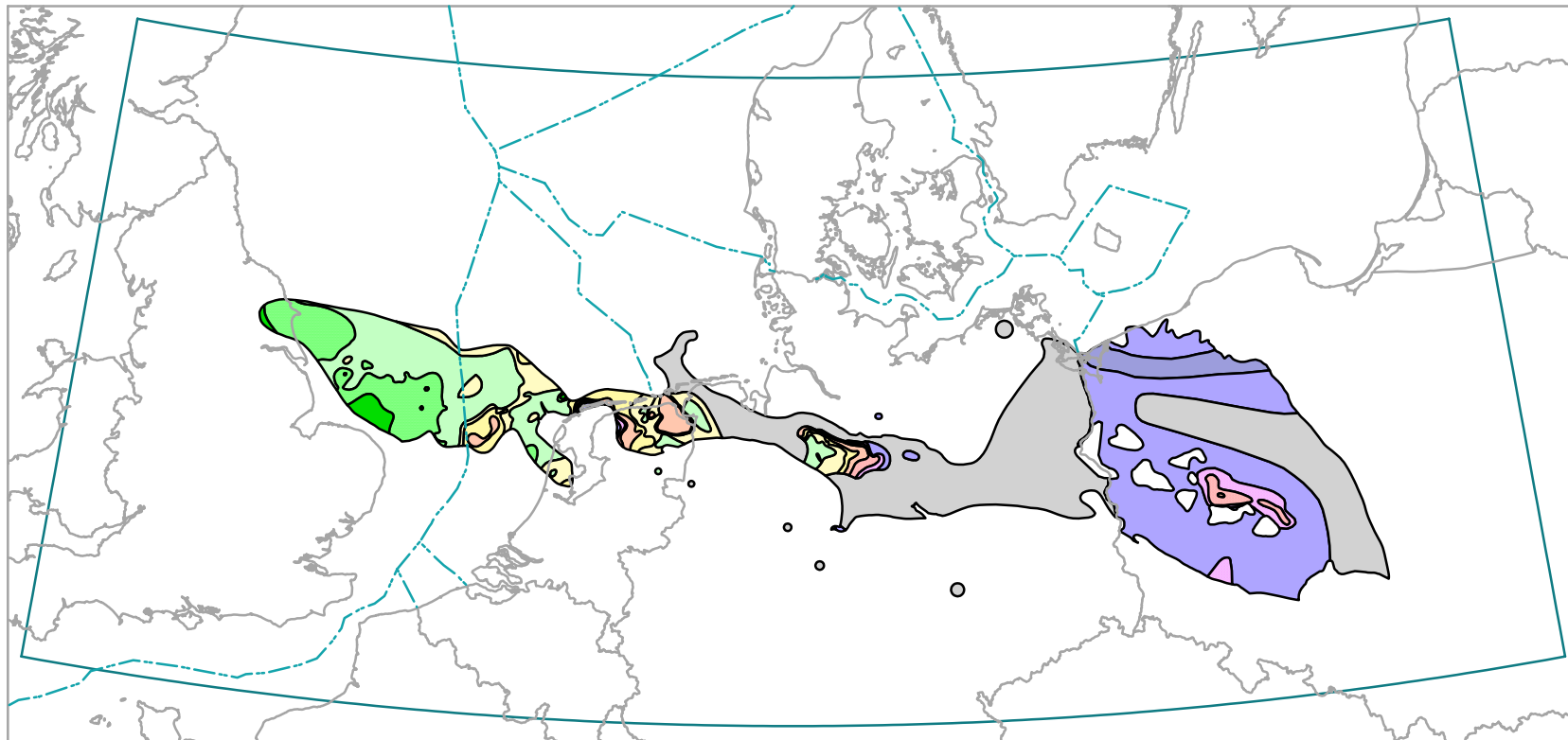
- Offshore boundaries
- Topographic overview
- Carboniferous Cal.Val.
- 0 - 15 MJ/m3
- 15 - 30 MJ/m3
- 30 - 32 MJ/m3
- 32 - 34 MJ/m3
- 34 - 36 MJ/m3
- 36 - 38 MJ/m3
- 38 - 40 MJ/m3
- 40 - 42 MJ/m3
- 42 - 44 MJ/m3
- 44 - 46 MJ/m3
- uncertain
- Study area outline

0 110 220 330 440 550 660 Kilometers



Projection : Lambert Conformal Conic  
 Spheroid : Bessel, 1841  
 Standard parallels : 51 N and 54 N  
 Central meridian : 9 E  
 Latitude of projection origin : 48 N  
 False easting : 7,500,000 m  
 False northing : 0 m

# Calorific Value contour map - Upper Rotliegend reservoir gas

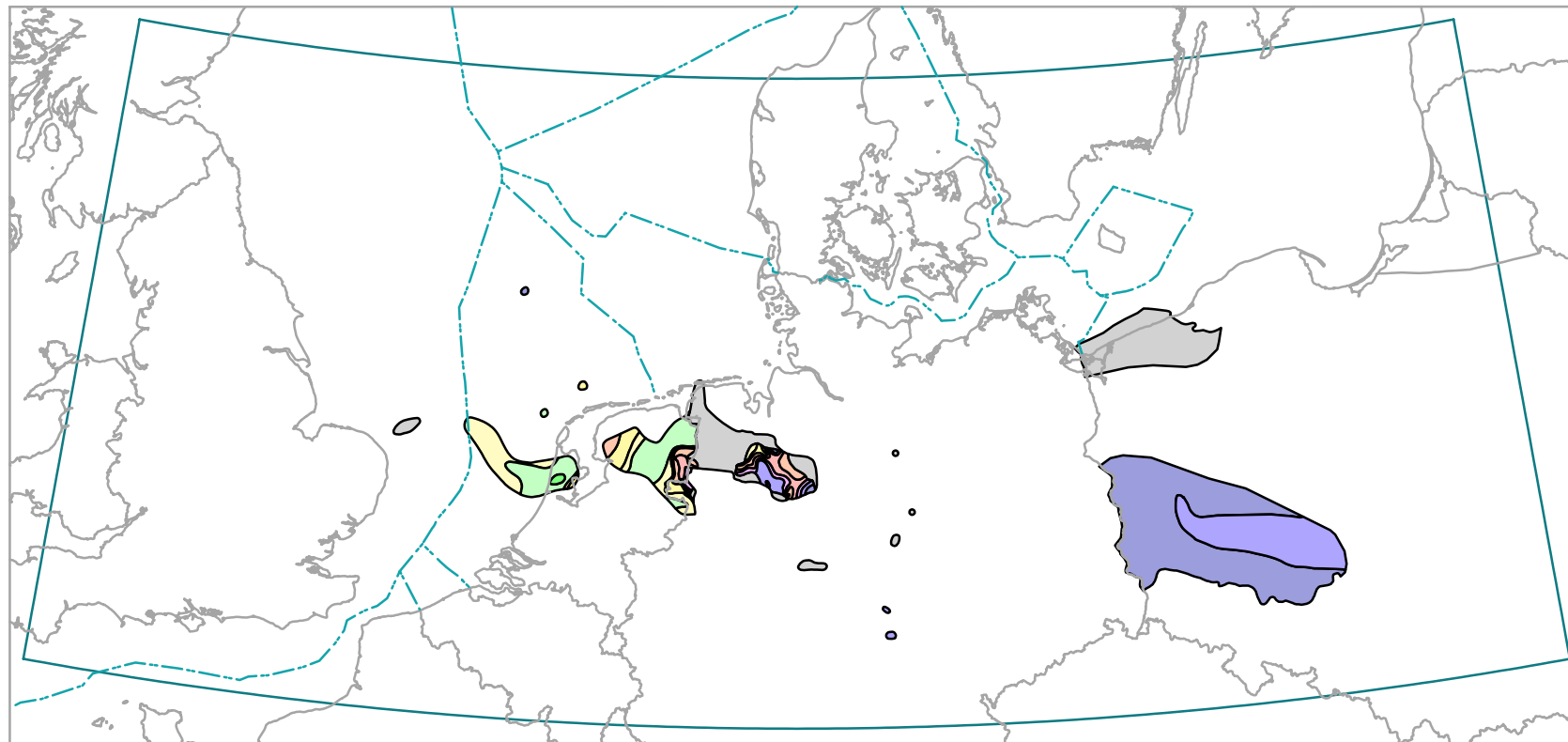







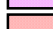


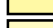




0 110 220 330 440 550 660 Kilometers



Projection : Lambert Conformal Conic  
Spheroid : Bessel, 1841  
Standard parallels : 51 N and 54 N  
Central meridian : 9 E  
Latitude of projection origin : 48 N  
False easting : 7,500,000 m  
False northing : 0 m

# Calorific Value contour map - Zechstein reservoir gas



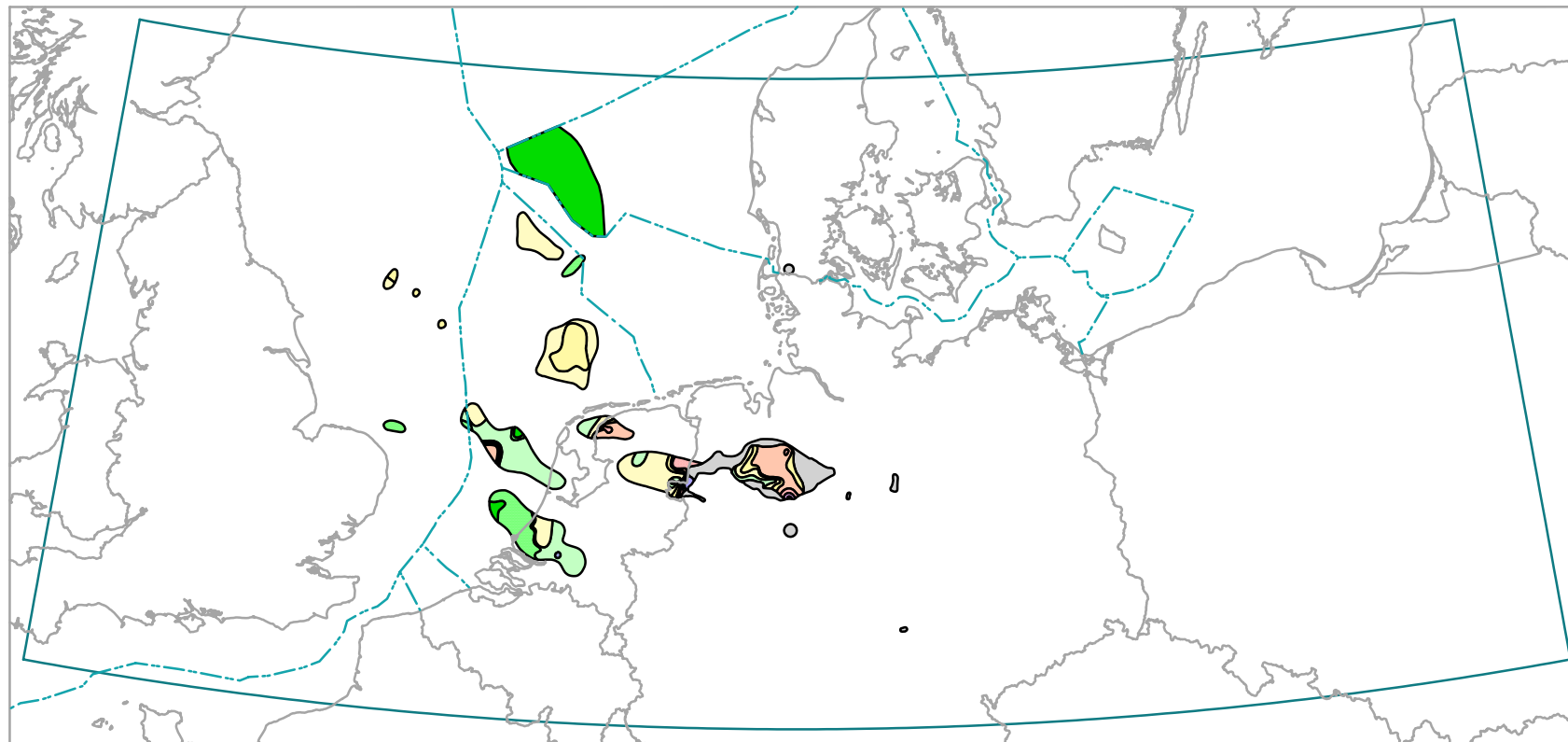
-  Offshore boundaries
-  Topographic overview
- Zechstein Cal.Val.
-  0 - 15 MJ/m<sup>3</sup>
-  15 - 30 MJ/m<sup>3</sup>
-  30 - 32 MJ/m<sup>3</sup>
-  32 - 34 MJ/m<sup>3</sup>
-  34 - 36 MJ/m<sup>3</sup>
-  36 - 38 MJ/m<sup>3</sup>
-  38 - 40 MJ/m<sup>3</sup>
-  40 - 42 MJ/m<sup>3</sup>
-  42 - 44 MJ/m<sup>3</sup>
-  uncertain
-  Study area outline

0 110 220 330 440 550 660 Kilometers



Projection : Lambert Conformal Conic  
 Spheroid : Bessel, 1841  
 Standard parallels : 51 N and 54 N  
 Central meridian : 9 E  
 Latitude of projection origin : 48 N  
 False easting : 7,500,000 m  
 False northing : 0 m

# Calorific Value contour map - Post-Zechstein reservoir gas



- Offshore boundaries
- Topographic overview
- Post-Zechstein Cal.Val.
- 0 - 15 MJ/m3
- 15 - 30 MJ/m3
- 30 - 32 MJ/m3
- 32 - 34 MJ/m3
- 34 - 36 MJ/m3
- 36 - 38 MJ/m3
- 38 - 40 MJ/m3
- 40 - 42 MJ/m3
- 42 - 44 MJ/m3
- 44 - 46 MJ/m3
- uncertain
- Study area outline

0 110 220 330 440 550 660 Kilometers



Projection : Lambert Conformal Conic  
 Spheroid : Bessel, 1841  
 Standard parallels : 51 N and 54 N  
 Central meridian : 9 E  
 Latitude of projection origin : 48 N  
 False easting : 7,500,000 m  
 False northing : 0 m

## 4.7 Density

Density measurements were not always available, and if so, it was not always clear whether they were measured or calculated. Therefore it was decided to calculate the densities on the basis of gas compositions derived from GC-analyses and thermodynamic properties.

There are quite a few methods for the calculation of densities of non ideal gases, each with their own confidence intervals and applicability ranges. Using molar masses and the compressibility factor of the gas mixture the density, expressed relative to air can be calculated (GEERSSEN, 1988). In this study we used ISO 6976-1983 for the calculation of the compressibility factor. The procedure followed is which is shortly summarised here. Considering the accuracy we needed for the preparation of our maps this method was considered satisfactory. The density  $\xi$  of a gas mixture at a certain temperature and pressure can be calculated according to:

$$\xi_{g[V(T_v;101.325)]} = \frac{1}{100 \cdot V_m \cdot Z_g} \cdot \frac{T_0}{T_v} \cdot \sum_1^n n_i \cdot M_i$$

where,

$\xi$	=	density, relative to air
$g\{V(T_v;101.325)\}$	=	density of gas mixture at 101.325 kPa and $T_v$ K
$T_0$	=	normal temperature (298.15 K)
$T_v$	=	temperature of gas mixture in K
$V_m$	=	normal molar volume, $22.41383 \cdot 10^{-3} \text{ m}^3/\text{mole}$
$Z$	=	compressibility factor of gas mixture
$n$	=	number of components
$n_i$	=	volume percentage of gas component $i$
$M$	=	molar mass of component $i$

The compressibility factor can be approximated in various ways. According to ISO 6976-1983, the calculation of the compressibility factor  $z$  can be calculated in a relative simple way if the concentration of  $H_2$  is negligible. This is the case in the investigated gases and the following formula was applied:

$$z = 1 - \left[ \sum_1^n \frac{n_i \sqrt{B_i}}{100} \right]^2$$

where:

$n$	=	number of gas components
$n_i$	=	concentration of component $i$ (mole%)
$\sqrt{B_i}$	=	summation factor = $\sqrt{(1-z_i)}$ , while
$z_i$	=	compressibility factor $z$ for component $i$ at $T$ K

In the table below the densities of various gas components are given:

<u>component</u>	<u>density</u> (relative to air)
CH <sub>4</sub>	0.555
C <sub>2</sub> H <sub>6</sub>	1.048
C <sub>3</sub> H <sub>8</sub>	1.555
n-C <sub>4</sub> H <sub>10</sub>	2.089
n-C <sub>5</sub> H <sub>12</sub>	2.671
n-C <sub>6</sub> H <sub>14</sub>	3.251
H <sub>2</sub> S	1.536
O <sub>2</sub>	1.429
N <sub>2</sub>	1.250
CO <sub>2</sub>	1.977
He	0.178
H <sub>2</sub>	0.090

From the table it can be seen that generally the lightest gas consists of pure methane, because the contributions of Hydrogen and Helium to the gas compositions are negligible in NW-Europe. As the presence of all other gas components will raise the density, density maps are even more difficult to interpret than calorific value maps.



The densities of **Carboniferous** gases show a clear geographical separation. Relatively low density gases, close to the densities of pure methane are found in the central part of the study area, i.e. in the Lower Saxony Basin and the Friesland Platform. These density occurrences coincide with areas of relatively pure methane rich gases. The highest densities are found in the eastern study area, where relatively high concentrations of nitrogen are responsible for the density increase. Intermediate densities are encountered in the Southern North Sea.

A similar pattern is observed for the density distribution in the **Rotliegend** gases. The lowermost gas densities are observed at the eastern and western edges of the Pompeckj block. At both sides there is a gradual increase to higher gas densities away from this structure. Like in the Carboniferous reservoirs, the highest densities are found in the easternmost part of the area.

The **Zechstein** gases display lowest densities in the Southern North Sea and the border area between the Netherlands and Germany. Locally, high densities occur here in relation to locally increased Nitrogen contents. Highest densities occur in SW Poland.

The **Post-Zechstein** gas density distribution is entirely different. East of the Ems depression relatively low density gases, with high percentages of methane are observed. To the west, at many places high density gases are frequently observed in the Southern and Central North Sea area, due to either the occurrence of carbon dioxide or the presence of wet gases.

## 4.8 Miscellaneous

Several constituents of natural gas occur either only locally or in a certain area or they occur just in minute concentrations. An example of the former group is hydrogen sulphide, whereas noble gases like helium or mercury belong to the latter group. Moreover, data from the latter group are rarely known. Consequently, these components are neither shown in any map nor will they be extensively discussed in Chapter 5. However, we don't want to exclude them. In the following paragraphs brief explanations about their generation and occurrence will be given.

### 4.8.1 Hydrogen Sulphide

Natural gases with more than 1% hydrogen sulphide are called sour gases. These sour gases only occur in Zechstein deposits in the area of interest. On a world-wide scale, sour gases with more than 10% H<sub>2</sub>S occur for example in the French gas field Lacq (U Jurassic and L Cretaceous carbonates), in Devonian and Lower Carboniferous reefs in Alberta / Canada, and in Upper Jurassic reservoirs at the US Gulf Coast. Reservoir depths in these areas is usually below 4.500 m and temperatures are rather high.

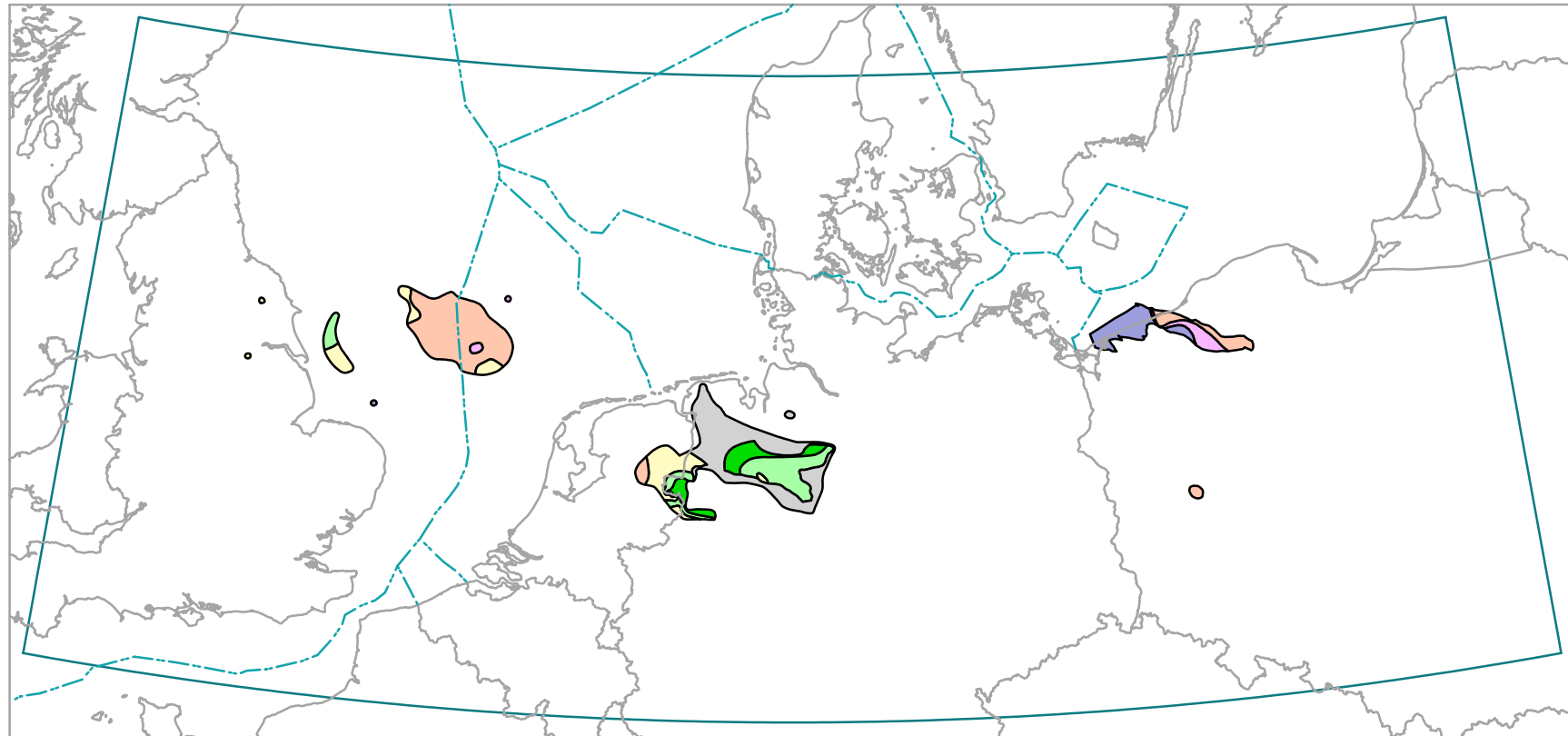
Thermochemical sulphate reduction (TSR) is believed to be the sulphide generating process. Hydrocarbons (HC) are decomposed during this process. The higher HCs (ethane, propane and higher homologues) are predominantly reduced. The remaining gases have heavier carbon and hydrogen isotopes (cf. paragraph 5.3.1) and isotopically lighter carbon dioxide (CO<sub>2</sub>) is produced. Finally, as the H<sub>2</sub>S level rises, methane is also decomposed.











MITTAG-BRENDEL (1994) has discussed the genesis of hydrogen sulphide in the west German Zechstein natural gas deposits and their dependence on the temperatures in the deposits as well as the facies-structural formations of the Werra anhydrite and the Staßfurt carbonates. Due to these results, TSR is a locally occurring phenomenon which is, amongst other things, strongly influenced by the reservoir temperature.

### 4.8.2 Mercury

Mercury is often found naturally as sulphide (HgS; red: cinnabarite, black: metacinnabarite), as by-product or trace element in a variety of ore minerals (sulphides, e.g. zinc-blende, pyrite) or selenides, as oxide (HgO) or depending on the pT-conditions as pure Hg in a liquid or gas phase.

# Density contour map - Carboniferous reservoir gas



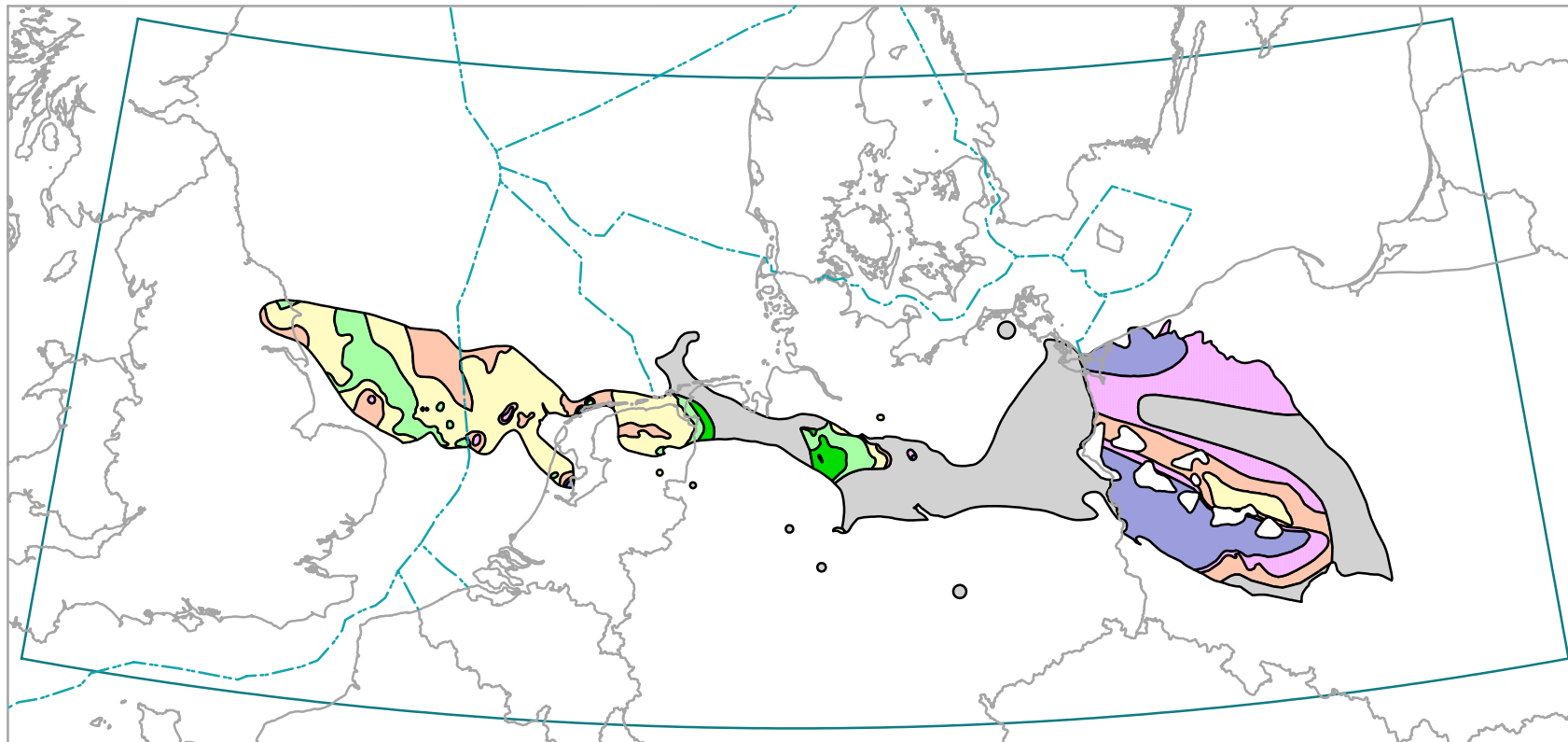
-  Offshore boundaries
-  Topographic overview
- Carboniferous Density**
-  0.50 - 0.55 r.t.a.
-  0.55 - 0.60 r.t.a.
-  0.60 - 0.65 r.t.a.
-  0.65 - 0.70 r.t.a.
-  0.70 - 0.75 r.t.a.
-  0.75 - 0.80 r.t.a.
-  uncertain
-  Study area outline

0 110 220 330 440 550 660 Kilometers



Projection : Lambert Conformal Conic  
Spheroid : Bessel, 1841  
Standard parallels : 51 N and 54 N  
Central meridian : 9 E  
Latitude of projection origin : 48 N  
False easting : 7,500,000 m  
False northing : 0 m

# Density contour map - Upper Rotliegend reservoir gas



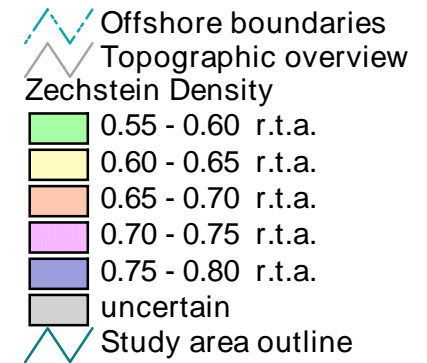
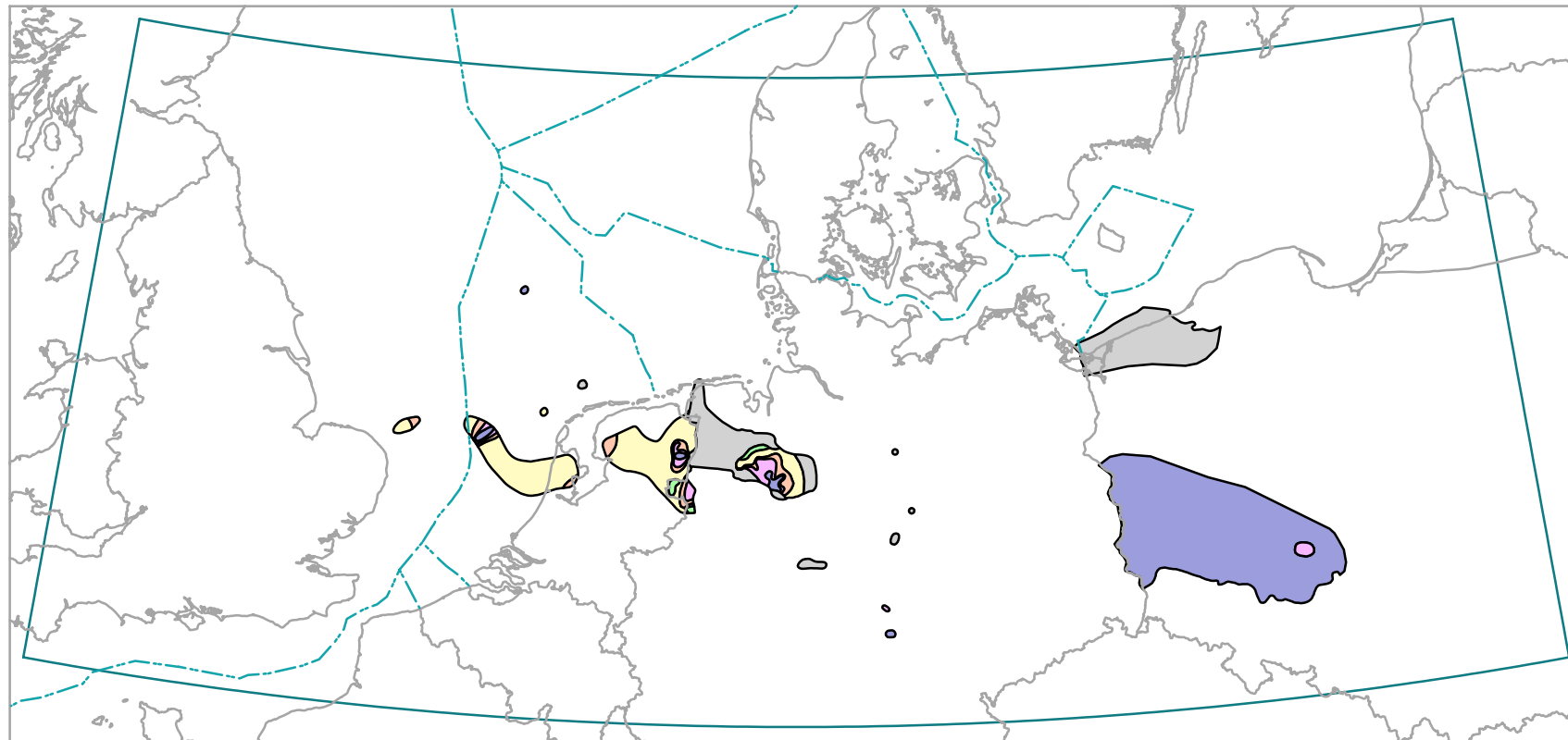
- Offshore boundaries
- Topographic overview
- Rotliegend Density
  - 0.50 - 0.55 r.t.a.
  - 0.55 - 0.60 r.t.a.
  - 0.60 - 0.65 r.t.a.
  - 0.65 - 0.70 r.t.a.
  - 0.70 - 0.75 r.t.a.
  - 0.75 - 0.80 r.t.a.
  - uncertain
- Study area outline

0 110 220 330 440 550 660 Kilometers



Projection : Lambert Conformal Conic  
Spheroid : Bessel, 1841  
Standard parallels : 51 N and 54 N  
Central meridian : 9 E  
Latitude of projection origin : 48 N  
False easting : 7,500,000 m  
False northing : 0 m

# Density contour map - Zechstein reservoir gas

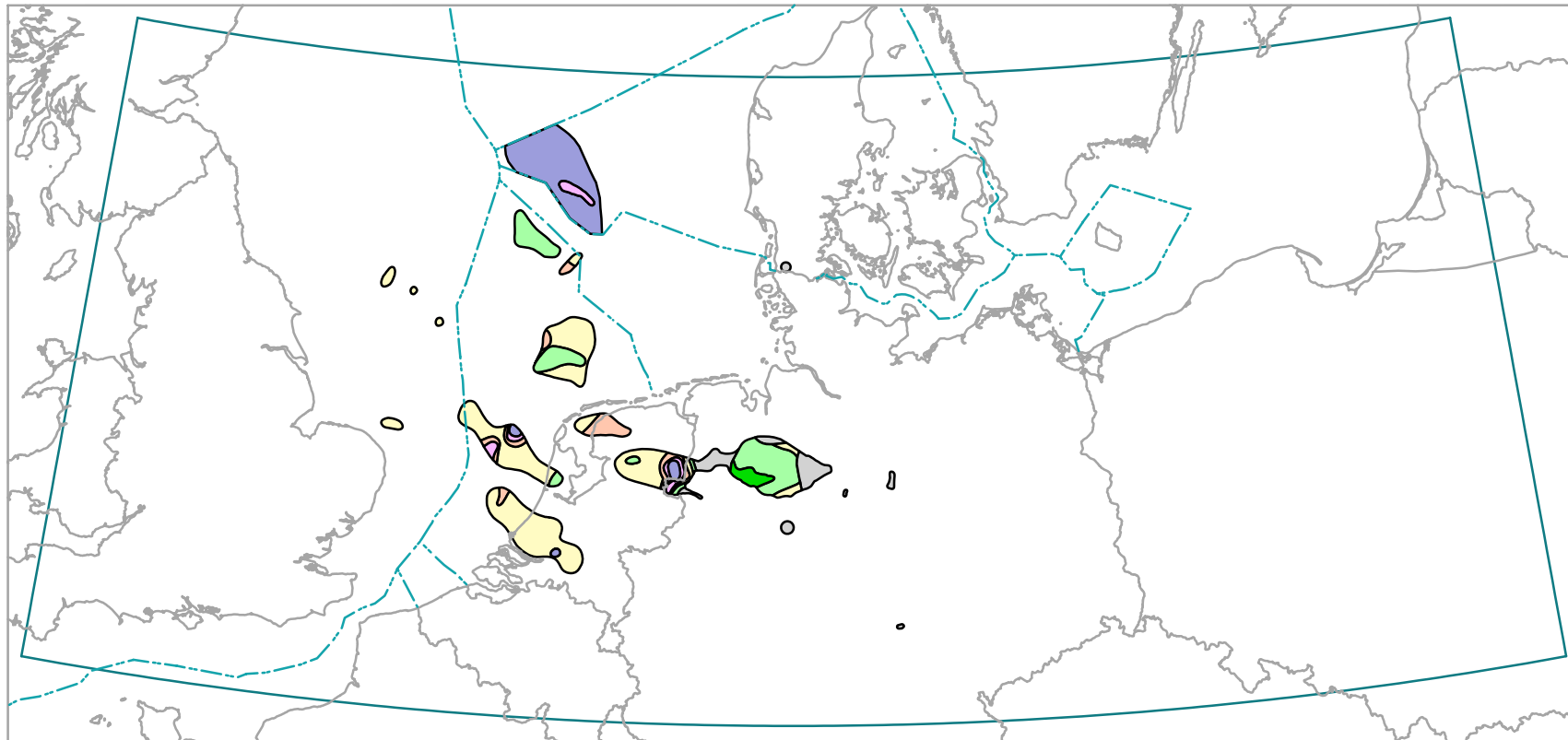


0 110 220 330 440 550 660 Kilometers



Projection : Lambert Conformal Conic  
Spheroid : Bessel, 1841  
Standard parallels : 51 N and 54 N  
Central meridian : 9 E  
Latitude of projection origin : 48 N  
False easting : 7,500,000 m  
False northing : 0 m

# Density contour map - Post-Zechstein reservoir gas



- Offshore boundaries
- Topographic overview
- Post-Zechstein Density
  - 0.50 - 0.55 r.t.a.
  - 0.55 - 0.60 r.t.a.
  - 0.60 - 0.65 r.t.a.
  - 0.65 - 0.70 r.t.a.
  - 0.70 - 0.75 r.t.a.
  - 0.75 - 0.80 r.t.a.
  - uncertain
- Study area outline

0 110 220 330 440 550 660 Kilometers



Projection : Lambert Conformal Conic  
Spheroid : Bessel, 1841  
Standard parallels : 51 N and 54 N  
Central meridian : 9 E  
Latitude of projection origin : 48 N  
False easting : 7,500,000 m  
False northing : 0 m

As well as these inorganic compounds mercury occurs often paragenetically with organic substances (BEUGE, 1982). After many analyses it was shown that rocks with organic content have significantly higher levels of Hg than those without organic components. The following combinations can occur simultaneously:

- sorptive on clay minerals and organic substances
- sulphidically in particular Fe-sulphides
- organo-metallically
- emulgated in organic substances

These organo-metallic connections are instable as of 60°C and - apart from the sulphide ones - do not exist above 300°C.

Currently the following mercury origins are being discussed:

- Hg originates from the upper earth's mantle and degasses through fractures into the upper crust,
- Hg is connected to basic to intermediary rocks,
- a metamorphic mobilisation is considered in crystalline areas,
- Hg is syngenetically enriched in coals and black shales,
- Hg is emitted by weathering/oxidation of sulphides along fault zones or under the influence of oxidizing waters which decompose sulphides.

Apart from that, the sorption ability of coals as well as mobilisation from it as a result of the thermal alteration must be taken into account.

The occurrence of mercury in hydrocarbon deposits in the mapped area has already been discussed by various authors (e.g. MORRISON , 1972; TUNN, 1973; RONTELTAP ,1973; DIKENSTEJN et al., 1973; KAEMMEL et al., 1978; PHILIPP & REINICKE, 1982; LUBAS, 1986). Some of these authors published the following data:

<u>Country</u>	<u>Strata</u>	<u>Minimum</u> ( $\mu\text{g}/\text{m}^3$ )	<u>Maximum</u> ( $\mu\text{g}/\text{m}^3$ )	<u>Average</u> ( $\mu\text{g}/\text{m}^3$ )	<u>Reference</u>
Germany	Carboniferous	300	340		TUNN, 1973
	Rotliegend	600	2000-4000		PHILIPP & REINICKE, 1982
	Buntsandstein	15	200		TUNN, 1973
	Jurassic	15	100		TUNN, 1973
The Netherlands	Rotliegend			180	RONTELTAP, 1973
Poland	L Carboniferous	65	85		LUBAS, 1986
	U Carboniferous	40	60		LUBAS, 1986
	Rotliegend	5	2000		LUBAS, 1986

Table 4.1: Mercury levels in natural gas fields

Two potential sources of mercury in natural gases are discussed in here cited literature. These are the Rotliegend volcanics (e.g RYKA, 1981) and also the Carboniferous coals (e.g. PHILIPP & REINICKE, 1982).

However, the database is quite small, and does not cover the entire area of the gas atlas. Therefore it is rather speculative to consider about the origin and distribution although mercury is an important but undesirable (toxic) component in natural gas.

### 4.8.3 Helium

Under the framework of the German 'Deep Gas Project' a total of 63 natural gas wells were selected for a study of the rare gas contents and isotope levels ( STAHL et al., 1996). The wells were chosen more or less statistically from all producing gas fields in northern Germany.

The helium contents of the North German natural gas fields (Fig. 4.6A) vary between about 150 and about 5000 ppm (0.015 - 0.5 vol%). Regional trends are recognisable in some gas provinces; for example, the He concentration in the East Hannover gas province (part of production province R3) decreases from east to west (PHILIPP & REINICKE, 1982). This phenomenon is, however, restricted to distinct areas. Moreover, distinct differences of in the content of noble gases between the reservoir formations within "stacked deposits" have been observed. Therefore the possibility of specific migration pathways, different times of accumulation, different distances to the sources, or even differences in the efficiency of the cap rock must be taken into consideration when the data are interpreted with respect to possible source rocks. At present it is assumed that the main reason for elevated He contents in gas fields is the proximity to deep-reaching faults that are open at least for the small He atoms.

Helium-isotope characteristics are a criterion for the genetic characterisation of this gas, e.g. the  $^3\text{He}/^4\text{He}$  ratio permits conclusions about the proportion of mantle helium (cf. OXBURGH et al., 1986). The unstable isotopes  $^3\text{He}$  and  $^4\text{He}$  occur in helium. In the atmosphere,  $^4\text{He}$  is about  $10^6$  times more concentrated.  $^4\text{He}$  is the product of the radiogene decomposition of U and Th, in particular in the earth's crust. On the other hand  $^3\text{He}$  occurs first and foremost in the earth's mantle. Its appearance in the earth's crust marks areas in which melting of the earth's mantle in the deeper underground occurs or has occurred. Mantle and crust helium can be clearly distinguished using the ratio R of both isotopes in gases. Crustal helium ( $R/R_a < 0.03$ ) and mantle helium ( $R/R_a = 9$ , defined from gases from the mid-ocean ridges) can be distinguished due to the normalisation of the  $^3\text{He}/^4\text{He}$  ratio in the atmosphere ( $R_a \approx 1.4 \times 10^{-6}$ ). Ratios falling in between describe helium-mixed gases.

Ten of the 63 samples of natural gas contained between 1 and 3% mantle helium (Fig. 4.6B) in addition to the crustal helium, which was the main component. The deposits from which these ten samples were taken are grouped in a small area north and northwest of the Uchte intrusive. A flow of gas may be assumed from very great depths, which means there must be a deep-reaching, sufficiently permeable migration path.

Further data on helium concentrations in reservoir horizons from Germany and Poland are given in the following table:

Country	Strata	Minimum (vol%)	Maximum (vol%)	Average (vol%)	Reference
Germany	Rotliegend	0.03	0.2		PHILIPP & REINICKE (1982)
Poland	Cambrian			0.18	KOTARBA*
	L Carboniferous	0.14	0.19		KOTARBA*
	U Carboniferous	0.11	0.30		KARNKOWSKI (1993), KOTARBA*
	Rotliegend	0.02	0.50		KARNKOWSKI (1993), KOTARBA*
	Zechstein (Ca2)	0.01	0.76		KARNKOWSKI (1993), KOTARBA*

Table 4.2: Helium levels in natural gas fields. \* unpublished data

This database is too small to present a basinwide interpretation.

## 5. THE GENETIC CHARACTERISATION OF GASEOUS HYDROCARBONS AND NITROGEN

General information about the generation and occurrence of various gas parameter have already been given in chapter 4. More information, especially on the genetic characterisation of the gases, can be of great help to describe and to understand the specific reservoir conditions in an production province. Moreover, this information may be very useful while correlating different production provinces.

Our approach is focusing on methane and nitrogen which are, beside carbon dioxide, the dominating natural gas components. The genetic characterisation of carbon dioxide is rather problematic (see chapter 4.5) and has therefore not been included in these considerations. From the minor gas constituents, we included ethane which can as well give important and additional information about type and maturity of a gas producing source rocks.

Concerning other minor gas constituents, e.g. hydrogen sulphide, mercury, and helium, we refer to the relevant explanations in Chapter 4.

The genetic interpretation of the natural gases will be given separately for the four reservoir horizons. These horizons have been further subdivided in production provinces. The total number of production provinces is 14. The areas of these were established around well clusters. Consequently, single wells are excluded from explanations about the natural gas occurrences in the production provinces. Since these from different reservoir horizons do in no case have identical spatial distributions, the number of wells inside as well as the area of the various production provinces differ.

Bulk genetic explanations about natural gases from a production province are given using a composition of four diagnostic plots. The genetic interpretation of gaseous hydrocarbons is based on

- the so-called 'Bernard-diagram' (after BERNARD et al. 1976, FABER & STAHL 1984) in which the molecular ratio  $C_1/(C_2+C_3)$  is compared with its methane stable carbon isotope ratio. This combination is particularly suitable to distinguish gases where there is a large range in the relative amount  $C_{2+}$  hydrocarbons, e.g. distinguishing wet thermogenic from dry thermogenic gases,
- the 'CD-diagram' (after SCHOELL 1980, 1984; WHITICAR et al. 1986) which is specifically designed to identify methane of various origins by using the carbon and hydrogen isotope ratios,
- the methane/ethane maturity lines (after BERNER & FABER 1996; see below) which are used to estimate type and maturity of the producing source rock

The genetic interpretation of nitrogen is based on

- a correlation of nitrogen content in a natural gas and its  $^{15}N/^{14}N$  ratios (after GERLING et al. 1997) which allow to distinguish between nitrogen from terrestrial and marine sources.

However, before applying these diagrams, certain remarks have to be given in order to understand the estimates about the type and maturity of source rocks, especially if taken from the combination of carbon isotope ratios of methane and ethane.

### Carbon isotope / maturity relationships for methane and ethane

During the last two decades a variety of models has been proposed that relate carbon isotope ratios of natural gases to source rock types and maturities. The pioneering works of STAHL (1968) and STAHL & CAREY (1975) have shown that empirical relations exist between the maturity of source rocks (vitrinite reflectance, VR) and the isotopic composition of related gaseous hydrocarbons.

Generally, carbon isotope values of thermal gases are thought to increase with increasing maturity of their precursors. This is explained through a kinetic isotope effect by which  $^{12}C$ - $^{12}C$  bonds of the kerogen are preferentially cracked, leading to an enrichment of  $^{13}C$  in the precursor sites of the gases, whereas light hydrocarbons are depleted in  $^{13}C$  compared to the kerogen.

Several researchers ( SUNDBERG & BENNETT 1983; PING & YONGCHANG 1986; SCHÜTZE & MÜHLE 1986; FABER 1987; CHUNG et al., 1988; GALIMOV 1988; BERNER 1989; ZHANG & FENG 1990; JAMES 1990; CLAYTON 1991; BERNER et al. 1992) have proposed how to use carbon isotopes of gases in hydro-



carbon exploration. The advantages and disadvantages of the individual models are discussed elsewhere (BERNER et al. 1993).

Pyrolyses experiments (dry, open-system) on algal kerogens and landplant material (BERNER et al., 1995) have shown that carbon isotopic variations of methane, ethane and propane obtained from laboratory experiments mimic isotope variations of natural thermal gases. These isotope variations can be approximated through kinetic models (BERNER et al., 1995). Also, maturity parameters like vitrinite reflectance and Rock-Eval  $T_{max}$  are reliably calculated from kinetic models that are based on pyrolysis experiments. User-friendly versions of isotope/maturity models for methane, ethane and propane were obtained from application of statistical curve-fitting procedures to the results of instantaneous kinetic models (BERNER & FABER 1996). The resulting simple empirical functions relate carbon isotopic variations of light hydrocarbons directly to source rock maturity and can be applied where gases have accumulated. They allow flexible calculations that account for carbon isotopic variability of precursor sites of the individual gases.

In this gas atlas we use the variable methane/ethane maturity lines proposed by BERNER & FABER (1996) in order to estimate the type and maturity of the gas producing source rocks (in the here discussed production provinces). The following algorithms have been installed in the relevant diagnostic plot:

- Gases from Type II kerogens

$$(1) \delta_{1III} = -4.0613VR^5 + 34.924VR^4 - 113VR^3 + 171.26VR^2 - 111.86VR - 20.735 + [30 - |\delta_{II}|] \quad (\text{instantaneous methane}),$$

$$(2) \delta_{2III} = 7.4991VR^6 - 81.906VR^5 + 354.73VR^4 - 772.76VR^3 + 881.75VR^2 - 482.97VR + 60.083 + [30 - |\delta_{II}|] \quad (\text{instantaneous ethane})$$

$\delta_{1III}$  and  $\delta_{2III}$  denote the variation of isotope ratios of methane and ethane as a function of maturity (VR) whereas  $\delta_{II}$  denotes the initial carbon isotope ratios of algal gas precursors. Function (1) is valid between 0.6 and 2.5% VR, function (2) between 0.6 and 2.0% VR.

- Gases from landplant kerogens and coals (Type III gases)

$$(3) \delta_{1III} = 3.6848VR - 31.292 + [22.0 - |\delta_{II}|] \quad (\text{instantaneous methane})$$

$$(4) \delta_{2III} = 3.1987VR - 26.901 + [22.4 - |\delta_{II}|] \quad (\text{instantaneous ethane})$$

$\delta_{1III}$  and  $\delta_{2III}$  denote the variation of isotope ratios of methane and ethane as a function of maturity (VR) whereas  $\delta_{III}$  denotes the initial carbon isotope ratios of landplant gas precursors. Functions (3) and (4) are valid between 0.6% and 2.5% VR.

Figure 5.1 shows the methane/ethane maturity lines for sapropelic or terrestrial organic matter. If a hydrocarbon gas only contains kogenetic methane and ethane from one of these source rocks, the corresponding pair of data should plot on or nearby a maturity line depending on the maturity of the source rock.

In Fig. 5.1 we have chosen  $-23\text{‰}$  and  $-29\text{‰}$  as default values for the carbon isotope ratios of the terrestrial and sapropelic gas precursors. Since these isotope ratios are variable in the different gas provinces due to specific source rock conditions, we have demonstrated in Fig. 5.2 how the flexibility of  $\delta_{II}$  and  $\delta_{III}$  has influence on the maturity lines and subsequently on the maturity estimates. To allow the customer the adaptation of the maturity line to a specific gas province,  $\delta_{II}$  and  $\delta_{III}$  are flexible in the relevant diagnostic plot on the CD ROM.

## Mixing Phenomena

In natural gas deposits very often the natural gas has not solely been generated from one source rock but contains gas components from a second, possibly even from several other source rocks. Isotope data of these mixed gases generally plot off the maturity lines.

The isotope ratios of the individual gases in the mixed gas depend on the isotopic and molecular composition of each mixing member which again are related to the type and maturity of the corresponding source rocks. In case of three or more mixing partners the interpretation of gas and isotope data is difficult, if not even impossible. However, in case of just two mixing gases which - to our current knowledge - is a very common feature in natural gas reservoirs, carbon isotope data of methane, ethane and propane of a mixed gas can be calculated using simple algorithms, including the molecular gas ratios of the mixing partners. Considering variable source types and maturities, mixing corridors can be established for the specific two mixing partners. These are presented in Fig. 5.3:

- If the mixed gas is a product of a dry gas from a terrestrial precursor and a wet gas from a sapropelic precursor it always lie in the corridor above the two mature lines.
- If the mixed gas is a composition of a gas from a rather low mature terrestrial source with a dry gas from a higher mature sapropelic organic matter it lies in the mixing corridor below the two maturity lines.

An example is given in Fig. 5.4 showing real data from production province R3 (see chapter 5.2.3). The carbon isotope ratio and the maturity of the marine precursor is known to be  $-29\text{‰}$  and 1.1% VR, respectively. The maturity of the terrestrial source rock is unknown, its carbon isotope ratio is assumed to be around  $-23\text{‰}$ . By iteration through the gas data it can be concluded that the gas is a mixture of a predominant coal-derived gas from a highly mature source with an admixture of about 0.5% gas from the lower mature marine source rock. It should be noticed that even this small admixture results in a large carbon isotope shift for ethane of about 5‰.

Finally, an important statement for the following chapters on the bulk genetic interpretation of gases from the individual production provinces will be given here. Quite often not all of the parameter shown in the four diagnostic plots are available for all individual reservoirs. Hence, the number of data points in the four plots will not always be identical.

## 5.1 Carboniferous Reservoirs

According to the distribution of natural gas fields producing from Carboniferous reservoirs, three production provinces have been established (Fig. 5.5). The reservoirs in the production provinces C1 and C2, lying in the North Sea and NW Germany, only produce from Upper Carboniferous strata. The corresponding Polish gas fields, however, produce from Lower and Upper Carboniferous strata.

Specific information about facies and distribution of the reservoir horizons is given in Chapter 3.

### 5.1.1 Production province C1: Upper Carboniferous Reservoirs in the UK and Dutch North Sea Sectors

The molecular gas ratios ( $C_1/(C_2+C_3)$ ) are plotted versus  $\delta^{13}C_1$  (the normalised  $^{13}C/^{12}C$  ratios of methane) in Figure 5.6A. The diagram permits bacterially generated methane to be distinguished from thermogenic hydrocarbon gases, with a further distinction between thermogenic gases from marine and terrestrial source rocks.

All investigated gases from reservoirs of production province C1 have  $C_1/(C_2+C_3)$  ratios between 8 and 45 and  $\delta^{13}C_1$  values between  $-44$  and  $-30\text{‰}$ , clearly indicating thermogenic origin. All of these gases seem to derive from a marine precursor. However, the most negative and the most positive isotope ratios (both from the UK sector of the production province) indicate a rather typical oil-associated gas in the first case (cf. production provinces Z3 and M1) and a rather typical gas from a terrestrial precursor material in the second case.

In Figure 5.6B, carbon ( $\delta^{13}\text{C}_1$ ) and hydrogen ( $\delta\text{D-C}_1$ ) isotope ratios of methane are used to distinguish between methane generation processes. Although this diagnostic plot was mainly designed for the discrimination of bacterial methanogenesis, it is also useful for determining the thermogenic origin of methane.

The methane from the reservoirs of production province C1 have  $\delta^{13}\text{C}_1$  values between -44 and -30‰ and  $\delta\text{D-C}_1$  values between -198 and -139‰, indicating all are of thermogenic origin. The isotopic ratios of most gases indicate a mixture from both a marine and a terrestrial source. Again (cf. Figure 5.6A), the most negative and the most positive carbon isotope values point to a rather typical associated gas and a gas from a terrestrial precursor, respectively.

Carbon isotope ratios of methane and ethane can be used to estimate the type and maturity of the precursor material. Correspondingly, Figure 5.6C shows two maturity lines for a sapropelic and a terrestrial source rock. A selection mode (see chapter 5: carbon isotope / maturity relationships for methane and ethane) allows the user to choose the carbon isotope ratio for each precursor material for the interpretation of the data. Since the default values of -23 and -29‰ are not necessarily the appropriate ones for every production province, all maturity estimates have to be categorised as qualitative statements.

The gases from production province C1 have  $\delta^{13}\text{C}_1$  values between -44 and -30‰ and  $\delta^{13}\text{C}_2$  values between -30 and -21‰. The majority of the data clearly indicate a gas mixture from a predominant marine source with a maturity of about 1.5 – 2% vitrinite reflectance and a minor amount of gas from a terrestrial source, most probably of lower maturity. Only the UK gas with the most positive  $\delta^{13}\text{C}_1$  value seems to contain a higher proportion of the gas from the terrestrial source. The most negative  $\delta^{13}\text{C}_1$  value indicates the presence of (?) bacterial methane, which is rather typical for oil-associated gases (cf. production provinces Z3 and M1).

Isotopic and molecular nitrogen data from pyrolysis experiments and from autochthonous Zechstein reservoirs are the basis for the interpretation of nitrogen gas in gas fields (Figure 5.6D). Especially the differences in the isotopic ratios allow nitrogen from a marine source rock to be distinguished from nitrogen from terrestrial precursor materials.

All five gases from production province C1 ( $\text{N}_2$  contents of 0.2 – 21%,  $\delta^{15}\text{N}$  values between 5 and 13‰) indicate a mixture of nitrogen from both a terrestrial and a marine source. The gas with the highest nitrogen content has the highest percentage of nitrogen from the marine precursor.

#### Conclusion:

The natural gases from production province C1 are in most cases mixtures from two source rocks. The predominant proportion derives from a sapropelic source having a moderate maturity (~ 1.5 - 2.0% vitrinite reflectance), a rather small gas proportion stems from a lower mature terrestrial source (probably Westphalian coals).

### **5.1.2 Production province C2: Upper Carboniferous Reservoirs in the eastern part of the Netherlands and in NW Germany**

The molecular gas ratios ( $\text{C}_1/(\text{C}_2+\text{C}_3)$ ) are plotted versus  $\delta^{13}\text{C}_1$  (the normalised  $^{13}\text{C}/^{12}\text{C}$  ratios of methane) in Figure 5.7A. The diagram permits bacterially generated methane to be distinguished from thermogenic hydrocarbon gases, with a further distinction between thermogenic gases from marine and terrestrial source rocks.

All investigated gases from reservoirs of production province C2 have  $\text{C}_1/(\text{C}_2+\text{C}_3)$  ratios between 11 and 315 and  $\delta^{13}\text{C}_1$  values between -32 and -22‰, clearly indicating thermogenic origin. Moreover, the gases display with the synchronous increase of carbon isotope ratios and molecular gas compositions an almost ideal case of a maturity trend. All of these gases seem to derive from a terrestrial precursor, although the most 'dry' and the most 'wet' gases lie outside the area of coal-derived gases.

In Figure 5.7B, carbon ( $\delta^{13}\text{C}_1$ ) and hydrogen ( $\delta\text{D-C}_1$ ) isotope ratios of methane are used to distinguish between methane generation processes. Although this diagnostic plot was mainly designed for the discrimination of bacterial methanogenesis, it is also useful for determining the thermogenic origin of methane.

The methane from the reservoirs of production province C2 have  $\delta^{13}\text{C}_1$  values between -32 and -22‰ and  $\delta\text{D-C}_1$  values between -164 and -121‰, indicating all are of thermogenic origin. The isotopic ratios indicate for most gases a terrestrial source. The distribution of the data show a classical maturity trend.

Carbon isotope ratios of methane and ethane can be used to estimate the type and maturity of the precursor material. Correspondingly, Figure 5.7C shows two maturity lines for a sapropelic and a terrestrial source rock. A selection mode (see chapter 5: carbon isotope / maturity relationships for methane and ethane) allows the user to choose the carbon isotope ratio for each precursor material for the interpretation of the data. Since the default values of -23 and -29‰ are not necessarily the appropriate ones for every production province, all maturity estimates have to be categorised as qualitative statements.

Most of the gases from production province C2 have  $\delta^{13}\text{C}_1$  values between -32 and -22‰ and  $\delta^{13}\text{C}_2$  values between -28 and -22‰, clearly indicating a mixture of gas from a predominant terrestrial source with a wide spread of maturity up to more than 2% vitrinite reflectance and - in some cases - a minor amount of gas from a lower mature marine source. The latter source can be found most probably in the Zechstein.

Isotopic and molecular nitrogen data from pyrolysis experiments and from autochthonous Zechstein reservoirs are the basis for the interpretation of nitrogen gas in gas fields (Figure 5.7D). Especially the differences in the isotopic ratios allow nitrogen from a marine source rock to be distinguished from nitrogen from terrestrial precursor materials.

The gases from production province C2 ( $\text{N}_2$  contents of 0.7 – 20%,  $\delta^{15}\text{N}$  values between -3 and 16‰) can be clearly divided in groups with  $\delta^{15}\text{N}$  values  $\geq 5$ ‰ and  $\delta^{15}\text{N}$  values  $< 1$ ‰. The first group clearly indicates a mixture of nitrogen from both a terrestrial and a marine source, whereas the nitrogen of the latter group seems to derive from terrestrial organic matter only. Since these gases are from reservoirs close to igneous intrusions of Bramsche-Vlotho-Uchte (cf. GERLING et al. 1997) one may consider as well an influence from those.

#### Conclusion:

The natural gases from production province C2 derive in most cases only from coaly organic matter. Some reservoirs contain additionally minor amounts of gaseous hydrocarbons and nitrogen from a lower mature, marine source (probably Zechstein).

### **5.1.3 Production province C3: Carboniferous Reservoirs in northern Poland**

The molecular gas ratios ( $\text{C}_1/(\text{C}_2+\text{C}_3)$ ) are plotted versus  $\delta^{13}\text{C}_1$  (the normalised  $^{13}\text{C}/^{12}\text{C}$  ratios of methane) in Figure 5.8A. The diagram permits bacterially generated methane to be distinguished from thermogenic hydrocarbon gases, with a further distinction between thermogenic gases from marine and terrestrial source rocks.

All investigated gases from reservoirs of production province C3 have  $\text{C}_1/(\text{C}_2+\text{C}_3)$  ratios between 14 and 45 and  $\delta^{13}\text{C}_1$  values between -31 and -28‰, clearly indicating thermogenic origin. However, the source rock character is not clearly to determine since the gas data - except one sample - plot in a very narrow cluster in a transition between thermogenic gases from marine and from terrestrial organic matter.

In Figure 5.8B, carbon ( $\delta^{13}\text{C}_1$ ) and hydrogen ( $\delta\text{D-C}_1$ ) isotope ratios of methane are used to distinguish between methane generation processes. Although this diagnostic plot was mainly designed for the discrimination of bacterial methanogenesis, it is also useful for determining the thermogenic origin of methane.

The methane from the reservoirs of production province C3 have  $\delta^{13}\text{C}_1$  values between -31 and -28‰ and  $\delta\text{D-C}_1$  values between -106 and -133‰, indicating all are of thermogenic origin. The isotopic ratios of all gases indicate a mixture from both a marine and a terrestrial source.

Carbon isotope ratios of methane and ethane can be used to estimate the type and maturity of the precursor material. Correspondingly, Figure 5.8C shows two maturity lines for a sapropelic and a terrestrial source rock. A selection mode (see chapter 5: carbon isotope / maturity relationships for methane and ethane) allows the user to choose the carbon isotope ratio for each precursor material for the interpretation of the data. Since the default values of -23 and -29‰ are not necessarily the appropriate ones for every production province, all maturity estimates have to be categorised as qualitative statements.

Most of the gases from production province C3 have  $\delta^{13}\text{C}_1$  values between -31 and -28‰ and  $\delta^{13}\text{C}_2$  values between -34 and -27‰, clearly indicating a mixture of gas from a predominant terrestrial source with a moderate maturity and a minor amount of gas from a lower mature, marine source.

Isotopic and molecular nitrogen data from pyrolysis experiments and from autochthonous Zechstein reservoirs are the basis for the interpretation of nitrogen gas in gas fields (Figure 5.8D). Especially the differences in the isotopic ratios allow nitrogen from a marine source rock to be distinguished from nitrogen from terrestrial precursor materials.

All gases from production province C3 ( $\text{N}_2$  contents of 31 – 60%,  $\delta^{15}\text{N}$  values between 4 and 13‰) clearly indicate a mixture of nitrogen from both a terrestrial and a marine source. Moreover, the data seem to indicate that the terrestrial organic matter occurs in dispersed form and not as solid coal seams.

#### Conclusion:

The natural gases from production province C3 are mixtures from two source rocks. The predominant proportion derives from terrestrial organic matter having a moderate maturity, a rather small gas proportion stems from a lower mature marine source (probably from Zechstein).

## **5.2 Rotliegend Reservoirs**

According to the distribution of natural gas fields producing from Rotliegend reservoirs, five production provinces have been established (Fig. 5.9). All reservoirs in these production provinces are found in sandstone deposits. These sand are aeolian deposits along the southern shore of the Rotliegend desert lake. More information about facies and distribution of the reservoir horizons is given in Chapter 3.

The Rotliegend production provinces do not overlap with those in the Carboniferous.

### **5.2.1 Production province R1: Rotliegend Reservoirs in the UK and Dutch North Sea (west of the island of Ameland)**

The molecular gas ratios ( $\text{C}_1/(\text{C}_2+\text{C}_3)$ ) are plotted versus  $\delta^{13}\text{C}_1$  (the normalised  $^{13}\text{C}/^{12}\text{C}$  ratios of methane) in Figure 5.10A. The diagram permits bacterially generated methane to be distinguished from thermogenic hydrocarbon gases, with a further distinction between thermogenic gases from marine and terrestrial source rocks.

All investigated gases from reservoirs of production province R1 have  $\text{C}_1/(\text{C}_2+\text{C}_3)$  ratios between 8 and 88 and  $\delta^{13}\text{C}_1$  values between -38 and -27‰, clearly indicating thermogenic origin. Most of these gases seem to derive from a marine precursor. The good correlation of increasing carbon isotope ratios and increasing gas compositions displays either a classical maturity trend of gases from one marine source or may as well be indicative for varying proportions of gases from marine and terrestrial precursor materials.. A few gases may be generated from pure terrestrial organic matter.

In Figure 5.10B, carbon ( $\delta^{13}\text{C}_1$ ) and hydrogen ( $\delta\text{D-C}_1$ ) isotope ratios of methane are used to distinguish between methane generation processes. Although this diagnostic plot was mainly

designed for the discrimination of bacterial methanogenesis, it is also useful for determining the thermogenic origin of methane.

The methane from the reservoirs of production province R1 have  $\delta^{13}\text{C}_1$  values between -38 and -27‰ and  $\delta\text{D-C}_1$  values between -160 and -117‰, indicating all are of thermogenic origin. Almost half of the data have the isotopic signature of associated methane whereas most of the other half indicate a mixture from both a marine and a terrestrial source. Some gases seem to derive from a pure terrestrial precursor, one gas from marine organic matter.

Carbon isotope ratios of methane and ethane can be used to estimate the type and maturity of the precursor material. Correspondingly, Figure 5.10C shows two maturity lines for a sapropelic and a terrestrial source rock. A selection mode (see chapter 5: carbon isotope / maturity relationships for methane and ethane) allows the user to choose the carbon isotope ratio for each precursor material for the interpretation of the data. Since the default values of -23 and -29‰ are not necessarily the appropriate ones for every production province, all maturity estimates have to be categorised as qualitative statements.

The gases from production province R1 have  $\delta^{13}\text{C}_1$  values between -38 and -27 ‰ and  $\delta^{13}\text{C}_2$  values between -30 and -18‰. About one half of the gases seem to be generated from a highly mature marine source, whereas most of the other gases seem to contain as well a minor proportion of hydrocarbons from a terrestrial organic matter. Only a few gases may stem either from a rather low mature coaly or marine precursor.

Isotopic and molecular nitrogen data from pyrolysis experiments and from autochthonous Zechstein reservoirs are the basis for the interpretation of nitrogen gas in gas fields (Figure 5.10D). Especially the differences in the isotopic ratios allow nitrogen from a marine source rock to be distinguished from nitrogen from terrestrial precursor materials.

The gases from production province R1 ( $\text{N}_2$  contents of 0.5 – 11%,  $\delta^{15}\text{N}$  values between -4.7 and 14‰) can be divided into two groups which indicate either a nitrogen generation from a coaly precursor or a mixture of nitrogen from both a terrestrial and a marine source.

#### Conclusion:

The natural gases from production province R1 seem to be generated in many cases from a rather highly mature marine source rocks. Even in case of mixed gases, the predominant proportion derives from a sapropelic source, only a rather small gas proportion stems from a comparatively lower mature terrestrial source (probably Westphalian coals).

## **5.2.2 Production province R2: Rotliegend Reservoirs on the Friesland platform, the Groningen High and the Ems Estuary**

The molecular gas ratios ( $\text{C}_1/(\text{C}_2+\text{C}_3)$ ) are plotted versus  $\delta^{13}\text{C}_1$  (the normalised  $^{13}\text{C}/^{12}\text{C}$  ratios of methane) in Figure 5.11A. The diagram permits bacterially generated methane to be distinguished from thermogenic hydrocarbon gases, with a further distinction between thermogenic gases from marine and terrestrial source rocks.

All investigated gases from reservoirs of production province R2 have  $\text{C}_1/(\text{C}_2+\text{C}_3)$  ratios between 8 and 85 and  $\delta^{13}\text{C}_1$  values between -38 and -22‰, clearly indicating thermogenic origin. Almost all of these gases seem to derive from a marine precursor. Only a few gases seem to derive from a rather typical terrestrial precursor material.

In Figure 5.11B, carbon ( $\delta^{13}\text{C}_1$ ) and hydrogen ( $\delta\text{D-C}_1$ ) isotope ratios of methane are used to distinguish between methane generation processes. Although this diagnostic plot was mainly designed for the discrimination of bacterial methanogenesis, it is also useful for determining the thermogenic origin of methane.

The methane from the reservoirs of production province R2 have  $\delta^{13}\text{C}_1$  values between -38 and -22‰ and  $\delta\text{D-C}_1$  values between -166 and -104‰, indicating all are of thermogenic origin. The isotope ratios of most gases indicate a mixture from both a marine and a terrestrial source. A few gases stem only from terrestrial organic matter.

Carbon isotope ratios of methane and ethane can be used to estimate the type and maturity of the precursor material. Correspondingly, Figure 5.11C shows two maturity lines for a sapropelic and a terrestrial source rock. A selection mode (see chapter 5: carbon isotope / maturity relationships for methane and ethane) allows the user to choose the carbon isotope ratio for each precursor material for the interpretation of the data. Since the default values of -23 and -29‰ are not necessarily the appropriate ones for every production province, all maturity estimates have to be categorised as qualitative statements.

The gases from production province R2 have  $\delta^{13}\text{C}_1$  values between -38 and -22‰ and  $\delta^{13}\text{C}_2$  values between -28 and -20‰, clearly indicating a mixture of gas from a predominant marine source with a maturity of about 2% vitrinite reflectance and a minor amount of gas from a terrestrial source, probably of comparatively lower maturity. Three gases seem to be generated only from terrestrial organic matter, one gas (from the easternmost area of this production province) is a mixture of predominant gaseous hydrocarbons from a coaly organic matter plus a minor amount of gaseous hydrocarbons from a lower mature marine source.

The difference between this sample and the other ones in production province R2 marks the E/W boundary in Rotliegend gasfields between gas mixtures with dominating marine or terrestrial gases.

Isotopic and molecular nitrogen data from pyrolysis experiments and from autochthonous Zechstein reservoirs are the basis for the interpretation of nitrogen gas in gas fields (Figure 5.11D). Especially the differences in the isotopic ratios allow nitrogen from a marine source rock to be distinguished from nitrogen from terrestrial precursor materials.

Most gases from production province R2 ( $\text{N}_2$  contents of 0.5 – 14%,  $\delta^{15}\text{N}$  values between -2 and 19‰) indicate a mixture of nitrogen from both a terrestrial and a marine source. Only two gases seem to contain pure coal-derived nitrogen..

#### Conclusion:

The natural gases from production province R2 are in most cases mixtures from two source rocks. The predominant proportion derives from a sapropelic source having a maturity of about 2.0% vitrinite reflectance, a rather small gas proportion stems from a lower mature terrestrial source (probably Westphalian coals).

### **5.2.3 Production province R3: Rotliegend Reservoirs between Bremen and the Altmark area (northern Germany)**

The molecular gas ratios ( $\text{C}_1/(\text{C}_2+\text{C}_3)$ ) are plotted versus  $\delta^{13}\text{C}_1$  (the normalised  $^{13}\text{C}/^{12}\text{C}$  ratios of methane) in Figure 5.12A. The diagram permits bacterially generated methane to be distinguished from thermogenic hydrocarbon gases, with a further distinction between thermogenic gases from marine and terrestrial source rocks.

All investigated gases from reservoirs of production province R3 have  $\text{C}_1/(\text{C}_2+\text{C}_3)$  ratios between 44 and 154 and  $\delta^{13}\text{C}_1$  values between -28 and -20‰, clearly indicating thermogenic origin. All of these gases derive from a terrestrial precursor.

In Figure 5.12B, carbon ( $\delta^{13}\text{C}_1$ ) and hydrogen ( $\delta\text{D}-\text{C}_1$ ) isotope ratios of methane are used to distinguish between methane generation processes. Although this diagnostic plot was mainly designed for the discrimination of bacterial methanogenesis, it is also useful for determining the thermogenic origin of methane.

The methane from the reservoirs of production province R3 have  $\delta^{13}\text{C}_1$  values between -28 and -20‰ and  $\delta\text{D}-\text{C}_1$  values between -125 and -107‰, indicating all are of thermogenic origin. The isotopic ratios of all gases indicate a generation in a terrestrial source.

Carbon isotope ratios of methane and ethane can be used to estimate the type and maturity of the precursor material. Correspondingly, Figure 5.12C shows two maturity lines for a sapropelic and a terrestrial source rock. A selection mode (see chapter 5: carbon isotope / maturity relationships for methane and ethane) allows the user to choose the carbon isotope ratio for each precursor material for

the interpretation of the data. Since the default values of -23 and -29‰ are not necessarily the appropriate ones for every production province, all maturity estimates have to be categorised as qualitative statements.

The gases from production province R3 have  $\delta^{13}\text{C}_1$  values between -28 and -20‰ and  $\delta^{13}\text{C}_2$  values between -24 and -19‰, clearly indicating a generation from a terrestrial source of a maturity of more than 1.5% vitrinite reflectance. In some cases, an admixture of a minor proportion of gas from a marine source of low maturity is indicated by the data.

Isotopic and molecular nitrogen data from pyrolysis experiments and from autochthonous Zechstein reservoirs are the basis for the interpretation of nitrogen gas in gas fields (Figure 5.12D). Especially the differences in the isotopic ratios allow nitrogen from a marine source rock to be distinguished from nitrogen from terrestrial precursor materials.

All gases from production province R3 ( $\text{N}_2$  contents of 4 – 81%,  $\delta^{15}\text{N}$  values between 6 and 15‰) indicate a mixture of nitrogen from both a terrestrial and a marine source. Interestingly, the content-related division of the gases indicates a differentiation between 'terrestrial' nitrogen from coals and that from dispersed coaly matter. Moreover, the latter nitrogen occurs only in the eastern part of production province R3 whereas the reservoirs in the western area contain only relatively small amounts of  $\text{N}_2$ .

#### Conclusion:

The natural gases from production province R3 contain in most cases gaseous hydrocarbon from a terrestrial precursor but nitrogen mixtures from a marine and a terrestrial source rocks. In case of mixed hydrocarbon gases, the predominant proportion derives from a terrestrial source having a maturity of more than 1.5% vitrinite reflectance, a rather small gas proportion stems from a lower mature marine source (probably Zechstein).

### **5.2.4 Production province R4: Rotliegend Reservoirs in Poland northeast of the Wolsztyn High**

The molecular gas ratios ( $\text{C}_1/(\text{C}_2+\text{C}_3)$ ) are plotted versus  $\delta^{13}\text{C}_1$  (the normalised  $^{13}\text{C}/^{12}\text{C}$  ratios of methane) in Figure 5.13A. The diagram permits bacterially generated methane to be distinguished from thermogenic hydrocarbon gases, with a further distinction between thermogenic gases from marine and terrestrial source rocks.

All investigated gases from reservoirs of production province R4 have  $\text{C}_1/(\text{C}_2+\text{C}_3)$  ratios between 27 and 488 and  $\delta^{13}\text{C}_1$  values between -33 and -26‰, clearly indicating thermogenic origin. All of these gases seem to derive from a marine precursor. The rather dry molecular gas compositions indicate a relatively high source rock maturity.

In Figure 5.13B, carbon ( $\delta^{13}\text{C}_1$ ) and hydrogen ( $\delta\text{D}-\text{C}_1$ ) isotope ratios of methane are used to distinguish between methane generation processes. Although this diagnostic plot was mainly designed for the discrimination of bacterial methanogenesis, it is also useful for determining the thermogenic origin of methane.

The methane from the reservoirs of production province R4 have  $\delta^{13}\text{C}_1$  values between -33 and -26‰ and  $\delta\text{D}-\text{C}_1$  values between -141 and -112‰, indicating all are of thermogenic origin. The isotopic ratios of most gases indicate a mixture from both a marine and a terrestrial source.

Carbon isotope ratios of methane and ethane can be used to estimate the type and maturity of the precursor material. Correspondingly, Figure 5.13C shows two maturity lines for a sapropelic and a terrestrial source rock. A selection mode (see chapter 5: carbon isotope / maturity relationships for methane and ethane) allows the user to chose the carbon isotope ratio for each precursor material for the interpretation of the data. Since the default values of -23 and -29‰ are not necessarily the appropriate ones for every production province, all maturity estimates have to be categorised as qualitative statements.

The gases from production province R4 have  $\delta^{13}\text{C}_1$  values between -33 and -26‰ and  $\delta^{13}\text{C}_2$  values between -37 and -27‰, clearly indicating a mixture of gas from a marine source and of gas from a



higher mature terrestrial source. The mixing proportions are rather difficult to evaluate since they are depending on the maturity of the involved source rocks for every individual reservoir. However, it is interesting to notice that the data spread represents an East-West maturity trend similar to the carbon isotope ratios of ethane. Moreover, the data indicate that the proportion of 'marine hydrocarbons' seem to increase from East to West.

Isotopic and molecular nitrogen data from pyrolysis experiments and from autochthonous Zechstein reservoirs are the basis for the interpretation of nitrogen gas in gas fields (Figure 5.13D). Especially the differences in the isotopic ratios allow nitrogen from a marine source rock to be distinguished from nitrogen from terrestrial precursor materials.

Many gases from production province R4 ( $N_2$  contents of 13 – 51%,  $\delta^{15}N$  values between 5 and 13‰) indicate a mixture of nitrogen from both a terrestrial and a marine source, some even a generation from a pure terrestrial source. Especially the latter indication is somehow irritating since the gaseous hydrocarbons indicate either a mixed gas or even a generation alone from a marine organic matter.

#### Conclusion:

The natural gases from production province R4 display a somehow enigmatic character. All gaseous hydrocarbons seem to be a gas mixture from a terrestrial organic source and lower mature marine organic matter. The nitrogen data is partly in agreement with this interpretation. Several gases, however, seem to be generated only from terrestrial organic matter.

### **5.2.5 Production province R5: Rotliegend Reservoirs in Poland southwest of the Wolsztyn High**

The molecular gas ratios ( $C_1/(C_2+C_3)$ ) are plotted versus  $\delta^{13}C_1$  (the normalised  $^{13}C/^{12}C$  ratios of methane) in Figure 5.14A. The diagram permits bacterially generated methane to be distinguished from thermogenic hydrocarbon gases, with a further distinction between thermogenic gases from marine and terrestrial source rocks.

All investigated gases from reservoirs of production province R5 have  $C_1/(C_2+C_3)$  ratios between 14 and 419 and  $\delta^{13}C_1$  values between -33 and -23‰, clearly indicating thermogenic origin. Almost all of these gases seem to derive from a marine precursor, only a few gases seem to be generated from terrestrial organic matter.

In Figure 5.14B, carbon ( $\delta^{13}C_1$ ) and hydrogen ( $\delta D-C_1$ ) isotope ratios of methane are used to distinguish between methane generation processes. Although this diagnostic plot was mainly designed for the discrimination of bacterial methanogenesis, it is also useful for determining the thermogenic origin of methane.

The methane from the reservoirs of production province R5 have  $\delta^{13}C_1$  values between -33 and -23‰ and  $\delta D-C_1$  values between -145 and -113‰, indicating all are of thermogenic origin. The isotopic ratios of most gases indicate a mixture from both a marine and a terrestrial source.

Carbon isotope ratios of methane and ethane can be used to estimate the type and maturity of the precursor material. Correspondingly, Figure 5.14C shows two maturity lines for a sapropelic and a terrestrial source rock. A selection mode (see chapter 5: carbon isotope / maturity relationships for methane and ethane) allows the user to choose the carbon isotope ratio for each precursor material for the interpretation of the data. Since the default values of -23‰ and -29‰ are not necessarily the appropriate ones for every production province, all maturity estimates have to be categorised as qualitative statements.

The gases from production province R5 have  $\delta^{13}C_1$  values between -33 and -23‰ and  $\delta^{13}C_2$  values between -34 and -28‰. The majority of the data clearly indicate a gas mixture from a terrestrial source and a gas from a lower mature marine source. The proportion of gas from the marine precursor seems to increase with increasing carbon isotope ratio of the ethane.

It is important to know that many reservoirs in this production province produce simultaneously from Rotliegend and Zechstein (Ca1) reservoirs.

Isotopic and molecular nitrogen data from pyrolysis experiments and from autochthonous Zechstein reservoirs are the basis for the interpretation of nitrogen gas in gas fields (Figure 5.14D). Especially the differences in the isotopic ratios allow nitrogen from a marine source rock to be distinguished from nitrogen from terrestrial precursor materials.

All gases from production province R5 ( $N_2$  contents of 17 – 78%,  $\delta^{15}N$  values between 3 and 14‰) indicate a mixture of nitrogen from both a terrestrial (dispersed coaly matter) and a marine source.

#### Conclusion:

The natural gases from production province R5 are mixtures from two source rocks. The predominant proportion derives from a terrestrial source, a rather small gas proportion stems from a lower mature sapropelic source (probably organic matter in Zechstein 2 strata).

### **5.3 Zechstein Reservoirs**

According to the distribution of natural gas fields producing from Zechstein reservoirs, two production provinces have been established (Fig. 5.15). The reservoirs are situated in Zechstein 2 carbonates which are in certain areas as well source rocks (e.g. GERLING et al. 1996). Due to its rather moderate maturity in the entire area of interest, Zechstein 2 reservoirs frequently produce oil. More information on facies and distribution of the reservoir horizons is given in chapter 3.

The production province Z1 overlaps with C2 and production province Z2 overlaps with R5, respectively.

#### **5.3.1 Production province Z1: Zechstein Reservoirs in the eastern part of the Netherlands and in NW Germany**

The molecular gas ratios ( $C_1/(C_2+C_3)$ ) are plotted versus  $\delta^{13}C_1$  (the normalised  $^{13}C/^{12}C$  ratios of methane) in Figure 5.16A. The diagram permits bacterially generated methane to be distinguished from thermogenic hydrocarbon gases, with a further distinction between thermogenic gases from marine and terrestrial source rocks.

All investigated gases from reservoirs of production province Z1 have  $C_1/(C_2+C_3)$  ratios between 15 and 32.136! and  $\delta^{13}C_1$  values between -45 and -6‰. Only one of these gases derives from a marine precursor which is probably situated inside the Zechstein strata itself (probably Ca2; cf. GERLING et al. 1996). All other gases seem to derive from terrestrial organic matter. However, many gases are influenced by a thermochemical sulphate reduction (TSR). Gaseous hydrocarbons are oxidised during this secondary process. This leads to (1.) an increase of  $CO_2$ -content in the gases, (2.) an increasing dryness of gaseous hydrocarbons and (3.) an successive increase of  $^{13}C$  and Deuterium in the individual homologues of the gaseous hydrocarbons. Consequently, many gases in Figure 5.16A lie outside the window of thermogenic gases.

In Figure 5.16B, carbon ( $\delta^{13}C_1$ ) and hydrogen ( $\delta D-C_1$ ) isotope ratios of methane are used to distinguish between methane generation processes. Although this diagnostic plot was mainly designed for the discrimination of bacterial methanogenesis, it is also useful for determining the thermogenic origin of methane.

The here shown methane data from the reservoirs of production province Z1 have  $\delta^{13}C_1$  values between -45 and -10‰ and  $\delta D-C_1$  values between -218 and -81‰. Only one methane has a typical character of an associated gas from a marine organic matter, which is most probably a precursor inside the Zechstein strata. The isotopic ratios of most other gases indicate clearly a genesis from a terrestrial source. Since TSR leads to an oxidation of the gaseous hydrocarbons, including methane in the final stage, many gases lie even outside the window of thermogenic hydrocarbons.

Carbon isotope ratios of methane and ethane can be used to estimate the type and maturity of the precursor material. Correspondingly, Figure 5.16C shows two maturity lines for a sapropelic and a terrestrial source rock. A selection mode (see chapter 5: carbon isotope / maturity relationships for methane and ethane) allows the user to chose the carbon isotope ratio for each precursor material for the interpretation of the data. Since the default values of -23 and -29‰ are not necessarily the

appropriate ones for every production province, all maturity estimates have to be categorised as qualitative statements.

The here shown gases from production province Z1 have  $\delta^{13}\text{C}_1$  values between -45 and -15‰ and  $\delta^{13}\text{C}_2$  values between -31 and -13‰. The carbon isotope ratios of one gas indicate a marine source rock. The position of the gas - significantly below the maturity line - indicates an admixture of fossil bacterial methane. This phenomenon is typical for autochthonous Zechstein gases (cf. GERLING et al. 1996 and production provinces Z2 and M1).

All other gases stem from a terrestrial source. If we exclude data sets with  $\delta^{13}\text{C}$ -values  $> -20$ ‰ of both methane and ethane due to the influence of TSR, we can see that the gases are dominated by coal-derived hydrocarbons, only small amounts of gas from a marine source seem to be admixed. The maturity-span of the terrestrial precursor extends from ca. 0.6 up to about 2.5% vitrinite reflectance.

Isotopic and molecular nitrogen data from pyrolysis experiments and from autochthonous Zechstein reservoirs are the basis for the interpretation of nitrogen gas in gas fields (Figure 5.16D). Especially the differences in the isotopic ratios allow nitrogen from a marine source rock to be distinguished from nitrogen from terrestrial precursor materials.

The gases from production province Z1 ( $\text{N}_2$  contents of 2 – 19%,  $\delta^{15}\text{N}$  values between -4 and 18‰) can be divided into a group of Westphalian coal-derived nitrogen and a second group of a mixture of Westphalian coal-generated nitrogen and Zechstein-derived nitrogen (GERLING et al. 1997).

#### Conclusion:

The natural gases from production province Z1 are in most cases mixtures generated in Westphalian coals. Sometimes, a minor admixture of gaseous hydrocarbons and nitrogen from a marine source rock occurs. As a complication, thermochemical sulphate reduction has caused in many cases secondary gas alterations which changed the molecular and isotopic compositions.

Disregarding the TSR-influenced gases, there exists a certain similarity between gases from production province C2 and those from Z1.

### **5.3.2 Production province Z2: Zechstein Reservoirs in Poland**

The molecular gas ratios ( $\text{C}_1/(\text{C}_2+\text{C}_3)$ ) are plotted versus  $\delta^{13}\text{C}_1$  (the normalised  $^{13}\text{C}/^{12}\text{C}$  ratios of methane) in Figure 5.17A. The diagram permits bacterially generated methane to be distinguished from thermogenic hydrocarbon gases, with a further distinction between thermogenic gases from marine and terrestrial source rocks.

All investigated gases from reservoirs of production province Z2 have  $\text{C}_1/(\text{C}_2+\text{C}_3)$  ratios between 4 and 21 and  $\delta^{13}\text{C}_1$  values between -52 and -34‰, indicating thermogenic origin. All of these gases seem to derive from a marine precursor. The four gases with the  $\delta^{13}\text{C}_1$  values around -50‰ indicate typical associated gases, the data of the fifth gas, however, is more indicative for a mixture of an associated gas with a gas from a terrestrial organic matter.

In Figure 5.17B, carbon ( $\delta^{13}\text{C}_1$ ) and hydrogen ( $\delta\text{D}-\text{C}_1$ ) isotope ratios of methane are used to distinguish between methane generation processes. Although this diagnostic plot was mainly designed for the discrimination of bacterial methanogenesis, it is also useful for determining the thermogenic origin of methane.

The methane from the reservoirs of production province Z2 have  $\delta^{13}\text{C}_1$  values between -52 and -34‰ and  $\delta\text{D}-\text{C}_1$  values between -256 and -201‰. All gases are of thermogenic origin, although the four gases with the most negative isotope ratios indicate that they are even at a transition between bacterial and thermogenic methane whereas the fifth methane has a typical isotopic signature of an associated gas.

Carbon isotope ratios of methane and ethane can be used to estimate the type and maturity of the precursor material. Correspondingly, Figure 5.17C shows two maturity lines for a sapropelic and a terrestrial source rock. A selection mode (see chapter 5: carbon isotope / maturity relationships for methane and ethane) allows the user to choose the carbon isotope ratio for each precursor material for

the interpretation of the data. Since the default values of -23 and -29‰ are not necessarily the appropriate ones for every production province, all maturity estimates have to be categorised as qualitative statements.

Most of the gases from production province Z2 have  $\delta^{13}\text{C}_1$  values between -52 and -34‰ and  $\delta^{13}\text{C}_2$  values between -37 and -30‰. Four gases lie significantly below the maturity line for sapropelic source rocks, indicating the presence of (?) bacterial methane, which is rather typical for associated gases (cf. production province M1). The fifth gas clearly indicates a mixture of gas from a predominant marine source with a maturity of about 1.2% vitrinite reflectance and a minor amount of gas from a terrestrial source of higher maturity.

Isotopic and molecular nitrogen data from pyrolysis experiments and from autochthonous Zechstein reservoirs are the basis for the interpretation of nitrogen gas in gas fields (Figure 5.17D). Especially the differences in the isotopic ratios allow nitrogen from a marine source rock to be distinguished from nitrogen from terrestrial precursor materials.

The two gases from production province Z2 ( $\text{N}_2$  contents of 70 and 73%,  $\delta^{15}\text{N}$  values of 14 and 16‰) indicate a nitrogen from a marine source, most probably autochthonous nitrogen from a Zechstein precursor.

#### Conclusion:

The natural gases from production province Z2 are in most cases typical products from a marine organic matter of rather low to moderate maturity. The source rock is most probably the organic matter within the Zechstein carbonates (Ca2).

Although both production provinces overlie each other, absolutely no similarities in the gas data have been identified.

## 5.4 Post-Zechstein Reservoirs

Post-Zechstein gas fields are mainly situated in Triassic, especially in Bunter strata. Additionally, gas fields occur in Jurassic, Lower Cretaceous, and even in some Cenozoic strata (e.g. RONDEEL et al. (eds.) 1996). According to the distribution of natural gas fields producing from post-Zechstein reservoirs, four production provinces have been established (Fig. 5.18). Specific information about facies and distribution of the various reservoir horizons are given in Chapters 3.

Production province M4 totally overlaps with C2 and Z1.

### 5.4.1 Production province M1: Post-Zechstein Reservoirs in the Danish North Sea Sector

The molecular gas ratios ( $\text{C}_1/(\text{C}_2+\text{C}_3)$ ) are plotted versus  $\delta^{13}\text{C}_1$  (the normalised  $^{13}\text{C}/^{12}\text{C}$  ratios of methane) in Figure 5.19A. The diagram permits bacterially generated methane to be distinguished from thermogenic hydrocarbon gases, with a further distinction between thermogenic gases from marine and terrestrial source rocks.

All investigated gases from reservoirs of production province M1 have  $\text{C}_1/(\text{C}_2+\text{C}_3)$  ratios between 3 and 20 and  $\delta^{13}\text{C}_1$  values between -53 and -39‰, clearly indicating for all but one gas a thermogenic origin. The only gas outside the thermal window contains a little of bacterially generated gas. All of these gases seem to derive from a marine precursor.

In Figure 5.19B, carbon ( $\delta^{13}\text{C}_1$ ) and hydrogen ( $\delta\text{D}-\text{C}_1$ ) isotope ratios of methane are used to distinguish between methane generation processes. Although this diagnostic plot was mainly designed for the discrimination of bacterial methanogenesis, it is also useful for determining the thermogenic origin of methane.

The methane from the reservoirs of production province M1 have  $\delta^{13}\text{C}_1$  values between -53 and -39‰ and  $\delta\text{D}-\text{C}_1$  values between -183 and -173‰, indicating all are of thermogenic origin or even may

contain some bacterially generated methane too. The isotopic ratios of most gases indicate a genesis from a marine source.

Carbon isotope ratios of methane and ethane can be used to estimate the type and maturity of the precursor material. Correspondingly, Figure 5.19C shows two maturity lines for a sapropelic and a terrestrial source rock. A selection mode (see Chapter 5: carbon isotope / maturity relationships for methane and ethane) allows the user to choose the carbon isotope ratio for each precursor material for the interpretation of the data. Since the default values of -23 and -29‰ are not necessarily the appropriate ones for every production province, all maturity estimates have to be categorised as qualitative statements.

The gases from production province M1 have  $\delta^{13}\text{C}_1$  values between -53 and -39‰ and  $\delta^{13}\text{C}_2$  values between -36 and -26‰, clearly indicating a mixture of gas from a predominant marine source with a varying maturity of about 0.8 – 1.8% vitrinite reflectance. The spread of data below the maturity line for sapropelic source rocks indicates the presence of (?) bacterial methane, which often occurs in associated gases (cf. production provinces Z1).

Isotopic and molecular nitrogen data from pyrolysis experiments and from autochthonous Zechstein reservoirs are the basis for the interpretation of nitrogen gas in gas fields (Figure 5.19D). Especially the differences in the isotopic ratios allow nitrogen from a marine source rock to be distinguished from nitrogen from terrestrial precursor materials.

There are no  $\delta^{15}\text{N}$  values available from gases from production province M1.

#### Conclusion:

The natural gases from production province M1 have in all cases a typical signature of associated gases from a marine source rock. The source rock maturity varies between 0.8 and 1.8% vitrinite reflectance.

### **5.4.2 Production province M2: Post-Zechstein Reservoirs in the Central Graben of the Dutch North Sea**

The molecular gas ratios ( $\text{C}_1/(\text{C}_2+\text{C}_3)$ ) are plotted versus  $\delta^{13}\text{C}_1$  (the normalised  $^{13}\text{C}/^{12}\text{C}$  ratios of methane) in Figure 5.20A. The diagram permits bacterially generated methane to be distinguished from thermogenic hydrocarbon gases, with a further distinction between thermogenic gases from marine and terrestrial source rocks.

All investigated gases from reservoirs of production province M2 have  $\text{C}_1/(\text{C}_2+\text{C}_3)$  ratios between 5 and 366 and  $\delta^{13}\text{C}_1$  values between -44 and -24‰, clearly indicating thermogenic origin. All but one of these gases seem to derive from marine organic matter. The gas with the most negative carbon isotope ratio and a rather wet gas composition has the typical character of an associated gas. The gas with the least negative  $\delta^{13}\text{C}_1$  value, however, has a very methane-rich gas composition. It probably derives from a terrestrial source rock.

In Figure 5.20B, carbon ( $\delta^{13}\text{C}_1$ ) and hydrogen ( $\delta\text{D}-\text{C}_1$ ) isotope ratios of methane are used to distinguish between methane generation processes. Although this diagnostic plot was mainly designed for the discrimination of bacterial methanogenesis, it is also useful for determining the thermogenic origin of methane.

The methane from the reservoirs of production province M2 have  $\delta^{13}\text{C}_1$  values between -44 and -24 ‰ and  $\delta\text{D}-\text{C}_1$  values between -269 and -119‰, indicating all are of thermogenic origin. Nevertheless, the gases seem to have very heterogeneous origins. Three gases have the typical isotopic signature of associated gases, another four gases indicate a mixture from both a marine and a terrestrial source, one gas stems from a terrestrial source alone.

Carbon isotope ratios of methane and ethane can be used to estimate the type and maturity of the precursor material. Correspondingly, Figure 5.20C shows two maturity lines for a sapropelic and a terrestrial source rock. A selection mode (see chapter 5: carbon isotope / maturity relationships for methane and ethane) allows the user to choose the carbon isotope ratio for each precursor material for the interpretation of the data. Since the default values of -23 and -29‰ are not necessarily the

appropriate ones for every production province, all maturity estimates have to be categorised as qualitative statements.

The here shown gases from production province M2 have  $\delta^{13}\text{C}_1$  values between -44 and -30‰ and  $\delta^{13}\text{C}_2$  values between -30 and -20‰, indicating for five gases a mixture of gas from a predominant marine source with a maturity of more than 1.5% vitrinite reflectance and a minor amount of gas from a terrestrial source, probably of lower maturity. The two gases with the most negative  $\delta^{13}\text{C}_1$  values indicate the presence of (?) bacterial methane admixed to thermogenic hydrocarbons from a marine source with a source rock maturity of about 1.3% vitrinite reflectance. Such a isotopic gas signature is rather typical for associated gases (cf. production provinces Z1 and M1).

Isotopic and molecular nitrogen data from pyrolysis experiments and from autochthonous Zechstein reservoirs are the basis for the interpretation of nitrogen gas in gas fields (Figure 5.20D). Especially the differences in the isotopic ratios allow nitrogen from a marine source rock to be distinguished from nitrogen from terrestrial precursor materials.

Three gases from production province M2 ( $\text{N}_2$  contents of 1 – 5%,  $\delta^{15}\text{N}$  values between -1 and 12‰) indicate a generation of nitrogen from a terrestrial source alone. The other two gases indicate a mixture of nitrogen from a terrestrial and a marine precursor.

#### Conclusion:

The natural gases from production province M2 are in most cases mixtures from two source rocks. The predominant proportion derives from a sapropelic source having a maturity of more than 1.5% vitrinite reflectance, a rather small gas proportion stems from a lower mature terrestrial source.

### **5.4.3 Production province M3: Post-Zechstein Reservoirs in the SW Netherlands**

The molecular gas ratios ( $\text{C}_1/(\text{C}_2+\text{C}_3)$ ) are plotted versus  $\delta^{13}\text{C}_1$  (the normalised  $^{13}\text{C}/^{12}\text{C}$  ratios of methane) in Figure 5.21A. The diagram permits bacterially generated methane to be distinguished from thermogenic hydrocarbon gases, with a further distinction between thermogenic gases from marine and terrestrial source rocks.

All investigated gases from reservoirs of production province M3 have  $\text{C}_1/(\text{C}_2+\text{C}_3)$  ratios between 8 and 35 and  $\delta^{13}\text{C}_1$  values between -38 and -30‰, clearly indicating thermogenic origin. All of these gases seem to derive from a marine precursor.

In Figure 5.21B, carbon ( $\delta^{13}\text{C}_1$ ) and hydrogen ( $\delta\text{D}-\text{C}_1$ ) isotope ratios of methane are used to distinguish between methane generation processes. Although this diagnostic plot was mainly designed for the discrimination of bacterial methanogenesis, it is also useful for determining the thermogenic origin of methane.

The methane from the reservoirs of production province M3 have  $\delta^{13}\text{C}_1$  values between -38 and -30‰ and  $\delta\text{D}-\text{C}_1$  values between -176 and -142‰, indicating all are of thermogenic origin. Moreover, the isotopic ratios of most gases indicate a character of associated gases.

Carbon isotope ratios of methane and ethane can be used to estimate the type and maturity of the precursor material. Correspondingly, Figure 5.21C shows two maturity lines for a sapropelic and a terrestrial source rock. A selection mode (see Chapter 5: carbon isotope / maturity relationships for methane and ethane) allows the user to chose the carbon isotope ratio for each precursor material for the interpretation of the data. Since the default values of -23 and -29‰ are not necessarily the appropriate ones for every production province, all maturity estimates have to be categorised as qualitative statements.

The gases from production province M3 have  $\delta^{13}\text{C}_1$  values between -38 and -30‰ and  $\delta^{13}\text{C}_2$  values between -27 and -23‰, most of these clearly indicating a mixture of gas from a predominant marine source with a maturity of 1.5 to 2% vitrinite reflectance and a minor amount of gas from a terrestrial source of lower maturity.

Isotopic and molecular nitrogen data from pyrolysis experiments and from autochthonous Zechstein reservoirs are the basis for the interpretation of nitrogen gas in gas fields (Figure 5.21D). Especially

the differences in the isotopic ratios allow nitrogen from a marine source rock to be distinguished from nitrogen from terrestrial precursor materials.

Most nitrogen gases from production province M3 ( $N_2$  contents of 0.4 – 10%,  $\delta^{15}N$  values between -4 and 12 ‰) indicate a genesis from a lower mature terrestrial source. Two gases show a small amount of nitrogen from the marine precursor admixed.

#### Conclusion:

The natural gases from production province M3 are in most cases generated in a sapropelic source rock, having a rather high maturity (~ 1.5 - 2.0% vitrinite reflectance), a rather small gas proportion stems from a lower mature terrestrial source. Whether this sapropelic source rock is a pre-Westphalian one or the Jurassic Posidonia Shale (cf. DE JAGER et al. 1996) has to be decided from case to case. Most nitrogen data indicate a gas generation from a low mature terrestrial source (Westphalian) only.

### **5.4.4 Production province M4: Post-Zechstein Reservoirs in the eastern part of the Netherlands and in NW Germany**

The molecular gas ratios ( $C_1/(C_2+C_3)$ ) are plotted versus  $\delta^{13}C_1$  (the normalised  $^{13}C/^{12}C$  ratios of methane) in Figure 5.22A. The diagram permits bacterially generated methane to be distinguished from thermogenic hydrocarbon gases, with a further distinction between thermogenic gases from marine and terrestrial source rocks.

All investigated gases from reservoirs of production province M4 have  $C_1/(C_2+C_3)$  ratios between 28 and 239 and  $\delta^{13}C_1$  values between -32 and -19‰, clearly indicating thermogenic origin. All but one of these gases derive from a terrestrial precursor. The exception seems to be generated in a highly mature marine source rock.

In Figure 5.22B, carbon ( $\delta^{13}C_1$ ) and hydrogen ( $\delta D-C_1$ ) isotope ratios of methane are used to distinguish between methane generation processes. Although this diagnostic plot was mainly designed for the discrimination of bacterial methanogenesis, it is also useful for determining the thermogenic origin of methane.

The methane from the reservoirs of production province M4 have  $\delta^{13}C_1$  values between -36 and -19‰ and  $\delta D-C_1$  values between -151 and -107‰, indicating all are of thermogenic origin. The isotopic ratios of all but two gases indicate gas generation from a terrestrial precursor.

Carbon isotope ratios of methane and ethane can be used to estimate the type and maturity of the precursor material. Correspondingly, Figure 5.22C shows two maturity lines for a sapropelic and a terrestrial source rock. A selection mode (see chapter 5: carbon isotope / maturity relationships for methane and ethane) allows the user to choose the carbon isotope ratio for each precursor material for the interpretation of the data. Since the default values of -23‰ and -29‰ are not necessarily the appropriate ones for every production province, all maturity estimates have to be categorised as qualitative statements.

Most of the gases from production province M4 have  $\delta^{13}C_1$  values between -32 and -19‰ and  $\delta^{13}C_2$  values between -34 and -20‰, clearly indicating for almost all gases a mixture of gas from a predominant terrestrial source with a maturity between about 1.5 and more than 2.5% vitrinite reflectance and a minor amount of gas from a marine source of lower maturity. One gas seems to be generated from a marine source rock with a maturity of 0.9% vitrinite reflectance.

Isotopic and molecular nitrogen data from pyrolysis experiments and from autochthonous Zechstein reservoirs are the basis for the interpretation of nitrogen gas in gas fields (Figure 5.22D). Especially the differences in the isotopic ratios allow nitrogen from a marine source rock to be distinguished from nitrogen from terrestrial precursor materials.

Most gases from production province M4 ( $N_2$  contents of 0.2 – 74%,  $\delta^{15}N$  values between -1 and 10‰) indicate a nitrogen from a terrestrial source, some from coals and those with the elevated nitrogen contents from dispersed coaly matter. A few gases indicate a nitrogen mixture from both a terrestrial and a marine precursor.

Conclusion:

The natural gases from production province M4 are in most cases dominated by components from a rather high mature terrestrial source rock (probably Westphalian coals). In some cases, a small gas proportion stems from a lower mature marine source (probably Zechstein).

There exist certain similarities with gases from production provinces C2 and Z1.



## 6. REFERENCES

### Chapter 2

- DUMKE, I., FABER, E. & POGGENBURG, J. (1989). Determination of stable carbon and hydrogen isotopes of light hydrocarbons, *Anal. Chem.* 61: 2149-2154.
- HUT, G., BEGEMANN, M.J.S. & WEERKAMP, H.R. (1984): Determination of isotope ratios in the natural gas components CH<sub>4</sub> and N<sub>2</sub> separated by gas chromatography, *Isotope Geoscience* 2: 75-83.
- JENDEN, P.D., KAPLAN, I.R., POREDA, R.J. & CRAIG, H. (1988): Origin of nitrogen-rich natural gases in the California Great Valley: Evidence from helium, carbon and nitrogen isotope ratios, *Geochim. Cosmochim. Acta* 52: 851-861.
- SOHNS, E., GERLING, P. & FABER, E. (1994): Improved stable nitrogen isotope ratio measurements of natural gases, *Anal. Chem.* 66: 2614-2620.
- MORRISON, J. (1972): NAM recovers mercury produced with Dutch natural gas. - *Oil and Gas Journ.*, April 17, 1972: 72-73
- OZIMA, M. & PODOSEK, F.A. (1983): *Noble gas geochemistry*. - 367 S.; Cambridge University Press
- THODE, H.G., MONSTER, J. & DUNFORD, H.B. (1961): Sulphur isotope geochemistry. - *Geochim. Cosmochim. Acta* 25: 159-174

### Chapter 3

- ADRICHEM-BOOGAERT, VAN, H.A. & KOUWE, W.F. P. (1993-1996): Stratigraphic nomenclature of the Netherlands, revision and update by RGD and NOGEPa. - *Meded. Rijks Geol. Dienst*, 50, sect A-J, Haarlem
- AGHABAWA, M.A. (1992): Petrology and geochemistry of Rotliegendes volcanic rocks in Denmark and their tectonic implication. Unpubl. PhD thesis, University of Aarhus, 335 pp.
- BALDSCHUHN, R., FRISCH, U. & KOCKEL, F. (1996): *Geotektonische Atlas von NW-Deutschland* 1:300.000. 17 encl. Bundesanstalt für Geowissenschaften u. Rohstoffe, Hannover (BGR)
- BENEK, R. (1995): Late Variscan calderas/volcanotectonic depressions in eastern Germany. - *Terra nostra*, 7: 16-19.
- BERTELSEN, F. (1980): Lithostratigraphy and depositional history of the Danish Triassic. - *Geological Survey Denmark, Series B, No. 4*: 91-102; Kopenhagen
- BINOT, F., GERLING, P., HILTMANN, W., KOCKEL, F. & WEHNER, H. (1993): The Petroleum System in the Lower Saxony Basin. - In: SPENCER (ed.): *Generation, accumulation and production of Europe's hydrocarbons*. Special Publ. Europ. Ass. Petrol. Geosc., 3: 121-139, 14 figs., 1 tab.; Berlin, Heidelberg
- BRAUN, A. & WOLF, M. (1995): Eine neue Inkohlungskarte des nördlichen rechtsrheinischen Schiefergebirges. - *N. Jb. Geol. Paläont. Mh.* 1994 H. 8: 449-475, 7 figs, 1 tab.
- CAMERON, T. D. J. (1993): Carboniferous and Devonian (southern North Sea). - In: KNOX & CORDEY (eds.): *Lithostratigraphic nomenclature of the UK North Sea*, 5: 1-93; Nottingham (BGS & UKOOA)
- CAMERON, T.D.J., CROSSBY, A., BALSON, P.S., JEFFEREY, D.H. LOTT, G.K., BULAT, J. & HARRISON, D.J. (1992): The geology of the southern North Sea. - *UK offshore regional rep.*: 1-152, 128 figs.; Keyworth (BGS)

- CLARK, D. N. & TALLBACKA, L. (1980): The Zechstein deposits of Southern Denmark. - In: FÜCHTBAUER, H. & PERYT, T.M. (eds): The Zechstein basin with emphasis on carbonate sequences.- Contrib. Sedim., 9: 205 - 231; Stuttgart (Schweizerbart)
- CORNFORD, C. (1984): Source rocks and hydrocarbons of the North Sea.- In GLENNIE, K.W. (ed). 1984. Introduction to the Petroleum Geology of the North Sea. Blackwell Scientific Publications, Oxford: 197-236.
- DADLEZ, R. (1977): Tectonic position of western Pomerania (Northwestern Poland) prior to the Upper Permian. - Instytut Geologiczny Buletyn, 285: 1-22; Warszawa
- DADLEZ, R. (ed.) (1980): Tectonic map of the Zechstein-Mesozoic structural complex in the Polish Lowlands, 1:500 000. - Warszawa (Wydawnictwa Geologiczne)
- DALLMEYER, R. D., FRANKE, W. & WEBER, K. (EDS.) (1995): Pre-Permian Geology of Central and Eastern Europe. - 1-604, 233 figs., 30 tables; Berlin, Heidelberg (Springer)
- DAMTOFT, K., NIELSEN, L. H., JOHANNESSEN, P., THOMSEN, E. & ANDERSEN, P. R. (1992): Hydrocarbon plays in the Danish Central Trough. - In: SPENCER (ed.): Generation, Accumulation and Production of Europe's Hydrocarbons II. Spec. Publ. Eur. Ass. Petrol. Geosc. No. 2: 35-58; Berlin, Heidelberg (Springer)
- DONATO, J.A., MARTINDALE, W. & TULLY, M.C. (1983): Buried granites within the Mid North Sea High. - Journ. Geol. Soc. London, 140, 825-837.
- DRONKERT & REMMELTS, G. (1996): Influence of salt structures on reservoir rocks in block L2, Dutch continental shelf. - In: RONDEEL et. al. (eds.): Geology of gas and oil under the Netherlands: 159-167.
- DROZDZEWSKI, G. (1992): Zur Faziesentwicklung im Oberkarbon des Ruhrbeckens, abgeleitet aus Mächtigkeitkarten und lithostratigraphischen Gesamtprofilen. - Z. angew. Geol., 38,1: 41-48 , 9 figs.; Berlin
- DROZDZEWSKI, G., ENGEL, H., WOLF, R. & WREDE, V. (1985): Beiträge zur Tiefentektonik westdeutscher Steinkohlenlagerstätten. - 1-236, 149 figs., 7 tab., 33 plates im Anlagebd.; Krefeld (Geologisches Landesamt)
- DULCE, G., HARMS, F., KATSCHOREK, T. & KOCKEL, F. (1993): Paläogeographie und synsedimentäre Tektonik im Oberjura des Niedersachsenbeckens, Abschlußbericht DFG-Projekt Ko 499/2-1. - Unveröff. Bericht BGR, Archiv-Nr. 1108120: 112 pp., 47 encl.; Hannover
- EDMONDS, E.A., MCKEOWN, M.C. AND WILLIAMS, M. (1975): British Regional Geology: South-West England, HMSO for the British Geological Survey, London.
- EISERBECK, W., MEHLHORN, S., MÜLLER, E.P., SCHMANSKI, W. & SCHRETZENMAYR, S. (1992): Zum Kohlenwasserstoffpotential des Präperm im östlichen Bereich der Bundesrepublik. - DGMK-Fachtagung Mai 1992: 31 - 54, 10 figs; Celle
- FELDMAN-OLSZEWSKA, A. (1988): The Lithological-Palaeogeographical Map of the Jurassic Coal-bearing Lithological Association. - Unpublished report.Archiv of Polish Geological Institute,Warsaw (In Polish).
- FRANKE, D. (1990): Der präpermische Untergrund der Mitteleuropäischen Senke - Fakten und Hypothesen. - Nieders. Akad. Geowiss. Veröff., 4: 19-75, 22 figs.; Hannover
- FRANKE, D. (ed.) (1990): Pre-Permian geologic-structural map of Central Europe, external Variscides and pre-Variscan foreland 1:1.500.000 - Zentrales Geologisches Institut & Panstwowy Instytut Geologiczny; Berlin, Warschau

- FRANKE, D., HOFFMANN, N. & LINDERT, W. (1995): The Variscan deformation front in East Germany, Part I: Geological and geophysical constraints. - *Z. angew. Geol.*, 41,2: 83-91; Hannover
- FRANKE, D., HOFFMANN, N. & LINDERT, W. (1996): The Variscan deformation front in Eastern Germany, Part II: Tectonic interpretation. - *Z. angew. Geol.*, 42,1: 44-56, 6 figs; Hannover
- GAST, R. (1988): Rifting im Rotliegend Niedersachsens. - *Die Geowissenschaften* 6: 115-122.
- GAST, R. (1991): The perennial Rotliegend saline lake in NW Germany. - *Geol. Jb. A* 119: 25-59, 12 figs, Hannover
- GELUK, M.C. (1995): Stratigraphische Gliederung der Z2-(Staßfurt-) Salzfolge in den Niederlanden: Beschreibung und Anwendung bei der Interpretation von halokinetisch gestörten Sequenzen. - *Z. dt. geol. Ges.*, 146,2: 458-465, 6 figs.; Hannover
- GELUK, M. C., PLOMP, A. & VAN DOORN, TH. H. M. (1996): Development of the Permo-Triassic succession in the basin fringe area, southern Netherlands. - In: RONDEEL, BATJES & NIEUWENHUIJS (eds.): *Geology of gas and oil under the Netherlands*: 57-78, 21 figs., 1 tab.; Haarlem
- GELUK, M.C. (1997): Palaeogeographic maps of Moscovian and Artinskian; contributions from the Netherlands - In: CRASQUIN-SOLEAU & DE WEVER (eds.), *Peri-Tethys stratigraphic correlations*, *Geodiversitas* 19 (2): 229-234, 3 figs.
- GELUK, M.C. & RÖHLING, H.-G. (1997, in press): High resolution sequence stratigraphy of the Lower Triassic "Buntsandstein" in the Netherlands and northwestern Germany. - *Geol. Mijnb.*
- GELUK, M.C., J.D. VAN WEES, H. GRÖNLOH & A.B. VAN ADRICHEM BOOGAERT (1997, in press) Palaeogeography and paleotectonics of the Zechstein Group (Upper Permian) in the Netherlands - In: *Proceedings XIII Int. Congress Carboniferous-Permian*, Krakow, Poland, in press.
- GEORGE, G.T. & BERRY, J.K. (1994): A new palaeogeographic and depositional model for the Upper Rotliegend, offshore The Netherlands. - *First Break*, 12: 147-158
- GLENNIE, K. W. (1990): *Introduction to the Petroleum Geology of the North Sea*. - 3. ed., 1-402; Blackwell Science Publ., London
- GOLDSMITH, P.J., RICH, B. & STANDING, J. (1995): Triassic correlation and stratigraphy in the South Central Graben, U.K. North Sea. - In: Boldy, S.A.R. (ed). *Permian and Triassic Rifting in North West Europe*. *Geol. Soc. Spec. Publ* 91, Geological Society, London: 123-144
- GÖRING, H. H. & ZAGORA, I. (1993): Strukturentwicklung des basalen Zechsteins im westlichen Vorpommern. - *Zeitschr. geol. Wiss.*, 21,3/4: 281-290, 7 figs.; Berlin
- GROCHOLSKI, A. & RYKA, W. (1995): Carboniferous magmatism in Poland. - In: ZDANOWSKI & ZAKOWA (eds.): *The Carboniferous system in Poland*. - *Prace Panstwowego Instytutu Geologicznego*, 148: 181-189; Warszawa
- GROTEK, I. (1997): (in preparation). - In: (NARKIEWICZ (ed.): *Sedimentary basin analysis of the Polish Lowlands*. - *Prace Panstwowego Instytutu Geologicznego*,
- HAMBLIN, R.J.O., CROSBY, A., BALSON, P., JONES, S.M., CHADWICK, R.A., PENN. I.E. AND ARTHUR, M.J. (1992): *United Kingdom offshore regional report: the geology of the English Channel*, HMSO for the British Geological Survey, London.
- HARWOOD, G. M. & SMITH, D. B. (eds.) (1986): *The English Zechstein and related topics*. - *Geol. Soc. Spec. Pub.* 22: 1-244, Oxford (Blackwell).
- HEYBROEK, P. (1974): Explanation to tectonic maps of the Netherlands. - *Geol. Mijnb.* 53: 43-50.

- HOFFMANN, N. (1990): Zur paläodynamischen Entwicklung des Präzechstein in der Nordostdeutschen Senke. - *Nieders. Akad. Geowiss., Veröffent.*, 4: 5-18, 7 figs.; Hannover
- HOFFMANN, N., POKORSKI, J., LINDERT, W. & BACHMANN, G. H. (1997): Rotliegend stratigraphy, palaeogeography and facies in the eastern part of the Central European basin. - In: *Proceedings XIII Int. Congress Carboniferous-Permian, Krakow, Poland*
- HOTH, K., WEYER, D., KAHLERT, E. & DÖRING, H. (1990): Das Standardprofil des Oberkarbons von Vorpommern. - *Z. angew. Geol.*, 36,10: 361-368, 2 figs., 1 tab., 2 plates; Berlin
- HOTH, K., HÜBSCHER, KORICH, D., GABRIEL, W & ENDERLEIN, F. (1993a): Die Lithostratigraphie der permokarbonischen Effusiva im Zentralabschnitt der Mitteleuropäischen Senke. - *Geol. Jb.*, A 131: 179-196; Hannover
- HOTH, K., RUSBÜLT, J., ZAGORA, K, BEER, H. & HARTMANN, O. (1993b): Die tiefen Bohrungen im Zentralabschnitt der Mitteleuropäischen Senke - Dokumentation für den Zeitabschnitt 1962-1990. - *Schriftenreihe f. Geowissenschaften*, 2,7: 1-145, 1 figs., 2 tab.; Berlin (Ges. f Geowiss. e.V.)
- JACKOWICZ, E. (1994): Permian volcanic rocks from the northern part of the Fore-Sudetic monocline. - *Prace Panstwowego Instytutu Geologicznego*, 145:
- JACKSON, M.P.A., ROBERTS, D.G. & SNELSON, S. (1995): *Salt Tectonics: A Global Perspective.* - AAPG, Memoir 65.
- JENYON, M. K. (1985): *Salt tectonics.* - 1-191; London (Elsevier)
- JENYON, M. K. (1986): Some consequences of faulting in the presence of a salt rock interval. - *Journ. Petrol. Geol.*, 9,1: 29-52, 12 figs.
- JOHNSON, H., WARRINGTON, G. & STOKER, S.J. (1994): Volume 6. Permian and Triassic of the Southern North Sea. - In: Knox, R.W.O'B. and Cordey, W.G. (eds) *Lithostratigraphic nomenclature of the UK North Sea.* British Geological Survey, Nottingham.
- KOCH, J., KOCKEL, F. & KRULL, P. (1997): Coalification at the base Zechstein and the Pre-Permian surface in northern Germany. - *Geol. Jb.*, D 103: 33-43, 2 figs; Hannover
- KOCKEL, F. with contributions by BALDSCHUHN, R., BEST, G., DENECKE, E., FRISCH, U., JÜRGENS, U. & SCHMITZ, J. (1990): Morphology and Genesis of Northwest German Salt Structures - *Proc. Sympos. on Diapirism with spec. reference to Iran* : 6 p., 21 fig., Bander Abbas
- KOCKEL, F. with contributions by. BALDSCHUHN, R., BEST, G., BINOT, F., FRISCH, U., GROSS, U., JÜRGENS, U., RÖHLING, H.-G. & SATTLER-KOSINOWSKI, S. (1995): Structural and palaeogeographical development of the German North Sea sector. - *Beitr. z. regionalen Geologie der Erde*, 26: 1-96, 7 figs., 16 encl.; Berlin-Stuttgart (Borntträger)
- LANGENAEKER, V. & DUSAR, M. (1992): Subsurface facies analysis of the Namurian and earliest Westphalian in the western part of the Campine Basin (N Belgium). - *Geol. Mijnb.*, 71: 161-172, 8 figs.Dordrecht (Kluwer Acad. Publ.)
- LEEDER, M. R. (1992): Dinantian.- In DUFF & SMITH (eds): *Geology of England and Wales*: 207 - 238; London
- LINDERT, W., WARNCKE, D. & STUMM, M. (1990) Probleme der lithostratigraphischen Korrelation des Oberrotliegenden (Saxon) im Norder der DDR. - *Z. angew. Geol.* 36: 368-375.
- LOTT, G. K. & KNOX, R.W.O'B. (1995): Volume 7. Post Triassic of the Southern North Sea. - In: Knox, R.W.O'B. and Cordey, W.G. (eds) *Lithostratigraphic nomenclature of the UK North Sea.* British Geological Survey, Nottingham.

- MICHELSEN, O. (1971): Lower Carboniferous foraminiferal faunas of the boring Orslev No 1, island of Falster, Denmark. - Danmarks Geol. Unders. II R (98): 1-86; Kopenhagen
- MICHELSEN, O. (1989a): Revision of the Jurassic lithostratigraphy of the Danish Subbasin. Geological Survey of Denmark, series A 24: 22pp.
- MICHELSEN, O., (1989b): Log-sequence analysis and environmental aspects of the Lower Jurassic Fjerritslev Formation in the Danish Subbasin. - Geological Survey of Denmark, series A 25.
- MÜLLER, E. P. (1994): Development of oil and gas exploration in the eastern part of Germany. - In: POPESCU (ed.): Hydrocarbons of Eastern Europe - habitat, exploration and production history: 119-146, 26 figs.; Berlin
- NIEMCZYCKA, T. (1997): Upper Jurassic. - In: MAREK, S. (ed.): The epicontinental Permian and Mesozoic in Poland. - Prace Państwowego Instytutu Geologicznego, 153
- OUDMAYER, B. & DE JAGER, J. (1993): Fault reactivations and oblique-slip in the southern North Sea. -In: PARKER (ed.) Petr. Geol. Northwest Europe: Proc. 4th Conf.: 1281-1293
- PAPROTH, E., CONIL, R., BLESS, J. M. J., BOONEN, P., BOUCKAERT, J. et al. (1983a): Bio- and lithostratigraphic subdivisions of the Dinantian in Belgium, a review. - Ann. Soc. Géol. Belgique 106: 185-239, 13 figs, 1 pl.; Liege
- PAPROTH, E., DUSAR, M., BLESS, M. J. M., BOUCKAERT, J., DELMER, A., FAIRON-DEMARET, M., HOULLEBERGHS, E., LALOUX, M., PIERAT, P., SOMERS, Y., STREEL, M., THOREZ, J. & TRICOT, J. (1983b): Bio- and lithostratigraphic subdivision of the Silesian in Belgium, a review. - Ann. Soc. Géol. Belgique 106: 241-283, 13 figs, 1 pl.; Liege
- PERYT, T. M. (1992): Debris-flow deposits in the Zechstein (Upper Permian) Main Dolomite of Poland. Significance for the evolution of the basin. - N. Jb. Geol. Paläontol., Abh., 185: 1-19; Stuttgart
- PHAROAH, T.C., MORRIS, J.H., LONG, C.B. AND RYAN, P.D. (1996) Tectonic Map of Britain, Ireland & Adjacent areas 1:1.500.000. British Geological Survey.
- PIESKE, J. & SCHRETZENMAYR, S. (1984): Sedimentationszyklen im Staßfurt-Karbonat und ihre Modifikation durch azyklische Vorgänge. - Z. geol. Wiss., 12,1: 83-100; 7 figs., 2 tab.; Berlin
- PLEIN, E. (ed.) (1995): Norddeutsches Rotliegend-Becken. - Rotliegend-Monographie, Teil II Courier Forsch.-Inst. Senckenberg, 183: 1-193, 80 figs., 10 tab., 8 plates; Frankfurt/M.
- POKORSKI, J. (1989): Evolution of the Rotliegend Basin in Poland. - Bull. 7, Polish Acad. Sciences, 37: 49-55; Warszawa
- POZARYSKI, W. & KARNOWSKI, P. (eds.) (1992): Tectonic map of Poland during the Varsican time, 1:1 Mio. - Państwowy Instytut Geologiczny (PIG); Warschau
- RASCH, H.-J. & ZAGORA, K. (1993): Paläostrukturen im basalen Zechstein des westlichen Vorpommern. - Zeitschr. geol. Wiss., 21, 3/4: 303-317, 10 figs., 3 plates; Berlin
- REMMELTS, G. (1995): Fault-related salt tectonics in the Southern North Sea, The Netherlands. - In: M.P.A. Jackson et al. (eds.) Salt tectonics: a global perspective, AAPG Memoir 656: 261-272
- REMMELTS, G. (1996): Salt tectonics in the southern North Sea, the Netherlands. - In: RONDEEL, BATJES & NIEUWENHUIJS (eds.): Geology of gas and oil under the Netherlands: 143-158, 13 figs.; Kluwer Acad. Publ.
- RÖHLING, H.-G. (1991): A lithostratigraphic subdivision of the Early Triassic in the Northwest German Lowlands and the German Sector of the North Sea, based on Gamma Ray and Sonic Log. - Geol. Jb., A 119: 3-23, 1 figs., 12 Anl.; Hannover

- SANNEMANN, D., ZIMDARS, J. & PLEIN, E. (1978): Der basale Zechstein (A2-T1) zwischen Weser und Ems. - Z. dt. geol. Ges., 129: 33-69, 7 figs., 1 tab., 11 plates; Hannover
- SØRENSEN, S. & MARTINSEN, B. B. (1987): A palaeogeographic reconstruction of the Rotliegend deposits in the Northeastern Permian basin. - In: BROOKS & GLENNIE (eds.): Petroleum Geology of North West Europe: 497-508; London (Graham & Trotman)
- STROHMENGER, C., ANTONINI, M., JÄGER, G., ROCKENBAUCH, K. & STRAUSS, C. (1996): Zechstein 2 Carbonate reservoir facies distribution in relation to Zechstein sequence stratigraphy (Upper Permian, Germany): an integrated approach. - Bull. Centres Rech. Explor.-Prod. Elf Aquitaine, 20,1: 1-35, 21 figs, 3 tab.; Pau
- SZYPERKO-TELLER, A. (1997): Lower Triassic. - In: MAREK, S. (ed.): The epicontinental Permian and Mesozoic in Poland. - Prace Panstwowego Instytutu Geologicznego, 153:
- TAYLOR, J. C. M. (1986): Late Permian-Zechstein. - In: GLENNIE (ed.): Introduction to the Petroleum Geology of the North Sea: 87-1111; Oxford (Blackwell)
- TAYLOR, J. C. M. & COLTER, V. S. (1975): Zechstein of the English sector of the Southern North Sea Basin. -
- TEICHMÜLLER, M. & TEICHMÜLLER, R. (1950): Das Inkohlungsbild des Niedersächsischen Wealdenbeckens. - Z. dt. geol. Ges., 100: 498-517; Hannover
- TEICHMÜLLER, M. & TEICHMÜLLER, R. (1982): Das Inkohlungsbild des Lippstädter Gewölbes. - Fortschr. Geol. Rheinld. u. Westf., 30: 223-239, 3 figs., 4 tab.; Krefeld
- TEICHMÜLLER, M., TEICHMÜLLER, R. & BARTENSTEIN, H. (1984): Inkohlung und Erdgas - eine neue Inkohlungskarte der Karbon-Oberfläche in Nordwestdeutschland. - Fortschr. Geol. Rheinld. u. Westf., 32: 11 - 34, 3 figs., 3 tab., 1 plates; Krefeld
- VAN DE SANDE, J. M. M., REIJERS, T. J. A. & CASSON, N. (1996): Multidisciplinary exploration strategy in the Northeast Netherlands Zechstein 2 Carbonate play, guided by 3D seismic. - In: RONDEEL, BATJES & NIEUWENHUIJS (eds.): Geology of gas and oil under the Netherlands: 125-142, 18 figs.; Kluwer Acad. Publ.
- VAN DER BAAN, D. (1990): Zechstein reservoirs in the Netherlands. - In: BROOKS (ed.): Classic petroleum provinces - Geol. Soc. Spec. Publications, 50: 379-398, 29 figs.; London
- VAN WIJHE, D. H. (1987): Structural evolution of inverted basins in the Dutch offshore. - Tectonophysics, 137: 171-219, 12 figs.; Amsterdam-Oxford
- VAN WIJHE, D. H., LUTZ, M. & KAASSCHIETER, J. P. H. (1980): The Rotliegend in the Netherlands and its gas accumulations. - Geol. Mijnb., 59,1: 2-24; Haarlem
- VEJBÆK, O. V. (1990): The Horn Graben and its relationship to the Oslo Graben and the Danish Basin. - Tectonophysics, 178: 29-49, 18 figs.; Amsterdam
- VEJBÆK, O. V. (1992): Geodynamic modelling of the Central Danish Trough. - In: LARSEN, BREKKE, LARSEN & TALLERAAS (eds.): Structural and tectonic modelling and its application to petroleum geology. - NPF Special Publ., 1: 1-17
- VEJBÆK, O. V. & BRITZE, P. (EDS.) (1994): Geological map of Denmark 1: 750 000, Top pre-Zechstein (two-way travelttime and depth). - Ministry of Environment and Energy (DGU) Map series No. 45: 1-3, 5 maps; Kopenhagen
- VERDIER, J. P. (1996): The Rotliegend sedimentation history of the southern North Sea and adjacent countries. - In: : RONDEEL, BATJES & NIEUWENHUIJS (eds.): Geology of Gas and Oil under the Netherlands: 45-56, 7 figs., 13 encl.; Dordrecht

- WALTER R. (1992) Geologie von Mitteleuropa. 5. Auflage. - Schweizerbart, Stuttgart, 561 pp., 151 figs.
- WAGNER, R. (1994): Stratigraphy and evolution of the Zechstein basin in the Polish Lowlands. - Prace Panstwowego Instytutu Geologicznego, 146: 1-71, 18 figs., 11 tabs.; Warszawa
- WHITTAKER, A. (ED.) (1985): Atlas of onshore sedimentary basins in England and Wales. - 71 pp., 27 maps, sections; Glasgow, London (Blackie)
- WONG, TH.E., VAN DOORN, TH.H.M. & SCHROOT, B. (1989) "Late Jurassic" petroleum geology of the Dutch Central North Sea Graben. - Geol. Rundsch. 78: 319-336
- ZDANOWSKI, A. & ZAKOWA, H. (EDS.) (1995): The Carboniferous System in Poland. - Prace Panstwowego Instytutu Geologicznego, 148: 1-215, 82 figs.; Warszawa
- ZGI (1990): Geologische Karte der Deutschen Demokratischen Republik - Geologische Karte ohne känozoische Sedimente, 1:500 000. - ZGI, Berlin.

## Chapter 4-6

- BERNARD, B.B., BROOKS, J.M. & SACKETT, W.M. (1976): Natural gas seepage in the Gulf of Mexico. - Earth and Planet. Sci.Lett. 31: 45-54
- BERNER, U. (1989) Entwicklung und Anwendung empirischer Modelle für die Kohlenstoffisotopenvariationen in Mischungen thermogener Erdgase. Ph.D. Thesis Techn. University Clausthal, 162 pp.
- BERNER, U., FABER, E. & STAHL, W. (1992) Mathematical simulation of carbon isotopic fractionation between huminitic coals and related methane. Chem. Geol.: 94: 315-319.
- BERNER, U. & FABER, E. (1993) Zusammenführung und Weiterentwicklung isotopengeochemischer Methoden in der Exploration von Kohlenwasserstoffen. BGR-Report 112 083, 48p, Fed. Inst. Geosc. Nat. Res, Hannover.
- BERNER, U., FABER, E., SCHEEDER, G. & PANTEN, D. (1995) Primary Cracking of Algal and Landplant Kerogens: Kinetic Models of Isotope Variations in Methane, Ethane, and Propane. In: RICE & SCHOELL (guest-editors): Processes of Natural Gas Formation, Chem. Geol., 126: 233-245 .
- BERNER, U. & FABER, E. (1996): Empirical carbon isotope/maturity relationships for gases from algal kerogens and terrigenous organic matter, based on dry, open-system pyrolysis. - Org.Geochem. 10/11: 947-955
- BEUGE, P. (1982): Paragenetische Beziehungen zwischen Quecksilber-Mineralen und organischen Substanzen. - Freib.Forsch.-H. C374: 53-62
- BOIGK, H., HAGEMANN, H.W., STAHL, W. & WOLLANKE, G. (1976): Zur Herkunft und Migration des Stickstoffs nordwestdeutscher Erdgase aus Oberkarbon und Rotliegend. - Erdöl und Kohle - Erdgas - Petrochemie 29: 103-112
- CLAYTON C. (1991) Carbon isotope fractionation during natural gas generation from kerogen. Marine and Petroleum Geology, 8: 232 - 240.
- DIKENSTEJN, G.CH., GLUSCHKO, W.W., GOLDBECKER, K., MÜLLER, E.P., THEILIG, F., PANKINA, R.I. & MAKSIMOW, S.P. (1973): Zum Auftreten von Quecksilber in Erdgasen am Beispiel der Rotliegend-erdgaslagerstätten. - Z.angew.Geol. 19: 492-494
- DUMKE, I., FABER, E. & POGGENBURG, J. (1989): Determination of stable carbon and hydrogen isotopes of light hydrocarbons. - Anal.Chem. 61: 2149-2154
- EVERLIEN, G. & HOFFMANN, U. (1991): Nitrogen in Natural Gas. Erdöl und Kohle 44: 166-172.

- FABER E. (1987) Zur Isotopengeochemie gasförmiger Kohlenwasserstoffe. Erdöl, Erdgas, Kohle 103: 210-218.
- FABER, E. & STAHL, W.J. (1984): Geochemical surface exploration for hydrocarbons in the North Sea. - AAPG Bull. 68: 363-386
- GALIMOV, E.M. (1988) Sources and mechanisms of formation of gaseous hydrocarbons in sedimentary rocks. Origins of Methane in the Earth. Chemical Geology, 71: 77-95.
- GERLING, P., PISKE, J., RASCH, H.J. & WEHNER, H. (1996): Paläogeographie, Organofazies und Genese von Kohlenwasserstoffen im Staßfurt-Karbonat Ostdeutschlands - (2) Genese von Erdölen und Erdölbegleitgasen. - Erdöl Erdgas Kohle 112: 152-156
- GERLING, P., IDIZ, E., EVERLIEN, G. & SOHNS, E. (1997): New aspects on the origin of nitrogen in natural gas in northern Germany. - Geol.Jb. D103: 65-84
- HAENDEL, D., MÜHLE, K., NITZSCHE, H.-M., STIEHL, G. & WAND, U. (1986): Isotopic variations of the fixed nitrogen in metamorphic rocks. - Geochim.Cosmochim.Acta 50: 749-758
- HUNT, J.M. (1979): Petroleum geochemistry and geology. - Freeman and Company, San Francisco
- JAGER; J. de, DOYLE, M.A.; GRANTHAM, P.J. & MABILLARD, J.E. (1996): Hydrocarbon habitat of the West Netherlands Basin. In: RONDEEL et al. [eds], Geology of gas and oil under the Netherlands, 191-209.
- JAMES, A.T. (1983) Correlation of natural gas by use of carbon isotopic distribution between hydrocarbon components. AAPG Bull. 67: 1176 - 1191.
- JENDEN, P.D., KAPLAN, I.R., POREDA, R.J. & CRAIG, H. (1988): Origin of nitrogen-rich natural gases in the California Great Valley: Evidence from helium, carbon and nitrogen isotope ratios. - Geochim. Cosmochim. Acta 52: 851-861
- KARNKOWSKI, P. (1983): Oil and gas fields in the Polish Lowlands. Vol. 1. The Polish Lowlands. 'Geos' Ed., Krakow, 214 pp. (in Polish, with English abstract).
- KAEMMEL, T., MÜLLER, E.P., KROSSNER, L., NEBEL, J., UNGER, H. & UNGETHÜM, H. (1978): Sind HgPb<sub>2</sub> und (Hg, Pb), gebildet aus natürlichen Begleitkomponenten der Erdgase der Lagerstätte der Altmark, Minerale? - Z.angew.Geol. 24: 90-96
- KETTEL, D. (1982): Norddeutsche Erdgase - Stickstoffgehalt und Isotopenvariationen als Reife- und Faziesindikatoren. - Erdöl und Kohle, Erdgas, Petrochemie 35: 557-559
- KLEIN, J. & JÜNTGEN, H. (1972): Studies on the emission of elemental nitrogen from coals of different rank and its release under geochemical conditions. - In: v.Gaertner, H.R. & Wehner, H. [eds.]: Advances in Organic Geochemistry 1971: 647-656
- KROOSS, B., LEYTHAEUSER, D. & LILLACK, H. (1993): Nitrogen-rich natural gases - Qualitative and quantitative aspects of natural gas accumulation in reservoirs. - Erdöl und Kohle, Erdgas, Petrochemie vereinigt mit Brennstoff-Chemie 46: 271-276
- MITTAG-BRENDEL, E. (1994): Schwefelwasserstoff-Genese in den Zechstein-Erdgaslagerstätten in NW-Deutschland. - BGR report 110.982 (confidential)
- MORRISON, J. (1972): NAM recovers mercury produced with Dutch natural gas. - Oil and Gas Journ., April 17, 1972: 72-73
- MÜLLER, E.P., MAY, F. & STIEHL, G. (1976): Zur Isotopengeochemie des Stickstoffs und zur Genese stickstoffreicher Erdgase. - Z. ang.Geol. 22: 319-324



- LUBAS, J. (1986): Mercury in Permian-Carbonian natural gases of the Polish Lowlands (in Polish). - Prace Instytutu Gornictwa Naftowego i Gasownictwa Nr. 56; ISSN 0209-0724
- OXBURGH, E.R., O'NIONS R.K. & HILL, R.I. (1986): Helium isotopes in sedimentary basins. - Nature 324: 632-635
- OZIMA, M. & PODOSEK, F.A. (1983): Noble gas geochemistry. - 367 S.; Cambridge University Press
- PHILIPP, W. & REINICKE, K.M. (1982): Zur Entstehung und Erschließung der Gasprovinz Ostthannover. - Erdoel Erdgas Zeitschrift 98: 85-90.
- PING S. AND XU, Y. (1986): Continental sediments in China. Academia Sinica: 185-199.
- RICE, D.D. & CLAYPOOL, G.E. (1981): Generation, accumulation and resource potential of biogenic gas. - AAPG Bull. 65: 5-25
- ROHRBACK, B.G., PETERS, K.E., SWEENEY, R.E. & KAPLAN, I.R. (1981): Ammonia formation in laboratory simulated thermal maturation: Implications related to the origin of nitrogen in natural gas. - in M. Bjorøy et al., [eds.]: Advances in Organic Geochemistry 1981: 819-823
- RYKA, W. (1981): Some problems of the Autunian volcanism in Poland. - In: Proceedings of the International Symposium Central European Permian, Warsaw: 165-179
- SCHOELL, M. (1980): The hydrogen and carbon isotopic composition of methane from natural gases of various origins. - Geochim.Cosmochim.Acta 44: 649-661
- SCHOELL, M. (1984): Wasserstoff- und Kohlenstoffisotope in organischen Substanzen, Erdölen und Erdgasen. - Geol.Jb. D67: 3-161
- SCHÜTZE, H. & MÜHLE, K. (1986) How to get relations between bedrocks and  $\delta^{13}\text{C}$  values of methane and ethane in natural gases. Proc. 4th Meeting Isotopes in Nature, Leipzig 1986: 589-603, Zentralinstitut für Isotopen- und Strahlenforschung, Leipzig.
- STAHL, W.J. (1968) Kohlenstoff-Isotopenanalysen zur Klärung der Herkunft norddeutscher Erdgase. PhD Thesis Techn. University Clausthal: 107 pp.
- STAHL, W.J. & CAREY, JR. B.D. (1975) Source-rock identification by isotope analyses of natural gases from fields in the Val Verde and the Delaware Basins, West Texas. Chemical Geology 16: 257-267.
- STAHL, W.J., GERLING, P., BANDLOWA, T., BRÜCKNER-RÖHLING, S., EVERLIEN, G., HOFFMANN, N., KESSEL, G., KOCH, J., KOCKEL, F., KRULL, P., MITTAG-BRENDEL, E., SOHNS, E. & WEHNER, H. (1996): Deep natural gas, a challenge for the future? - In: KÜRSTEN, M. [ed.], World Energy, a Changing Scene, Proc. of the 7th Int. Symp. held in Hannover, Germany, at the Federal Institute for Geosciences and Natural Resources, Oct. 25-27, 1994: 169-191
- STIEHL, G. & LEHMANN, M. (1980): Isotopenvariationen des Stickstoffs humoser und bituminöser natürlicher organischer Substanzen. - Geochim.Cosmochim.Acta 44: 1737-1746
- SOHNS, E., GERLING, P. & FABER, E. (1994): Improved stable nitrogen isotope ratio measurements of natural gases. - Anal.Chem. 66: 2614-2620
- SUNDBERG, K. R. & BENNETT, C. R. (1983) Carbon isotope paleothermometry of natural gas. Advances in Organic Geochemistry 1981: 769-774.
- SWEENEY, R.E., LIU, K.K. & KAPLAN, I.R. (1978): Oceanic nitrogen isotopes and their uses in determining the source of sedimentary nitrogen. - In: Robinson, B.W. [ed.]: Stable isotopes in earth sciences, D.S.I.R.Bull. 220: 9-26

- TUNN, W. (1973): Quecksilberspuren in Erdgasen aus deutschen Erdgasfeldern und ihr Einfluß auf die Luft. - Erdöl und Kohle, Erdgas, Petrochemie vereinigt mit Brennstoff-Chemie 26: 498-500
- WHITICAR, M.J. (1990): A geochemical perspective of natural gas and atmospheric methane. - Org.Geochem. 16: 531-547
- WHITICAR, M.J., FABER, E. & SCHOELL, M. (1986): Biogenic methane formation in marine and freshwater environments: CO<sub>2</sub> reduction vs. acetate fermentation-isotope evidence. - Geochim. Cosmochim.Acta 50: 693-709
- ZHANG, Y.G. & FENG, X.Z. (1990) Catalytic versus noncatalytic degradation of organic matter related to its gas productivity. In: ITTEKKOT V., KEMPE S., MICHAELIS W., & SPITZY A. (eds.) Facts of modern biogeochemistry: 402 - 415, Springer, Berlin.

Composition of Natural Gases in Northwest European Gasfields (vol%)

Table 2 - 1

Wellname/Fieldname	Reservoir	CH4	C2H6	C3H8	i-C4	n-C4	C4	i-C5	n-C5	C5	C6	N2	CO2	H2S	He	H2	others	Calval	Reference
<b>DENMARK</b>																			
Elly-3	M/T	81,15	6,87	1,62	0,35	0,35		0,18	0,15		4,65	0,25	4,62			0			
H-1x	M/T	88,75	4,25	1,41	0,43	0,54		0,32	0,20		2,58	0,89	0,55			0,08			
Roar-2x	M/T	84,59	5,78	2,47	0,53	1,01		0,36	0,43		3,02	0,21	1,63			na			
Alma-2	M/T	67,91	10,6	7,95	1,74	2,39		0,85	0,69		4,5	0,93	2,3			0			
W.Lulu-3	M/T	76,48	8,07	4,30	0,68	1,25		0,42	0,49		5,06	0,49	2,76			0			
Lulu-1	M/T	78,83	7,18	4,38	0,64	1,63		0,39	0,51		5,16	0,44	0,84			na			
E-2	M/T	86,2	5,15	2,24	0,49	0,94		0,41	0,69		2,70	0,23	1,14			0,06			
E-5x	M/T	87,69	4,71	1,99	0,52	0,87		0,43	0,37		2,58	0,58	0,28			0			
E-6x	M/T	85,78	4,66	2,04	0,5	0,87		0,41	0,38		4,6	0,38	0,38			0			
Boje-1	M/T	75,69	6,13	3,71	0,77	1,9		0,64	0,86		10,45	0,4	0,45			na			
Bo-1	M/T	84,32	6,35	4,26	0,56	1,55		0,28	0,4		0,46	0,23	1,59			0			
N.Jens-2	M/T	56,77	7,52	5,25	0,85	2,78		0,86	1,33		23,3	0,14	1,2			0			
G-1x	M/T	93,22	3,91	1,11	0,37	0,42		0,27	0,12		0,04	0,45	tr			0,09			
Adda-1		71,63	6,29	5,78	0,93	2,72		0,82	1,26		10,2	0,3	nd			na			
<b>GERMANY</b>																			
Langensalza 105	M/T	-	-	-	-	-		-	-			67	-	-	-	-	-		Mueller et al. (1976)
Hengstlage T4	M/T	-	-	-	-	-		-	-			9,52	-	-	0,051		Ar=0.002		Eichmann et al. (1969)
Adorf Z1	M/T	75	4,2	0,1	0,3	-		-	-			4,4	14	-	-	-	-		Faber et al. (1979)
Adorf Z10	M/T	-	-	-	-	-		-	-			29,8	0,85	-	-	-	-		Faber et al. (1979)
Adorf Z7	M/T	69,83	1,04	0,06	0	0,01		-	-			28,37	0,67	-	-	-	-		Faber et al. (1979)
Annaveen Z1	M/T	74,7	1,58	0,33	0,57	0,57		0,3	0,45			21,13	0,32	-	-	-	-		Gerling (1986)
Annaveen Z4	M/T	56,76	1,45	0,26	0,05	0,06		0,04	-			41,5	0,33	-	-	-	-		Faber et al. (1979)
Apeldorn T4	M/T	24,9	0,33	0	0	0		0	0			74,26	0,46	-	-	-	-		Gerling (1986)
Bahrenbostel T2	M/T	91,79	0,7	0,03	-	-		-	-			6,73	0,37	-	-	-	-		Faber et al. (1979)
Bahrenbostel T3	M/T	93,39	0,64	0,03	-	-		-	-			4,62	1,08	-	-	-	-		Faber et al. (1979)
Barenburg Z1	M/T	81,15	0,47	0,02	-	-		-	-			17,52	0,5	-	-	-	-		Faber et al. (1979)
Barrien 2T	M/T	-	-	-	-	-		-	-			18,29	-	-	0,069		Ar=0.0041		Eichmann et al. (1969)
Barrien 5T	M/T	85,01	0,2	0,01	0	0		-	-			13,97	0,43	-	-	-	-		Faber et al. (1979)
Barrien 5T	M/T	-	-	-	-	-		-	-			18,46	-	-	0,07		-		Eichmann et al. (1969)
Barrien 8T	M/T	-	-	-	-	-		-	-			18,15	-	-	0,067		Ar=0.0043		Eichmann et al. (1969)
Buchhorst Z4	M/T	85,2	0,43	0,02	-	-		-	-			13,4	0,83	-	-	-	-		Faber et al. (1979)
Code: D 1	M/T	83	2,9	0,6	-	-	C4+=0,3	-	-			12,5	0,7	-	-	-	-		Stahl (1968)
Code: F 1	M/T	91,4	-	-	-	-		-	-			6,4	1,3	-	-	-	-		Stahl (1968)
Code: F 2	M/T	90,1	-	-	-	-		-	-			8,2	1	-	-	-	-		Stahl (1968)
Code: F 3	M/T	90,9	-	-	-	-		-	-			7,3	1,8	-	-	-	-		Stahl (1968)
Code: F 4	M/T	91,7	-	-	-	-		-	-			6,5	1,4	-	-	-	-		Stahl (1968)
Code: G 1	M/T	88,1	1,3	-	-	-		-	-			10,1	0,1	-	-	-	-		Stahl (1968)
Code: G 2	M/T	87,7	1,5	0,1	-	-		-	-			9,2	0,3	-	-	-	-		Stahl (1968)
Code: G 3	M/T	87,4	1,9	0,1	-	-		-	-			10,2	0,1	-	-	-	-		Stahl (1968)
Code: G 4	M/T	87,7	1,5	0,1	-	-		-	-			9,7	0,3	-	-	-	-		Stahl (1968)
Code: G 5	M/T	87,4	1,8	0,1	-	-		-	-			10,6	0,1	-	-	-	-		Stahl (1968)
Code: G 6	M/T	86,9	1,5	0,1	-	-		-	-			9,9	0,3	-	-	-	-		Stahl (1968)
Code: G 8	M/T	82	1,2	-	-	-		-	-			16,5	0,3	-	-	-	-		Stahl (1968)
Code: G 9	M/T	82,3	1,2	-	-	-		-	-			16,4	0,2	-	-	-	-		Stahl (1968)
Code: L	M/T	85	0,2	-	-	-		-	-			14	0,4	-	-	-	-		Stahl (1968)
Doetlingen T1	M/T	85,11	1,24	-	-	-		-	-			13,25	0,4	-	-	-	-		Faber et al. (1979)

Composition of Natural Gases in Northwest European Gasfields (vol%)

Table 2 - 1

Wellname/Fieldname	Reservoir	CH4	C2H6	C3H8	i-C4	n-C4	C4	i-C5	n-C5	C5	C6	N2	CO2	H2S	He	H2	others	Calval	Reference
Doetlingen T1	M/T	-	-	-	-	-	-	-	-	-	-	15,76	-	-	0,074	-	Ar=0.004	-	Eichmann et al. (1969)
Doetlingen T2	M/T	82,3	1,2	-	-	-	-	-	-	-	-	16,4	0,2	-	-	-	-	-	Faber et al. (1979)
Doetlingen T2	M/T	-	-	-	-	-	-	-	-	-	-	15,8	-	-	0,073	-	Ar=0.004	-	Eichmann et al. (1969)
Fehndorf 4Z	M/T	47,69	0,48	0,07	-	-	-	-	-	-	-	51,65	0,11	-	-	-	-	-	Faber et al. (1979)
Fehndorf 5T	M/T	35,76	0,98	0,38	0,03	0,13	-	0,01	0,04	-	-	61,97	0,64	-	-	-	-	-	Faber et al. (1979)
Fehndorf 6Z	M/T	43,8	1,44	0,59	0,08	0,22	-	0,07	0,12	-	-	53,41	0,27	-	-	-	-	-	Faber et al. (1979)
Hengstlage T1	M/T	-	-	-	-	-	-	-	-	-	-	9,56	-	-	0,05	-	Ar=0.002	-	Eichmann et al. (1969)
Hengstlage T2	M/T	-	-	-	-	-	-	-	-	-	-	9,05	-	-	0,051	-	Ar=0.0021	-	Eichmann et al. (1969)
Hengstlage T3	M/T	-	-	-	-	-	-	-	-	-	-	9,48	-	-	0,05	-	Ar=0.0019	-	Eichmann et al. (1969)
Hengstlage T5	M/T	-	-	-	-	-	-	-	-	-	-	9,54	-	-	0,052	-	Ar=0.0018	-	Eichmann et al. (1969)
Hengstlage T6	M/T	86,9	1,5	0,1	-	-	-	-	-	-	-	5,86	0,27	-	-	-	-	-	Faber et al. (1979)
Hengstlage T6	M/T	-	-	-	-	-	-	-	-	-	-	9,49	-	-	0,05	-	Ar=0.0023	-	Eichmann et al. (1969)
Hengstlage T8a	M/T	-	-	-	-	-	-	-	-	-	-	9,46	-	-	0,051	-	Ar=0.0021	-	Eichmann et al. (1969)
Hengstlage T8b	M/T	-	-	-	-	-	-	-	-	-	-	9,3	-	-	0,054	-	Ar=0.0020	-	Eichmann et al. (1969)
Rehden T1	M/T	91,4	0,8	0,1	-	-	-	-	-	-	-	6,4	1,3	-	-	-	-	-	Faber et al. (1979)
Rehden T1	M/T	-	-	-	-	-	-	-	-	-	-	6,4	-	-	0,054	-	Ar=0.0024	-	Eichmann et al. (1969)
Rehden T11	M/T	91,03	0,59	0,04	0,01	0,01	-	-	-	-	-	6,44	1,89	-	-	-	-	-	Faber et al. (1979)
Rehden T2	M/T	90,1	0,7	-	-	-	-	-	-	-	-	8,2	1	-	-	-	-	-	Faber et al. (1979)
Rehden T2	M/T	-	-	-	-	-	-	-	-	-	-	7,33	-	-	0,056	-	Ar=0.0021	-	Eichmann et al. (1969)
Rehden T4	M/T	90,9	0,8	0,1	-	-	-	-	-	-	-	6,59	1,52	-	-	-	-	-	Faber et al. (1979)
Rehden T4	M/T	-	-	-	-	-	-	-	-	-	-	8,55	-	-	0,063	-	Ar=0.0028	-	Eichmann et al. (1969)
Rehden T6	M/T	91,7	0,4	-	-	-	-	-	-	-	-	6,46	1,39	-	-	-	-	-	Faber et al. (1979)
Ruetenbrock T1	M/T	-	-	-	-	-	-	-	-	-	-	12,07	2,02	-	-	-	-	-	Faber et al. (1979)
Ruetenbrock Z1	M/T	-	-	-	-	-	-	-	-	-	-	2,05	1	-	-	-	-	-	Faber et al. (1979)
Ruetenbrock Z7	M/T	84,16	0,35	0,03	0,01	0,01	-	-	-	-	-	14,31	0,97	-	-	-	-	-	Faber et al. (1979)
Siedenburg T3	M/T	85,64	0,34	0,01	-	-	-	-	-	-	-	12,65	1,08	-	-	-	-	-	Faber et al. (1979)
Staffhorst Z4	M/T	82,43	0,46	0,83	-	-	-	-	-	-	-	-	0,59	-	-	-	-	-	Faber et al. (1979)
Uelsen T1	M/T	83,95	2,07	0,51	0,08	0,17	-	0,06	0,08	-	-	12,86	0,02	-	-	-	-	-	Faber et al. (1979)
Uelsen T2	M/T	83,96	2,21	0,53	0,08	0,17	-	0,06	0,07	-	-	12,73	-	-	-	-	-	-	Faber et al. (1979)
Visbeck T1	M/T	69,27	0,98	0,04	0,01	0,01	-	0,01	-	-	-	29,35	0,36	-	-	-	-	-	Faber et al. (1979)
Voigtei T1	M/T	71,81	0,64	0,03	-	-	-	-	-	-	-	26,53	0,49	-	-	-	-	-	Faber et al. (1979)
Fahner Hoehe 7	M/T	17,6	0,7	0,1	-	-	-	-	-	-	-	62	17,9	-	0,83	-	-	-	Freund (1966)
Langensalza	M/T	33,5	-	-	-	-	-	-	-	-	-	66,3	-	-	0,5	-	-	-	Freund (1966)
Wiegleben 1	M/T	43,9	4,9	1	-	-	-	-	-	-	-	49,7	-	-	-	-	-	-	Freund (1966)
Fuhrberg E2	M/T	90,3	6,1	1	0,1	0,7	-	0,2	0,2	-	-	-	1,3	-	-	-	-	-	Gerling et al. (1991)
Grossburgwedel 4	M/T	72,5	9,9	6,8	1,8	4,1	-	1,8	2,2	-	-	-	0,9	-	-	-	-	-	Gerling et al. (1991)
Grossburgwedel 2	M/T	87,9	6,9	2,5	0,3	0,7	-	0,2	0,2	-	-	-	1,2	-	-	-	-	-	Gerling et al. (1991)
Messingen 5	M/T	94,7	0,58	0	0	0	-	0	0	-	-	4,35	0,39	-	-	-	-	-	Gerling (1986)
Grossburgwedel 5	M/T	88,6	4,8	1,5	0,3	0,5	-	0,2	0,2	-	-	-	4	-	-	-	-	-	Gerling et al. (1991)
Grossburgwedel 6	M/T	89,9	4,5	1,3	0,3	0,5	-	0,2	0,2	-	-	-	2,9	-	-	-	-	-	Gerling et al. (1991)
Annaveen Z4	C	83,03	0,35	0,01	-	-	-	-	-	-	-	7,35	9,72	-	-	-	C2+ =0.43	-	Faber et al. (1979)
Cappeln Z1	C	95,87	1,33	0,3	0,02	0,02	-	0,02	0,02	-	-	2,37	0,33	-	-	-	-	-	Faber et al. (1979)
Code: E 3	C	93,2	3,7	0,7	-	-	0,1	-	-	C5+=0.3	-	1,2	0,8	-	-	-	-	-	Stahl (1968)
Code: E 4	C	92,1	3,8	0,8	-	-	0,1	-	-	C5+=0.3	-	2,1	0,8	-	-	-	-	-	Stahl (1968)
Code: F 10	C	83,7	-	-	-	-	-	-	-	-	-	6,6	8,5	-	-	-	-	-	Stahl (1968)
Code: F 11	C	78,8	-	-	-	-	-	-	-	-	-	10	10,5	-	-	-	-	-	Stahl (1968)
Code: F 12	C	82,1	-	-	-	-	-	-	-	-	-	6,8	7,1	-	-	-	-	-	Stahl (1968)
Code: F 13	C	82,6	-	-	-	-	-	-	-	-	-	7	9,4	-	-	-	-	-	Stahl (1968)
Code: F 14	C	82,8	-	-	-	-	-	-	-	-	-	6,1	9	-	-	-	-	-	Stahl (1968)

Composition of Natural Gases in Northwest European Gasfields (vol%)

Table 2 - 1

Wellname/Fieldname	Reservoir	CH4	C2H6	C3H8	i-C4	n-C4	C4	i-C5	n-C5	C5	C6	N2	CO2	H2S	He	H2	others	Calval	Reference
Code: O	C	88,3	5,3	1,2	-	-	C4+=0,8	-	-	-	-	2,2	2,2	-	-	-	-	-	Stahl (1968)
Emlichheim T1	C	91,46	2,59	0,59	0,12	0,19	-	0,1	-	-	-	2,46	2,16	-	-	-	-	-	Faber et al. (1979)
Emlichheim T6	C	91,38	0,68	-	-	-	-	-	-	-	-	-	-	-	-	-	C2+ =0.8	-	Schoell (1984)
Emlichheim Z6	C	91,38	0,68	0,04	0,01	0,01	-	-	-	-	-	3,94	3,96	-	-	-	-	-	Faber et al. (1979)
Esche Z3	C	92,4	2,73	0,34	0,06	0,05	-	0,02	0,02	-	-	2,14	2,21	-	-	-	-	-	Faber et al. (1979)
Fehndorf 3Z	C	75,88	0,29	0,01	-	-	-	-	-	-	-	19,09	4,74	-	-	-	-	-	Faber et al. (1979)
Fehndorf 6Z	C	58,03	0,61	0,01	-	-	-	-	-	-	-	31,25	10,1	-	-	-	-	-	Faber et al. (1979)
Frenswegen 5	C	92,94	1,05	0,07	0,01	0,01	-	0,01	-	-	-	4,62	1,31	-	-	-	-	-	Faber et al. (1979)
Getelo Z1	C	91,9	4	0,84	0,13	0,1	-	0,06	0,06	-	-	1,88	0,97	-	-	-	-	-	Faber et al. (1979)
Goldenstedt Z6	C	88,17	0,44	0,01	-	-	-	-	-	-	-	4,68	4,68	-	-	-	-	-	Faber et al. (1979)
Hamwiede Z2	C	88,4	-	-	-	-	-	-	-	-	-	6,9	1,9	-	-	-	-	-	Boigk et al. (1975)
Itterbeck-Halle Z10	C	94,61	2,81	0,45	0,06	0,09	-	0,03	0,02	-	-	1,27	0,61	-	-	-	-	-	Faber et al. (1979)
Itterbeck-Halle Z5	C	95,34	1,97	0,41	0,06	0,09	-	0,08	-	-	-	1,76	0,29	-	-	-	-	-	Faber et al. (1979)
Itterbeck-Halle Z6	C	92,1	-	-	-	-	-	-	-	-	-	2,1	0,8	-	-	-	-	-	Faber et al. (1979)
Kalle Z4	C	92,49	1,48	0,24	0,05	0,04	-	0,03	-	-	-	2,43	2,89	-	-	-	-	-	Faber et al. (1979)
Oythe Z2	C	87,28	0,55	0,09	-	-	-	-	-	-	-	7,33	4,83	-	-	-	-	-	Faber et al. (1979)
Ratzel Z3	C	88,34	5,31	1,2	0,25	0,3	-	0,14	0,11	-	-	2,15	2,2	-	-	-	-	-	Faber et al. (1979)
Ratzel Z4	C	90,39	4	1,28	0,23	0,32	-	0,12	0,09	-	-	2,34	0,97	-	-	-	-	-	Faber et al. (1979)
Rehden 19	C	83,7	-	-	-	-	-	-	-	-	-	5,55	9,92	-	-	-	-	-	Faber et al. (1979)
Rehden 19	C	-	-	-	-	-	-	-	-	-	-	6,72	-	-	0,052	-	Ar=0.0022	-	Eichmann et al. (1969)
Rehden 21	C	78,4	0,9	0,2	-	-	-	-	-	-	-	9,97	10,46	-	-	-	-	-	Faber et al. (1979)
Rehden 21	C	78,4	-	-	-	-	-	-	-	-	-	6,78	10,5	-	0,054	-	C2+ =1.1	-	Stiehl (1980)
Rehden 23	C	83,03	0,61	0,04	-	-	-	-	-	-	-	7,08	9,27	-	-	-	-	-	Faber et al. (1979)
Rehden 24	C	82,1	-	-	-	-	-	-	-	-	-	6,79	7,05	-	-	-	-	-	Faber et al. (1979)
Rehden 24	C	82,1	-	-	-	-	-	-	-	-	-	6,72	7,1	-	0,053	-	C2+ =0.7	-	Stiehl (1980)
Rehden 27	C	82,6	-	-	-	-	-	-	-	-	-	7,03	9,4	-	-	-	-	-	Faber et al. (1979)
Rehden 27	C	82,6	-	-	-	-	-	-	-	-	-	6,92	9,4	-	0,05	-	C2+ =0.7	-	Stiehl (1980)
Rehden 28	C	82,8	1,7	0,3	0,1	-	-	-	-	-	-	6,05	9,02	-	-	-	-	-	Faber et al. (1979)
Rehden 28	C	-	-	-	-	-	-	-	-	-	-	6,53	-	-	0,048	-	Ar=0.0025	-	Eichmann et al. (1969)
Ruetenbrock Z1	C	-	0	-	-	-	-	-	-	-	-	2,1	1,2	-	-	-	-	-	Faber et al. (1979)
Twistringem Z1	C	95,88	0,54	0,01	-	-	-	-	-	-	-	2,43	-	-	-	-	-	-	Faber et al. (1979)
Uelsen Z1	C	92,89	2,84	0,64	0,14	0,15	-	0,05	0,07	-	-	2,26	0,69	-	-	-	-	-	Faber et al. (1979)
Wielen Z4	C	92,61	3,31	0,78	0,13	0,2	-	0,07	0,06	-	-	1,98	0,61	-	-	-	-	-	Faber et al. (1979)
Wietingsmoor Z1	C	-	-	-	-	-	-	-	-	-	-	0,5	3,37	-	-	-	-	-	Faber et al. (1979)
Code: C 2	C	91,7	0,1	0,1	-	-	-	-	-	-	-	5,8	1,4	-	-	-	-	-	Stahl (1968)
Code: D 3	C	90,8	4,6	1,1	-	-	C4+=0,6	-	-	-	-	2,1	1	-	-	-	-	-	Stahl (1968)
Bahnsen 9Z	R	76,1	0,98	0,03	0,01	0,01	-	-	-	-	-	-	-	-	-	-	C2+ =1.35	-	Schoell (1984)
North Sea 1	R	73,64	11,99	-	-	-	-	-	-	-	-	-	-	-	-	-	C2+ =19.87	-	Schoell (1984)
Alfeld-Elze Z1	R	65,7	-	-	-	-	-	-	-	-	-	31	3,1	-	-	-	-	-	Boigk et al. (1975)
Alfeld-Elze Z2	R	64,9	-	-	-	-	-	-	-	-	-	30,4	4,5	-	-	-	-	-	Boigk et al. (1975)
Bodenteich Z1	R	35	-	-	-	-	-	-	-	-	-	64,3	0,6	-	-	-	-	-	Boigk et al. (1975)
Dalum Z5	R	86,06	0,37	0,01	-	-	-	-	-	-	-	7,16	6,41	-	-	-	-	-	Faber et al. (1979)
Ebstorf Z1	R	61,8	0,51	0,02	0,02	0,02	-	-	-	-	-	-	-	-	-	-	C2+ =0.92	-	Schoell (1984)
Ebstorf-Nord Z1	R	63,2	0,51	0,07	0,03	0,03	-	-	-	-	-	-	-	-	-	-	C2+ =1.05	-	Schoell (1984)
Engerhafe Z1	R	93,18	2,8	0,29	0,03	0,06	-	0,01	0,02	-	-	2,89	0,71	-	-	-	-	-	Faber et al. (1979)
Greetsiel Z1	R	92,5	3,08	0,29	0,03	0,06	-	0,01	0,01	-	-	3,23	0,81	-	-	-	-	-	Faber et al. (1979)
Groothusen Z5	R	86,74	3,92	0,6	0,09	0,13	-	0,04	-	-	-	7,45	1,06	-	-	-	-	-	Faber et al. (1979)
Groothusen Z6	R	84,55	3,89	0,63	0,08	0,14	-	0,06	0,07	-	-	9,57	1,01	-	-	-	-	-	Faber et al. (1979)
Munster Z1	R	80,1	1,1	0,04	0,01	0,01	-	-	-	-	-	-	-	-	-	-	C2+ =1.45	-	Schoell (1984)

Composition of Natural Gases in Northwest European Gasfields (vol%)

Table 2 - 1

Wellname/Fieldname	Reservoir	CH4	C2H6	C3H8	i-C4	n-C4	C4	i-C5	n-C5	C5	C6	N2	CO2	H2S	He	H2	others	Calval	Reference
Niendorf II Z1	R	77,8	-	-	-	-	-	-	-	-	-	20,8	0,5	-	-	-	-	-	Boigk et al. (1975)
Ruetenbrock 8Z	R	80,56	0,22	0,02	0,01	0,01	-	0	-	-	-	18,72	0,41	-	-	-	-	-	Faber et al. (1979)
Schmarbeck Z1	R	76	1,04	0,04	0,01	0,01	-	-	-	-	-	-	-	-	-	-	C2+ =1.45	-	Schoell (1984)
Uttum Z1	R	93,19	2,84	0,26	0,03	0,06	-	0,01	0,02	-	-	2,48	1,11	-	-	-	-	-	Faber et al. (1979)
Wustrow Z1	R	35,2	-	-	-	-	-	-	-	-	-	64,1	0,3	-	-	-	-	-	Boigk et al. (1975)
Wustrow Z3	R	20,7	-	-	-	-	-	-	-	-	-	78,9	0,3	-	-	-	-	-	Boigk et al. (1975)
Wustrow-West Z1	R	41,8	0,57	0,02	0	0	-	-	-	-	-	-	-	-	-	-	C2+ =1.41	-	Schoell (1984)
Groothusen Z1	R	-	-	-	-	-	-	-	-	-	-	7,94	-	-	0,066	-	Ar=0.0016	-	Eichmann et al. (1969)
North Sea B2	R	-	-	-	-	-	-	-	-	-	-	62,61	-	-	0,064	-	Ar=0.013	-	Eichmann et al. (1969)
North Sea D1	R	-	-	-	-	-	-	-	-	-	-	46,87	-	-	0,085	-	Ar=0.0086	-	Eichmann et al. (1969)
Hohenkoerben 1	M/T	-	-	-	-	-	-	-	-	-	-	0,26	-	-	0,0098	-	Ar=0.00034	-	Eichmann et al. (1969)
Adorf Z1	Z	84,54	0,69	0,14	0,02	0,06	-	0,02	0,03	-	-	4,45	9,9	-	-	-	C2+ =1.29	-	Faber et al. (1979)
Adorf Z12	Z	79,48	1,08	0,14	0,02	0,05	-	0,06	-	-	-	6,91	12,22	-	-	-	-	-	Faber et al. (1979)
Adorf Z4	Z	79,87	0,95	0,15	0,03	0,07	-	0,08	-	-	-	6,65	12,2	-	-	-	-	-	Faber et al. (1979)
Adorf Z5	Z	82,32	0,63	0,13	0,02	0,05	-	0,02	0,03	-	-	6,27	10,4	-	-	-	C2+ =1.21	-	Faber et al. (1979)
Adorf Z6	Z	79,59	1,05	0,11	0,02	0,04	-	0,05	-	-	-	5,38	13,76	-	-	-	-	-	Faber et al. (1979)
Bentheim 10	Z	88,9	0,8	0,3	0,1	-	-	-	-	-	-	6,6	2	-	-	-	-	-	Faber et al. (1979)
Bentheim 15	Z	88,05	0,48	0,03	-	-	-	-	-	-	-	7,42	4,01	-	-	-	C2+ =0.58	-	Faber et al. (1979)
Cappeln Z1	Z	77,69	0,34	0,02	-	-	-	-	-	-	-	2,17	18,32	-	-	-	-	-	Faber et al. (1979)
Cloppenburg Z2	Z	89,32	0,4	-	-	-	-	-	-	-	-	1,33	7,98	-	-	-	-	-	Faber et al. (1979)
Emlichheim NZ3	Z	90,52	1,3	0,21	0,08	0,09	-	-	-	-	-	4,52	3,28	-	-	-	-	-	Faber et al. (1979)
Emlichheim NZ5	Z	87,28	0,54	0,06	0,02	0,02	-	-	-	-	-	3,39	6,48	-	-	-	-	-	Faber et al. (1979)
Emlichheim Z1	Z	86,35	0,61	0,2	0,04	0,02	-	-	-	-	-	5,29	7,38	-	-	-	-	-	Faber et al. (1979)
Emlichheim Z9	Z	87,82	1,2	0,22	0,04	0,1	-	-	-	-	-	4,84	5,78	-	-	-	-	-	Faber et al. (1979)
Emlichheim-Nord Z7	Z	91,67	0,31	0,04	0,01	0,02	-	0,01	0,01	-	-	3,93	3,92	-	-	-	-	-	Faber et al. (1979)
Emlichheim-Nord Z9	Z	91,31	2,33	0,49	0,11	0,12	-	0,06	0,04	-	-	2,16	3,22	-	-	-	-	-	Faber et al. (1979)
Esche Z1	Z	90,55	2,96	0,43	0,07	0,08	-	0,03	0,03	-	-	2,16	3,33	-	-	-	-	-	Faber et al. (1979)
Fehndorf 6Z	Z	0,27	-	-	-	-	-	-	-	-	-	90,34	9,39	-	-	-	-	-	Faber et al. (1979)
Frenswegen 3	Z	84,8	0,8	0,6	0,1	-	-	-	-	-	-	8,9	3,3	-	-	-	-	-	Faber et al. (1979)
Frenswegen Z5	Z	91,72	1,68	0,12	0,01	0,01	-	0,01	-	-	-	4,93	1,5	-	-	-	-	-	Faber et al. (1979)
Itterbeck-Halle Z1	Z	86,28	1,8	-	-	-	-	-	-	-	-	8,64	3,12	-	-	-	-	-	Faber et al. (1979)
Itterbeck-Halle Z2	Z	88,54	2,88	-	-	-	-	-	-	-	-	2,92	4,9	-	-	-	-	-	Faber et al. (1979)
Itterbeck-Halle Z3	Z	90,7	2,99	0,69	0,13	0,2	-	0,15	-	-	-	2,6	2,53	-	-	-	-	-	Faber et al. (1979)
Itterbeck-Halle Z4	Z	89,75	3,27	0,73	0,15	0,22	-	0,18	-	-	-	2,82	2,87	-	-	-	-	-	Faber et al. (1979)
Itterbeck-Halle Z7	Z	-	-	-	-	-	-	-	-	-	-	0,73	4,74	-	-	-	-	-	Faber et al. (1979)
Kalle Z1	Z	85,65	2,87	0,87	0,16	0,37	-	0,13	0,19	-	-	3,94	6,26	-	-	-	-	-	Faber et al. (1979)
Kalle Z6	Z	89,67	1,71	0,48	0,09	0,21	-	0,07	0,11	-	-	3,72	3,65	-	-	-	-	-	Faber et al. (1979)
Norddeutschland 2	Z	91	1,1	-	-	-	-	-	-	-	-	4,28	2,89	-	-	-	-	-	Faber et al. (1979)
Norddeutschland 5	Z	89,51	0,41	0,02	-	-	-	-	-	-	-	5,57	4,48	-	-	-	-	-	Faber et al. (1979)
Norddeutschland 7	Z	88,91	0,49	0,05	-	-	-	-	-	-	-	7,52	3,04	-	-	-	-	-	Faber et al. (1979)
Norddeutschland 8	Z	88,37	0,38	0,02	-	-	-	-	-	-	-	6,56	4,68	-	-	-	-	-	Faber et al. (1979)
Norddeutschland 9	Z	94,1	0,73	0,12	-	-	-	-	-	-	-	2,56	2,4	-	-	-	-	-	Faber et al. (1979)
Ratzel Z1	Z	90,33	2,86	0,8	0,16	0,21	-	0,09	0,07	-	-	2,61	2,63	-	-	-	-	-	Faber et al. (1979)
Rehden T11	Z	76,6	0,7	-	-	-	-	-	-	-	-	7,11	15,59	-	-	-	-	-	Faber et al. (1979)
Rehden T17	Z	80,8	0,3	-	-	-	-	-	-	-	-	10,7	8,2	-	-	-	-	-	Faber et al. (1979)
Rehden T5	Z	74,4	0,9	0,2	-	-	-	-	-	-	-	6,1	18,4	-	-	-	-	-	Faber et al. (1979)
Rehden T8	Z	75,8	0,7	-	-	-	-	-	-	-	-	7,6	14,3	-	-	-	-	-	Faber et al. (1979)
Rehden T9	Z	-	-	-	-	-	-	-	-	-	-	-	-	-	-	-	-	-	Faber et al. (1979)
Ruetenbrock 10Z	Z	84,92	0,27	0,04	0,01	0,02	-	0,01	0,01	-	-	12,6	2,11	-	-	-	-	-	Faber et al. (1979)

Composition of Natural Gases in Northwest European Gasfields (vol%)

Table 2 - 1

Wellname/Fieldname	Reservoir	CH4	C2H6	C3H8	i-C4	n-C4	C4	i-C5	n-C5	C5	C6	N2	CO2	H2S	He	H2	others	Calval	Reference
Ruetenbrock 11Z	Z	84,08	0,24	0,05	0,02	0,02		0,01	0,01			13,09	2,45	-	-	-	-	-	Faber et al. (1979)
Ruetenbrock 6Z	Z	92,25	0,19	0,04	0,01	0,02		0,01	0,01			4,54	2,84	-	-	-	-	-	Faber et al. (1979)
Ruetenbrock Z5	Z	80,33	0,37	0,05	0,02	0,03		-	-			15,39	3,81	-	-	-	-	-	Faber et al. (1979)
Staffhorst-N. Z2	Z	84,7	0,5	0,02	-	-		-	-			2,26	9,48	-	-	-	-	-	Faber et al. (1979)
Uelsen Z2	Z	6,44	0,19	0,05	0,01	0,02		0,01	0,01			91,22	2,03	-	-	-	-	-	Faber et al. (1979)
Wardenburg Z1	Z	88,11	0,61	0,05	0,01	0,02		0,01	0,1			5,3	4,48	-	-	-	-	-	Faber et al. (1979)
Wielen Z2	Z	90,62	2,71	0,74	0,12	0,2		0,08	0,08			2,59	2,47	-	-	-	-	-	Faber et al. (1979)
Wielen Z6	Z	90,34	2,85	0,77	0,13	0,22		0,09	0,08			3,07	2,1	-	-	-	-	-	Faber et al. (1979)
North Sea B1	Z	-	-	-	-	-		-	-			89,49	-	-	0,035	-	-	Ar=0.021	Eichmann et al. (1969)
Rehden 11	Z	-	-	-	-	-		-	-			7,1	-	-	0,05	-	-	Ar=0.0025	Eichmann et al. (1969)
Rehden 17	Z	-	-	-	-	-		-	-			9,77	-	-	0,062	-	-	Ar=0.0029	Eichmann et al. (1969)
Rehden 5	Z	-	-	-	-	-		-	-			6,9	-	-	0,05	-	-	Ar=0.0026	Eichmann et al. (1969)
Rehden 8	Z	-	-	-	-	-		-	-			6,92	-	-	0,049	-	-	Ar=0.0022	Eichmann et al. (1969)
Rehden 9	Z	-	-	-	-	-		-	-			6,98	-	-	0,05	-	-	Ar=0.0021	Eichmann et al. (1969)
Bentheim B10	Z	-	-	-	-	-		-	-			6,16	-	-	0,13	-	-	Ar=0.0027	Eichmann et al. (1969)
Bentheim ND7	Z	-	-	-	-	-		-	-			6	-	-	0,13	-	-	Ar=0.0027	Eichmann et al. (1969)
Altengottern 1	Z	46,2	-	-	-	-		-	-			52,7	2	-	-	-	-	-	Freund (1966)
Atterwasch	Z	23,3	5,4	3	0,42	1,33		-	-			65,6	0,39	0,008	0,09	-	-	-	Weinlich (1991)
Behringen 1	Z	56,6	2,5	-	-	-		-	-			40,8	-	-	-	-	-	-	Freund (1966)
Biegenbrueck	Z	6,9	2,4	1,9	0,2	0,6		-	-	C5+ =0.3		8,43	0,1	0,31	0,04	-	-	-	Weinlich (1991)
Bienstaedt 1	Z	59,3	11,3	4,6	0,4	0,7		-	-	-		18,7	4,3	-	-	-	-	-	Freund (1966)
Burg	Z	57	11,9	6,2	1,2	1,75		-	-	C5+ =0.58		19	-	-	2,4	-	-	-	Weinlich (1991)
Code: A 1	Z	88,9	0,8	0,3	-	-	0,1	-	-	-		6,6	2	-	-	-	-	-	Stahl (1968)
Code: A 2	Z	91,2	0,8	0,3	-	-	0,1	-	-	-		6,3	2	-	-	-	-	-	Stahl (1968)
Code: B 1	Z	75	4,2	0,1	-	-	C4+=0.1	-	-	-		4,4	14	-	-	-	-	-	Stahl (1968)
Code: B 2	Z	77,5	1	0,2	-	-	C4+=0.1	-	-	-		4,4	15,2	-	-	-	-	-	Stahl (1968)
Code: D 2	Z	85,1	4,7	1,4	-	-	C4+=0.1	-	-	-		4,2	4,2	-	-	-	-	-	Stahl (1968)
Code: F 5	Z	74,4	-	-	-	-	-	-	-	-		6,1	18,4	-	-	-	-	-	Stahl (1968)
Code: F 6	Z	75,8	-	-	-	-	-	-	-	-		7,6	14,3	-	-	-	-	-	Stahl (1968)
Code: F 8	Z	76,6	-	-	-	-	-	-	-	-		7,1	15,6	-	-	-	-	-	Stahl (1968)
Code: F 9	Z	80,8	-	-	-	-	-	-	-	-		10,7	7,9	-	-	-	-	-	Stahl (1968)
Code: M	Z	91	1,7	0,6	-	-	-	-	-	-		3,4	3,3	-	-	-	-	-	Stahl (1968)
Code: N	Z	86,4	2,4	0,4	-	-	C4+=0.1	-	-	-		3,9	6,2	-	-	-	-	-	Stahl (1968)
Dalum Z2	Z	80,1	0,97	0,16	0	0		0	-	-		2,66	16,15	-	-	-	-	-	Gerling (1986)
Drebkau	Z	58	9,3	3,7	0,75	1,14		-	-	C5+ =0.44		26,6	-	-	0,03	0,04	-	-	Weinlich (1991)
Drewitz	Z	33,9	8,4	4,2	0,65	1,93		-	-	-		49,9	0,34	0,16	0,12	-	-	-	Weinlich (1991)
Ettersberg 5h	Z	4,8	0,7	0,1	-	-		-	-	-		6,4	85,1	-	-	-	-	-	Freund (1966)
Fahner Hoehe 7	Z	40	1,4	0,3	-	-		-	-	-		25	34	-	-	0,14	-	-	Freund (1966)
Gotha 1	Z	30,9	1,3	-	-	-		-	-	-		35,5	30,3	-	-	-	-	-	Freund (1966)
Guben 1	Z	22,8	4,8	3,5	0,3	0,8		-	-	-		67,9	-	-	0,12	0,09	-	-	Weinlich (1991)
Hainich-Eigenrieden 2	Z	29,9	1,3	0,1	-	-		-	-	-		32,7	37	-	-	-	-	-	Freund (1966)
Hainich-Heyerode	Z	31,8	1,1	0,3	-	-		-	-	-		67,3	-	-	0,3	-	-	-	Freund (1966)
Hainich-Mihla	Z	30	1	0,3	-	-		-	-	-		68	-	-	0,3	-	-	-	Freund (1966)
Hainich-Nazza	Z	15,1	0,5	-	-	-		-	-	-		83,2	0,9	-	-	-	-	-	Freund (1966)
Keula 3	Z	33,3	4,3	5,5	0,3	1,3		-	-	-		10,2	44,9	-	-	-	-	-	Freund (1966)
Kirchheilingen	Z	61,8	10	4,3	0,3	0,7		-	-	-		22,8	-	-	0,1	-	-	-	Freund (1966)
Komptendorf	Z	37,4	11,9	6,3	0,9	1,51		-	-	-		41,4	0,05	-	0,11	-	-	-	Weinlich (1991)
Krahnberg 1	Z	28,7	1,1	-	-	-		-	-	-		18,8	51,5	-	0,16	-	-	-	Freund (1966)
Krahnberg 15	Z	-	-	-	-	-		-	-	-		38	-	-	-	-	-	-	Mueller et al. (1976)

Composition of Natural Gases in Northwest European Gasfields (vol%)

Table 2 - 1

Wellname/Fieldname	Reservoir	CH4	C2H6	C3H8	i-C4	n-C4	C4	i-C5	n-C5	C5	C6	N2	CO2	H2S	He	H2	others	Calval	Reference
Langensalza	Z	56,5	9,1	4,2	0,4	0,8		-	-			29,3	-	-	0,08		-		Freund (1966)
Langensalza 13	Z	-	-	-	-	-		-	-			30	-	-	-		-		Mueller et al. (1976)
Langensalza 26	Z	68,2	6,6	2,7	0,2	0,6		-	-			21,2	-	-	-		-		Freund (1966)
Leibsch	Z	5	2,2	1,6	0,2	0,8		-	-	C5+ =0.4		89,3	0,4	0,034	0,03				Weinlich (1991)
Luebben	Z	44,3	6,4	2,3	0,42	0,59		-	-	C5+ =0.27		44,3	0,1	1,2	0,38				Weinlich (1991)
Mechterstaedt 1	Z	45	2,3	0,4	-	-		-	-	-		49	3,8	-	-				Freund (1966)
Mittweide	Z	26,6	5,7	3,3	0,4	1,1		-	-	C5+ =0.5		61,9	-	0,064	0,04				Weinlich (1991)
Muehlhausen	Z	49,7	1,8	0,5	-	-		-	-			47,6	-	-	0,16		-		Freund (1966)
Neudietendorf 1h	Z	7,6	0,3	-	-	-		-	-			7,3	85,4	-	-		-		Freund (1966)
Obermehler 1	Z	59,2	11,9	3,9	0,4	0,8		-	-			23,8	-	-	-		-		Freund (1966)
Raden	Z	30,6	9,8	4,6	0,67	1,55		-	-	C5+ =0.4		52,2	0,2	0,0002	0,1				Weinlich (1991)
Schenkendoeborn	Z	21,1	5,6	2,7	0,4	0,8		-	-	C5+ =0.6		68,6	0,1	0,014	0,08				Weinlich (1991)
Schlagsdorf	Z	19,4	3,9	1,8	0,22	0,54		-	-	C5+ =0.09		73,7	0,07	0,0003	0,05				Weinlich (1991)
Schlepzig	Z	15,1	4,3	2,5	0,37	0,91		-	-	C5+ =0.31		76,8	-	0,077	0,06				Weinlich (1991)
Staakow	Z	56,6	2,1	0,8	0,25	0,5		-	-			27,5	7,6	4,8	0,04		-		Weinlich (1991)
Steinsdorf	Z	32,9	10,2	5,1	0,61	1,22		-	-	C5+ =0.4		49,4	0,1	0,033	0,12				Weinlich (1991)
Tauer 103	Z	47,3	10,2	4,7	0,11	0,19		-	-	C5+ =0.48		34,9	-	2,03	0,1				Weinlich (1991)
Tauer 7	Z	54,8	10,6	4,3	0,67	1,37		-	-			20,5	0,42	6,7	0,08		-		Weinlich (1991)
Uchte Z2	Z	88,2	0,53	0	0							2,8	8,48	-	-		-		Gerling (1986)
Volkenroda	Z	50,2	6,4					-	-			43,2	-	-	-		-		Freund (1966)
Wattesattel	Z	65,3	7,7	6,6	0,48	1,46		-	-			6,9	11,5	-	-		-		Freund (1966)
Wiegleben 1	Z	12,3	0,5					-	-			12,8	74,1	-	-		-		Freund (1966)
Code: C 1	Z	84,8	0,8	0,3	-		C4+=0.	-	-			8,9	3,3	-	-		-		Stahl (1968)
Bentheim ND5	Z	-	-	-	-	-		-	-			5,03	-	-	0,15		Ar=0.0021		Eichmann et al. (1969)
Bentheim ND8	Z	-	-	-	-	-		-	-			5	-	-	0,097		Ar=0.0028		Eichmann et al. (1969)
Code: A 3	Z	91	1,1					-	-			-	-	-	-		-		Stahl (1968)
Code: A 4	Z	90,1	0,7	0,2				-	-			5,8	2,5	-	-		-		Stahl (1968)
Code: A 5	Z	90,1	0,7	0,2			0,1	-	-			5,2	22,5	-	-		-		Stahl (1968)
Code: A 6	Z	91,2	0,7	0,2			0,1	-	-			5,3	2,5	-	-		-		Stahl (1968)
Code: E 1	Z	88,7	2,7	1				-	-	C5+=0.6		2,6	4,5	-	-		-		Stahl (1968)
Code: E 2	Z	88,3	4,5	1,3			0,2	-	-	C5+=0.7		2,3	2,4	-	-		-		Stahl (1968)
<b>THE NETHERLANDS</b>																			
Annerveen-Veendam	Z	76,4	C2+=5.5									14,4	2	+					Bandlova
Annerveen-Veendam	R	85,2										8,2	3,3						Bandlova
Annerveen-Veendam	R	90,6	C2+=4.5									4,5	0,6						Bandlova
Annerveen	Rotl.	90,83	3,39	C3+=1.19								3,87	0,66						Int. Map Gasfields 1985
Bergen	R	91,8	C2+=4.1									3,1	1						Bandlova
Bergen	Rotl.	89,68	3,89	C3+=1.1								4,52	0,67						Int. Map Gasfields 1985
Bergermeer	R	94,6	C2+=3.7									0,78	0,67						Bandlova
Bergermeer	Rotl.	94,8	3	C3+=0.52															Int. Map Gasfields 1985
Coevorden	Z	91,6	C2+=2.3									2,5	3,6	+					Bandlova
Coevorden	Zech/Carb	91,4	1,1	C3+=0.31								3,5	3,4				0,4		Int. Map Gasfields 1985
De Lier	Cretac.	90	8,6									1,4							Int. Map Gasfields 1985
De Lutte	Z	92,2	C2+=2.7									3,6	1,3						Bandlova
De Lutte	Zechst.	92,2	C2+=2.9									3,6	1,3						Int. Map Gasfields 1985
Denekamp	Z	88	-									7,8	-						Bandlova
De Wijk	M/T	87,7	C2+=5,4									7	-						Bandlova
De Wijk	R	85	C2+=8									6,4	0,4						Bandlova



Composition of Natural Gases in Northwest European Gasfields (vol%)

Table 2 - 1

Wellname/Fieldname	Reservoir	CH4	C2H6	C3H8	i-C4	n-C4	C4	i-C5	n-C5	C5	C6	N2	CO2	H2S	He	H2	others	Calval	Reference
De Wijk		90,5	2,6	C3+=1.28								4,9	0,6						Int. Map Gasfields 1985
Groet	Rotl.	92,1	3,1	0,63								3	0,9				0,1		Int. Map Gasfields 1985
Groningen	R	81,2	C2+=3,5									14,35	0,89						Bandlova
Groningen	Rotl.	81,25	2,85	C3+=0.57								14,35	0,89						Int. Map Gasfields 1985
Harlingen 1	Cret.	86,95	0,5	C3+=0.1								12,3	0,15						Int. Map Gasfields 1985
Harlingen	M/T	95,79	C2+=0,6									3,61	-						Bandlova
IJsselmonde	Cretac.	93,3	0,1									3,4	0,2						Int. Map Gasfields 1985
Leeuwarden	M/T	80,96	C2+>3,5									15	0,27						Bandlova
Middelie	R+Z	66,57	2,55	0,87								1,92	28						Int. Map Gasfields 1985
Noordwijk	Cretac.??	98,2	0,2									1,5	0,1						Int. Map Gasfields 1985
Oudega 3	Cret/Rotl	84,7	3,04	1,1								11,58							Int. Map Gasfields 1985
Rossum	Z	87,7	C2+=4.0									3	2,7						Bandlova
Rossum-Weerselo	Zech/Carb	90,16	2,86	C3+=1.16								2,94	2,69	0,14					Int. Map Gasfields 1985
Rijswijk	Cretac.	93,5	5,4									0,9	0,2						Int. Map Gasfields 1985
Schoonebeek	Z	87,9	-									5,1	6,6						Bandlova
Schoonebeek	Cret.	88,25	0,42	C3+=0.08								5,16	6,0						Int. Map Gasfields 1985
Sleen	M/T	45	-									55	-						Bandlova
Tijetjerkstradeel	Cret/Rotl	79,33	2,58	0,6								16,2	1,18						Int. Map Gasfields 1985
Tubbergen	Z	88	-									8,2	-						Bandlova
Tubbergen	Zech/Carb	90,3	3,4	C3+=1.41								2,9	1,6	0,3			0,1		Int. Map Gasfields 1985
Vries 1	Rotl.	89,7	4,3	1,59								3,9	0,4						Int. Map Gasfields 1985
Wanneperveen	M/T	88,9	-									6,6	-						Bandlova
Wanneperveen	Cretac.	89,23	2,89	c3+=1.11								6,6	0,11						Int. Map Gasfields 1985
Zuidwal	M/T	88,7	C2+>6.4									3	1,26						Bandlova
Zuidwal	Cretac.	88,56	5,26	C3+=1.7								3,21	1,27						Int. Map Gasfields 1985
D15-03	C	78,88	2,54	0,47			0,14			0,05	0,04	12,39	5,38	0			0,11	34,06	
E13-01	C	75,24	2,22	0,33			0,06			0,02	0,04	18,06	3,97	0			0,06	32,04	
F03-01	M/T	86,95	8,63	2,53			0,42			0,04	0	1,16	0,27	0			0	43,8	
F03-03A	M/T	80,71	11,45	2,75			0,5			0,07	0,01	0,34	4,17	0			0	43,7	
F03-03B	M/T	86,95	8,63	2,53			0,42			0,04	0	1,16	0,27	0			0	43,8	
F03-08	M/T	86,95	8,63	2,53			0,42			0,04	0	1,16	0,27	0			0	43,8	
F15-04	M/T	85,56	3,49	0,27			0,06			0,01	0,01	9,62	0,85	0			0,13	37,2	
F17-03	M/T	84,31	8,28	3,42			1,22			0,44	0,48	1,19	0,66	0			0	46,06	
G16-01	M/T	88,7	2,9	0,4			0,2			0	0,4	5,6	1,8	0			0	38,76	
J03-02	R	80,47	5	1,62			0,76			0,34	0,47	8,65	2,69	0			0	39,7	
J06-01	R	84,33	5,43	1,36			0,53			0,2	0,13	6,62	1,23	0			0,17	41,45	
K03-01A	C	81,19	6,09	1,24			0,47			0,19	0,55	8,1	2,17	0			0	40,04	
K03-01B	R	81,19	6,09	1,24			0,47			0,19	0,55	8,1	2,17	0			0	40,04	
K04-01A	C	84,01	3,9	1,05			0,44			0,2	0,59	8,45	1,36	0			0	38,86	
K04-01B	C	84,54	5,09	1,68			0,6			0,34	0,24	6	1,51	0			0	40,61	
K05-02	R	85,41	5,35	1,26			0,47			0,17	0,24	4,84	2,26	0			0	40,47	
K06-02	R	85,71	6,51	1,18			0,39			0,13	0,12	4,61	1,35	0			0	41,04	
K06-03	R	88,25	5,44	1,03			0,33			0,14	0,07	3,32	1,43	0			0	41,04	
K07-01	R	85,11	4,88	1,24			0,45			0,16	0,08	7,12	0,96	0			0	39,56	
K07-02	R	83,66	4,83	1,53			0,57			0,19	0,06	8,21	0,86	0			0,09	39,39	
K08-01	R	87,56	5,64	1,17			0,39			0,15	0,07	4,02	1	0			0	40,88	
K08-02	R	86,16	5,05	1,27			0,45			0,16	0,07	5,33	1,41	0			0,1	40,09	
K08-07	R	85,92	5,72	1,28			0,51			0,16	0,09	5,11	1,21	0			0	40,61	
K09-04	R	89,41	5,5	0,96			0,32			0,09	0,13	1,96	1,63	0			0	41,16	

Composition of Natural Gases in Northwest European Gasfields (vol%)

Table 2 - 1

Wellname/Fieldname	Reservoir	CH4	C2H6	C3H8	i-C4	n-C4	C4	i-C5	n-C5	C5	C6	N2	CO2	H2S	He	H2	others	Calval	Reference
K09-05	R	87,39	5,85	1,03			0,33			0,09	0,31	3,24	1,76	0			0	41,29	
K10-05	R	85,91	5,49	1,11			0,4			0,12	0,1	5,05	1,67	0			0,15	40,24	
K10-06	R	86,82	5,6	1,13			0,4			0,14	0,12	4,34	1,26	0			0,19	40,83	
K11-02	R	87,25	5,59	1,15			0,4			0,15	0,09	4,23	1,14	0			0	40,76	
K11-08	R	88,08	5,37	0,99			0,33			0,1	0,11	3,55	1,47	0			0	40,62	
K12-02	R	86,83	6,49	1,43			0,45			0,16	0,13	3,13	1,38	0			0	41,52	
K12-06	R	81,22	4,05	0,71			0,28			0,1	0,24	1,9	11,49	0			0,01	36,95	
K12-08A	R	89,93	4,88	0,72			0,25			0,07	0,21	1,75	2,14	0			0,05	40,72	
K12-08B	R	87,79	5,68	1,12			0,4			0,12	0,41	2,32	2,16	0			0	41,55	
K13-01	M/T	84,54	5,68	1,33			0,5			0,23	0	7,54	0,18	0			0	38,02	
K13-02	M/T	84	4,04	1,24			0,46			0,15	0,13	9,88	0,1	0			0	38,69	
K13-04	R	85,38	5,45	1,13			0,4			0,13	0,14	5,58	1,71	0			0,08	40,16	
K13-05	R	85,48	5,57	1,13			0,39			0,12	0,16	5,44	1,63	0			0,08	40,36	
K14-01	R	87,46	2,86	0,41			0,21			0,09	0,06	5,32	3,59	0			0	37,79	
K14-08	R	86,92	1,04	0,07			0,02			0	0,01	6,83	5,11	0			0	35,46	
K15-02	R	89,86	5,44	0,93			0,37			0,22	0,21	1,5	1,47	0			0	41,83	
K15-03	R	68,75	2,93	0,58			0,16			0,06	0,03	1,42	26,07	0			0	30,42	
K15-06	R	80,78	3,5	1,37			1,38			0,1	0,04	4,4	8,43	0			0	38,03	
K15-07	R	89,18	4,63	0,61			0,19			0,05	0,21	0,8	4,33	0			0	40,21	
K15-08	R	90,58	4,6	0,63			0,22			0,06	0,12	1,15	2,64	0			0	40,59	
K15-09	R	90,63	4,88	0,82			0,26			0,08	0,22	1,26	1,85	0			0	41,32	
K16-05	Z	82,04	5,22	0,89			0,38			0,14	0,08	10,05	1,11	0			0,09	38,19	
K17-02A	R	92,7	0,6	0,03			0			0	0	4,73	1,86	0			0,08	37,36	
K17-02B	Z	61,92	6,9	3,15			1,91			0,83	0,78	20,6	1,06	2,8			0,05	38,67	
K17-05	R	86,18	0,51	0,02			0			0	0	10,4	2,89	0			0	34,69	
K18-01	C	70,71	8,46	7,82			3,52			1,04	0,51	5,68	2,26	0			0	49,29	
L01-04-A	R	85,03	2,76	0,36			0,12			0,04	0,06	7,75	3,88	0			0	34,65	
L02-01	M/T	93,96	0,78	0,01			0			0	0	4,4	0,8	0			0,05	37,97	
L02-05	M/T	93,93	0,95	0,07			0			0	0	4,3	0,7	0			0,05	38,13	
L04-01	R	90,43	2,7	0,25			0,17			0	0	3,51	2,85	0			0,09	38,6	
L04-03	R	86,1	4,75	0,64			0,24			0,06	0,28	6,07	1,86	0			0	38,95	
L07-01	R	84,71	6,61	1,05			0,31			0,08	0,06	4,5	2,67	0			0,01	40,24	
L07-02A	R	92,2	2,5	0,29			0,16			0,04	0,15	2,7	1,89	0			0,07	39,4	
L07-02B	R	92,8	2,3	0,26			0,15			0,02	0,12	2,7	1,64	0			0,01	39,4	
L07-03	R	91,4	2,8	0			0			0	0,8	3,1	1,9	0			0	39,4	
L07-05	R	86,14	5,53	1			0,33			0,11	0,31	4,92	1,66	0			0	39,77	
L07-06	R	94,61	2,44	0,21			0,04			0,01	0,02	1,9	0,77	0			0	39,82	
L08-01	R	94,36	2,41	0,05			0,08			0,02	0,04	1,25	1,79	0			0	39,6	
L08-05	R	90,72	3,08	0,24			0			0	0,22	1,55	4,19	0			0	38,74	
L08-09	R	91,11	2,17	0,18			0,04			0	0,07	1,91	4,52	0			0	38,15	
L10-01	R	89,58	4,91	0,75			0,27			0,11	0,4	2,82	1,16	0			0	41,11	
L10-03A	R	93,07	2,77	0,31			0,09			0,02	0,1	2,12	1,52	0			0	39,8	
L10-03B	R	93,07	2,77	0,31			0,09			0,02	0,1	2,12	1,52	0			0	39,8	
L10-04	R	90,46	4,73	0,79			0,25			0,06	0,07	1,69	1,95	0			0	40,74	
L10-06	R	84,75	5,01	1,13			0,42			0,13	0,09	6,1	2,37	0			0	39,19	
L10-07	R	92,6	3,4	0,51			0,14			0,04	0,06	1,53	1,72	0			0	40,1	
L10-10	R	90,56	3,48	0,47			0,14			0,04	0,25	3,2	1,86	0			0	39,61	
L10-19	R	93,21	2,62	0,31			0,09			0,03	0,28	1,07	2,39	0			0	40,15	
L11-01	R	89,65	5,16	1,06			0,33			0,12	0,13	0,68	2,87	0			0	41,11	

Composition of Natural Gases in Northwest European Gasfields (vol%)

Table 2 - 1

Wellname/Fieldname	Reservoir	CH4	C2H6	C3H8	i-C4	n-C4	C4	i-C5	n-C5	C5	C6	N2	CO2	H2S	He	H2	others	Calval	Reference
L11-04A	R	90,35	3,96	0,69			0,19			0,1	0,17	2,84	1,7	0			0	40,26	
L11-04B	R	89,95	3,95	0,61			0,2			0,08	0,17	3,11	1,93	0			0	40,26	
L11-10	R	86,53	5,92	1,56			0,52			0,12	0,07	3,79	1,49	0			0	41,07	
L11-11	R	93,39	2,59	0,31			0,15			0,01	0,03	1,45	2,04	0			0,03	40,5	
L12-01-AA	R	91,2	4,39	0,85			0,29			0,09	0,1	1,42	1,62	0			0,04	40,97	
L12-01-AB	R	91,2	4,39	0,85			0,29			0,09	0,1	1,42	1,62	0			0,04	40,97	
L12-02	R	91,2	4,39	0,85			0,29			0,09	0,1	1,42	1,62	0			0,04	40,97	
L12-03	R	82,41	7,15	1,9			0,63			0	0,06	2,43	5,25	0			0,17	40,74	
L12-05	R	86,51	6,95	1,93			0,71			0,27	0,69	1,44	1,5	0			0	44,13	
L13-01	R	76,9	9,5	3,09			1,24			0,38	0,18	7,5	1,05	0			0,16	42,95	
L13-02	R	84,44	6,75	1,85			0,62			0,17	0,07	4,97	1,06	0			0,07	41,42	
L13-06	R	92,36	3,48	0,57			0,19			0,06	0,1	1,64	1,6	0			0	40,36	
L13-07A	R	84,77	6,25	2			0,87			0,38	0,77	2,73	2,23	0			0	42,35	
L13-07B	R	92,36	3,48	0,57			0,19			0,06	0,1	1,64	1,6	0			0	40,36	
L13-08	R	92,36	3,48	0,57			0,19			0,06	0,1	1,64	1,6	0			0	40,36	
L13-09	R	90,75	4,05	0,7			0,23			0,07	0,1	2,4	1,7	0			0	39,51	
L14-01A	R	88,52	5,16	1			0,29			0,1	0,12	3,82	0,99	0			0	40,62	
L14-01B	R	88,52	5,16	1			0,29			0,1	0,12	3,82	0,99	0			0	40,62	
L14-01C	ZE	88,64	5,47	1,1			0,33			0,12	0,08	3,39	0,87	0			0	40,62	
L15-01	R	90,56	4,83	1			0,29			0,08	0,07	1,34	1,83	0			0	41,11	
M11-01	R	82,51	3,79	0,96			0,38			0,14	0,2	9,93	2,09	0			0	37,56	
P01-01A	R	61,7	2,44	0,19			0,02			0,01	0,02	2,51	33,1	0			0,01	26,6	
P01-01B	Z	62,42	9,08	4,34			1,71			0,36	0,03	18,84	3,22	0			0	38,4	
P01-03	R	83,43	1,38	0,08			0,03			0,01	0,01	9,72	5,34	0			0	34,35	
P02-01	M/T	64,73	1,15	0,12			0,03			0,01	0	33,58	0,38	0			0	26,8	
P02-04	R	85,65	2,09	0,29			0,09			0,03	0	7,49	4,36	0			0	36,05	
P02-05	R	88,35	3,16	0,46			0,14			0,03	0	3,87	2,84	0			1,15	38,16	
P02-07	R	91,19	3,21	0,3			0,04			0,01	0	1,96	3,17	0			0,12	39,03	
P06-01A	M/T	93,32	2,47	0,37			0,18			0,13	0,69	1,51	1,33	0			0	40,12	
P06-01B	Z	91,65	2,48	0,39			0,14			0,12	0,46	1,54	3,22	0			0	40,02	
P12-03	M/T	86,53	6,1	2,04			0,93			0,39	0,5	2,07	1,39	0			0,05	43,68	
P12-05	M/T	91,6	4,16	1,07			0,36			0,3	0,34	1,21	0,8	0			0,16	42,24	
P12-06	M/T	84,37	7,52	2,14			1,01			0,33	0,24	2,64	1,59	0			0,16	43,48	
P15-03	M/T	82,12	6,35	4,02			2,6			1,06	0,64	1,88	1,33	0			0	45,71	
Q01-02	R	85,02	7,06	2,08			0			0	1,28	3,8	0,76	0			0	42,8	
Q07-01	Z	91,2	4,44	0,77			0,29			0	0	1,6	1,7	0			0	40,57	
Q08-01A	M/T	89,88	4,49	0,91			0,3			0,09	0,11	3,97	0,25	0			0	40,54	
Q08-01B	Z	88,42	5,34	1,28			0,44			0,15	0,21	3,68	0,48	0			0	41,51	
Q08-04	M/T	90,63	3,43	0,68			0,4			0	0	4,4	0,46	0			0	39,91	
<b>POLAND</b>																			
Kargowa-6	Z	20,6	4,90	2,0	0,35	0,65		0,22	0,17		0,07	70,3	0,28	0,38		0,05		-15,61	
Rozansko-1	Z	54,7	1,67	0,89	0,31	0,38		0,17	0,12		0,17	31,3	0,74	9,5	0,01	0,01		-25,60	
Sulecin 21	Z	1,8	0,24	0,18	0,027	0,051		0,026	0,03		0,015	97,6	0,04					-1,28	
Zbaszyn-6	Z	17,8	3,0	1,4	0,22	0,49		0,17	0,14		0,12	75,2	0,21	1,1	0,02	0,01		-12,17	
Borzecin-22	Z	60,4	1,83	0,18	0,018	0,025		0,008	0,005		0,006	37,0	0,08	0,08	0,27	0,06		-25,72	
Czeszow-18	Z	63,0	0,61	0,07	0,005	0,011		0,004	0,003		0,005	35,7	n.a.	0	0,50	0,07		-25,74	
Henrykowice-5	Z	68,2	0,57	0,019	0,0016	0,0038		0,0009	0,0008		0,0003	30,9	0,05		0,32	0		-27,69	
Paproc-17	Z	49,9	1,74	0,08	0,012	0,017		0,008	0,002		0,001	47,9	0,06	n.a.	0,16	0,11		-21,36	

Composition of Natural Gases in Northwest European Gasfields (vol%)

Table 2 - 1

Wellname/Fieldname	Reservoir	CH4	C2H6	C3H8	i-C4	n-C4	C4	i-C5	n-C5	C5	C6	N2	CO2	H2S	He	H2	others	Calval	Reference
Paproc-19	Z	47,6	1,38	0,06	0,011	0,014		0,0044	0,002		0,0072	50,6	0,04	0	0,17	0,06		-20,19	
Wierzchowiec-3	Z	68,3	0,45	0,024	0,0019	0,004		0,001	0,0008		0,0006	30,8	0,03		0,34	0,049		-27,66	
Wierzowiec-4	Z	70,7	2,59	0,23	0,02	0,021		0,008	0,004		0,004	26,1	0,03	0	0,18	0,08		-30,37	
Aleksandrowka-3	R/Z	69,8	1,50	0,14	0,016	0,030		0,009	0,006		0,002	28,2	0,03	0	0,24	n.a.		-29,17	
Lipowiec-9	R/Z	55,3	3,35	0,49	0,048	0,085		0,02	0,0137		0,01	40,3	0,07	0	0,20	0,05		-25,22	
Niechlow-4	R/Z	38,8	0,91	0,09	0,013	0,025		0,006	0,0052		0,005	59,8	0,03		0,25	0,13		-16,40	
Szlichtyngowa-2	R/Z	38,0	0,98	0,1	0,012	0,033		0,018	0,018		0,03	60,6	0,03	0	0,22	0,009		-16,23	
Tarchaly-3	R/Z	53,6	0,12	0,008	0,0006	0,0016		0,0004	0,0004		0,0002	45,8	0,03		0,49	0		-21,57	
Buk-10W	R	79,7	0,87	0,02	0,001	0,002		0,0007	0,0009		0,0021	19,2	0,04	0	0,14	0		-32,46	
Ceradz-2	R	78,1	0,80	0,035	0,008	0,012		0,0060	0,002		0,001	20,8	0,04	0	0,14	0		-31,82	
Cicha Gora-1	R	70,5	1,14	0,047	0,008	0,002		0,0017	0,0015		0,0012	28,1	0,03	0	0,25	0		-29,02	
Debina-1	R	29,1	0,42	0,053	0,007	0,022		0,0037	0,0037		0,0025	70,1	0,04	0	0,22	0		-11,98	
Grochowice-39	R	36,5	1,04	0,07	0,0098	0,018		0,0088	0,0069		0,007	62,0	0,06	0	0,23	0,03		-15,55	
Grodzisk-30	R	80,8	0,80	0,052	0,003	0,005		0,0010	0,0007		0,0008	18,2	0,05	0	0,15	0		-32,88	
Jankowice-2	R	75,2	0,97	0,009	0,002	0,017		0,0015	0,001		0,001	23,6	0,04	0	0,17	0		-30,76	
Jarcin-5	R	80,9	0,37	0,01	0,0013	0,0028		0,0002	0,0002		0,0002	18,5	0,05	0	0,14	0		-32,57	
Kandlewo-1	R	24,2	0,73	0,11	0,002	0,031		0,012	0,010		0,01	74,5	0,06	n.a.	0,25	0,02		-10,33	
Kleka-8	R	79,4	0,35	0,013	0,0012	0,0027		0,0002	0,0001		0,0003	20,1	0,05	0	0,14	0		-31,96	
Lubinia-1 (!)	R	74,1	0,15	0,002	0,0001	0,0003		0,0001	0,0001		0,0001	25,6	0,04	0	0,11	0,025		-29,71	
Mlodasko-2	R	74,6	0,82	0,016	0,002	0,003		0,0013	0,0013		0,001	24,4	0,03	0	0,13	0		-30,40	
Niemierzyce-1 (!)	R	81,1	1,08	0,038	0,001	0,004		0,0009	0,0013		0,001	17,6	0,04	0	0,14	0		-33,18	
Paproc-6	R	69,7	1,12	0,04	0,004	0,006		0,0017	0,0015		0,0036	28,9	0,04	0	0,18	0,04		-28,70	
Radlin-3	R	80,6	0,61	0,009	0,0002	0,0006		0,0002	0,0002		0,0002	18,7	0,04		0,12	0		-32,61	
Rokietnica-1	R	85,4	1,01	0,024	0,002	0,003		0,0005	0,0003		0,0001	13,4	0,05	0	0,11	0,02		-34,81	
Szewce-3W	R	78,8	0,87	0,026	0,001	0,003		0,0007	0,0009		0,0009	20,1	0,04	0	0,15	0		-32,11	
Ujazd-12	R	80,2	0,80	0,02	0,001	0,002		0,0005	0,0006		0,0003	18,8	0,04	0	0,16	0		-32,60	
Wilcze-2	R	28,7	0,88	0,053	0,002	0,017		0,0019	0,0034		0,0015	70,1	0,04	0	0,24	0		-12,11	
Wilkow-26	R	37,6	1,28	0,1	0,019	0,032		0,011	0,013		0,01	60,6	0,05	0	0,21	0,01		-16,23	
Gorzyslaw-15	C	51,7	1,06	0,86	0,018	0,025			*	0,07		46,1	n.a.	0	0,12	0		-22,49	
Gorzyslaw-2	C	50,8	1,20	0,18	n.a.	n.a.		n.a.	n.a.		n.a.	47,4	0,05	0	0,30	0		-21,38	
Trzebusz-1	C	53,6	1,43	0,36	0,11	0,16			*	0,17		43,9	n.a.	0	0,26	0		-23,45	
Paproc-1	C	69,6	1,28	0,039	0,005	0,007		0,0014	0,0008		0,0017	28,8	0,03	0	0,19	0,08		-28,78	
Paproc-4	C	69,9	0,97	0,04	0,002	0,005		0,001	0,0008		0,0013	28,8	0,03	n.a.	0,18	0,04		-28,68	
Wierzchowo-11	C	58,0	1,40	0,24	0,052	0,073		0,026	0,025		0,033	40,0	0,08		0,14			-24,75	
Zbaszyn-1	Z	19,0	4,10	2,40	0,43	0,86		0,29	0,26		0,23	72,2	0,01		0,02	0,19		-15,73	
Brzostowo-2	Z	61,1	0,46	0,03	0,002	0,004		0,0009	0,0007		0,0010	37,7	0,35		0,31	0,035		-24,81	
Czeszow-17	Z	61,5	0,51	0,056	0,007	0,012		0,004	0,003		0,007	37,4	0,09		0,33	0,06		-25,07	
Koscian-6	Z	81,4	0,59	0,027	0,002	0,003		0,0008	0,0006		0,001	17,3	0,52		0,16	0,015		-32,94	
Radziadz-13	Z	69,6	1,56	0,21	0,023	0,032		0,011	0,006		0,013	28,2	0,10		0,02	0,17		-29,24	
Radziadz-7	Z	68,2	1,78	0,26	0,03	0,044		0,013	0,009		0,014	29,2	0,19		0,16	0,01		-28,93	
Bogdaj Uciechow-25	R/Z	54,7	0,35	0,018	0,001	0,003		0,0009	0,0006		0,001	44,2	0,27		0,47	0,002		-22,18	
Janowo-3	R/Z	51,0	0,48	0,075	0,007	0,016		0,004	0,004		0,005	47,8	0,29		0,38			-20,90	
Szklarka-4	R/Z	54,6	0,31	0,017	0,001	0,003		0,0007	0,0006		0,0007	44,6	0,05		0,46	0,006		-22,11	
Bialogard-10	R	50,5	1,12	0,13	0,0012	0,029		0,006	0,006		0,008	47,9	0,10		0,18			-21,23	
Borowo-4	R	81,0	0,33	0,012	0,0005	0,0014		0,0002	0,0002		0,0003	18,2	0,33		0,16	0,009		-32,58	
Buk-17	R	78,9	0,38	0,012	0,008	0,001		0,0002	0,0002		0,0004	20,2	0,32		0,14			-31,79	
Bukowiec-26	R	79,8	0,70	0,034	0,002	0,004		0,0008	0,0006		0,0013	18,9	0,32		0,16	0,001		-32,39	
Duszniki-1	R	79,4	0,43	0,013	0,0004	0,0015		0,0002	0,0002		0,0007	19,7	0,27		0,17			-32,02	
Duszniki-2	R	79,6	0,42	0,012	0,0002	0,0012		0,0002	0,0002		0,0007	19,5	0,30		0,17	0,002		-32,09	

Composition of Natural Gases in Northwest European Gasfields (vol%)

Table 2 - 1

Wellname/Fieldname	Reservoir	CH4	C2H6	C3H8	i-C4	n-C4	C4	i-C5	n-C5	C5	C6	N2	CO2	H2S	He	H2	others	Calval	Reference
Gora-5	R	44,2	1,0	0,16	0,019	0,031		0,01	0,006		0,009	54,2	0,16		0,26	0,001		-18,71	
Kaleje-9	R	79,6	0,24	0,013	0,004	0,008		0,002	0,002		0,002	19,8	0,17		0,15			-31,99	
Luszczanow-1	R	63,4	0,31	0,075	0,007	0,027		0,006	0,006		0,005	35,7	0,19		0,10	0,11		-25,73	
Mlodasko-3	R	76,1	0,47	0,013	0,0007	0,0012		0,0002	0,0001		0,0005	22,9	0,43		0,14			-30,74	
Naratow-5	R	47,4	1,40	0,21	0,026	0,05		0,014	0,009		0,014	50,5	0,05		0,27	0,003		-20,36	
Pakoslaw-2	R	52,1	0,61	0,11	0,023	0,04		0,014	0,014		0,019	46,1	0,38		0,35	0,29		-21,57	
Podrzewie-1	R	79,1	0,45	0,012	0,001	0,0009		0,0002			0,0003	19,9	0,36		0,18			-30,91	
Porazyn-2A	R	79,5	0,62	0,034	0,003	0,004		0,0011	0,0009		0,002	19,4	0,26		0,18			-32,22	
Slubow-4	R	62,5	0,84	0,064	0,005	0,0024		0,0013	0,0002		0,003	35,8	0,05		0,22	0,44		-25,67	
Turkowo-1	R	80,0	0,49	0,025	0,0015	0,002		0,0005	0,0001		0,001	19,0	0,23		0,16	0,11		-32,31	
Wiewierz-28	R	69,2	1,0	0,09	0,006	0,012		0,003	0,002		0,004	29,3	0,18		0,18			-28,49	
Wiewierz-3	R	68,4	1,10	0,11	0,008	0,016		0,041	0,003		0,006	30,0	0,11		0,18			-28,34	
Zbarzewo-1	R	20,6	0,36	0,064	0,011	0,024		0,008	0,01		0,011	78,5	0,10		0,27	0,04		-8,59	
Daszewo-21	C	66,0	1,50	0,19	0,031	0,046		0,012	0,011		0,022	31,9	0,24		0,11			-27,81	
Zarnowiec-7	C	82,0	10,0	3,60	0,3	0,6		0,12	0,17		0,24	1,8	0,92		0,18	0,006		-45,33	
Bialogard 2	R	49,6	1,23	0,15	0,01	0,04		0,01	0,01		0,01	48,8	0,12					-21,02	
Bogdaj Uciechow 68	R	55,9	0,35	0,03	0,01	0,02		0,01	0,01		0,01	43,4	0,27					-22,74	
Ciechnowo 1	R	47,7	1,81	0,69	0,24	0,34		0,14	0,20		0,01	48,8	0,11					-22,38	
Miedzzydroje 5	R	20,7	0,91	0,05	0,01	0,01		0,00	0,00		0,01	78,3	0,0					-8,95	
Piekary 2	R	83,0	0,49	0,02	0,00	0,00		0,00	0,00		0,00	16,3	0,19					-33,49	
Radlin 31	R	82,4	0,24	0,01	0,00	0,00		0,00	0,00		0,00	16,8	0,56					-33,07	
Steszew 4	R	82,9	0,41	0,02	0,00	0,01		0,00	0,00		0,00	16,2	0,48					-33,41	
Strykowo 1	R	83,7	0,54	0,07	0,03	0,04		0,01	0,02		0,01	15,3	0,30					-33,99	
Strzepin 1	R	84,1	0,55	0,03	0,00	0,00		0,00	0,00		0,00	14,8	0,49					-33,99	
Wierzchowice 29	R	71,7	0,42	0,03	0,01	0,01		0,00	0,01		0,00	27,5	0,32					-29,01	
Zuchlow 4	R	58,4	1,58	0,32	0,04	0,06		0,02	0,02		0,01	39,3	0,25					-25,00	
Daszewo 13k	C	66,4	1,34	0,15	0,03	0,04		0,01	0,01		0,01	31,8	0,28					-27,76	
Gorzyslaw 6	C	46,3	1,20	0,17	0,03	0,05		0,02	0,02		0,01	52,1	0,06					-19,76	
Wrzosowo 1	C	37,5	2,11	0,48	0,11	0,01		0,01	0,01		0,00	59,7	0,0					-17,23	
Bialogard 3	C	49,6	1,22	0,15	0,01	0,04		0,01	0,01		0,01	48,8	0,11					-21,02	
Wierzchowo 6	C	57,5	1,57	0,26	0,06	0,09		0,04	0,04		0,01	40,4	0,0					-24,73	
Antonin-3	Z	42,2	12,8	3,6	0,36	0,92		0,22	0,2		0,11	39,3	0,05	0	0,22	0		-32,03	
Babimost-1	Z	16,8	4,33	1,84	0,24	0,44		0,14	0,11		0,07	74,5	0,57	0,87	0,02	0,05		-12,91	
Bartniki-1	Z	32,1	2,18	0,69	0,07	0,16		0,088	0,08		0,059	64,2		0	0,28	0,017		-15,63	
Czeklin-1	Z	11,8	1,24	0,72			0,34			0,15	0,05	85,5	0,2	0				-7,03	
Kakolewo-2	Z	16,9	2,7	1,39			0,76			0,35	0,09	76,8	0,2	0,71	0,02			-11,67	
Rawicz-8	Z	17,9	4,04	1,83			0,76			0,19	0,03	74,6	0,46	0,03	0,16			-13,07	
Sekowice-1	Z	19,5	3,26	1,37			0,58			0,22	0,05	75						-12,56	
Unikow-1	Z	23,1	6,74	2,54	0,27	0,68		0,17	0,15		0,07	66,2		0,006		0		-18,24	
Wysocko Male-1	Z	67,5	1,27	0,55	0,002	0,12		0,1			0,12	29,9			0,14	0,006		-29,4	
Zakrzewo-1	Z	27,8	7,2	4,36			1,81			0,56	0,11	57,7	0,5	tr.				-23,79	
Piaski IG-2	R	21,3	0,19	0,006	0,0004	0,0016		0,0015			0,0006	78,4	0,05	0	n.a.	0		-8,61	
<b>UNITED KINGDOM</b>																			
AMETHYST	R	91,95	3,58	0,05			0,36					2,22	0,64		0,36				Garland, p 393
BARQUE	R	94,59	2,73	0,49	0,09	0,11		0,04	0,04		0,15	1,36	0,35						Farmer & Hillier, p 399
CAMELOT	R	90,7	4,1	1		0,4				1,3		2,4	0,1						Holmes, p 408
CLEETON	R	91,55	4,79	0,93	0,16	0,21		0,07	0,06		0,23	1,33	0,45		0,05				Heinrich, p 413
CLIPPER	R	95,76	2,24	0,47	0,07	0,13		0,04	0,03		0,07	0,71	0,47		0,01				Farmer & Hillier, p 421

Composition of Natural Gases in Northwest European Gasfields (vol%)

Table 2 - 1

Wellname/Fieldname	Reservoir	CH4	C2H6	C3H8	i-C4	n-C4	C4	i-C5	n-C5	C5	C6	N2	CO2	H2S	He	H2	others	Calval	Reference
ESMOND	M/T	91										8	1						Bifani, p 221
ESKDALE 2	R	98,8	0,9	0,3															Lees and Taitt, 1945; QJGS p255-317
FORBES	M/T	86										12							Bifani, p 221
GORDON	M/T	82										16							Bifani, p 221
HATFIELD MOORS	C	88,6	4,9	1,9		0,7						3,5							
HEWETT	M/T	83,19	5,32	2,14	0,21	0,15		0,08			0,41	8,4	0,08	0,02					Cumming & Wyndham, p 324
HEWETT	R	92,13	3,56	0,85	0,16	0,22		0,1	0,08		0,52	2,36	0,02						Cumming & Wyndham, p 324
INDEFATIGABLE	R	92	3,4									2,7	0,5						Pearson, Yougs & Smith, p 449
LEMAN	R	94,94	2,86	0,49	0,08	0,1		0,03	0,03		0,15	1,26	0,04		0,02				Hillier & Williams, p 458
LOCKTON	R	93,1	3	0,9								2,6	0,3	0,05			0,04		Map natural gas fields Europe 1986
MORECAMBE SOUTH	M/T	85	4,5	1			1,2					7,7	0,6	0-5ppm					Stuart & Cowan, p. 539
RAVENSPURN NORTH	R											2,5	>1					C6H6	Ketter, p 467
RAVENSPURN SOUTH	R	93,15	3,15	0,55			0,4					1,78	0,96		0,03				Heinrich, p 475
ROUGH	R	91	3,8	1,1			1,1					2,4	0,6						Stuart, p. 483
SEAN NORTH	R	92,06	2,94	0,64	0,12	0,13		0,04	0,03		0,17	3,07	0,76		0,04				Hobson & Hillier, p. 489
SEAN SOUTH	R	91,06	3,38	0,58	0,11	0,13		0,05	0,04		0,25	3,19	1,21						Hobson & Hillier, p. 489
THAMES	R	92											0,4						Werngren, p. 495
YARE	R	92											0,4						Werngren, p. 496
BURE	R	92											0,4						Werngren, p. 497
VIKING	R	91,2	4,1	1	0,4							2,5	0,4						Barnard & Cooper, p 25
WEST SOLE	R	94	3,1	0,5		0,2				0,4		1	0,8						Winter & King, p. 521
C=Carboniferous																			
R=Rotliegend																			
Z=Zechstein																			
M/T=post-Zechstein																			